

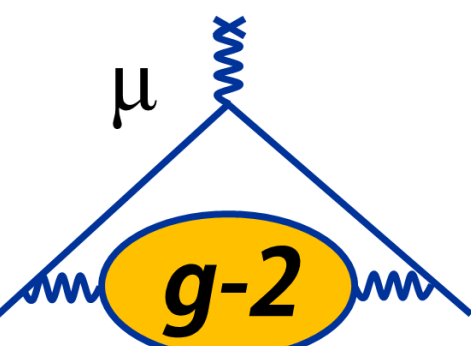
# Measuring the Muon Anomalous Magnetic Moment to High Precision

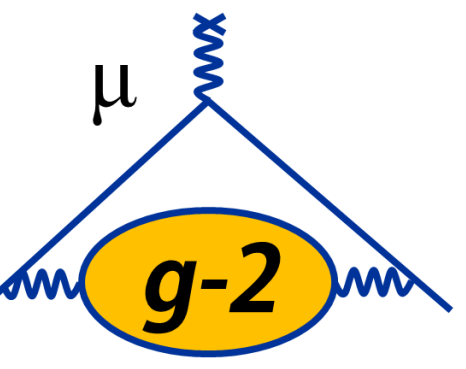
David Flay

Electromagnetic Interactions with Nucleons and Nuclei, Paphos, Cyprus

31 October 2019

This document was prepared by [Muon G-2 Collaboration] using the resources of the Fermi National Accelerator Laboratory (Fermilab), a U.S. Department of Energy, Office of Science, HEP User Facility. Fermilab is managed by Fermi Research Alliance, LLC (FRA), acting under Contract No. DE-AC02-07CH11359.





# Outline

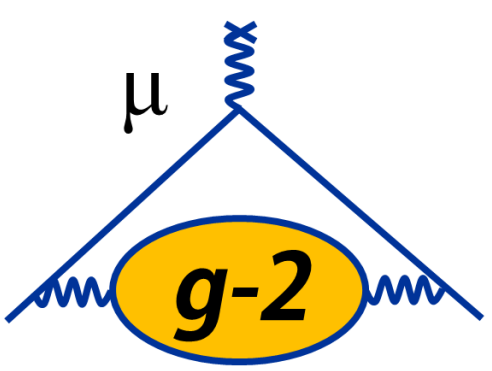
## Introduction

- The Magnetic Moment and the Anomaly
- Recent Theoretical Efforts

## The Muon g-2 Experiment at Fermilab

- Experimental Technique
- Overview of Operations to Date
- Analysis Status

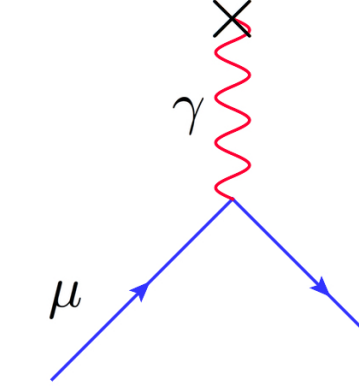
## Summary



# The Magnetic Moment and the Anomaly

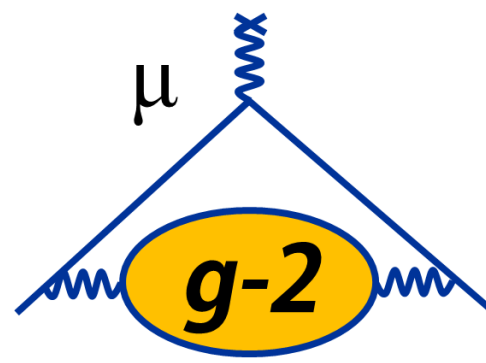
## The Magnetic Moment

$$\vec{\mu} = g \frac{q}{2m} \vec{s}$$



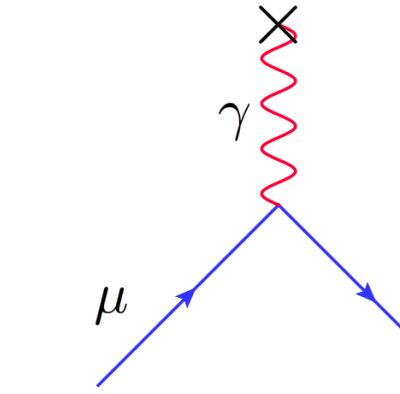
- Magnetic moment connected to spin via dimensionless g-factor
- Dirac:  $g = 2$  for  $s = 1/2$  particles (1928)
- Hyperfine structure experiments on hydrogen:  $g \neq 2$  (Nafe, Nelson, Rabi 1947)
  - Anomalous contribution  $a \equiv (g-2)/2 = a/2\pi$  (Schwinger, QED, 1948)
  - Radiative corrections from virtual particles in loops

# The Magnetic Moment and the Anomaly



## The Magnetic Moment

$$\vec{\mu} = g \frac{q}{2m} \vec{s}$$

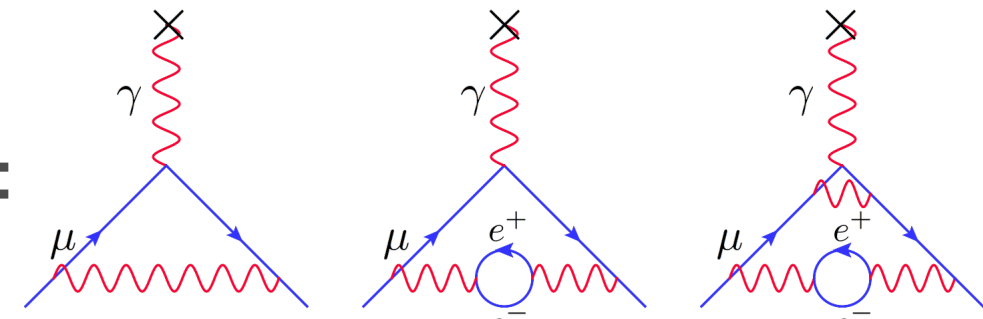


- Magnetic moment connected to spin via dimensionless g-factor
- Dirac:  $g = 2$  for  $s = 1/2$  particles (1928)
- Hyperfine structure experiments on hydrogen:  $g \neq 2$  (Nafe, Nelson, Rabi 1947)
  - Anomalous contribution  $a \equiv (g-2)/2 = a/2\pi$  (Schwinger, QED, 1948)
  - Radiative corrections from virtual particles in loops

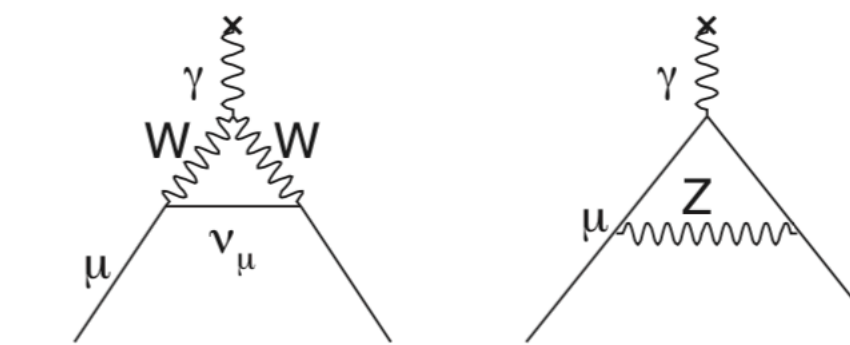
## The Muon Anomaly $a_\mu$

Schwinger  $O(a)$  Vacuum polarization  $O(a^2)$

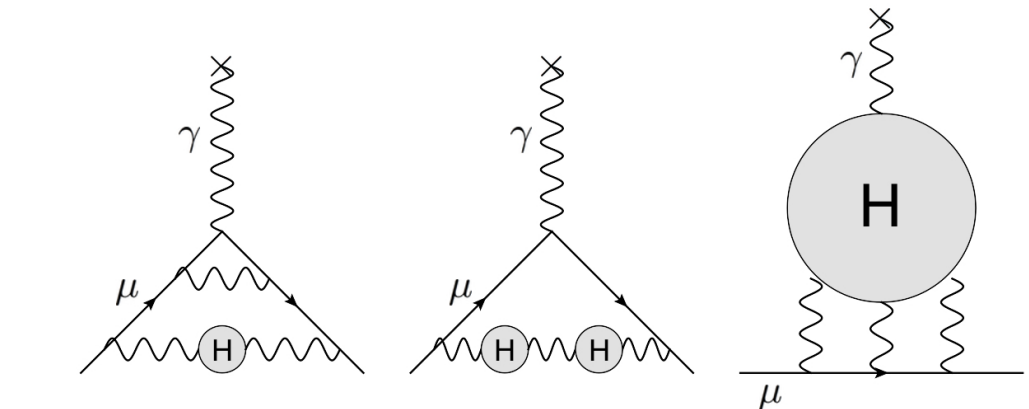
$$a_\mu =$$



+



+

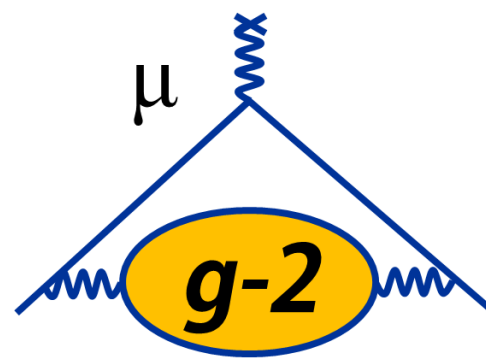


**QED**

**EW**

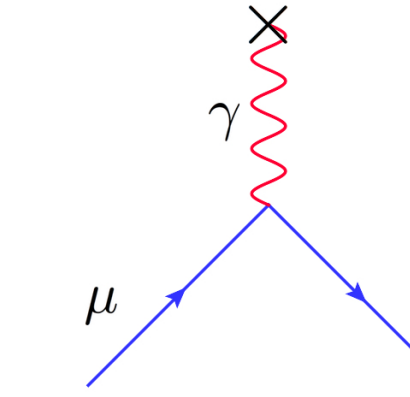
**QCD**

# The Magnetic Moment and the Anomaly



## The Magnetic Moment

$$\vec{\mu} = g \frac{q}{2m} \vec{s}$$

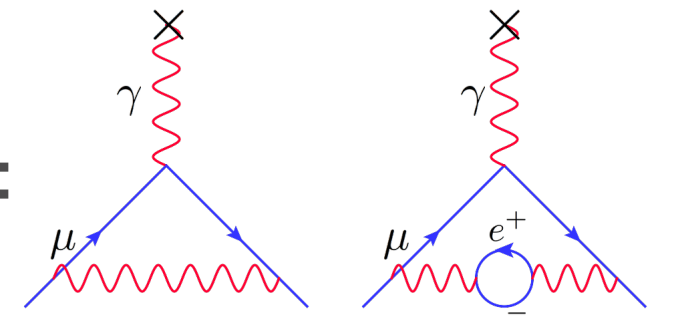


- Magnetic moment connected to spin via dimensionless g-factor
- Dirac:  $g = 2$  for  $s = 1/2$  particles (1928)
- Hyperfine structure experiments on hydrogen:  $g \neq 2$  (Nafe, Nelson, Rabi 1947)
  - Anomalous contribution  $a \equiv (g-2)/2 = a/2\pi$  (Schwinger, QED, 1948)
  - Radiative corrections from virtual particles in loops

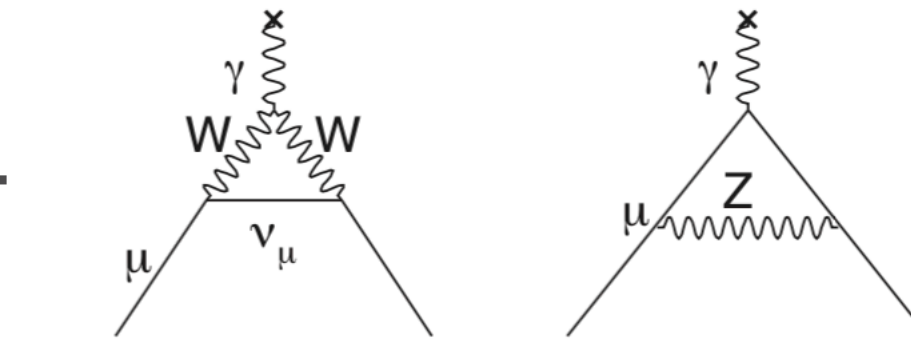
## The Muon Anomaly $a_\mu$

Schwinger  $O(a)$  Vacuum polarization  $O(a^2)$

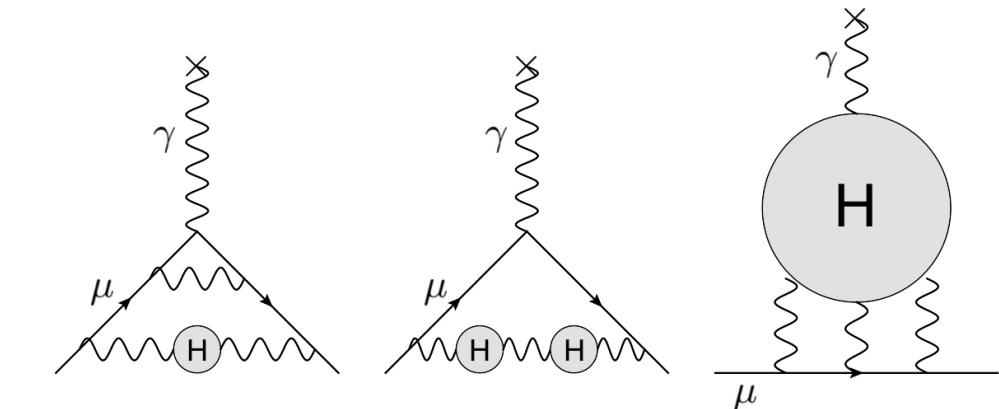
$$a_\mu =$$



+



+



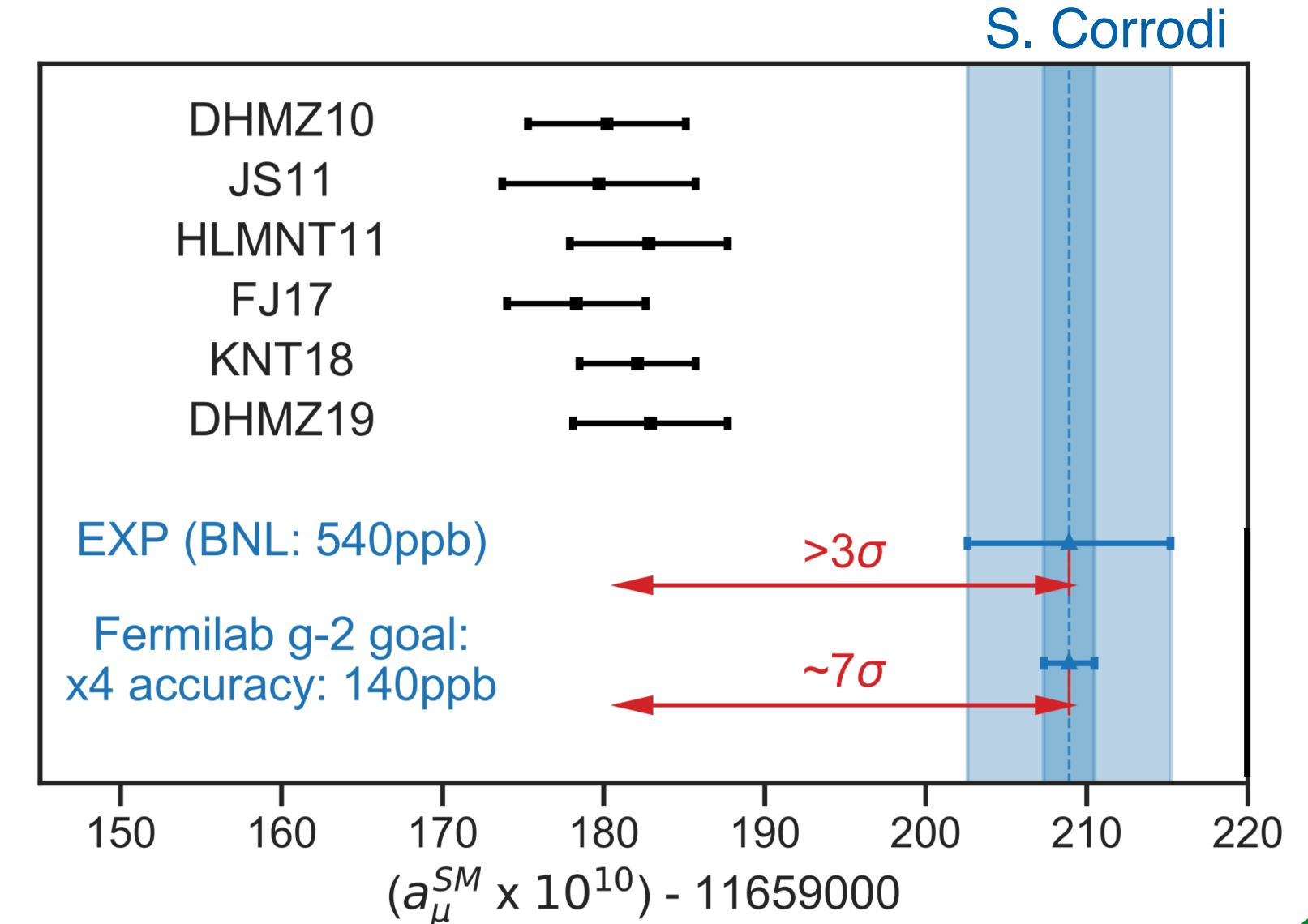
**QED**

**EW**

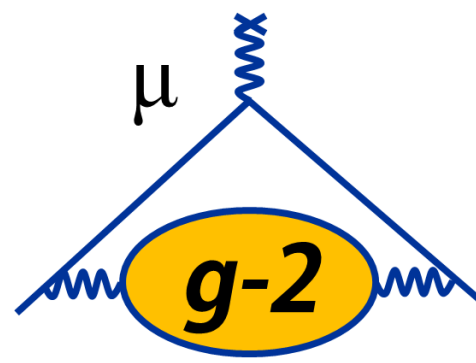
**QCD**

## Current Status

- Disagreement** between experiment and theory at  $> 3\sigma$
- Improvements**
  - Experiment:** more statistics, reduced systematics
  - Theory:** focus on QCD uncertainties



# The Magnetic Moment and the Anomaly



## Lattice groups making excellent progress (HVP LO, NLO, HLbL)

### Calculation of the hadronic vacuum polarization contribution to the muon anomalous magnetic moment

T. Blum, P.A. Boyle, V. Gülpers, T. Izubuchi, L. Jin, C. Jung, A. Jüttner, C. Lehner, A. Portelli, J.T. Tsang

(Submitted on 22 Jan 2018)

We present a first-principles lattice QCD+QED calculation at physical pion mass of the leading-order hadronic vacuum polarization contribution to the muon anomalous magnetic moment. The total contribution of up, down, strange, and charm quarks including QED and strong isospin breaking effects is found to be  $a_{\mu}^{\text{HVP LO}} = 715.4(16.3)(9.2) \times 10^{-10}$ , where the first error is statistical and the second is systematic. By supplementing lattice data for very small momenta, we significantly improve the precision of our calculation. We also estimate the remaining systematic, R-ratio statistical, and R-ratio systematic errors. The total uncertainty of the leading-order hadronic vacuum polarization contribution to the muon  $g - 2$  from lattice QCD is estimated to be  $\sim 1.5\%$ . This is the first calculation of the light-quark QED correction at physical pion mass.

Comments: 12 pages, 11 figures

Subjects: High Energy Physics – Lattice (hep-lat); High Energy Physics – Theory (hep-th)

Cite as: arXiv:1801.07224 [hep-lat]

(or arXiv:1801.07224v1 [hep-lat] for this version)

### Higher-order hadronic-vacuum-polarization contribution to the muon $g - 2$ from lattice QCD

B. Chakraborty, C. T. H. Davies, J. Koponen, G. P. Lepage, and R. S. Van de Water (Fermilab Lattice, HPQCD, and MILC Collaborations)

Phys. Rev. D **98**, 094503 – Published 9 November 2018

Article

References

Citing Articles (1)

PDF

HTML

Export Citation

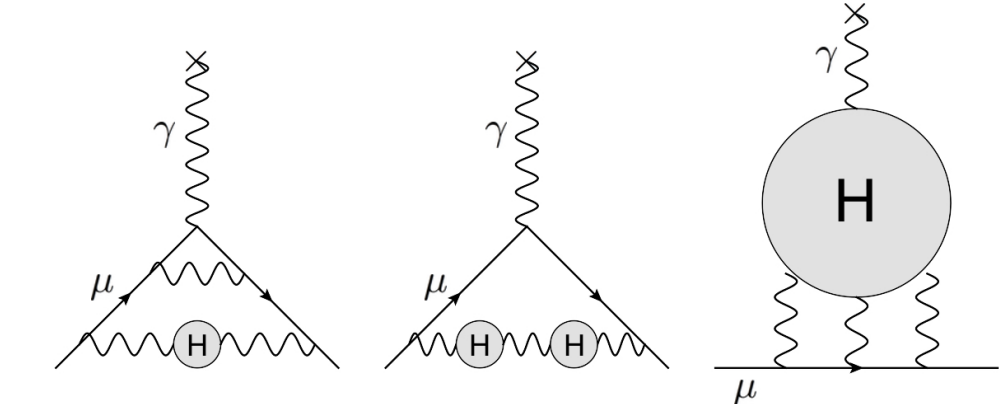
### ABSTRACT

We introduce a new method for calculating the  $O(\alpha^3)$  hadronic-vacuum-polarization contribution to the muon anomalous magnetic moment from *ab initio* lattice QCD. We first derive expressions suitable for computing the higher-order contributions either from the renormalized vacuum polarization function  $\hat{\Pi}(q^2)$  or directly from the lattice vector-current correlator in Euclidean space. We then demonstrate the approach using previously published results for the Taylor coefficients of  $\hat{\Pi}(q^2)$  that were obtained on four-flavor QCD gauge-field configurations with physical light-quark masses. We

VIRTUAL PARTICLES IN LOOPS

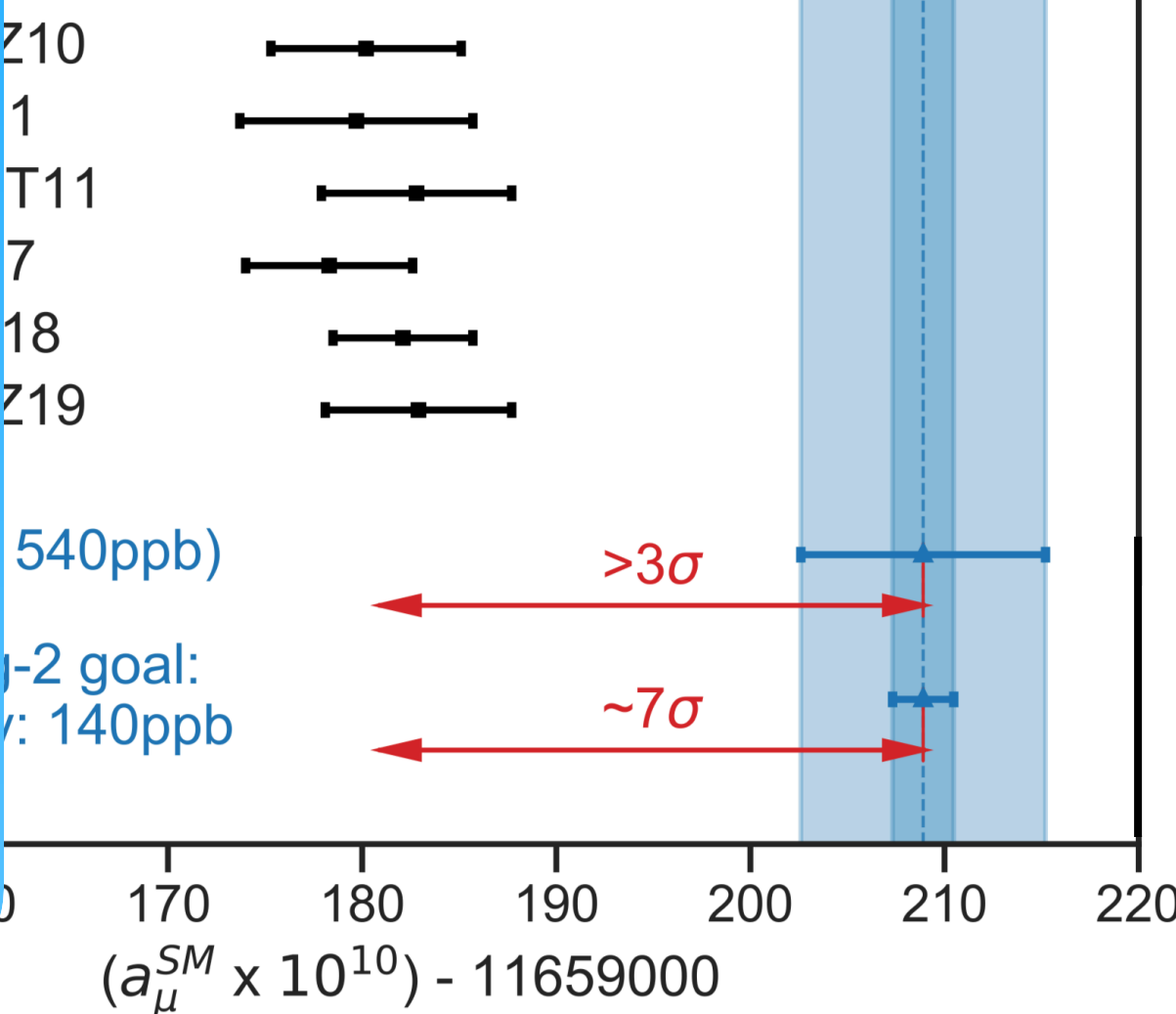
$a_{\mu}$

+



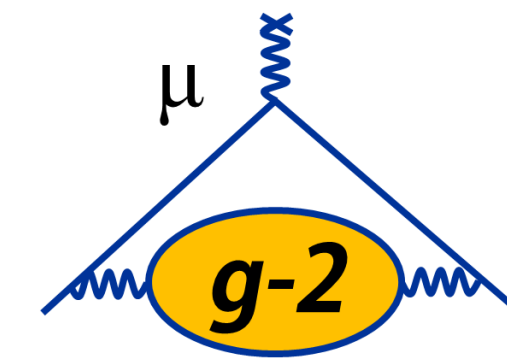
QCD

S. Corradi



UMassAmherst

# The Magnetic Moment and the Anomaly



# Lattice groups making excellent progress (HVP LO, NLO, HLbL)

# Calculation of the hadronic vacuum polarization and anomalous magnetic moment

T. Blum, P.A. Boyle, V. Gülpers, T. Izubuchi, L. Jin, C. Jung, A. Jüttner, C.

(Submitted on 22 Jan 2018)

We present a first-principles lattice QCD+QED calculation at physical pion mass contribution to the muon anomalous magnetic moment. The total contribution of strong isospin breaking effects is found to be  $a_\mu^{\text{HVP LO}} = 715.4(16.3)(9.2) \times 10^{-10}$ , which is significantly more precise than previous calculations. By supplementing lattice data for very small  $q^2$  and  $m_\pi^2$  and by including higher-order corrections, we significantly improve the precision of our calculation. We also include the leading-order hadronic vacuum polarization contribution to the calculation of the light-quark QED correction at physical pion mass.

Comments: 12 pages, 11 figure

Subjects: **High Energy Physics – Lattice (hep-lat);**

Cite as: arXiv:1801.07224 [hep-

(or [arXiv:1801.07224v1 \[hep-lat\]](https://arxiv.org/abs/1801.07224v1) for this

# Higher-order muon $g - 2$ fr

B. Chakraborty, C. T. H. Miller  
MILC Collaborations)  
Phys. Rev. D **98**, 094501

## Article

ABS

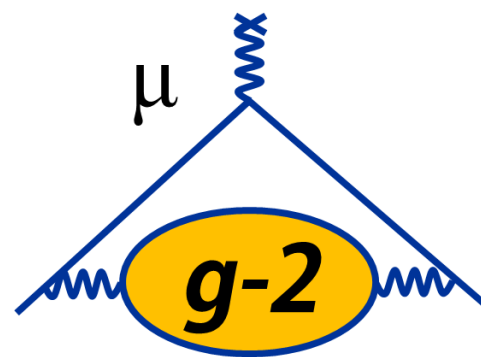
We introduce  
the model  
for con-

function  $\hat{\Pi}(q^2)$  or directly from the lattice vector-current correlator in Euclidean space. We then demonstrate the approach using previously published results for the Taylor coefficients of  $\hat{\Pi}(q^2)$  that were obtained on four-flavor QCD gauge-field configurations with physical light-quark masses. We

# virtual particles in loops



# The Magnetic Moment and the Anomaly



Lattice groups making excellent progress (HVP LO, NLO, HLbL)

## Calculation of the hadronic vacuum polarization contribution to the anomalous magnetic moment

T. Blum, P.A. Boyle, V. Gülpers, T. Izubuchi, L. Jin, C. Jung, A. Jüttner, C.

(Submitted on 22 Jan 2018)

We present a first-principles lattice QCD+QED calculation at physical pion mass of the hadronic vacuum polarization contribution to the muon anomalous magnetic moment. The total contribution from strong isospin breaking effects is found to be  $a_{\mu}^{\text{HVP LO}} = 715.4(16.3)(9.2) \times 10^{-9}$ , which is significantly more precise than previous calculations. By supplementing lattice data for very small momenta with experimental data, we significantly improve the precision of our calculation. We also include R-ratio statistical, and R-ratio systematic errors, leading to a total systematic error of 1.3%. The leading-order hadronic vacuum polarization contribution is obtained by a calculation of the light-quark QED correction at physical pion mass.

Comments: 12 pages, 11 figures

Subjects: High Energy Physics – Lattice (hep-lat); High Energy Physics – Theory (hep-th)

Cite as: arXiv:1801.07224 [hep-lat]

(or arXiv:1801.07224v1 [hep-lat] for this version)

Article References



ABS

We introduce a new method to calculate the muon g - 2 loop correction for contributions from the hadronic vacuum polarization function  $\hat{\Pi}(q^2)$  or directly from the lattice. We demonstrate the approach using previous results obtained on four-flavor QCD gauge theories.

VIRTUAL PARTICLES IN LOOPS

## 2<sup>nd</sup> g-2 Theory Initiative Meeting in June 2018



JOHANNES GUTENBERG  
UNIVERSITÄT MAINZ

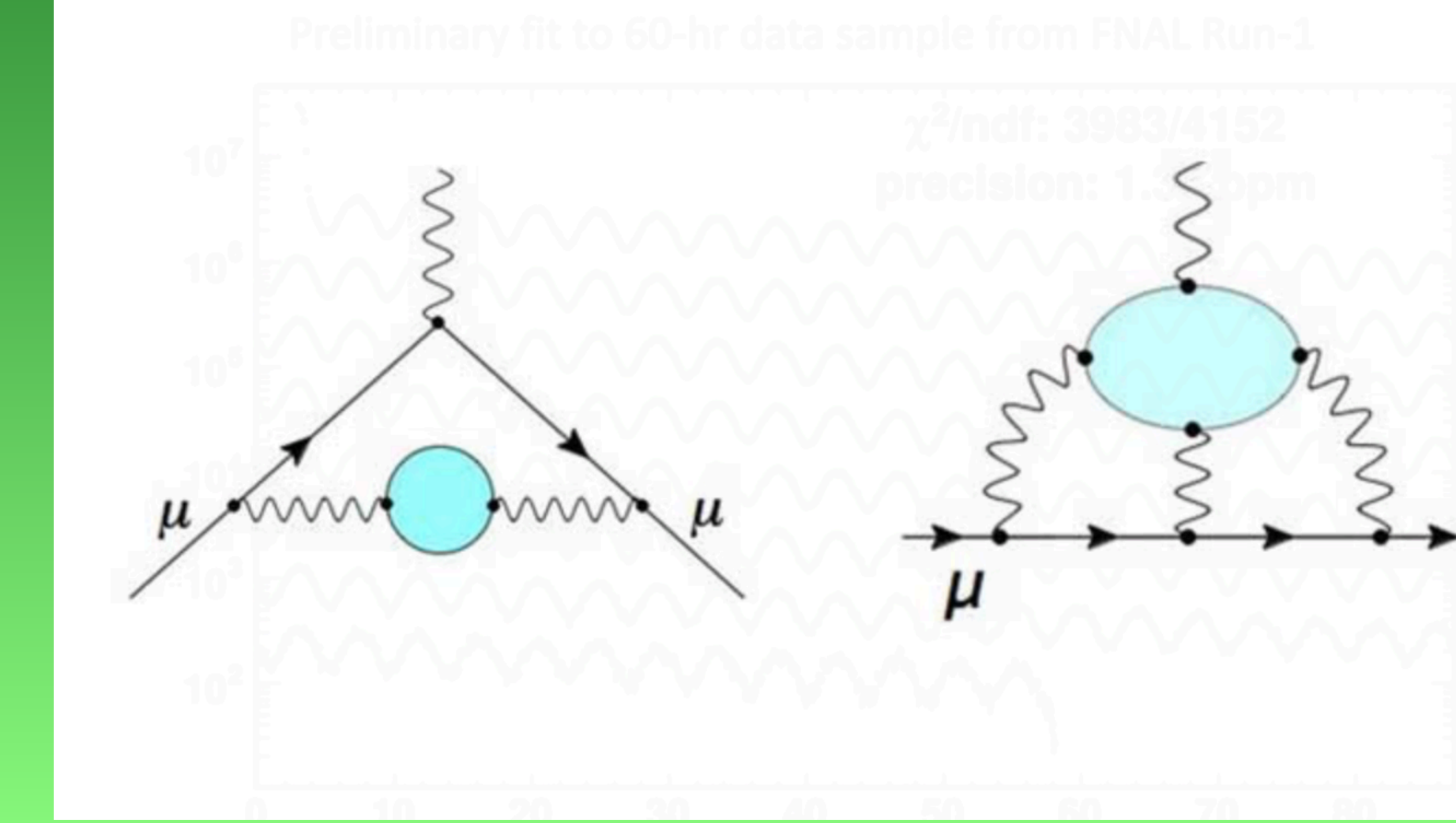
- [Home](#)
- [Research](#)
- [People](#)
- [Publications](#)
- [Teaching](#)
- [Events](#)
  - [Talks and Guest Speakers](#)
  - [Previous Events](#)
- [g-2 Workshop](#)
- [Press and Media](#)
- [Services](#)
- [Contact](#)

## 3<sup>rd</sup> g-2 Theory Initiative Meeting in Sept 2019

INT Workshop INT-19-74W

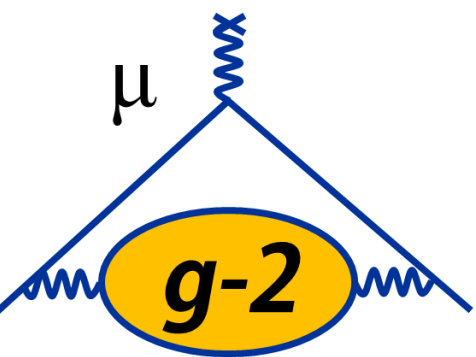
Hadronic contributions to  $(g-2)_\mu$

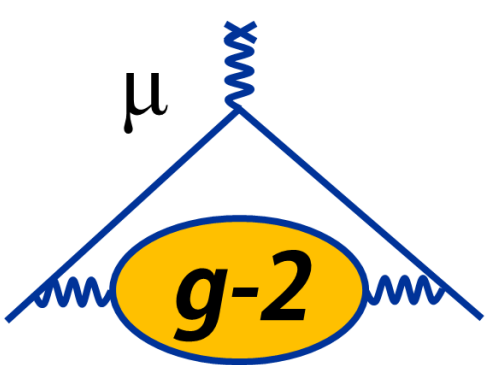
September 9 - 13, 2019



UMassAmherst

# a<sub>μ</sub> Theoretical Status





# $a_\mu$ Theoretical Status

| Contribution | Value (x 10 <sup>-11</sup> ) | Reference             |
|--------------|------------------------------|-----------------------|
| QED          | 116 584 718.95 ± 0.08        | PRL 109 111808 (2012) |
| EW           | 153.6 ± 1.0                  | PRD 88 053005 (2013)  |
| HVP (LO)     | 6931 ± 34                    | EPJ C 77 827 (2017)   |
| HVP (LO)     | 6933 ± 25                    | PRD 97 114025 (2018)  |
|              |                              |                       |
|              |                              |                       |
|              |                              |                       |
|              |                              |                       |
|              |                              |                       |
|              |                              |                       |

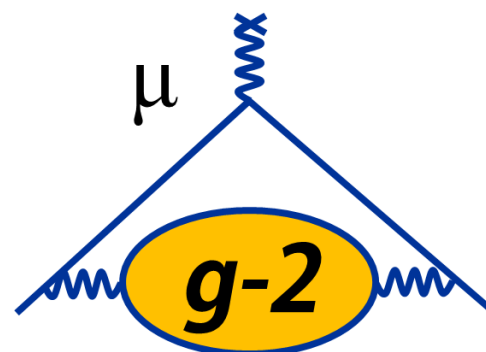
## HVP (LO): Lowest-Order Hadronic Vacuum Polarization

- **Critical input** from e<sup>+</sup>e<sup>-</sup> colliders (data from SND, CMD3, BaBar, KLOE, Belle, BESIII), extensive physics program running to reduce  $\delta a_\mu^{\text{HVP}}$  to ~ 0.3% in coming years
- **Progress on the lattice**: Calculations at physical  $\pi$  mass; approaching goal of  $\delta a_\mu^{\text{HVP}} \sim 1\%$  (cross-check with e<sup>+</sup>e<sup>-</sup> data)

$$a_\mu^{\text{had;LO}} = \left( \frac{\alpha m_\mu}{3\pi} \right)^2 \int_{m_\pi^2}^\infty \frac{ds}{s^2} K(s) R(s)$$

$$R \equiv \frac{\sigma_{\text{tot}}(e^+e^- \rightarrow \text{hadrons})}{\sigma(e^+e^- \rightarrow \mu^+\mu^-)}$$

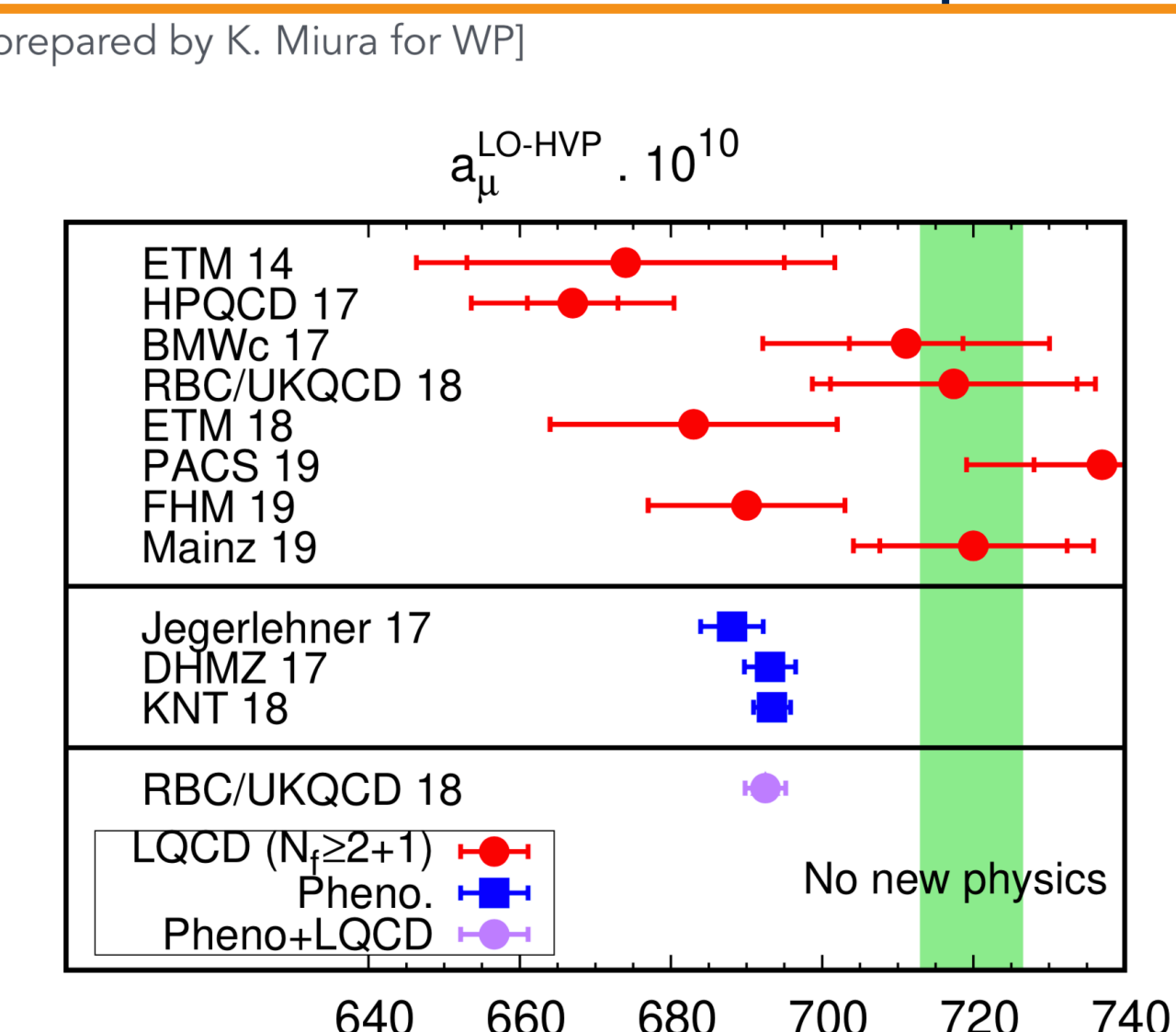
# $a_\mu$ Theoretical Status



| Contribution | Value (x 10 <sup>-11</sup> ) | Reference  |
|--------------|------------------------------|--|
| QED          | 116 584 718.95 ± 0.08        | PRL 109 111808 (2012)  |
| EW           | 153.6 ± 1.0                  | PRD 88 053005 (2013)   |
| HVP (LO)     | 6931 ± 34                    | EPJ C 77 827 (2017)  |
| HVP (LO)     | 6933 ± 25                    | PRD 97 114025 (2018)   |
|              |                              | [prepared by K. Miura for WP]  |
|              |                              | $a_\mu^{\text{LO-HVP}} \cdot 10^{10}$  |
|              |                              | ETM 14<br>HPQCD 17<br>BMWc 17<br>RBC/UKQCD 18<br>ETM 18<br>PACS 19<br>FHM 19<br>Mainz 19 |
|              |                              | Jegerlehner 17<br>DHMZ 17<br>KNT 18  |
|              |                              | RBC/UKQCD 18   |
|              |                              | LQCD ( $N_f \geq 2+1$ )<br>Pheno.<br>Pheno+LQCD  |
|              |                              | No new physics   |

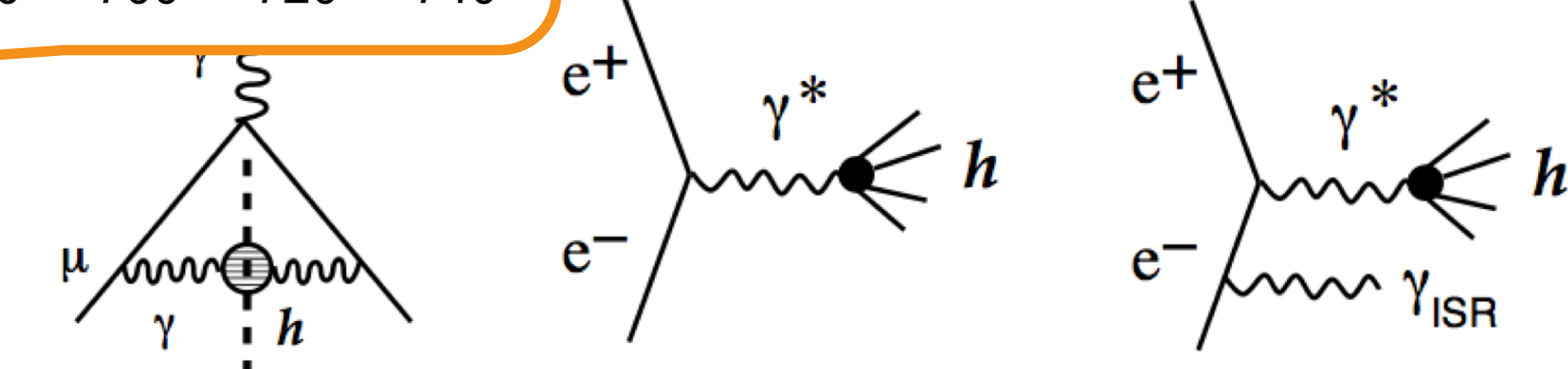
## HVP (LO): Lowest-Order Hadronic Value

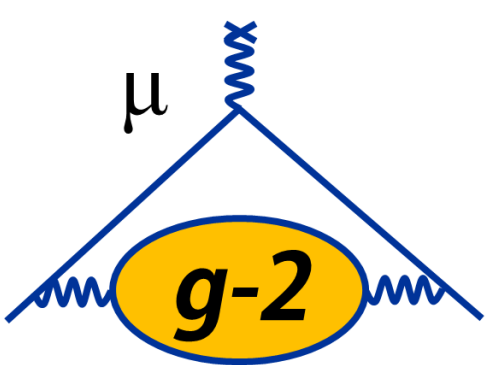
- Critical input** from  $e^+e^-$  colliders (data from SLAC, BaBar, KLOE, Belle, BESIII), extensive physics running to reduce  $\delta a_\mu^{\text{HVP}}$  to  $\sim 0.3\%$  in coming years
- Progress on the lattice**: Calculations at physical  $\pi$  mass; approaching goal of  $\delta a_\mu^{\text{HVP}} \sim 1\%$  (cross-check with  $e^+e^-$  data)



$$= \left( \frac{\alpha m_\mu}{3\pi} \right)^2 \int_{m_\pi^2}^{\infty} \frac{ds}{s^2} K(s) R(s)$$

$$R \equiv \frac{\sigma_{\text{tot}}(e^+e^- \rightarrow \text{hadrons})}{\sigma(e^+e^- \rightarrow \mu^+\mu^-)}$$





# $a_\mu$ Theoretical Status

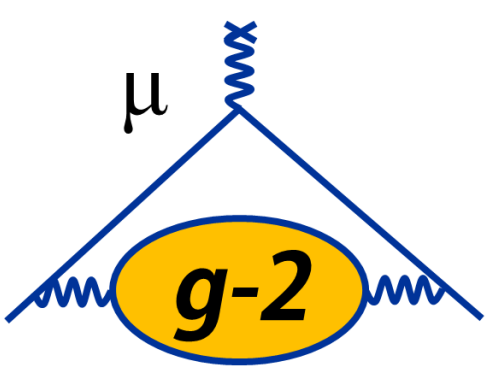
| Contribution      | Value (x 10 <sup>-11</sup> ) | Reference                    |
|-------------------|------------------------------|------------------------------|
| <b>QED</b>        | <b>116 584 718.95 ± 0.08</b> | PRL <b>109</b> 111808 (2012) |
| <b>EW</b>         | <b>153.6 ± 1.0</b>           | PRD <b>88</b> 053005 (2013)  |
| <b>HVP (LO)</b>   | <b>6931 ± 34</b>             | EPJ C <b>77</b> 827 (2017)   |
| <b>HVP (LO)</b>   | <b>6933 ± 25</b>             | PRD <b>97</b> 114025 (2018)  |
| <b>HVP (NLO)</b>  | <b>-98.7 ± 0.7</b>           | EPJ C <b>77</b> 827 (2017)   |
| <b>HVP (NLO)</b>  | <b>-98.2 ± 0.4</b>           | PRD <b>97</b> 114025 (2018)  |
| <b>HVP (NNLO)</b> | <b>12.4 ± 0.1</b>            | PLB <b>734</b> 144 (2014)    |
|                   |                              |                              |
|                   |                              |                              |

## HVP (LO): Lowest-Order Hadronic Vacuum Polarization

- **Critical input** from  $e^+e^-$  colliders (data from SND, CMD3, BaBar, KLOE, Belle, BESIII), extensive physics program running to reduce  $\delta a_\mu^{\text{HVP}}$  to  $\sim 0.3\%$  in coming years
- **Progress on the lattice**: Calculations at physical  $\pi$  mass; approaching goal of  $\delta a_\mu^{\text{HVP}} \sim 1\%$  (cross-check with  $e^+e^-$  data)

$$a_\mu^{\text{had;LO}} = \left( \frac{\alpha m_\mu}{3\pi} \right)^2 \int_{m_\pi^2}^\infty \frac{ds}{s^2} K(s) R(s)$$

$$R \equiv \frac{\sigma_{\text{tot}}(e^+e^- \rightarrow \text{hadrons})}{\sigma(e^+e^- \rightarrow \mu^+\mu^-)}$$



# $a_\mu$ Theoretical Status

New *ab initio* approaches [PRD **98** 094503 (2018)]  
finding consistent result of  $(-93 \pm 13) \times 10^{-11}$  —  
**lattice making big strides**

|            |                    | 2012)                       |
|------------|--------------------|-----------------------------|
| HVP (NLO)  | <b>-98.7 ± 0.7</b> | EPJ C <b>77</b> 827 (2017)  |
| HVP (NLO)  | <b>-98.2 ± 0.4</b> | PRD <b>97</b> 114025 (2018) |
| HVP (NNLO) | <b>12.4 ± 0.1</b>  | PLB <b>734</b> 144 (2014)   |
|            |                    |                             |
|            |                    |                             |

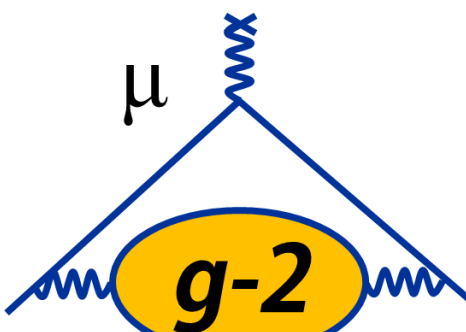
## HVP (LO): Lowest-Order Hadronic Vacuum Polarization

- **Critical input** from  $e^+e^-$  colliders (data from SND, CMD3, BaBar, KLOE, Belle, BESIII), extensive physics program running to reduce  $\delta a_\mu^{\text{HVP}}$  to  $\sim 0.3\%$  in coming years
- **Progress on the lattice:** Calculations at physical  $\pi$  mass; approaching goal of  $\delta a_\mu^{\text{HVP}} \sim 1\%$  (cross-check with  $e^+e^-$  data)

$$a_\mu^{\text{had;LO}} = \left( \frac{\alpha m_\mu}{3\pi} \right)^2 \int_{m_\pi^2}^\infty \frac{ds}{s^2} K(s) R(s)$$

$$R \equiv \frac{\sigma_{\text{tot}}(e^+e^- \rightarrow \text{hadrons})}{\sigma(e^+e^- \rightarrow \mu^+\mu^-)}$$

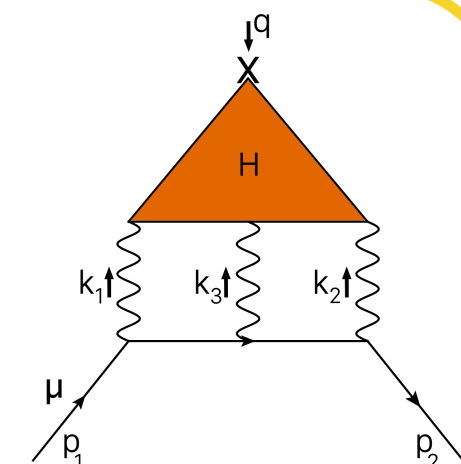
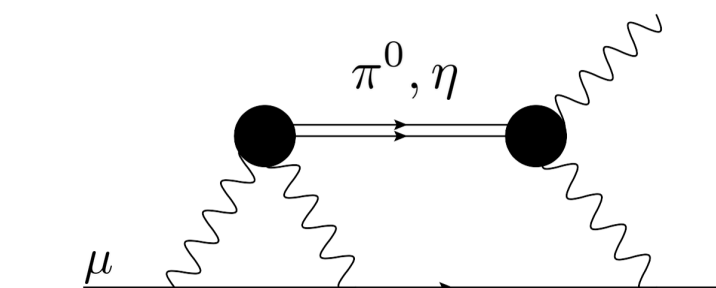
# $a_\mu$ Theoretical Status



New *ab initio* approaches [PRD **98** 094503 (2018)]  
finding consistent result of  $(-93 \pm 13) \times 10^{-11}$  —  
**lattice making big strides**

| HVP (LO)        | <b>-98.7 ± 0.7</b>   | EPJ C <b>77</b> 827 (2017)  |
|-----------------|--|---|
| HVP (NLO)       | <b>-98.2 ± 0.4</b>   | PRD <b>97</b> 114025 (2018)                                       |
| HVP (NNLO)      | <b>12.4 ± 0.1</b>  | PLB <b>734</b> 144 (2014)   |
| HLbL (LO + NLO) | <b>101 ± 26</b>  | PLB <b>735</b> 90 (2014),<br>EPJ Web Conf <b>118</b> 01016 (2016) |
| Total SM        | <b>116 591 818 ± 43 (368 ppb)</b><br><b>116 591 821 ± 36 (309 ppb)</b> |   |

## HLbL: Hadronic Light-by-Light



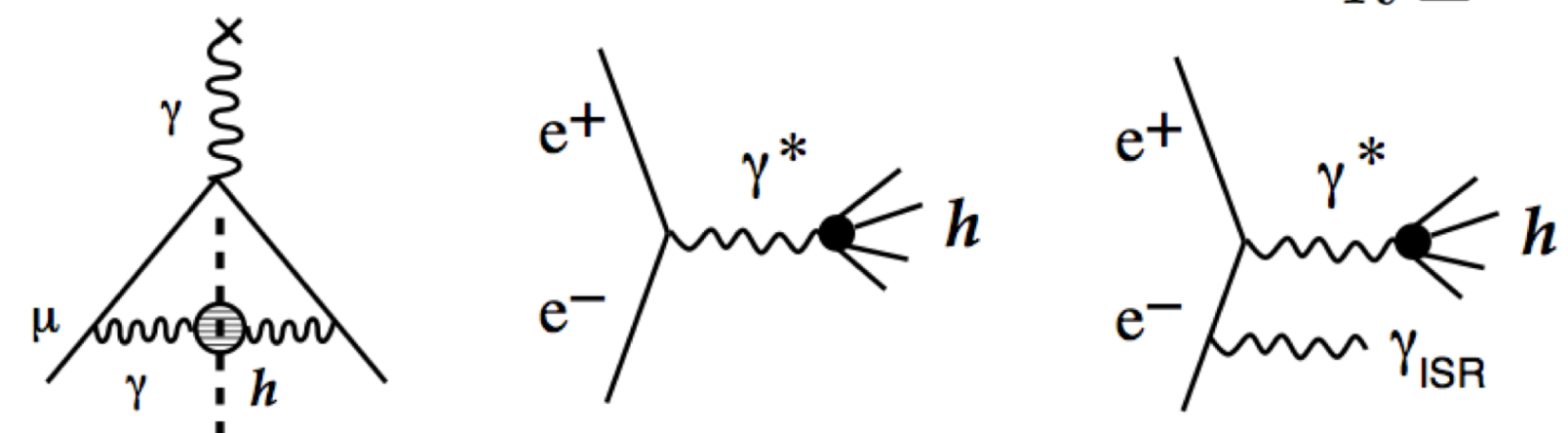
- Model dependent: based on xPT + short-distance constraints (operator product expansion)
- Difficult to relate to data like HVP (LO);  $\gamma^*$  physics,  $\pi^0$  data (BESIII, KLOE) important for constraining models
- **Theory Progress:** New dispersive calculation approach; extend the lattice (finite volume, disconnected diagrams); Blum et al. making excellent progress

## HVP (LO): Lowest-Order Hadronic Vacuum Polarization

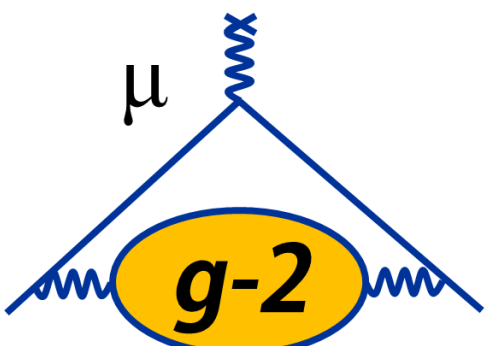
- **Critical input** from  $e^+e^-$  colliders (data from SND, CMD3, BaBar, KLOE, Belle, BESIII), extensive physics program running to reduce  $\delta a_\mu^{\text{HVP}}$  to  $\sim 0.3\%$  in coming years
- **Progress on the lattice:** Calculations at physical  $\pi$  mass; approaching goal of  $\delta a_\mu^{\text{HVP}} \sim 1\%$  (cross-check with  $e^+e^-$  data)

$$a_\mu^{\text{had;LO}} = \left( \frac{\alpha m_\mu}{3\pi} \right)^2 \int_{m_\pi^2}^{\infty} \frac{ds}{s^2} K(s) R(s)$$

$$R \equiv \frac{\sigma_{\text{tot}}(e^+e^- \rightarrow \text{hadrons})}{\sigma(e^+e^- \rightarrow \mu^+\mu^-)}$$



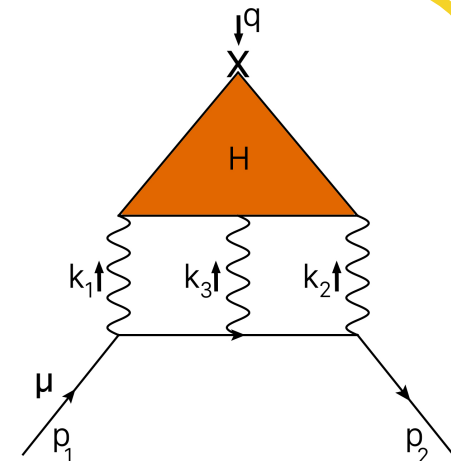
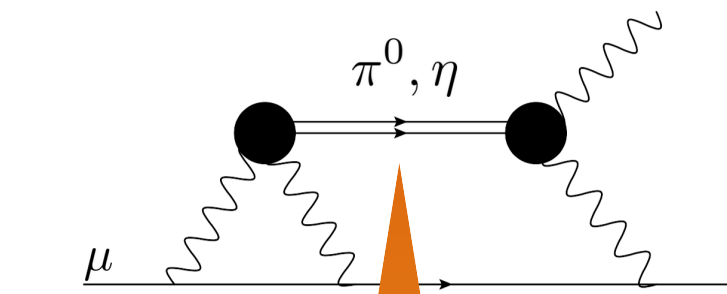
# $a_\mu$ Theoretical Status



New *ab initio* approaches [PRD **98** 094503 (2018)]  
finding consistent result of  $(-93 \pm 13) \times 10^{-11}$  —  
**lattice making big strides**

| HVP (LO)        | <b>-98.7 ± 0.7</b>   | EPJ C <b>77</b> 827 (2017)  |
|-----------------|--|---|
| HVP (NLO)       | <b>-98.2 ± 0.4</b>   | PRD <b>97</b> 114025 (2018)                                       |
| HVP (NNLO)      | $12.4 \pm 0.1$   | PLB <b>734</b> 144 (2014)   |
| HLbL (LO + NLO) | $101 \pm 26$   | PLB <b>735</b> 90 (2014),<br>EPJ Web Conf <b>118</b> 01016 (2016) |
| Total SM        | <b><math>116\,591\,818 \pm 43</math> (368 ppb)</b><br><b><math>116\,591\,821 \pm 36</math> (309 ppb)</b> |   |

## HLbL: Hadronic Light-by-Light



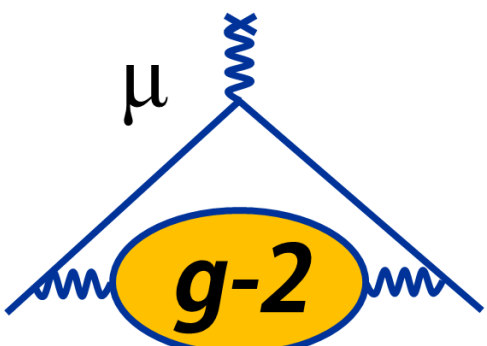
- Model dependence: based on xPT + short-distance constraints (operator product expansion)
- Difficult to relate to data like HVP (LO);  $\gamma^*$  physics,  $\pi^0$  data (BESIII, KLOE) important for constraining models
- **Theory Progress:** new dispersive calculation approach; extend the lattice (finite volume, disconnected diagrams); Blum et al. report excellent progress

## HVP (LO): Lowest-Order Hadronic Contribution

- **Critical input** from  $e^+e^-$  colliders (BaBar, KLOE, Belle, BESIII), running to reduce  $\delta a_\mu^{\text{HVP}}$  to  $\sim 10$  ppb
- **Progress on the lattice:** Calculations approaching goal of  $\delta a_\mu^{\text{HVP}} < 10$  ppb

Recent lattice & data-driven estimate [PRD **100** 034520 (2019)]  
for  $a_\mu^{\pi^0\text{-pole}}$  is consistent with lowest-meson dominance, +  
vector phenomenological models [PRD **51** 4939 (2005), PRL **83**  
5230 (1999), EJC **21** 659 (2001), PRD **65** 073034 (2002), PRD  
**94** 053006 (2016), EJC **75** 586 (2015)]

# $a_\mu$ Theoretical Status



New *ab initio* approaches [PRD **98** 094503 (2018)]  
finding consistent result of  $(-93 \pm 13) \times 10^{-11}$  —  
**lattice making big strides**

| HVP (NLO)       | <b>-98.7 ± 0.7</b>                      | EPJ C <b>77</b> 827 (2017)  | PRD <b>98</b> 094503 (2018) |
|-----------------|---|-----------------------------|-----------------------------|
| HVP (NLO)       | <b>-98.2 ± 0.4</b>                      | PRD <b>97</b> 114025 (2018) |                             |
| HVP (NNLO)      | $12.4 \pm 0.1$                          |                             |                             |
| HLbL (LO + NLO) | $101 \pm 26$                            |                             |                             |
|                 | <b><math>91.818 \pm 43</math> (368)</b> |                             |                             |
|                 | <b><math>91.821 \pm 36</math> (309)</b> |                             |                             |

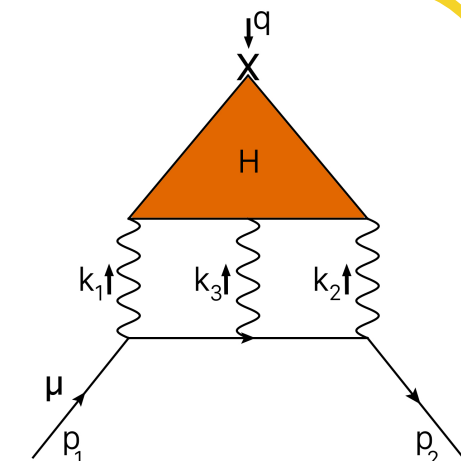
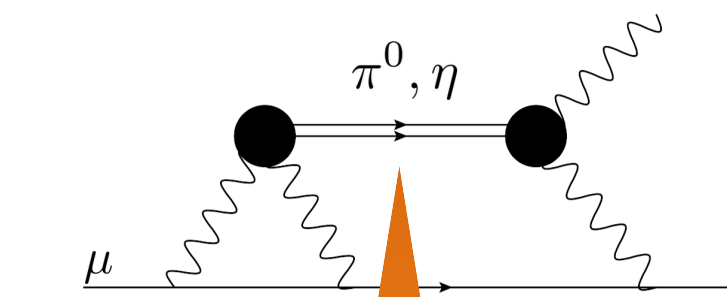
Builds confidence  
in HLbL term

See T. Blum's talk for  
updates on the lattice

- Critical input** from  $e^+e^-$  colliders (BaBar, KLOE, Belle, BESIII), + running to reduce  $\delta a_\mu^{\text{HVP}}$  to  $\sim 1\%$
- Progress on the lattice:** Calculations approaching goal of  $\delta a_\mu^{\text{HVP}} < 1\%$

Recent lattice & data-driven estimate [PRD **100** 034520 (2019)]  
for  $a_\mu^{\pi^0\text{-pole}}$  is consistent with lowest-meson dominance, +  
vector phenomenological models [PRD **51** 4939 (2005), PRL **83**  
5230 (1999), EJC **21** 659 (2001), PRD **65** 073034 (2002), PRD  
**94** 053006 (2016), EJC **75** 586 (2015)]

## HLbL: Hadronic Light-by-Light



- Model dependence: based on xPT + short-distance constraints (operator product expansion)
- Difficult to relate to other data like HVP (LO);  $\gamma^*$  physics,  $\pi^0$  data (BESIII, KLOE) important for constraining models
- Theory Progress:** New dispersive calculation approach; extend the lattice (finite volume, disconnected diagrams); Blum et al. report excellent progress

$$\frac{\sigma_{\text{tot}}(e^+e^- \rightarrow \text{hadrons})}{\sigma(e^+e^- \rightarrow \mu^+\mu^-)}$$

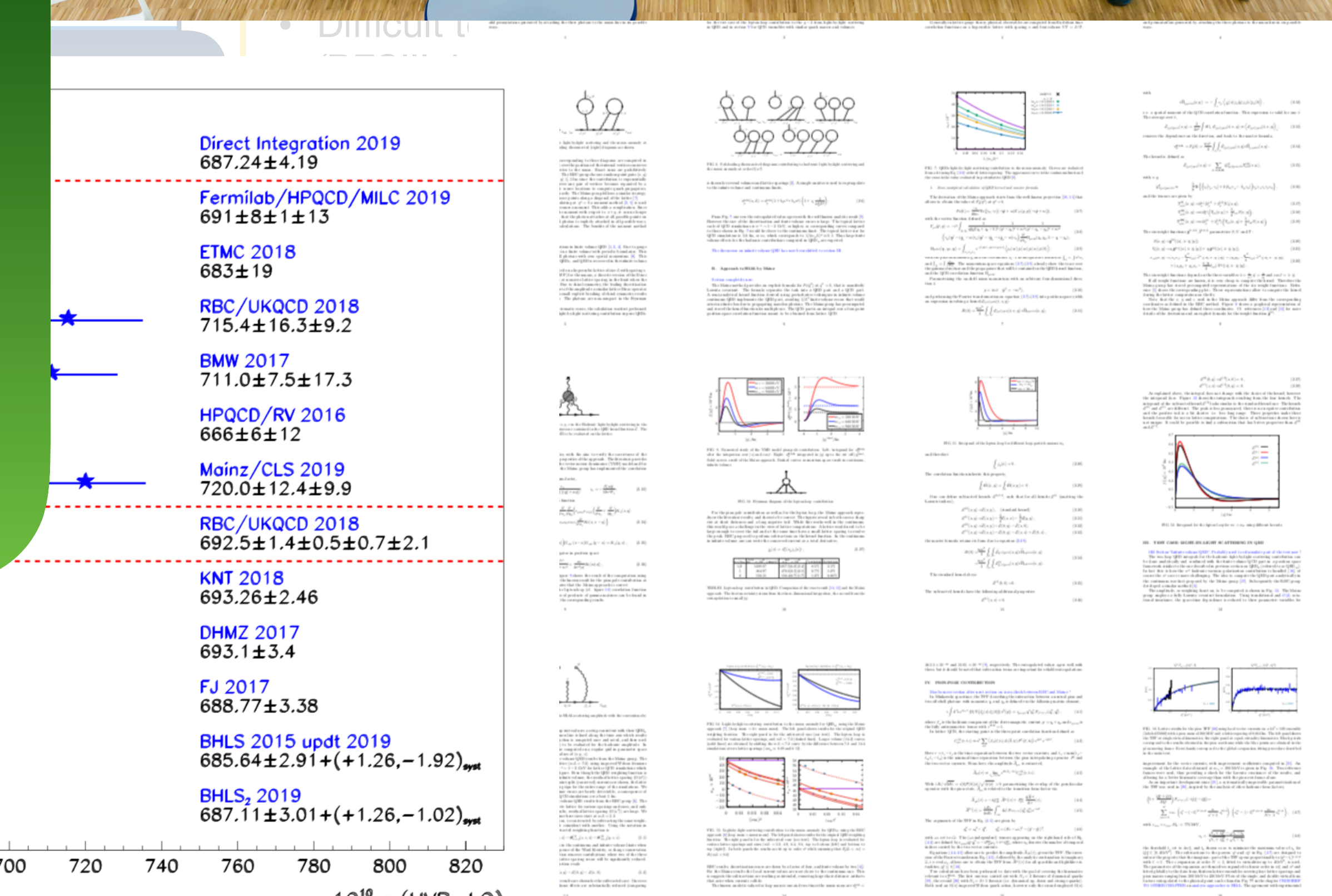
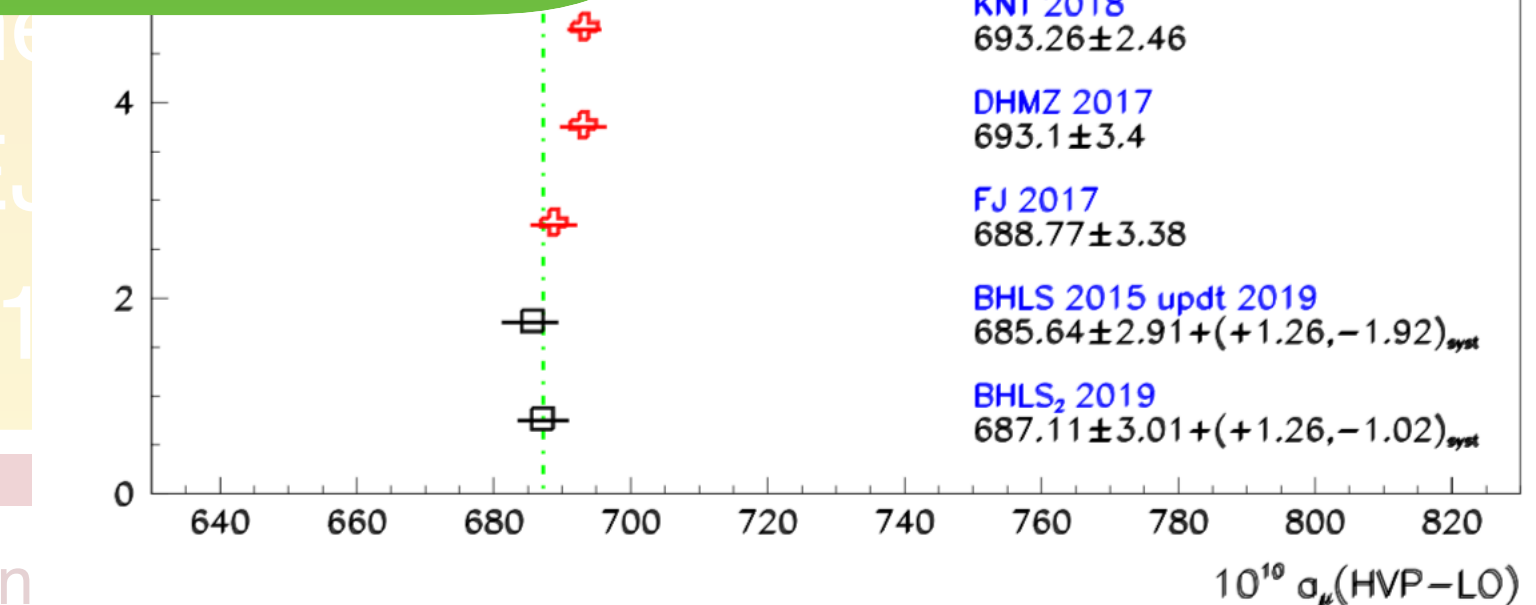
# $a_\mu$ Theoretical Status

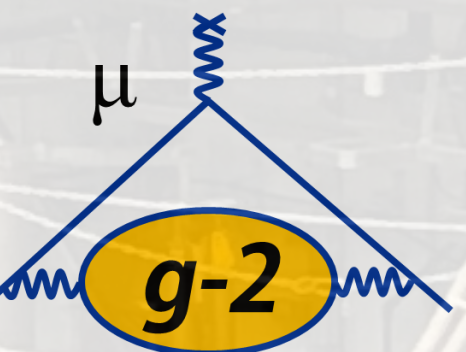
New *ab initio* approaches [PRD 98 094503 (2018)]  
finding consistent result of  $(-93 \pm 13) \times 10^{-11}$  —

- Theory groups are making steady progress to achieve competitive uncertainties on the same time scale as the FNAL experiment result
- White paper discussing all terms forthcoming



- Progress on the lattice: Calculations 5230 (1999), E94 053006 (2011) approaching goal of  $\delta a_\mu^{\text{HVP}}$

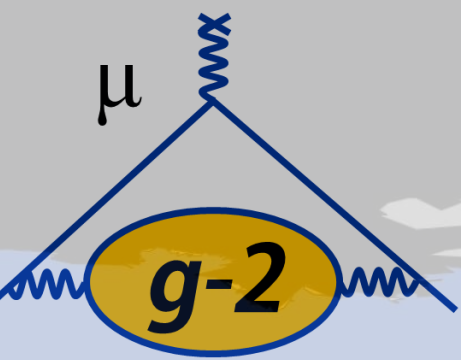




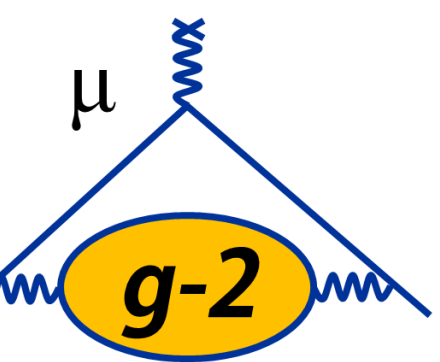
# The Muon g-2 Experiment at Fermilab

UMassAmherst

# Muon g-2: 33 Institutions, 7 countries, 203 Members



UMassAmherst

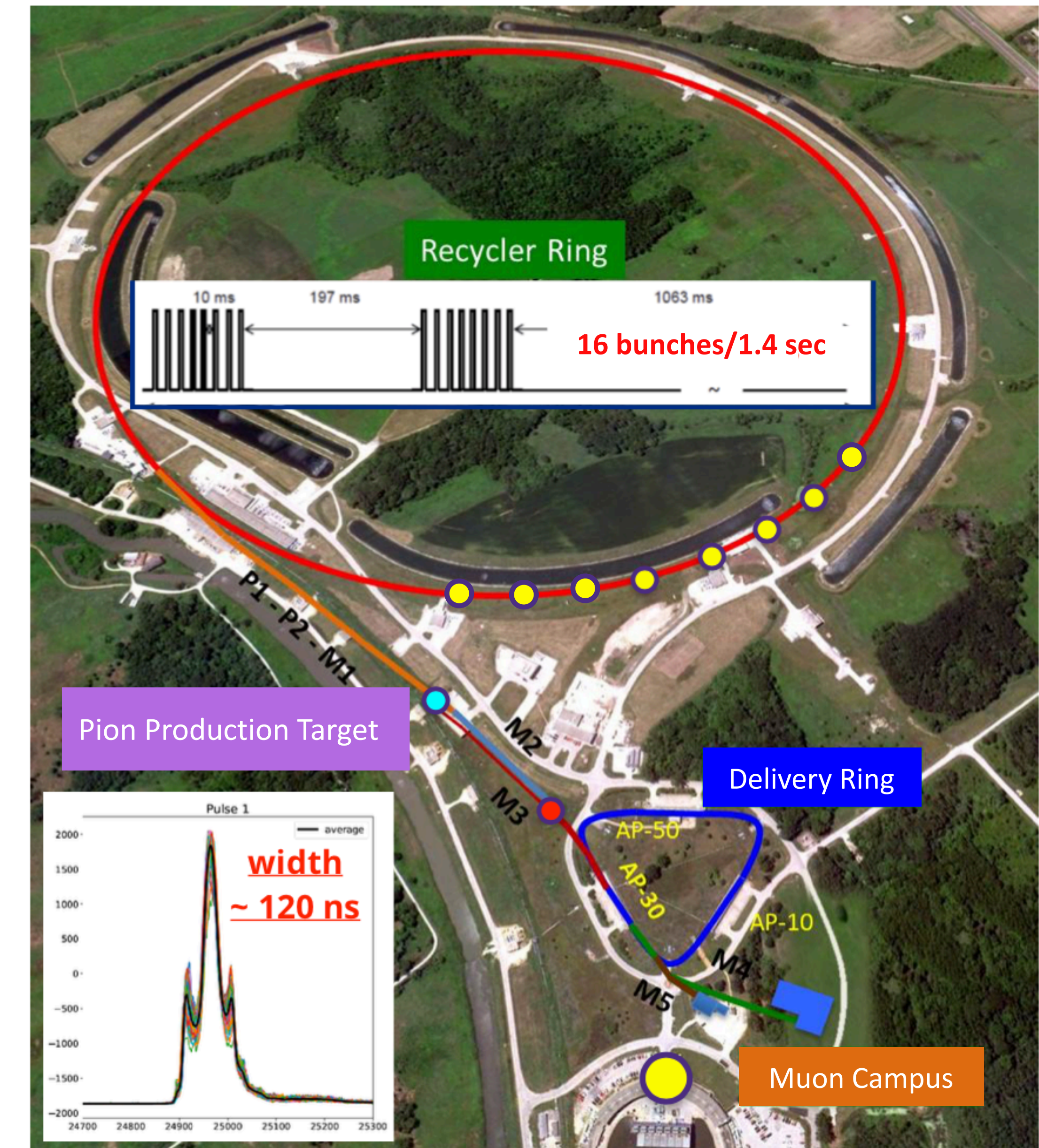


# Why Fermilab?

- BNL limited by statistics  
(540 ppb on  $9 \times 10^9$  detected  $e^+$ )
- E989 goal: Factor of 21 more statistics  
( $2 \times 10^{11}$  detected  $e^+$ )

## Fermilab advantages

- ✓ Long beam line to collect  $\pi^+ \rightarrow \mu^+$
- ✓ Much reduced amount of p,  $\pi$  in ring
- ✓ 4x higher fill frequency than BNL



UMassAmherst

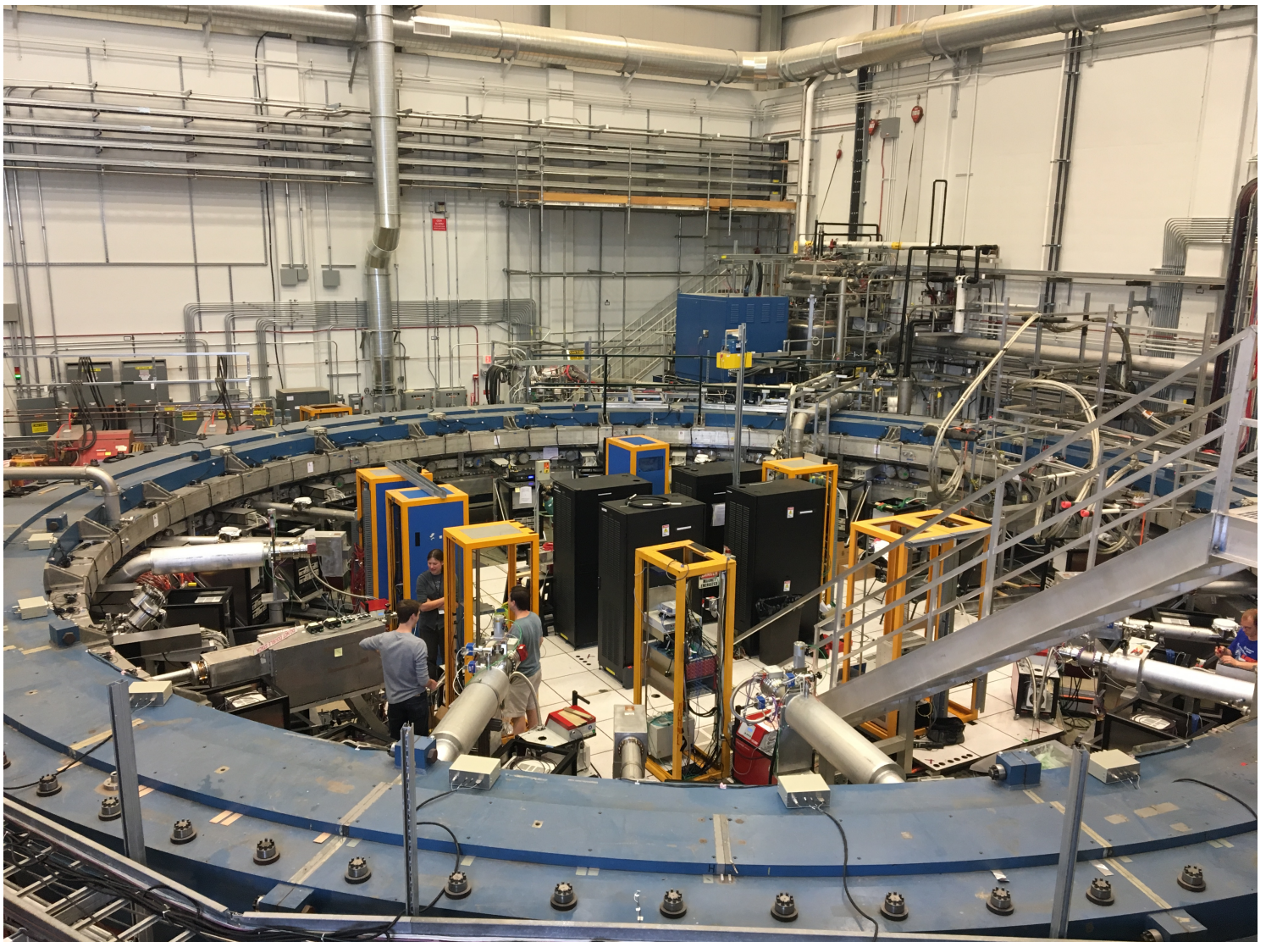
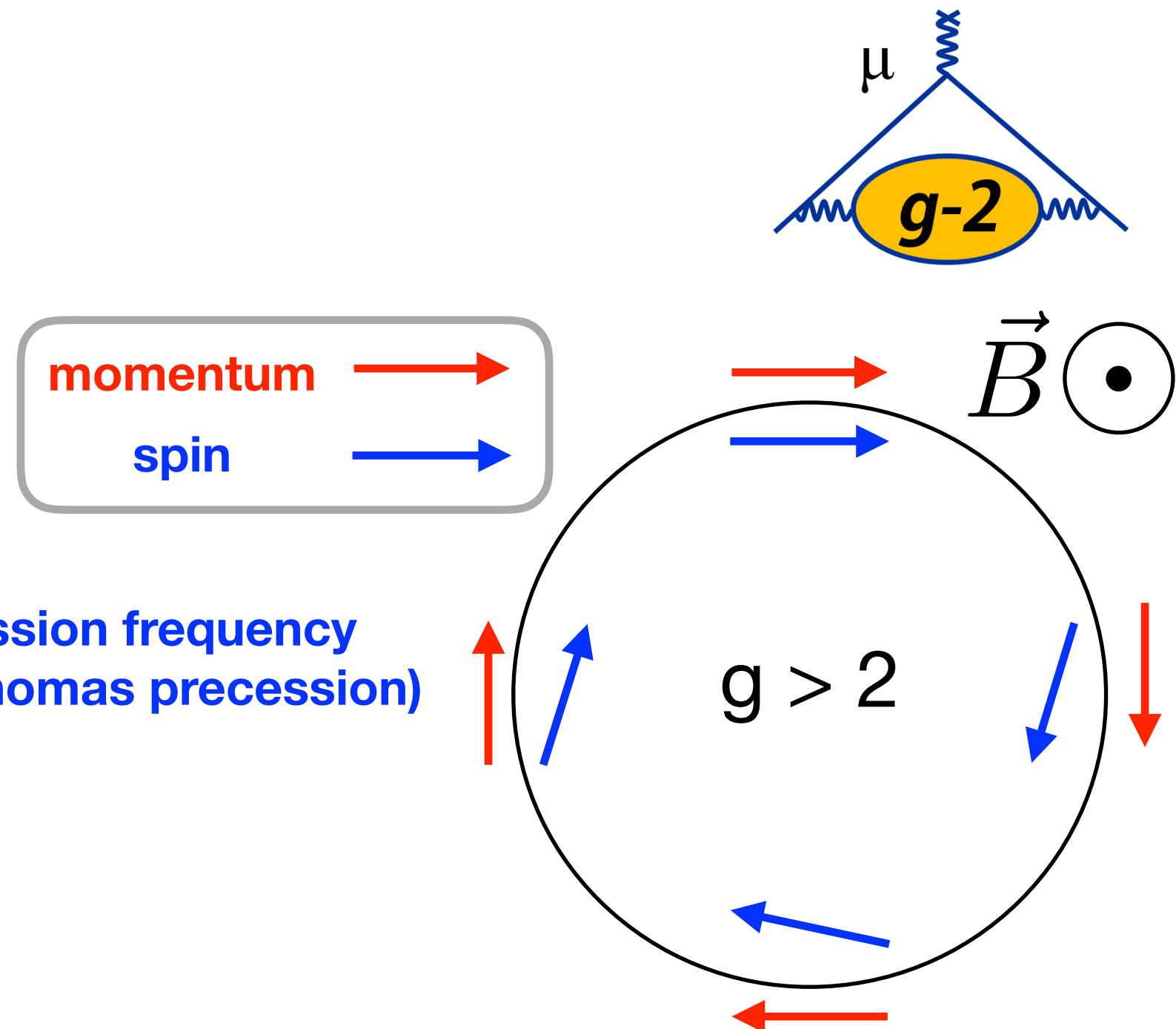
# Measuring the Muon Anomaly

- Inject polarized muon beam into magnetic storage ring
- Measure **difference** between spin precession and cyclotron frequencies
- If  $g = 2$ ,  $\omega_a = 0$
- $g \neq 2$ ,  $\omega_a \approx (e/m_\mu)a_\mu B$

$$\vec{\omega}_C = -\frac{e}{\gamma m} \vec{B} \quad \text{cyclotron frequency}$$

$$\vec{\omega}_S = -\frac{e}{\gamma m} \vec{B} (1 + \gamma a_\mu) \quad \text{spin precession frequency (Larmor, Thomas precession)}$$

$$\vec{\omega}_a \equiv \vec{\omega}_S - \vec{\omega}_C$$



UMassAmherst

# Measuring the Muon Anomaly

- Inject polarized muon beam into magnetic storage ring
- Measure **difference** between spin precession and cyclotron frequencies
- If  $g = 2$ ,  $\omega_a = 0$
- $g \neq 2$ ,  $\omega_a \approx (e/m_\mu)a_\mu B$
- Using  $\hbar\omega_p = 2\mu_p|\vec{B}|$ :

$$a_\mu = \frac{\omega_a}{\tilde{\omega}_p} \frac{\mu_p}{\mu_e} \frac{m_\mu}{m_e} \frac{g_e}{2}$$

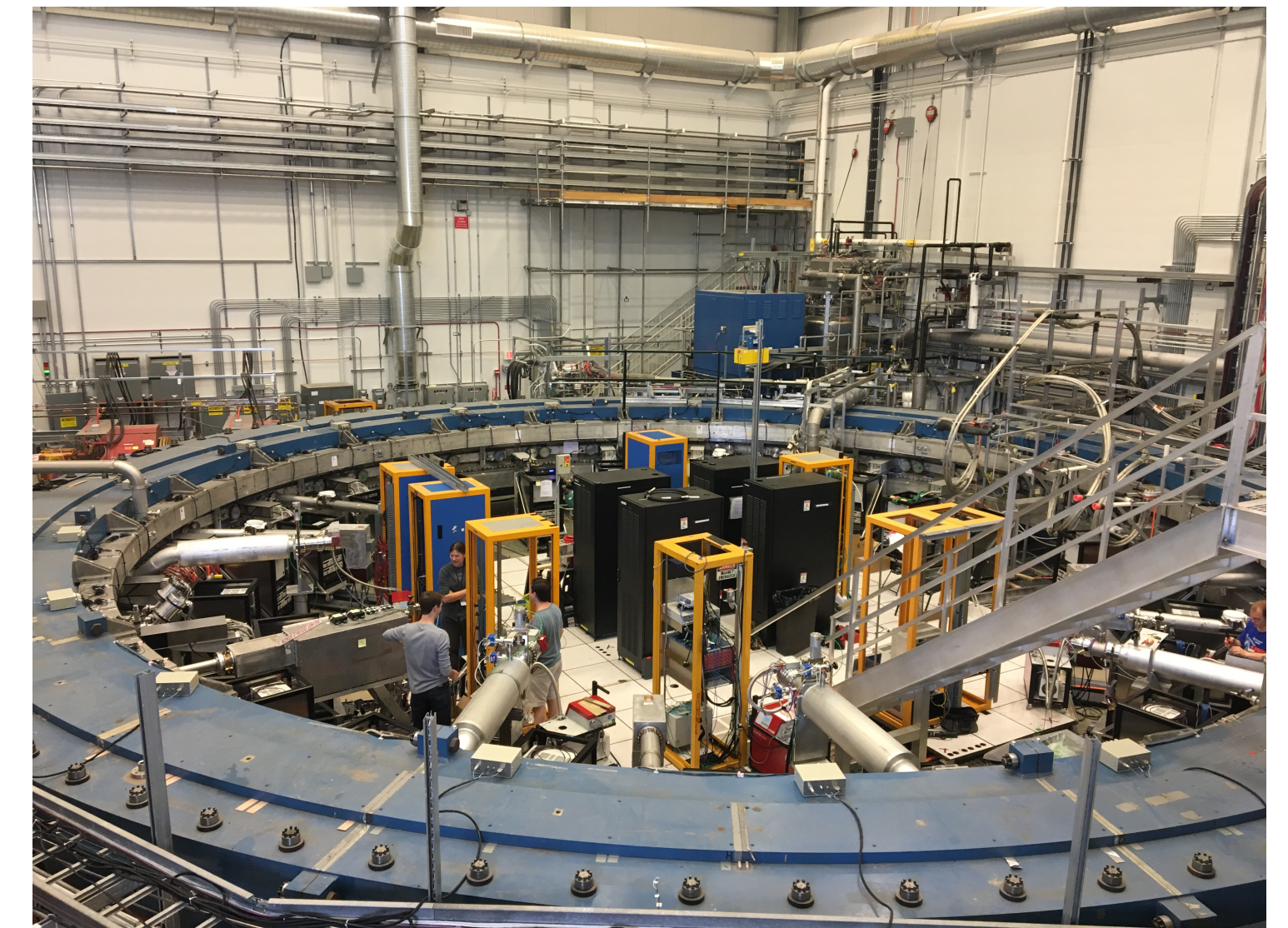
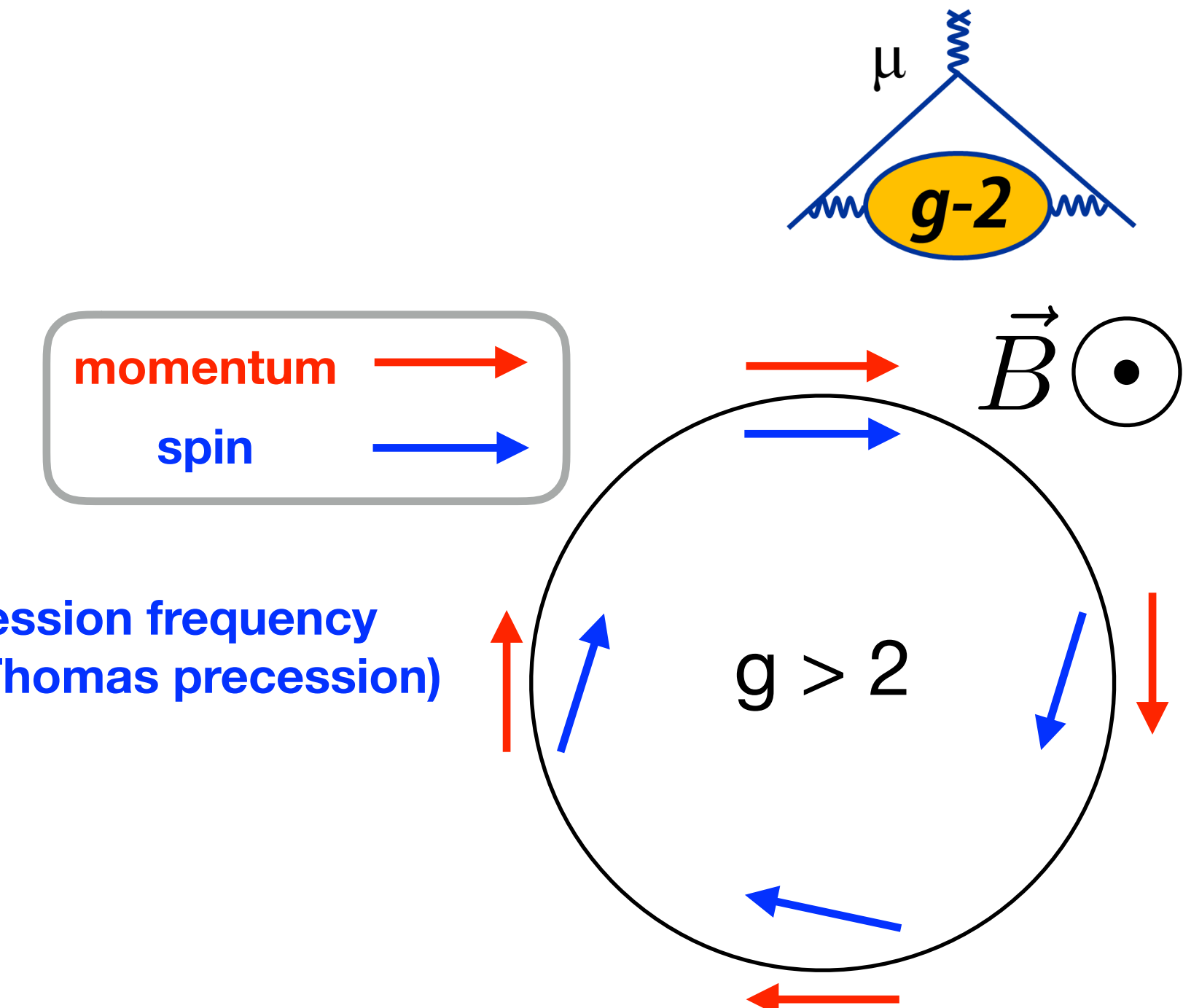
↑      ↑      ↑  
 3 ppb      22 ppb      0.3 ppt

Rev. Mod. Phys. 88, 035009 (2016)

$$\vec{\omega}_C = -\frac{e}{\gamma m} \vec{B} \quad \text{cyclotron frequency}$$

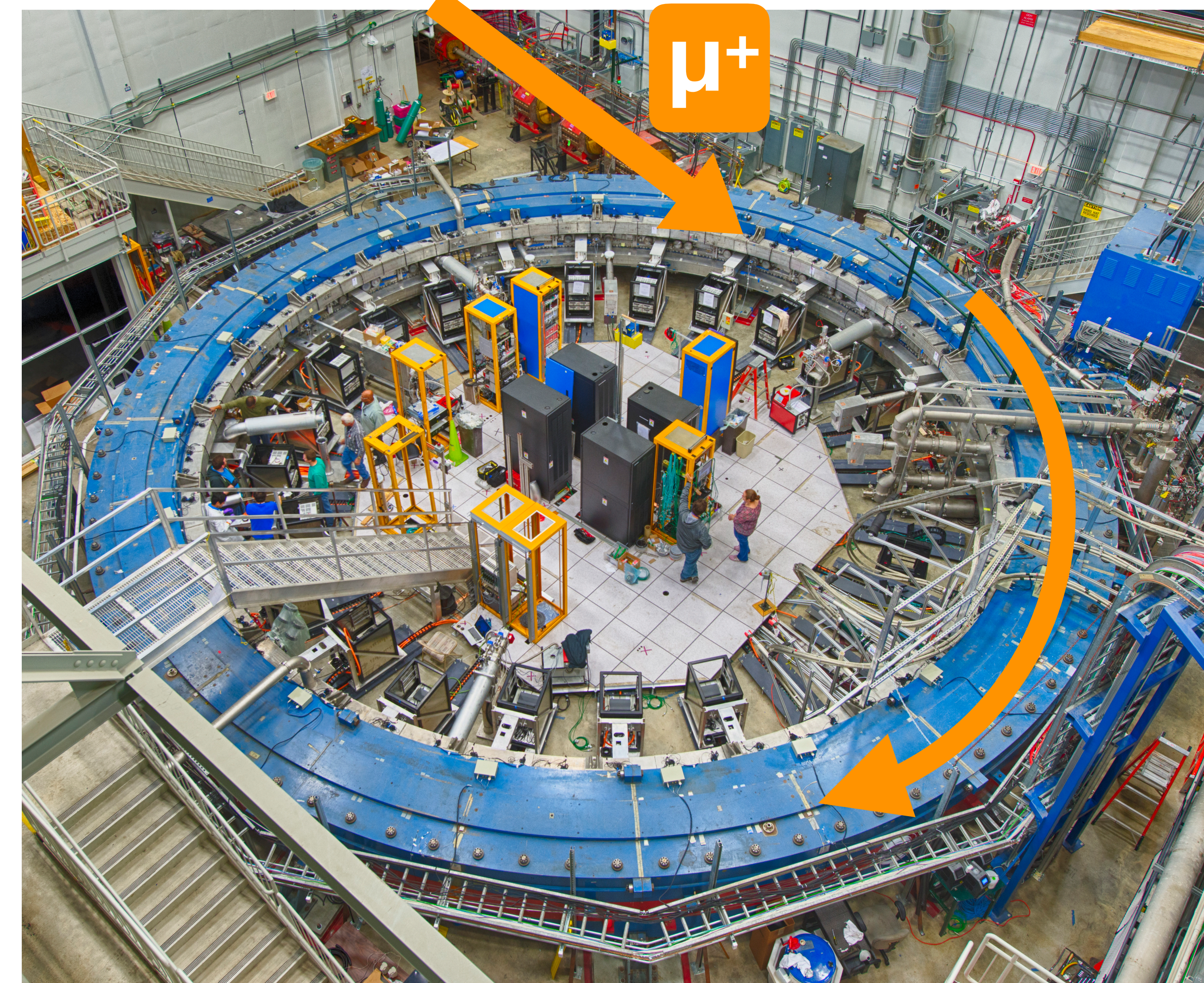
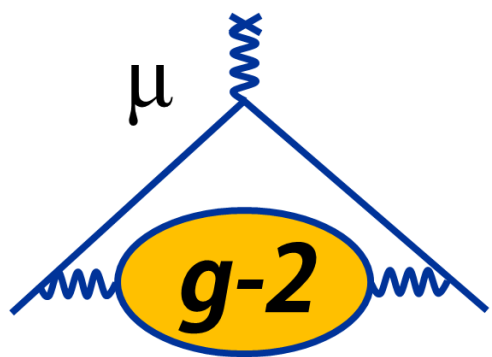
$$\vec{\omega}_S = -\frac{e}{\gamma m} \vec{B} (1 + \gamma a_\mu) \quad \text{spin precession frequency (Larmor, Thomas precession)}$$

$$\vec{\omega}_a \equiv \vec{\omega}_S - \vec{\omega}_C$$



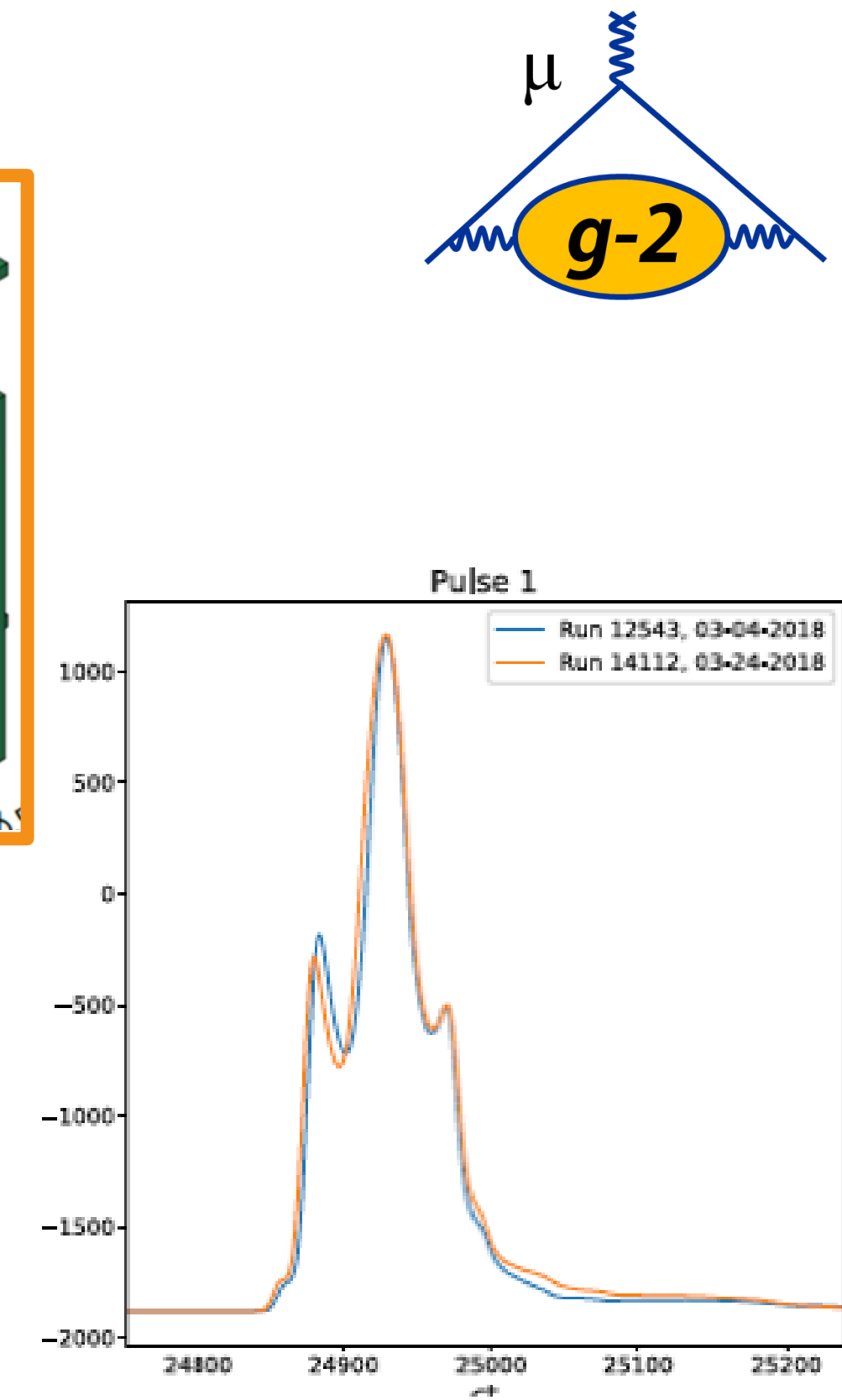
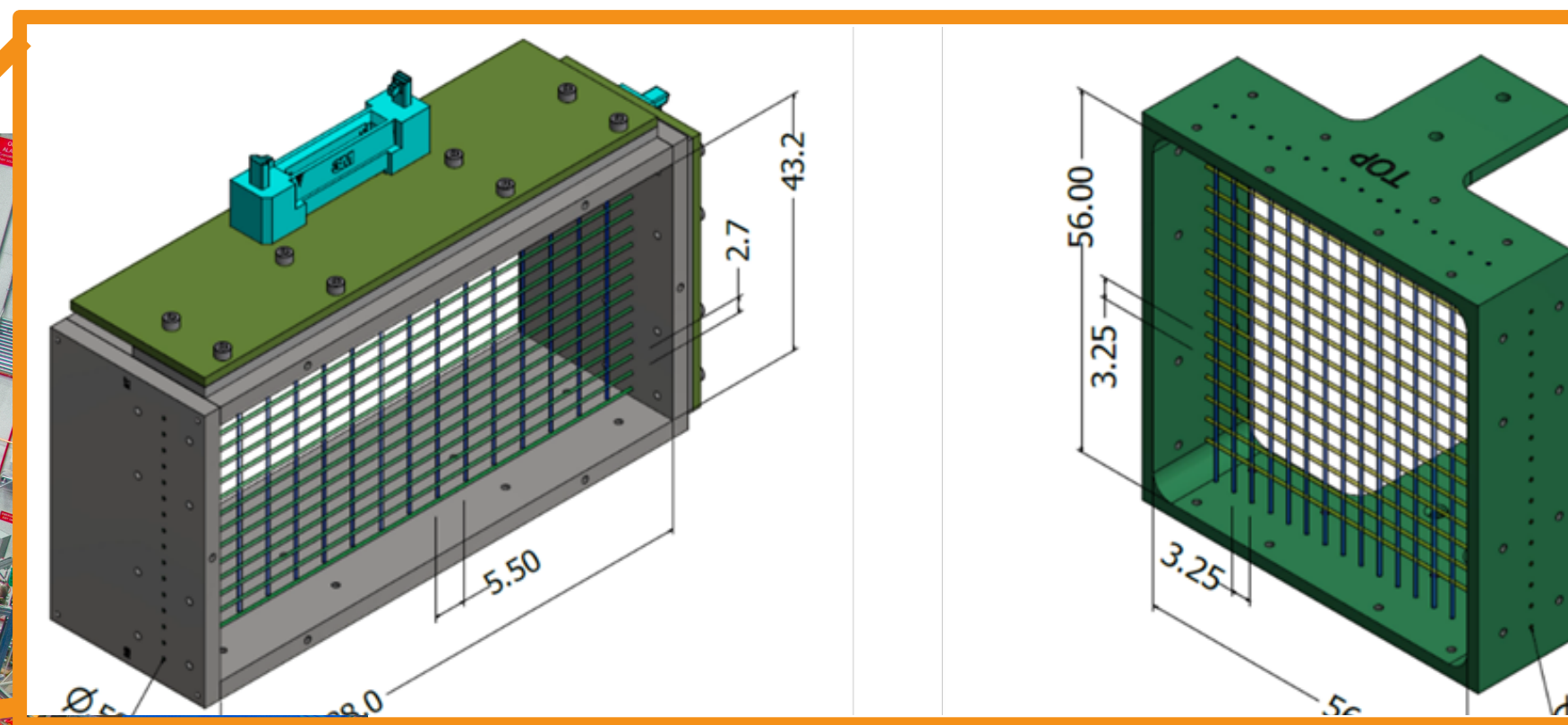
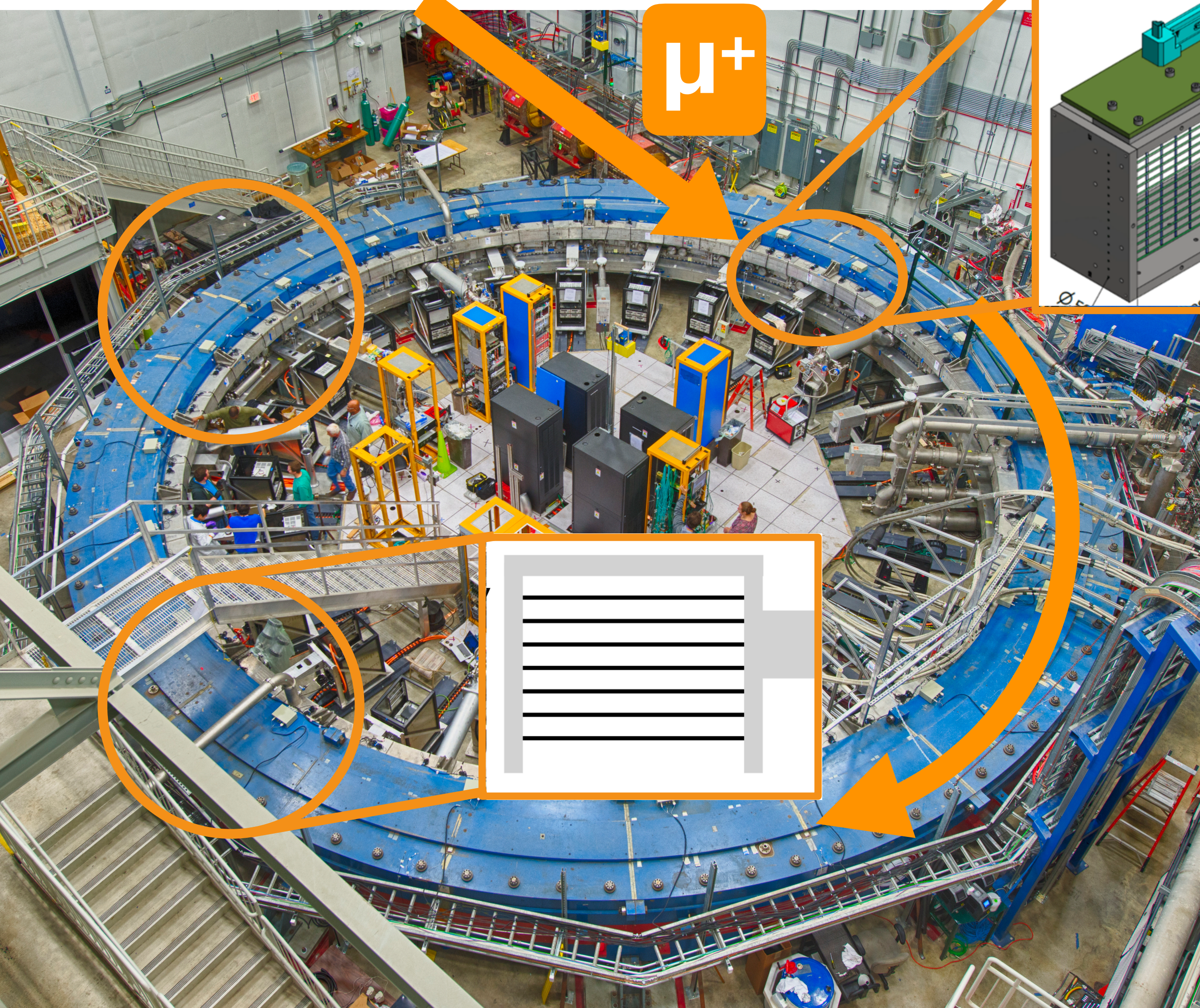
- We measure  $\omega_a$  and  $\omega_p$  separately
- Aiming for 70 ppb precision on each (systematic)
- **Target:  $\delta a_\mu = 140$  ppb; factor of 4 improvement over BNL**

# Muon Beam Injection



UMassAmherst

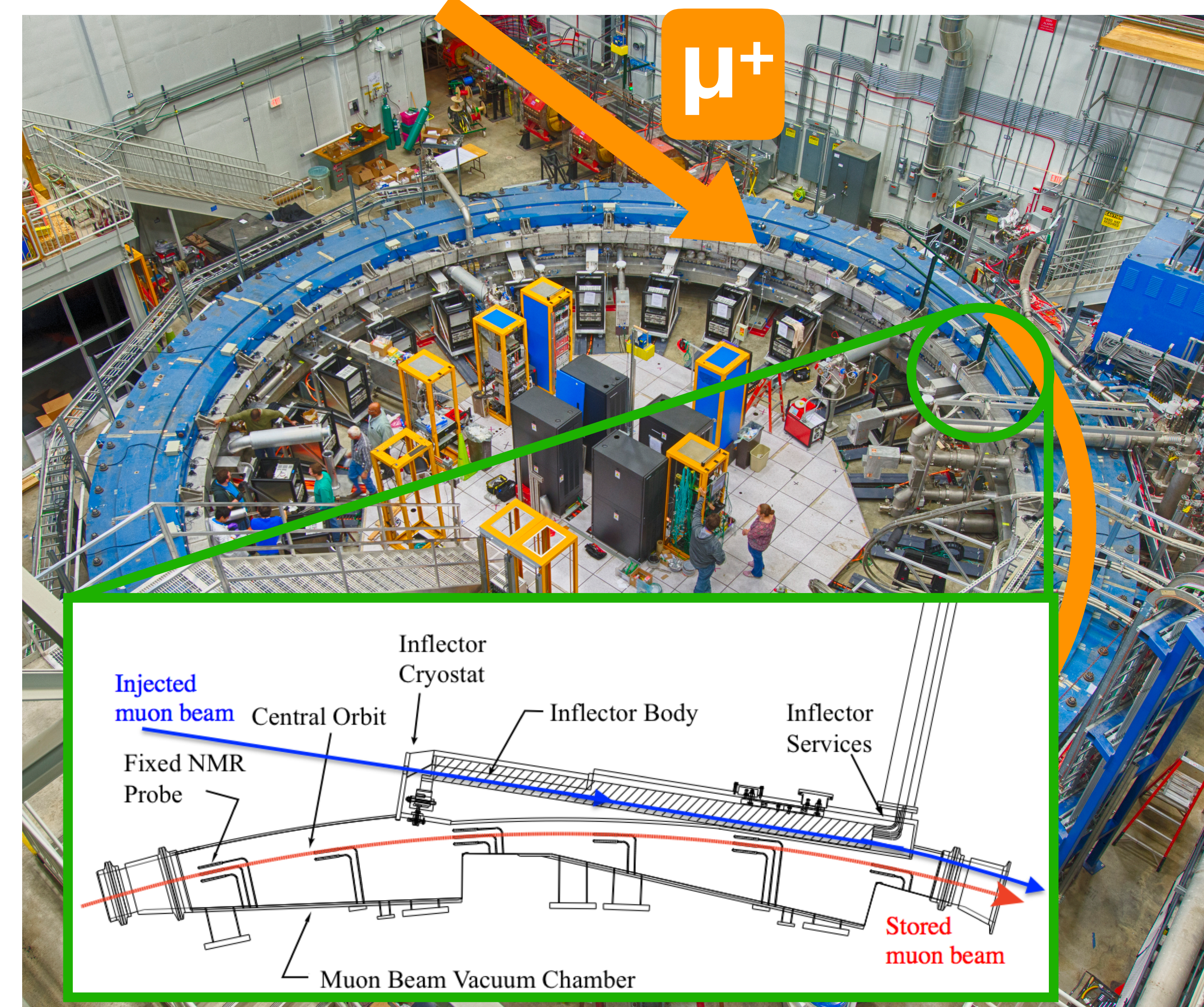
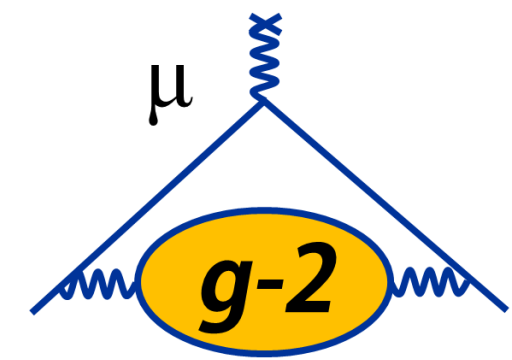
# Muon Beam Injection



## Monitoring the Incoming Muon Beam

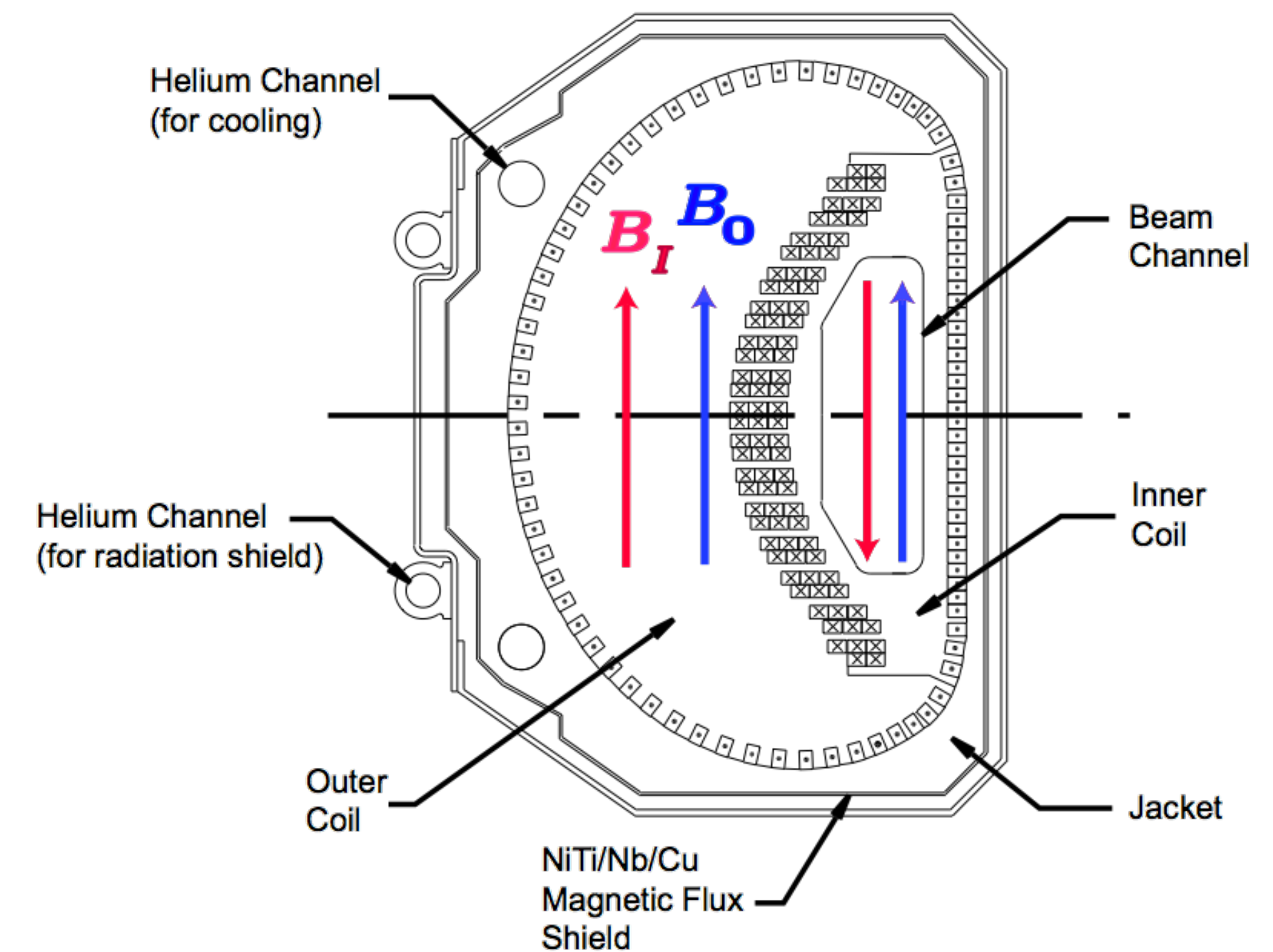
- **Scintillating Paddles:** Monitoring temporal distribution
- **Scintillating Fibers:** Map of transverse profile, guides  $\mu$  tuning into the ring

# Muon Beam Injection



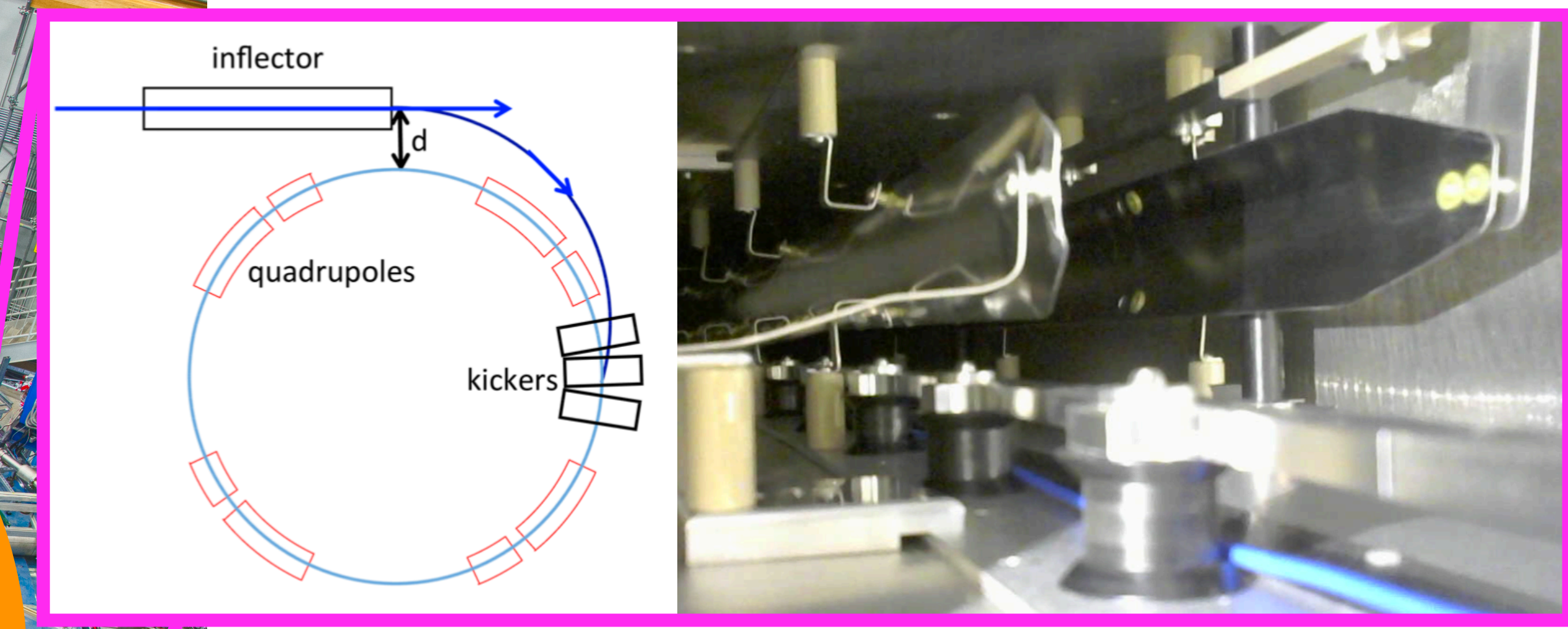
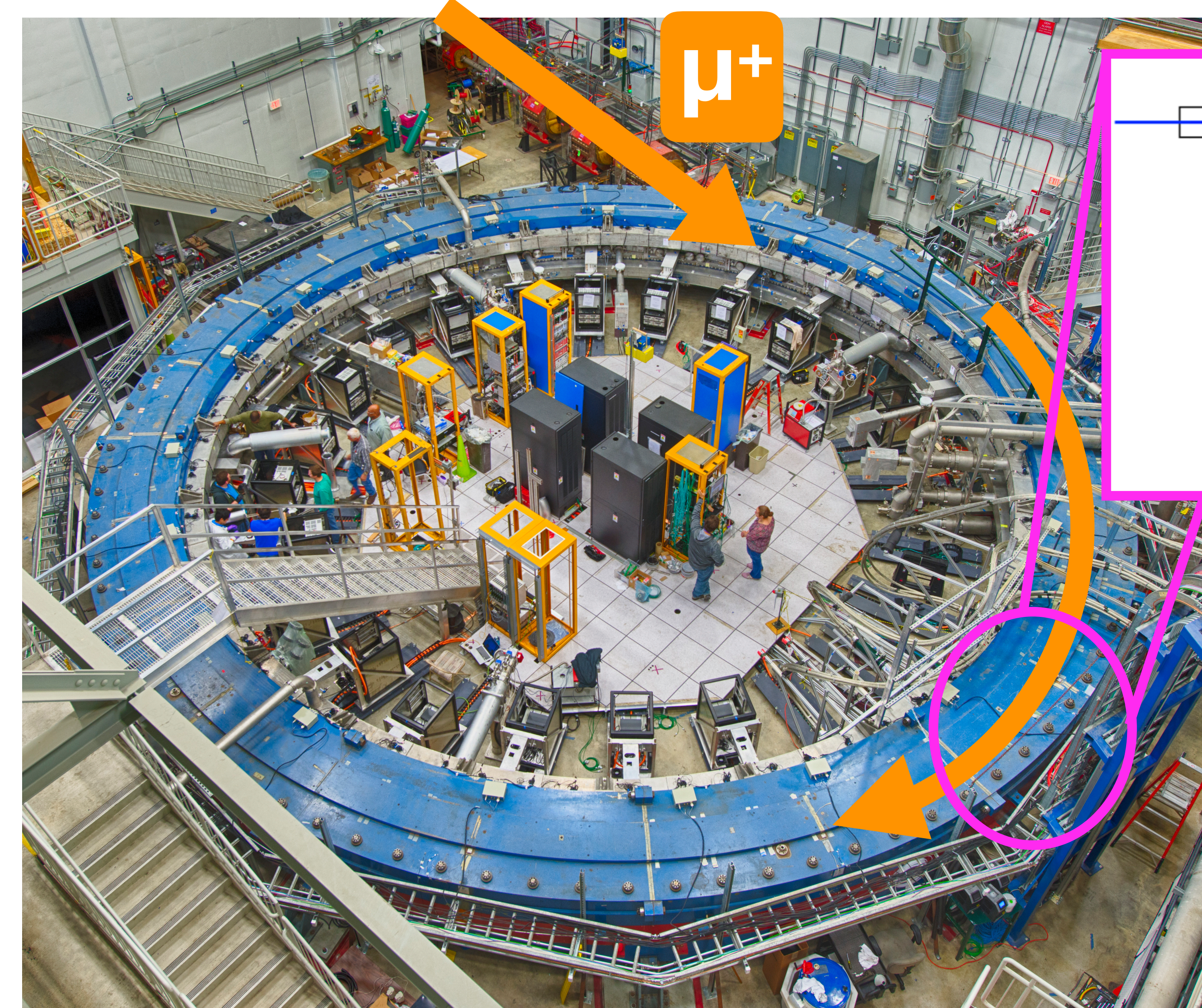
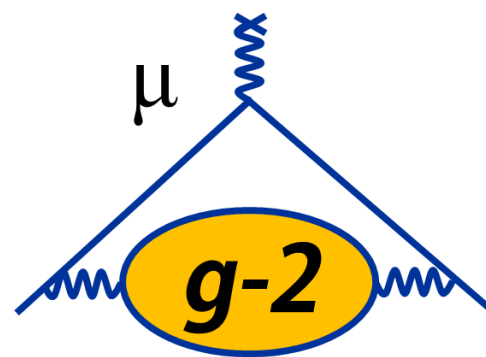
## Inflector Magnet

- Need to cancel field in beam channel
- Prevents strong deflection of the beam
- Minimal perturbation to storage magnetic field



UMassAmherst

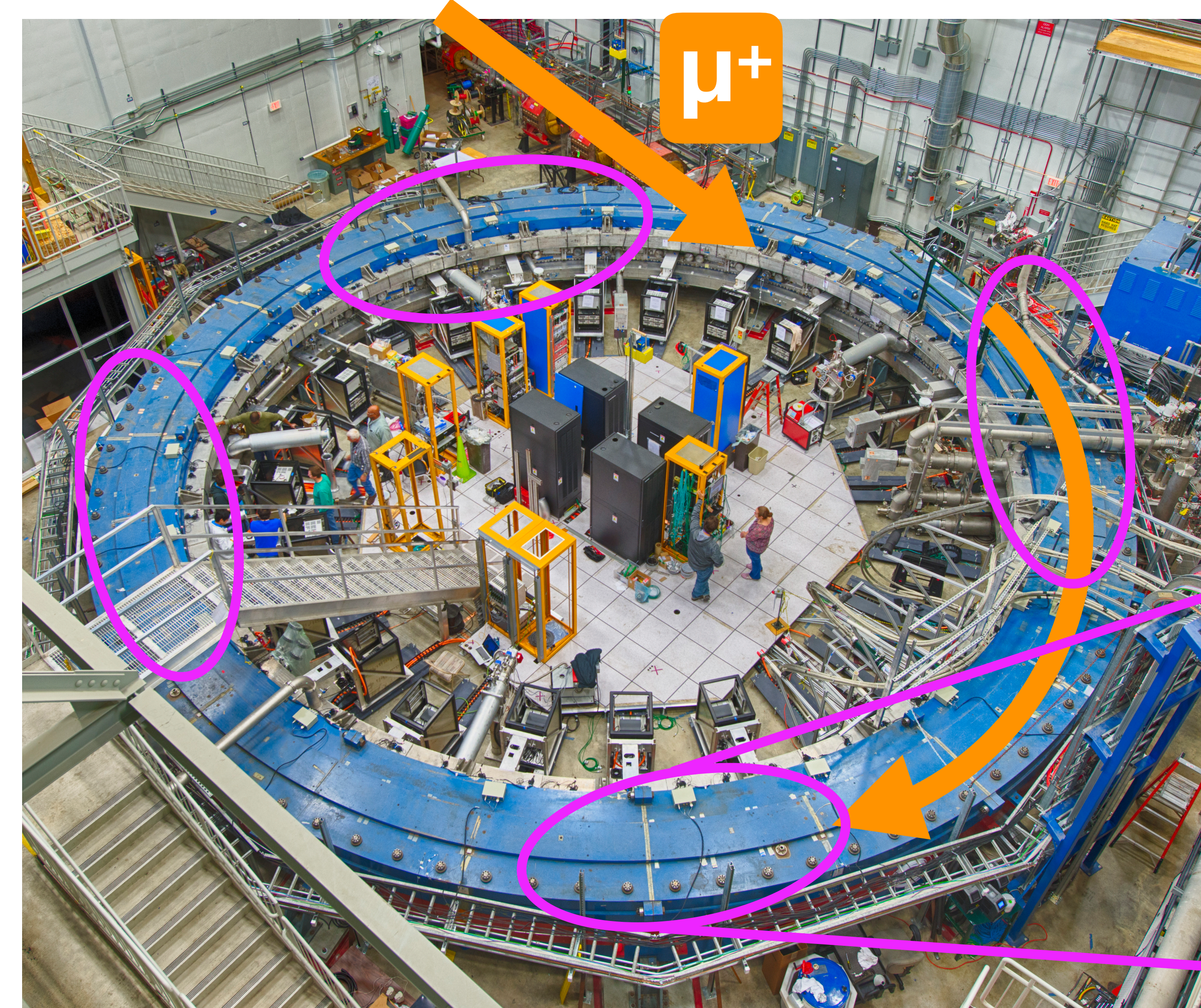
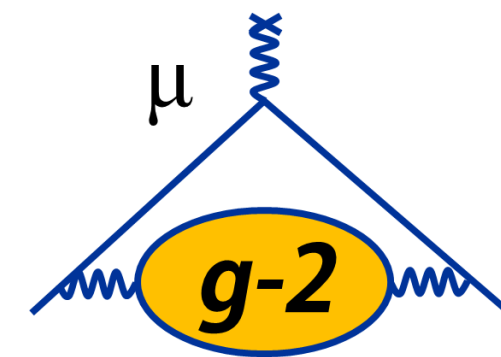
# Muon Beam Storage and Focusing



## 3 Kicker Magnets

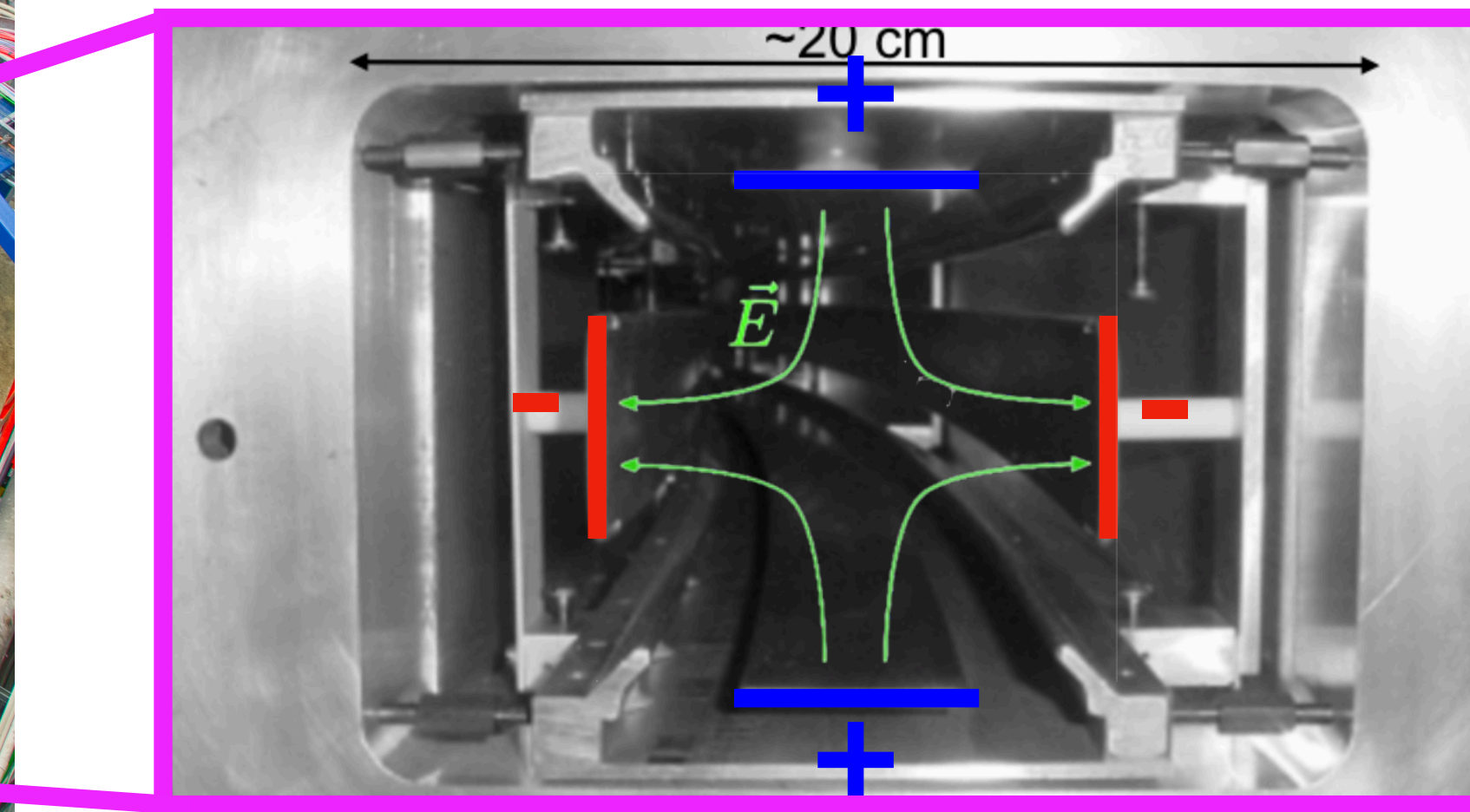
- After inflector, muons enter storage region at  $r = 77$  mm outside central closed orbit
- Deliver pulse in  $< 149$  ns to muon beam
- Steer muons onto stored orbit

# Muon Beam Storage and Focusing



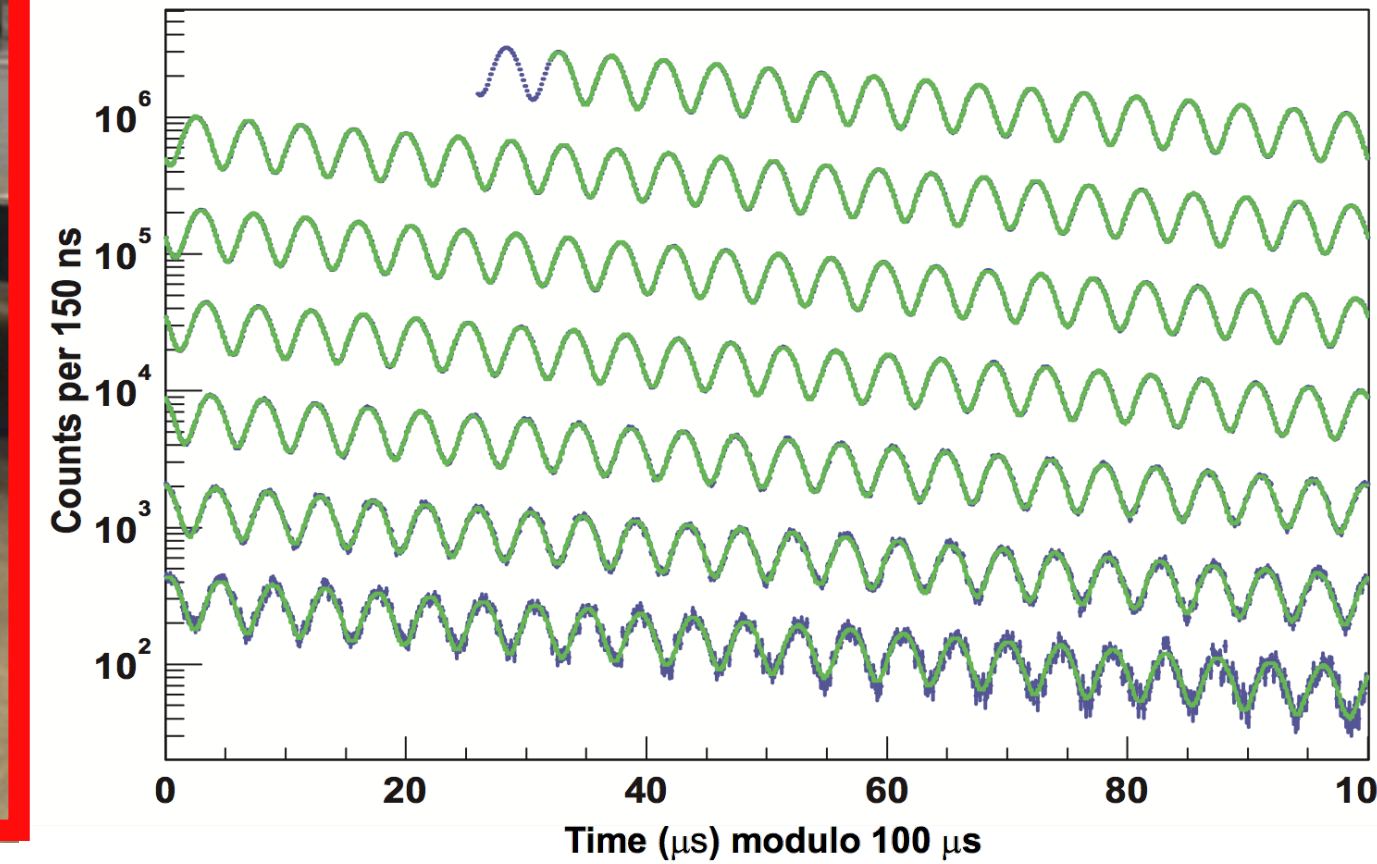
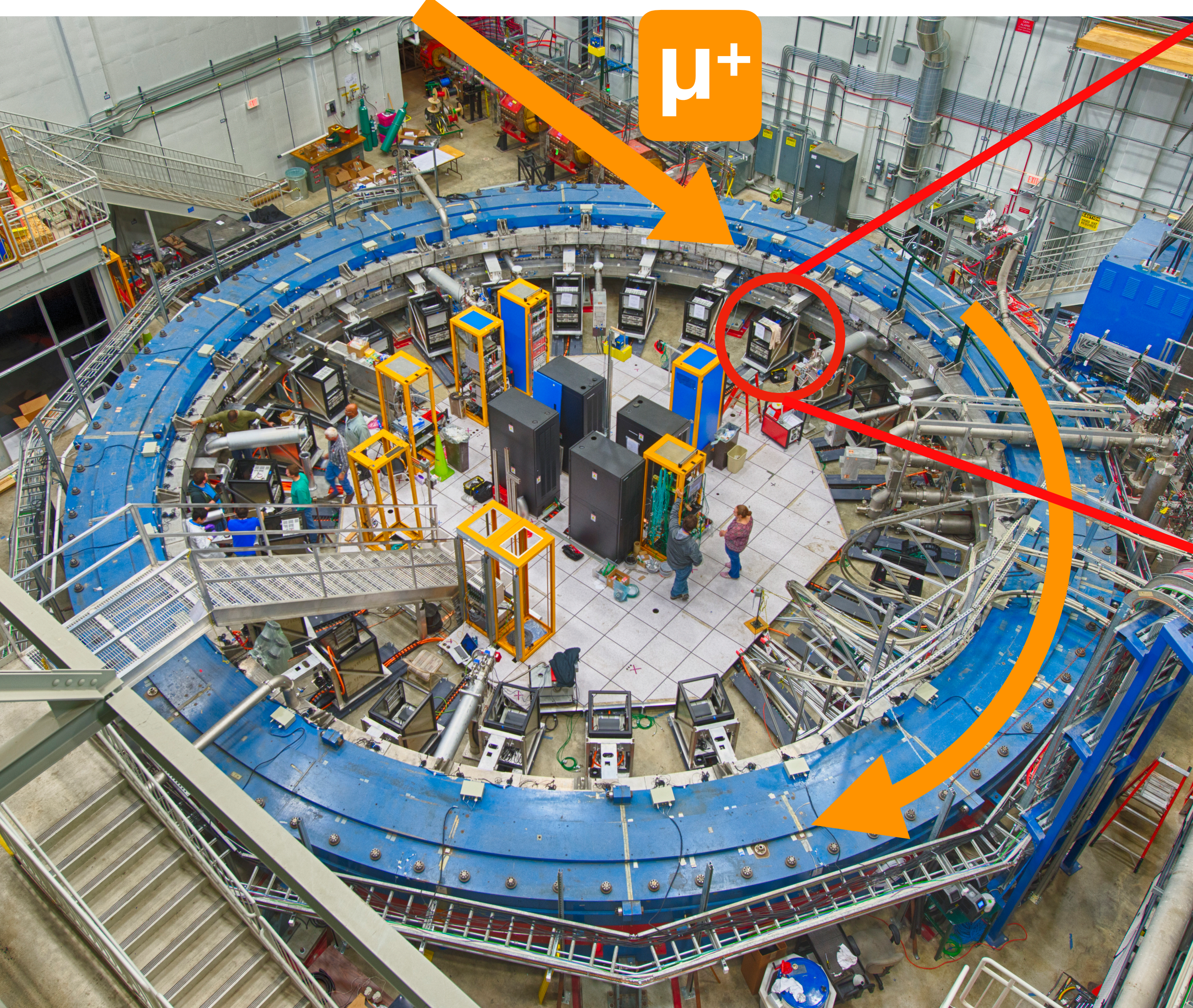
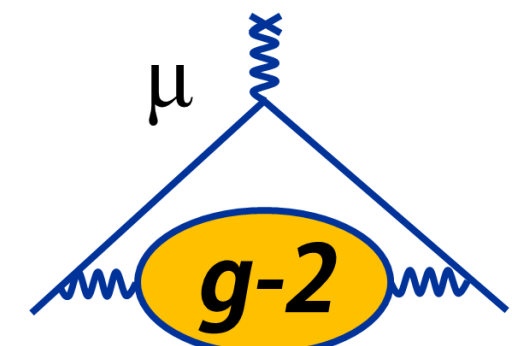
## Electrostatic Quadrupoles

- Drives the muons towards the central part of storage region vertically
- Aluminum electrodes cover ~43% of total circumference



UMassAmherst

# Measuring Muon Spin Precession ( $\omega_a$ )

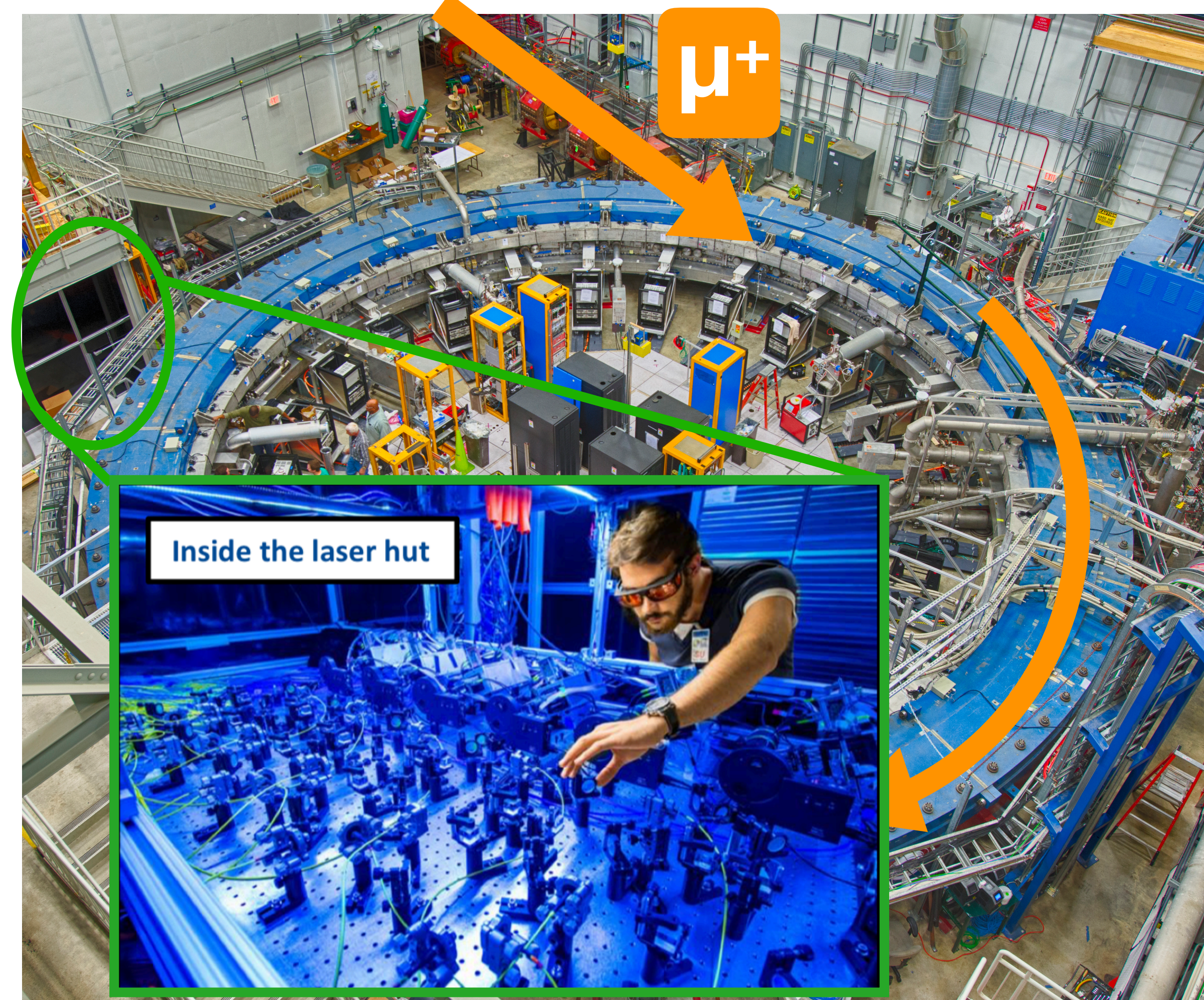
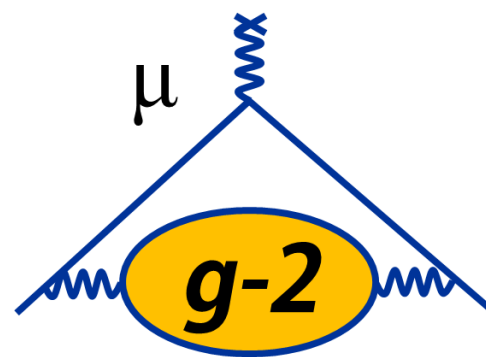


## 24 finely-segmented PbF<sub>2</sub> crystal calorimeters

- Self-analyzing decay:  $\mu^+ \rightarrow e^+ \bar{\nu}_\mu \nu_e$
- Highest-energy  $e^+$  emitted preferentially along muon spin
- Results in sinusoidally-oscillating arrival time of these  $e^+$  in calorimeters

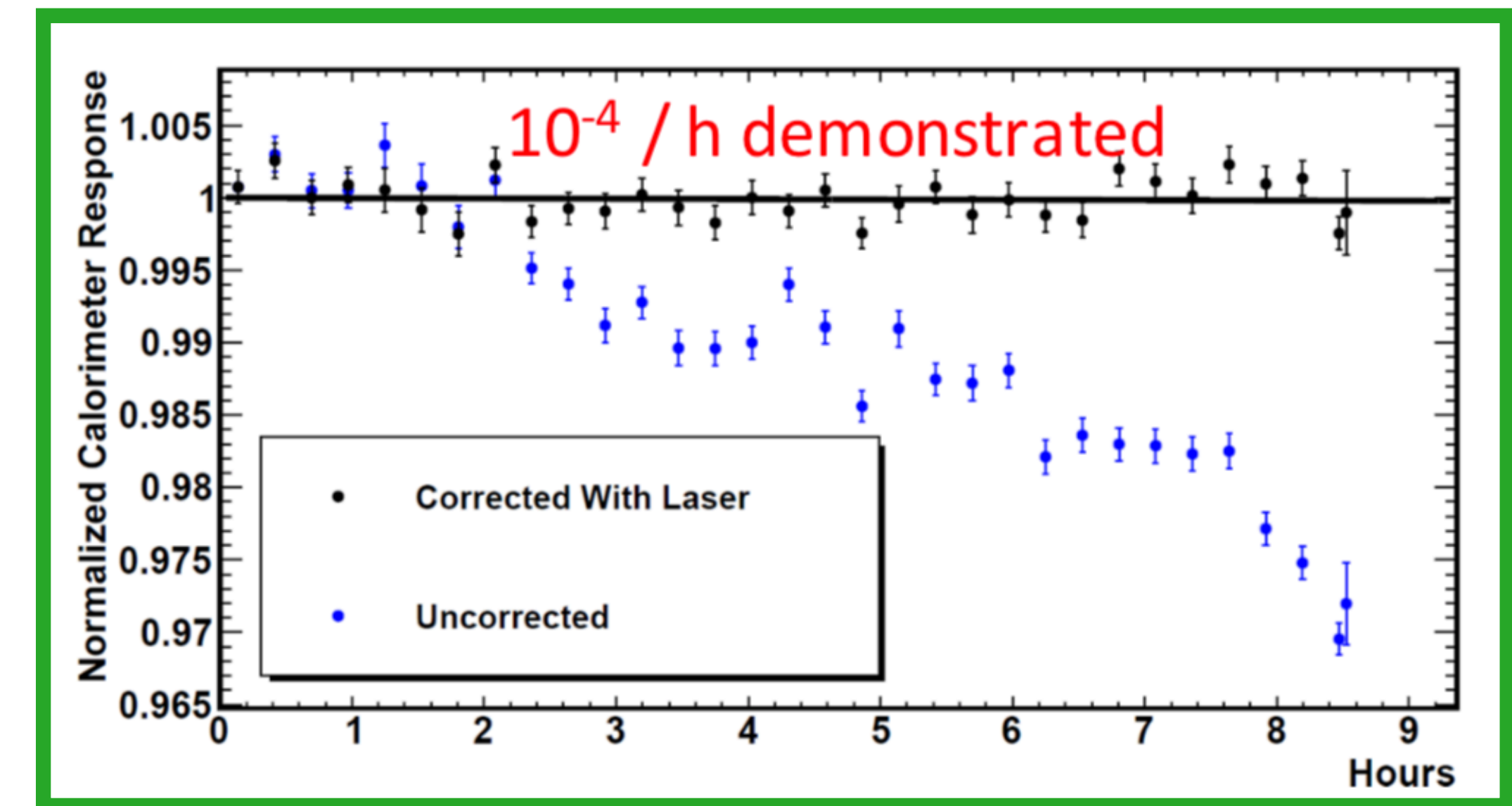
UMassAmherst

# Measuring Muon Spin Precession ( $\omega_a$ )



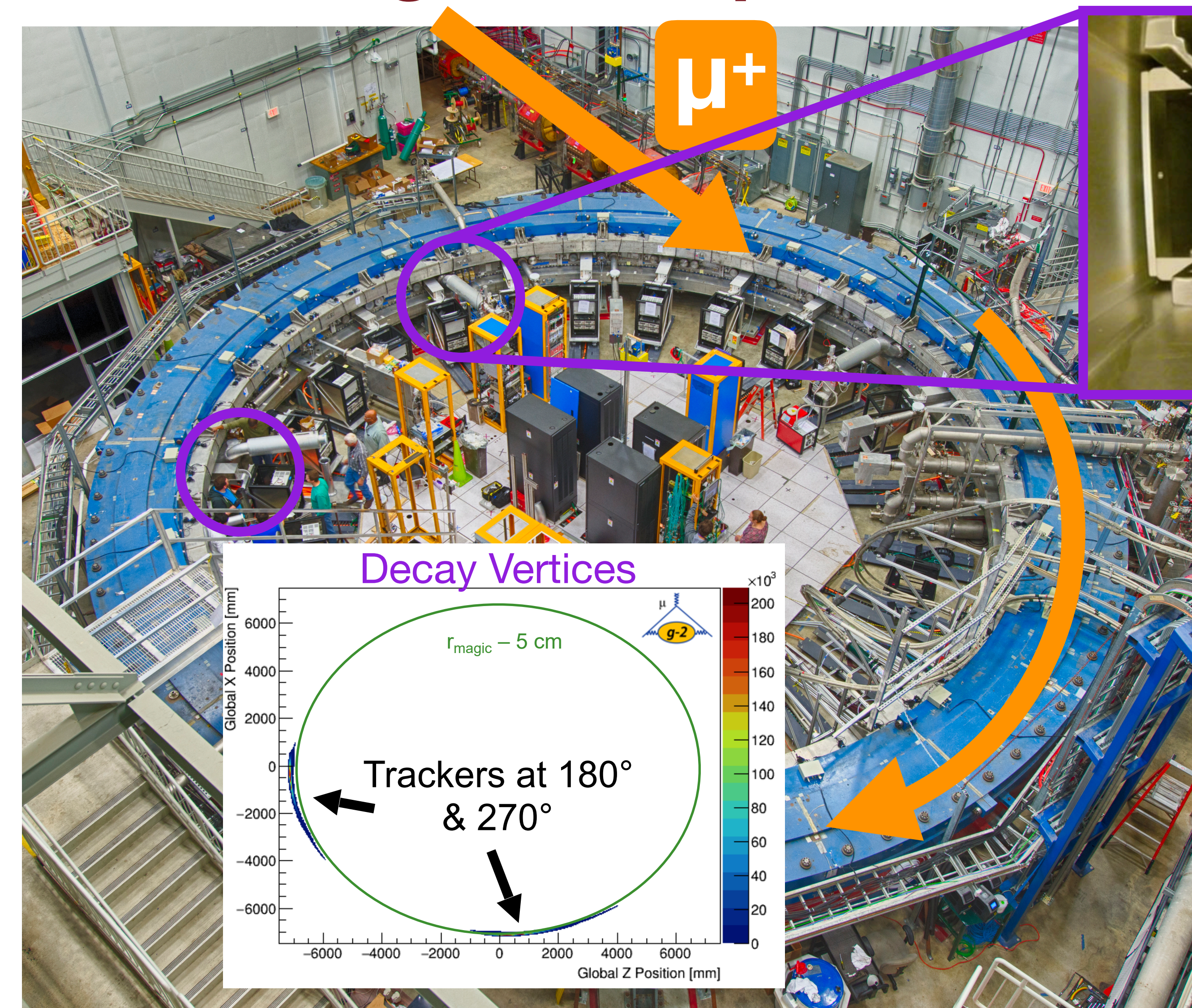
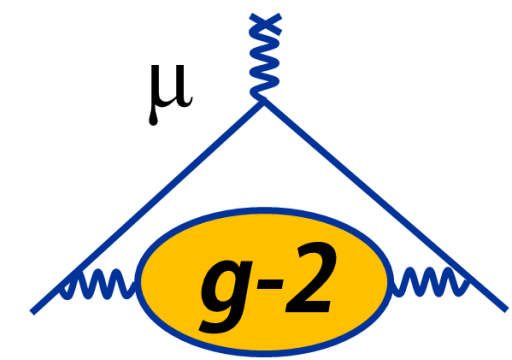
## Laser System

- Calibrate calorimeter gain response throughout data taking
- Demonstrated stability to  $10^{-4}/\text{hr}$

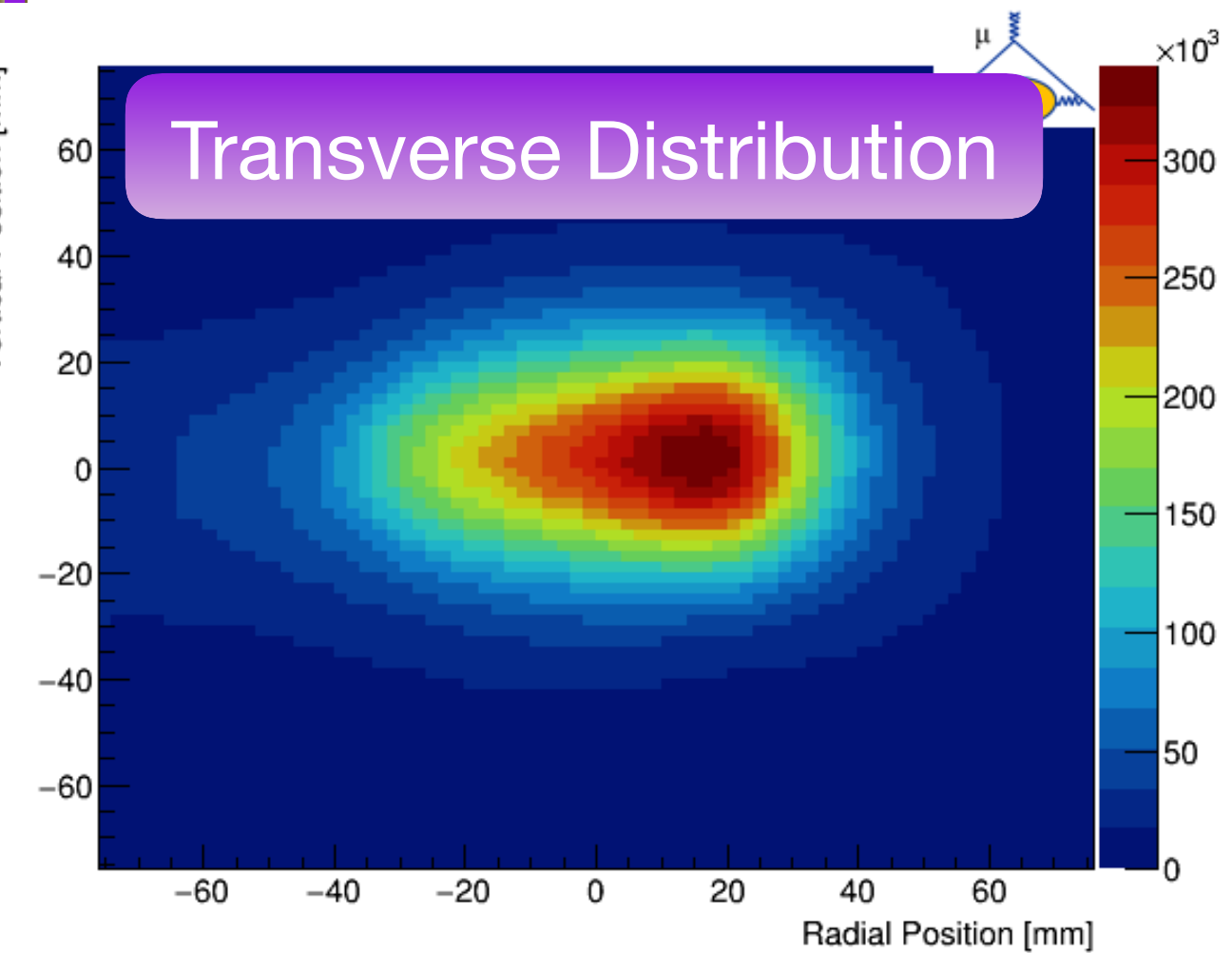


UMassAmherst

# Measuring Muon Spin Precession ( $\omega_a$ )



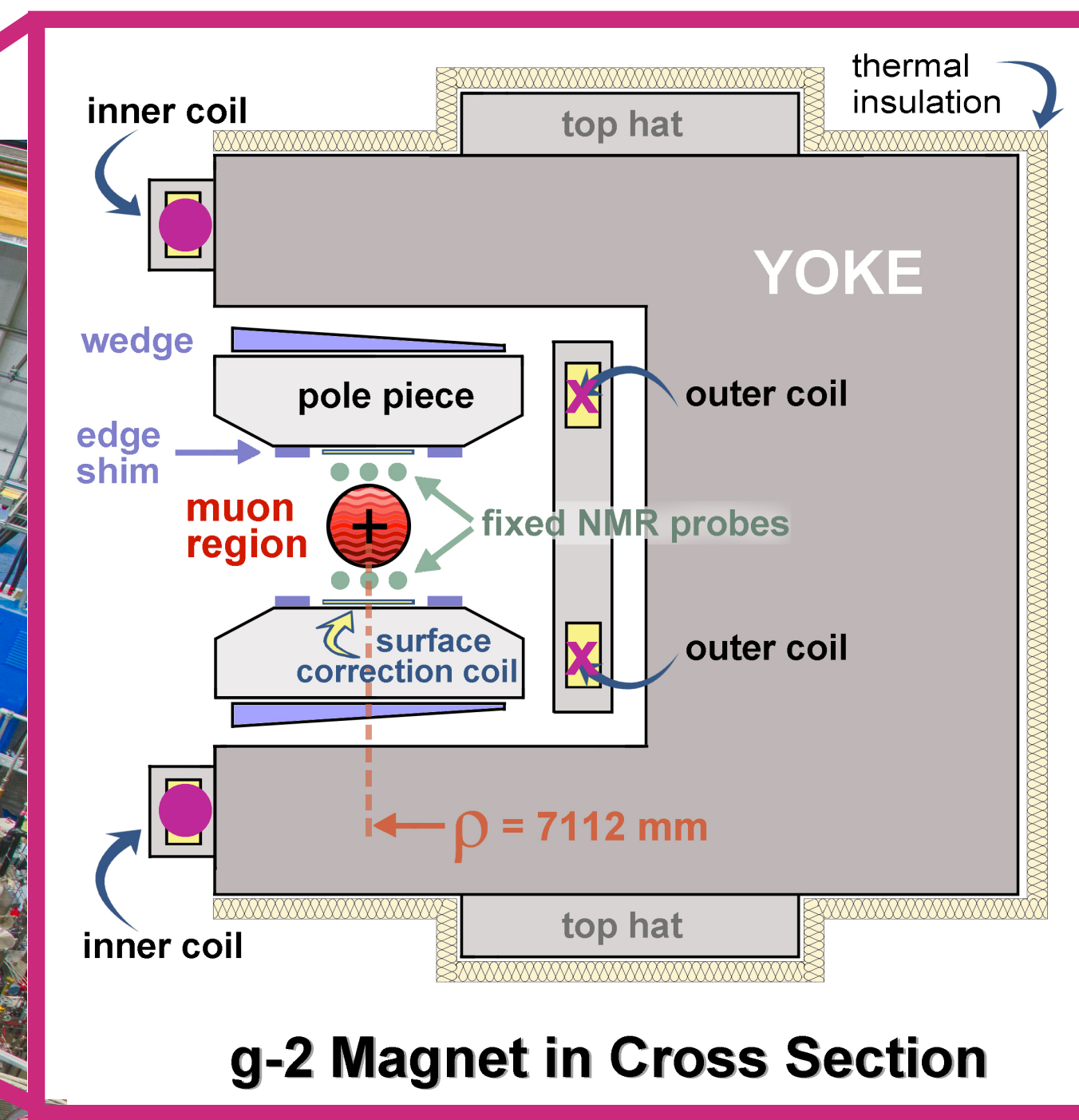
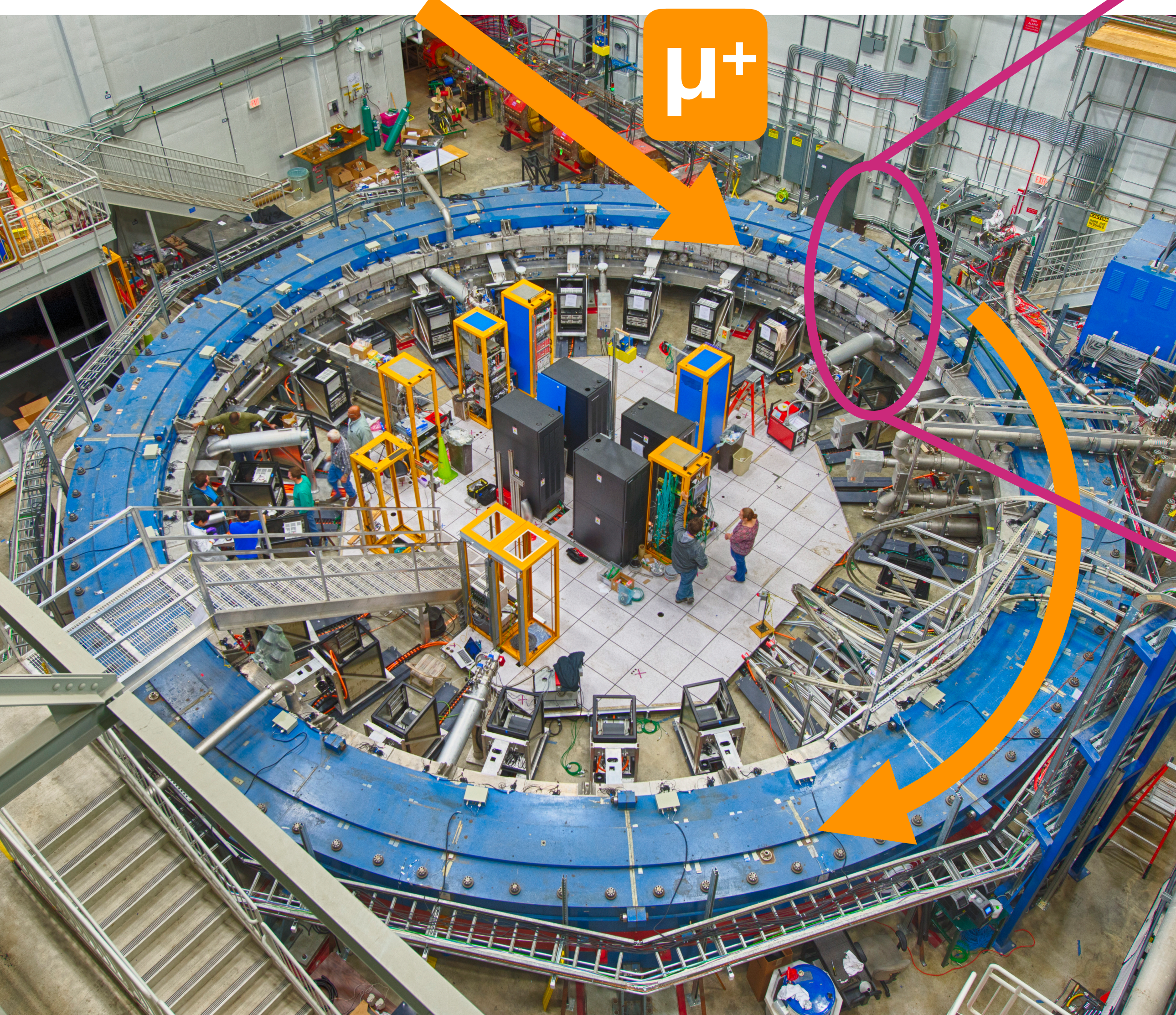
Muon's view of the storage region



## Two straw-tracker stations

- Reconstruct the muon beam distribution from  $e^+$  hits
- Tracker module: 128 straws/module
- 8 modules per station

# Magnet Anatomy



$$B = 1.45 \text{ T } (\sim 5200 \text{ A})$$

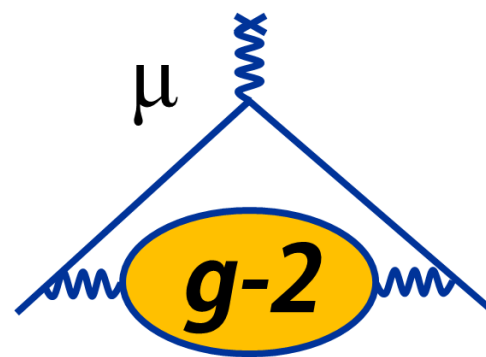
- Power supply with feedback to fine-tune field in real time

## 12 C-shaped yokes

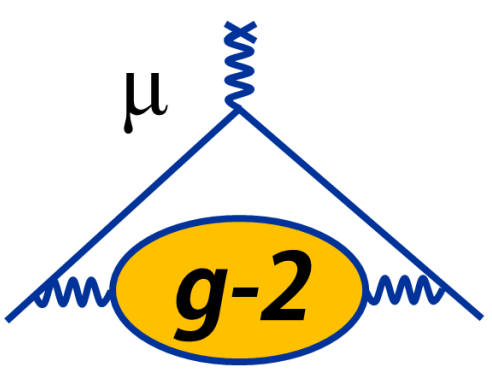
- 3 upper and 3 lower poles per yoke
- 72 total poles

## Field Shape

- Determined by positioning of pole pieces, wedge-shaped pieces of steel, programmable surface coils

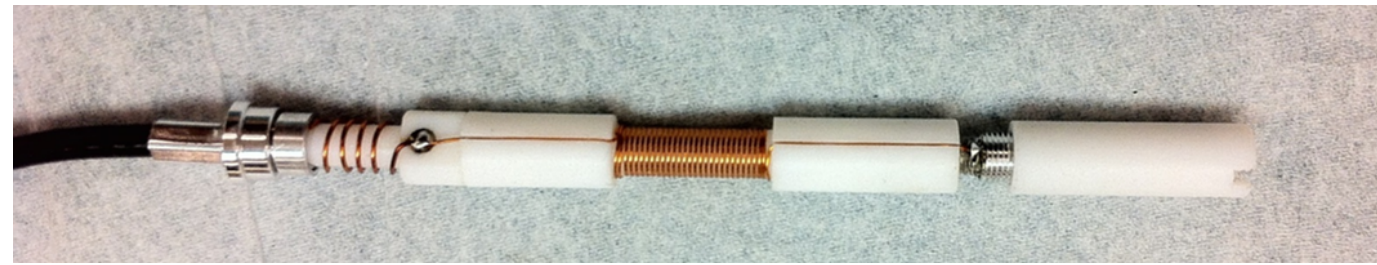


Current direction indicated by ● and x

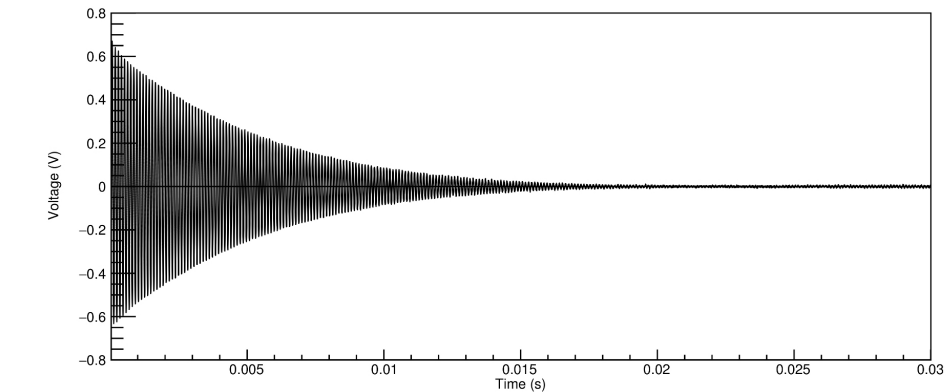


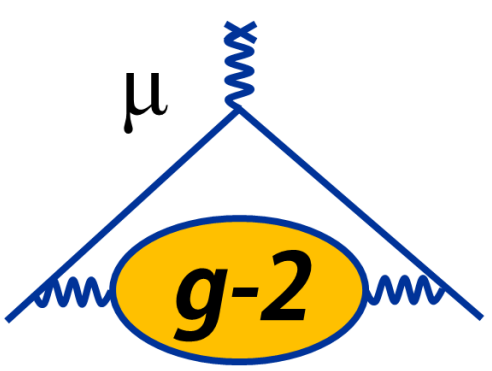
# Monitoring and Mapping the Magnetic Field

## Pulsed NMR



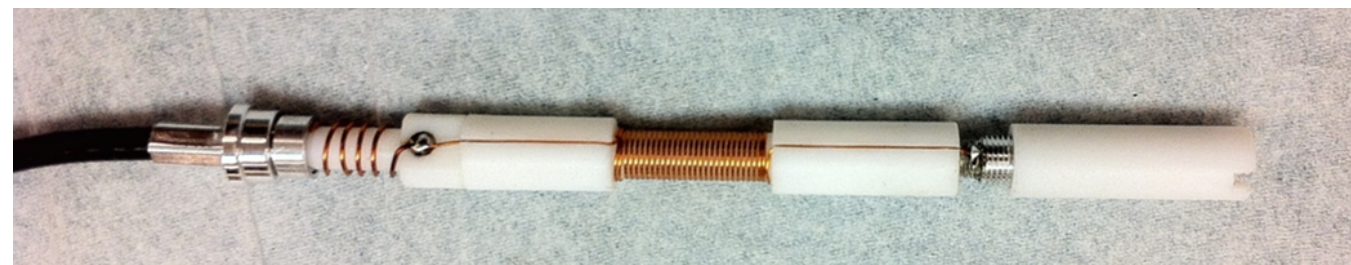
- Deliver  $\pi/2$  pulse to probe, induce & record the free-induction decay (FID)
- Extracted frequency precision: 10 ppb/FID



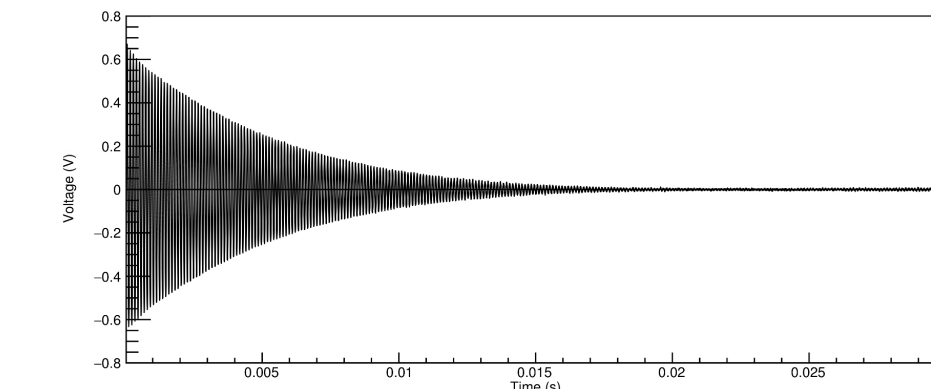


# Monitoring and Mapping the Magnetic Field

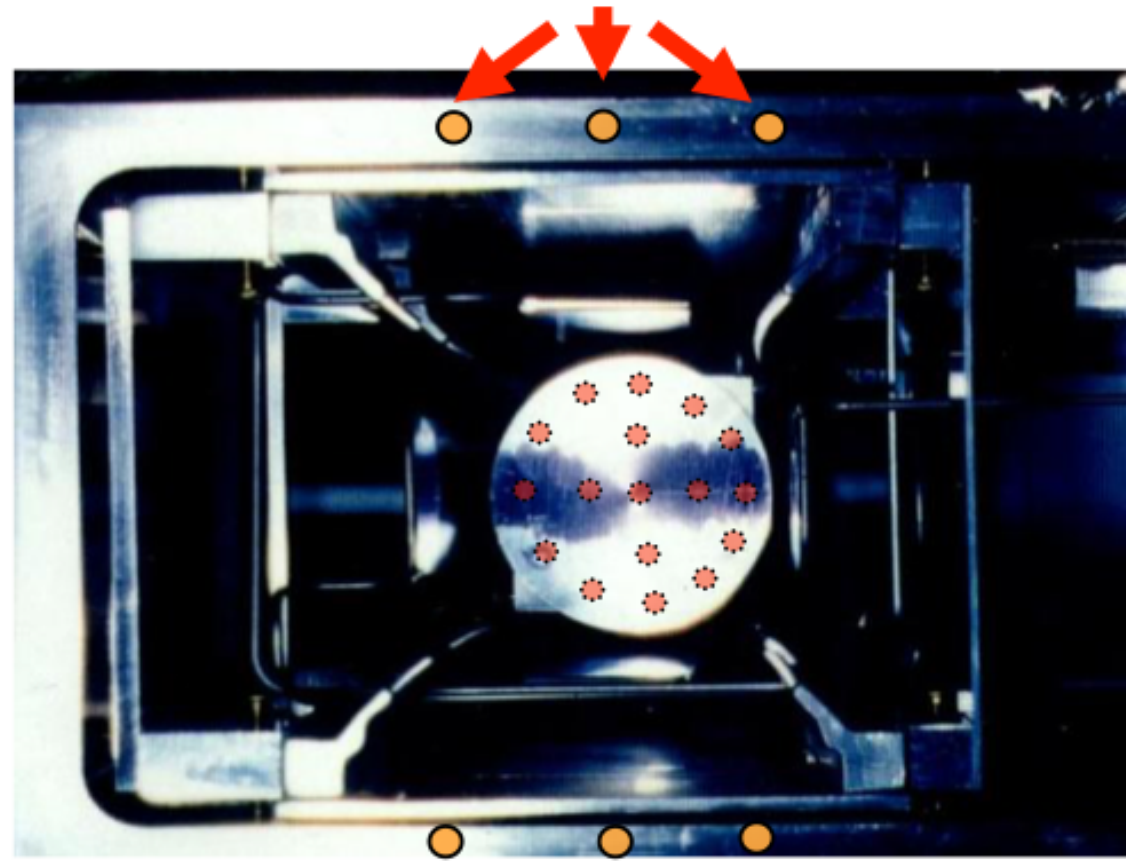
## Pulsed NMR



- Deliver  $\pi/2$  pulse to probe, induce & record the free-induction decay (FID)
- Extracted frequency precision: 10 ppb/FID

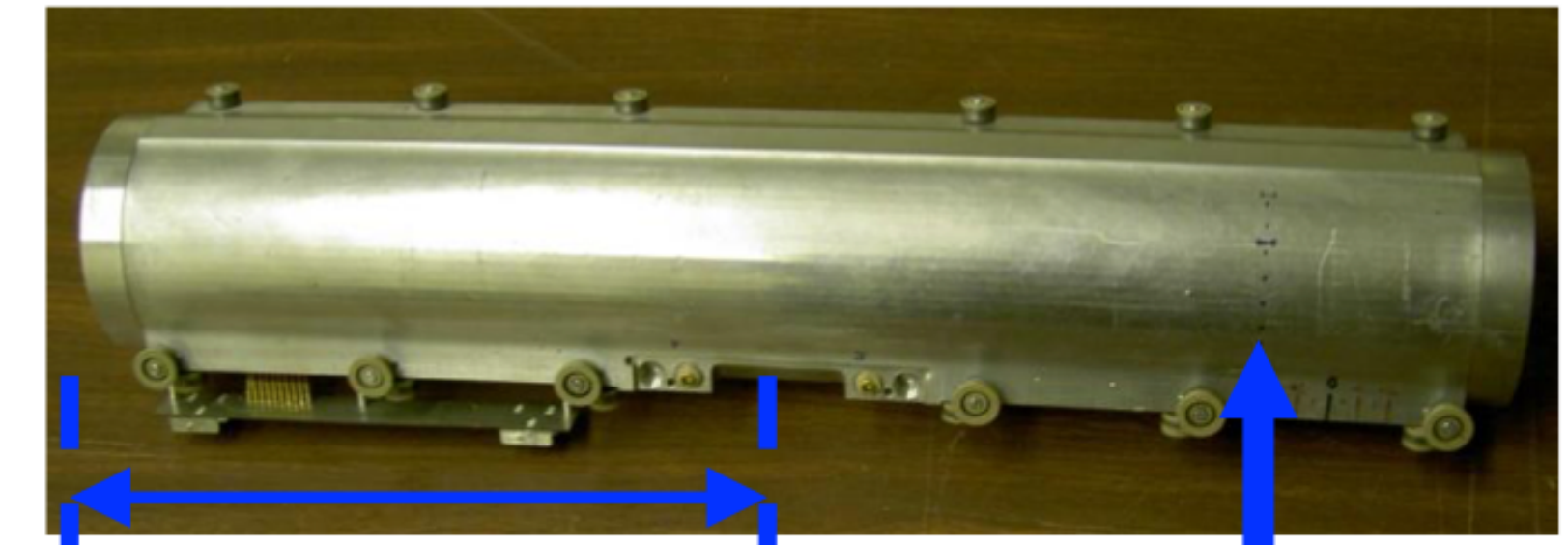


## Fixed probes on vacuum chambers



- Measure field while muons are in ring  
– 378 probes **outside** storage region

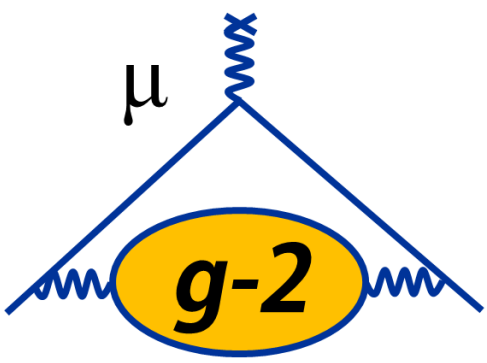
## Trolley matrix of 17 NMR probes



Legend:

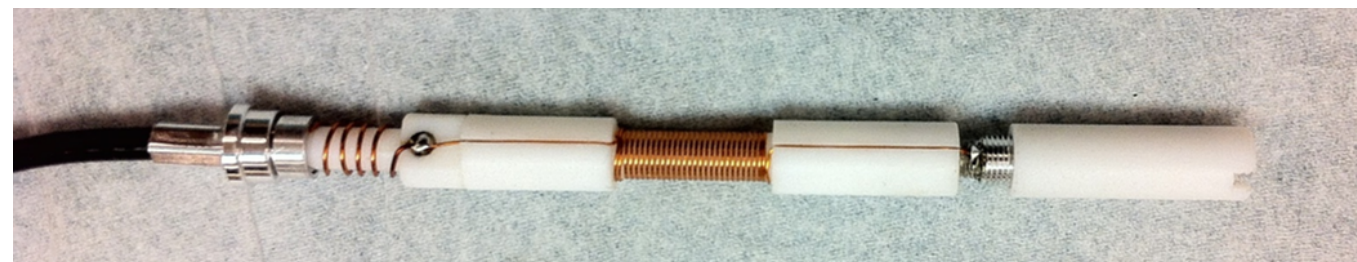
- Electronics, Microcontroller, Communication
- Position of NMR probes

- Measure field in storage region during **specialized runs** when **muons are not being stored**

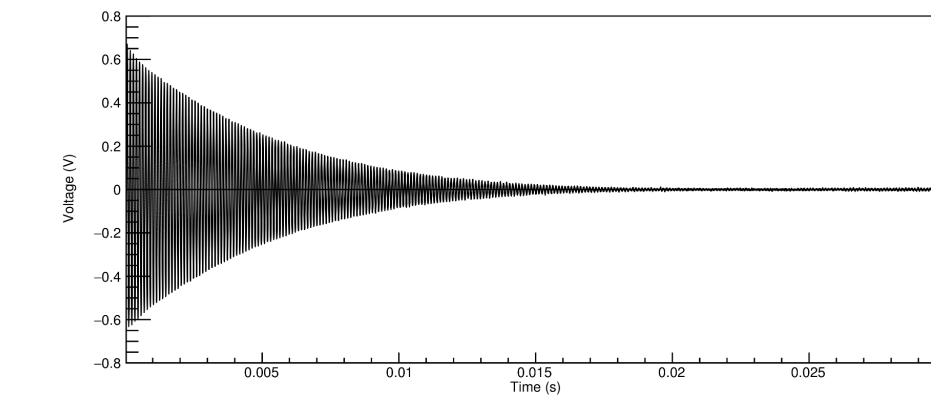


# Monitoring and Mapping the Magnetic Field

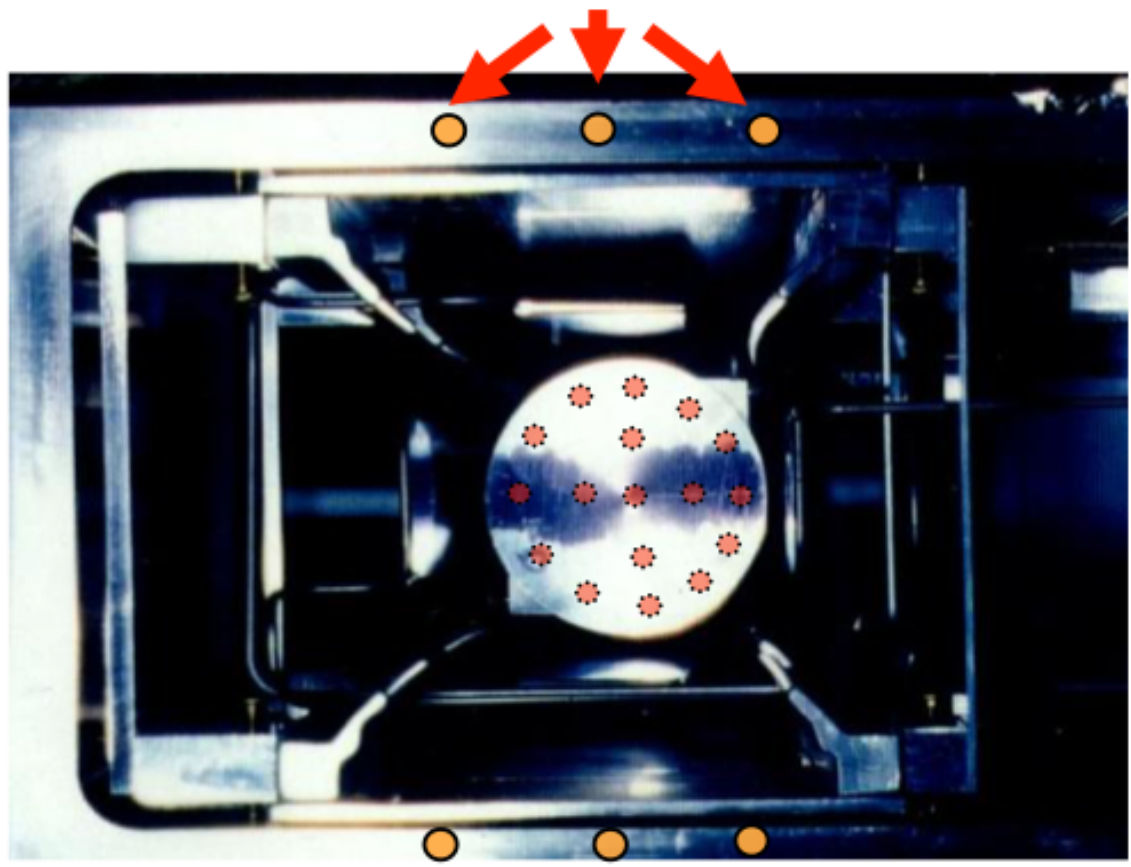
## Pulsed NMR



- Deliver  $\pi/2$  pulse to probe, induce & record the free-induction decay (FID)
- Extracted frequency precision: 10 ppb/FID



## Fixed probes on vacuum chambers



- Measure field while muons are in ring  
– 378 probes **outside** storage region

## Trolley matrix of 17 NMR probes

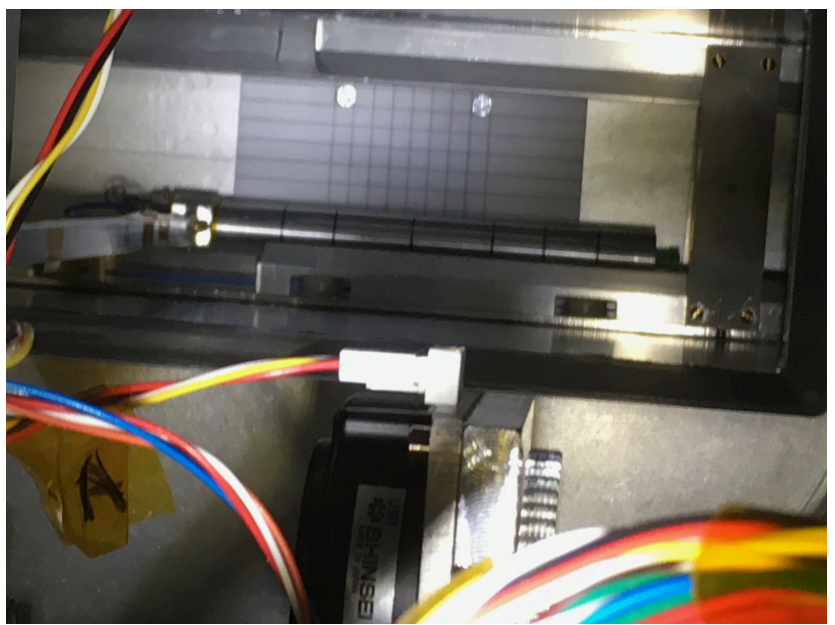
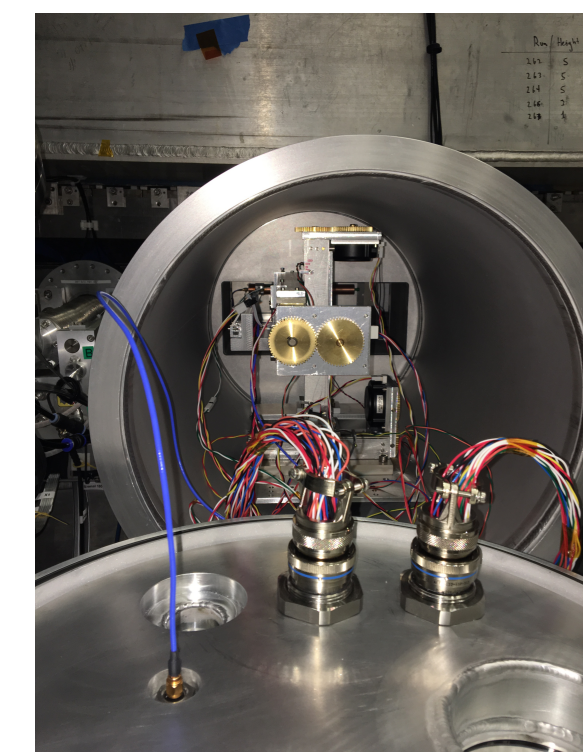


Electronics,  
Microcontroller,  
Communication

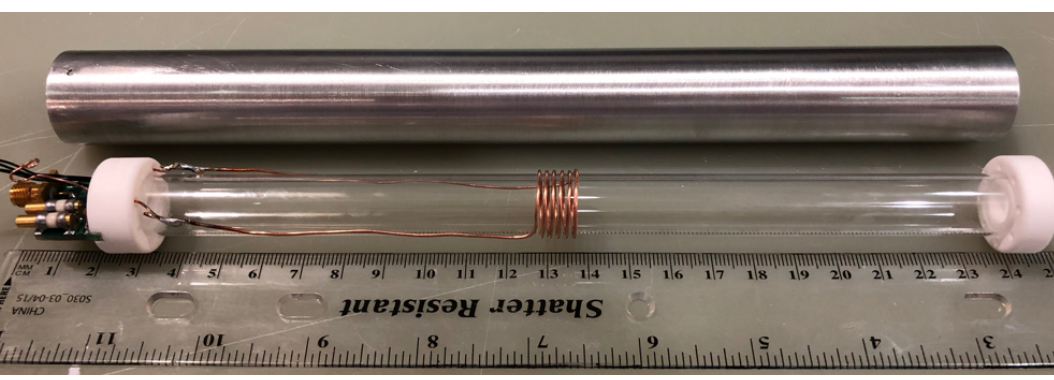
- Measure field in storage region during **specialized runs** when **muons are not being stored**

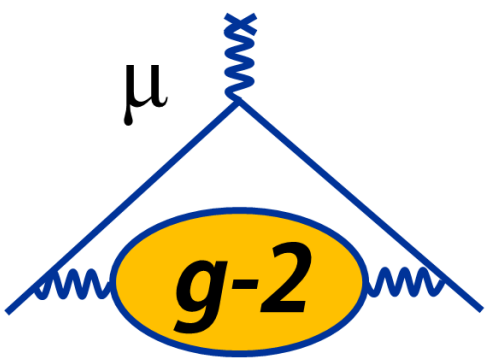
## Trolley probes calibrated to free-proton Larmor frequency

- Calibrate trolley probes using a special probe that uses a water sample
- Measurements in specially-shimmed region of ring



Plunging Probe





# Systematic Uncertainty Comparison: E821 and E989

$$a_\mu = \frac{\omega_a}{\tilde{\omega}_p} \frac{\mu_p}{\mu_e} \frac{m_\mu}{m_e} \frac{g_e}{2}$$

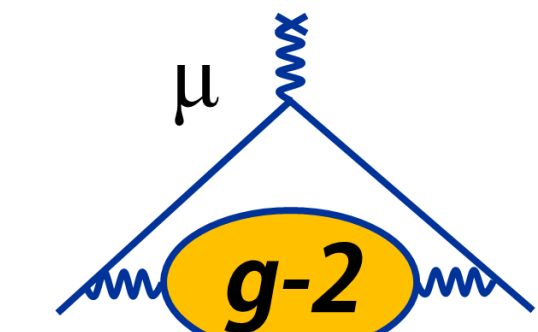
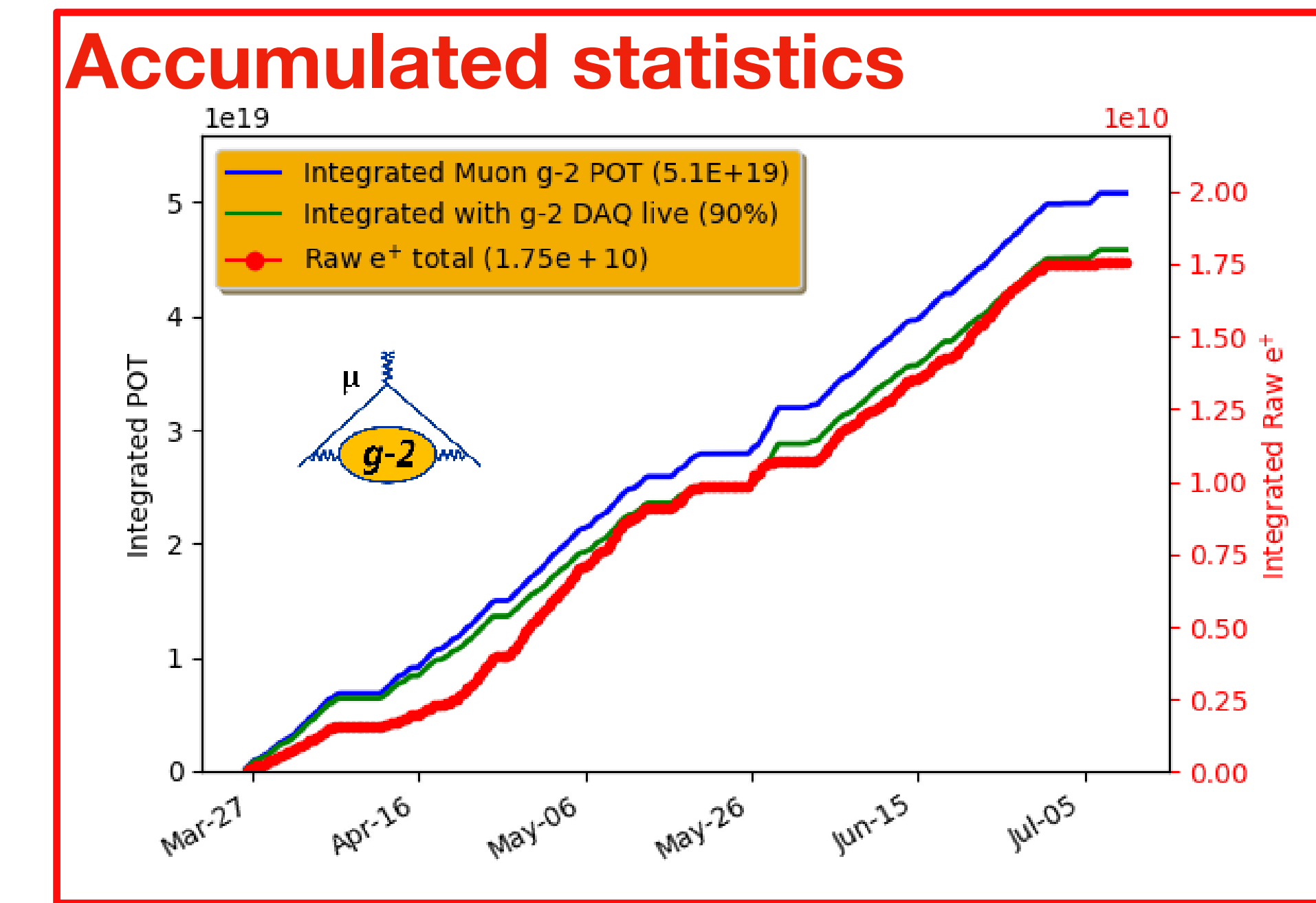
| $\omega_a$ Goal: Factor of 3 Improvement |            |                 |
|--|------------|-----------------|
| Category                                 | E821 (ppb) | E989 Goal (ppb) |
| Gain Changes                             | 120        | 20              |
| Lost Muons                               | 90         | 20              |
| Pileup                                   | 80         | 40              |
| Horizontal CBO                           | 70         | < 30            |
| E-field/pitch                            | 110        | 30              |
| <b>Quadrature Sum</b>                    | <b>214</b> | <b>70</b>       |

- New hardware (calorimeters, trackers, NMR)
- Improved analysis techniques
- Reduce uncertainties by at least a factor of 2.5

| $\omega_p$ Goal: Factor of 2.5 Improvement |            |                 |
|--|------------|-----------------|
| Category                                   | E821 (ppb) | E989 Goal (ppb) |
| Field Calibration                          | 50         | 35              |
| Trolley Measurements                       | 50         | 30              |
| Fixed Probe Interpolation                  | 70         | 30              |
| Muon Convolution                           | 30         | 10              |
| Time-Dependent Fields                      | –          | 5               |
| Others                                     | 100        | 50              |
| <b>Quadrature Sum</b>                      | <b>170</b> | <b>70</b>       |

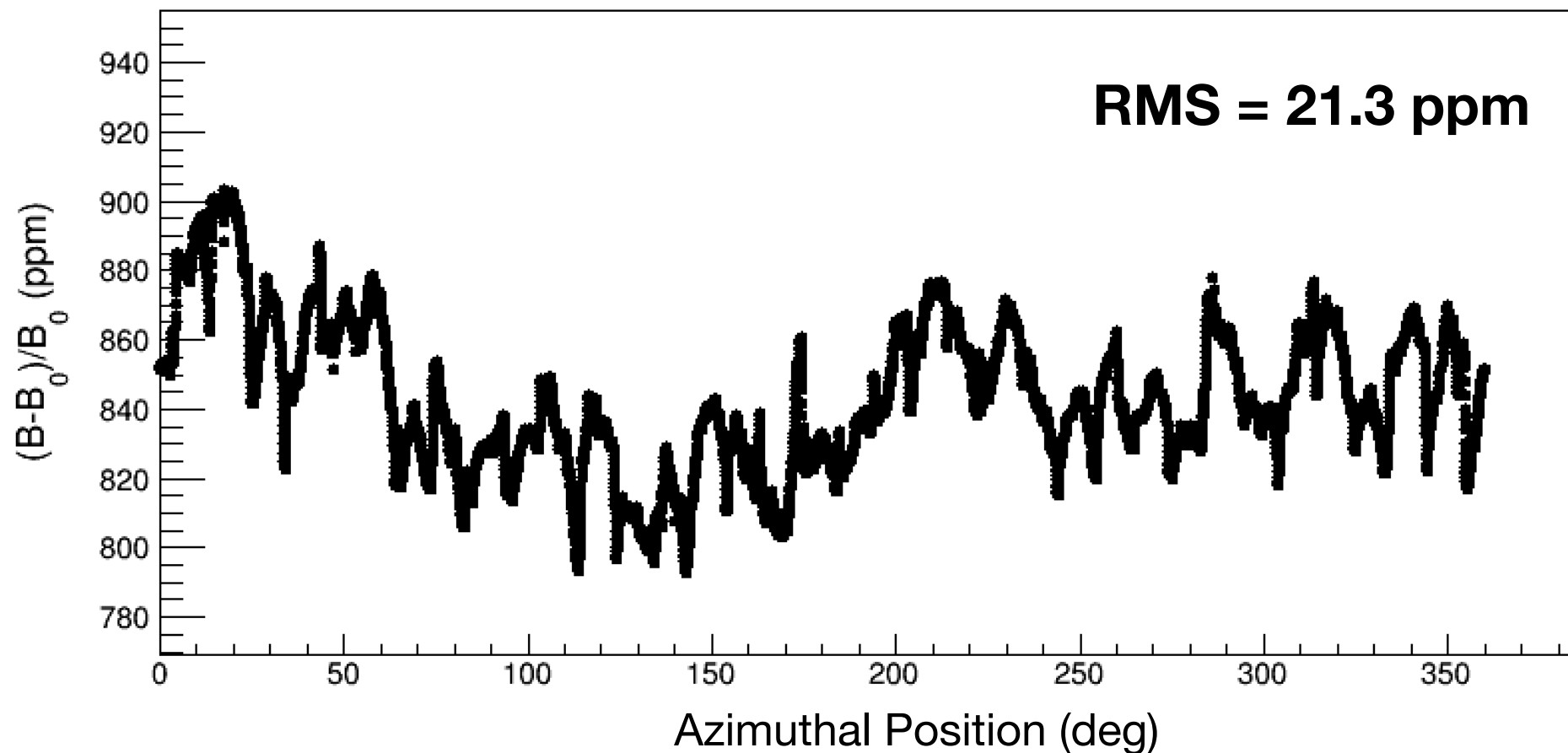
# Run 1 Overview

- Data taking period: April—July 2018
- A number of changing conditions as we optimized hardware
- Accumulated  $\sim 1.1 \times$  BNL statistics (after data quality cuts) —  $\delta\omega_a(\text{stat}) \sim 410 \text{ ppb}$
- Field uniformity  $\sim 2x$  better than BNL

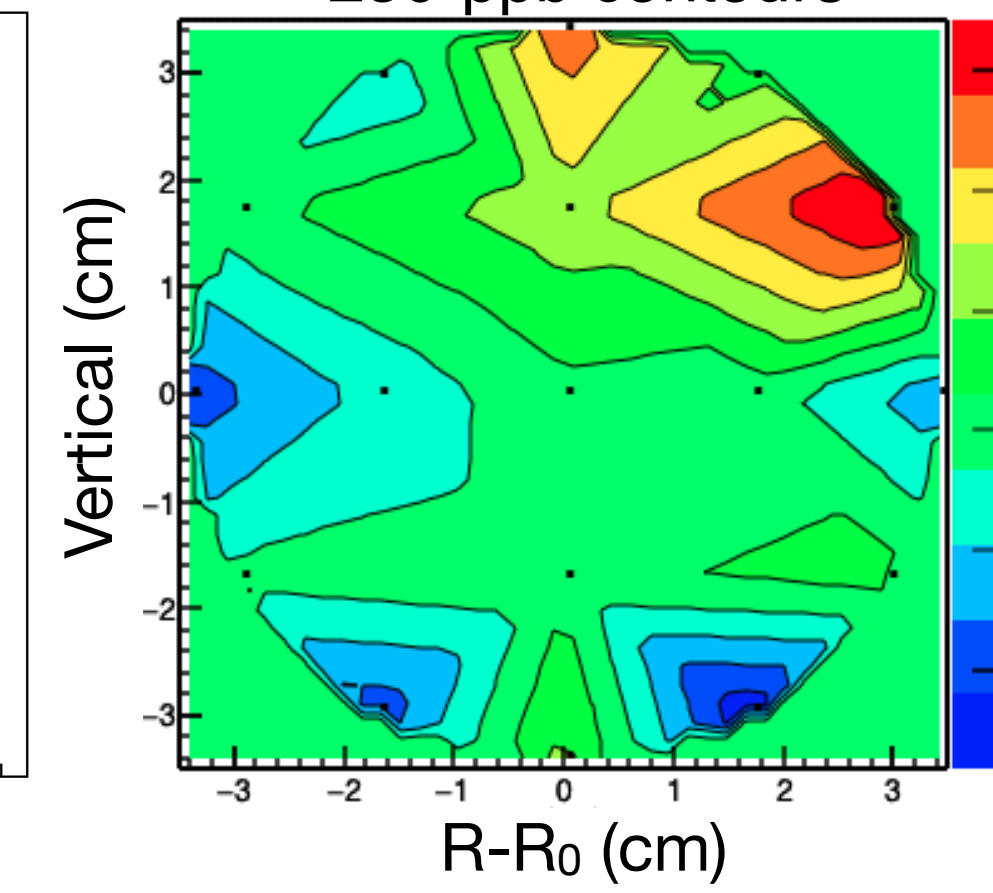


## Typical Field Map

Dipole Moment

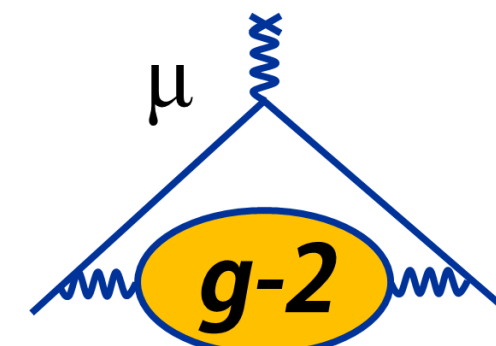


Azimuthal average  
250-ppb contours

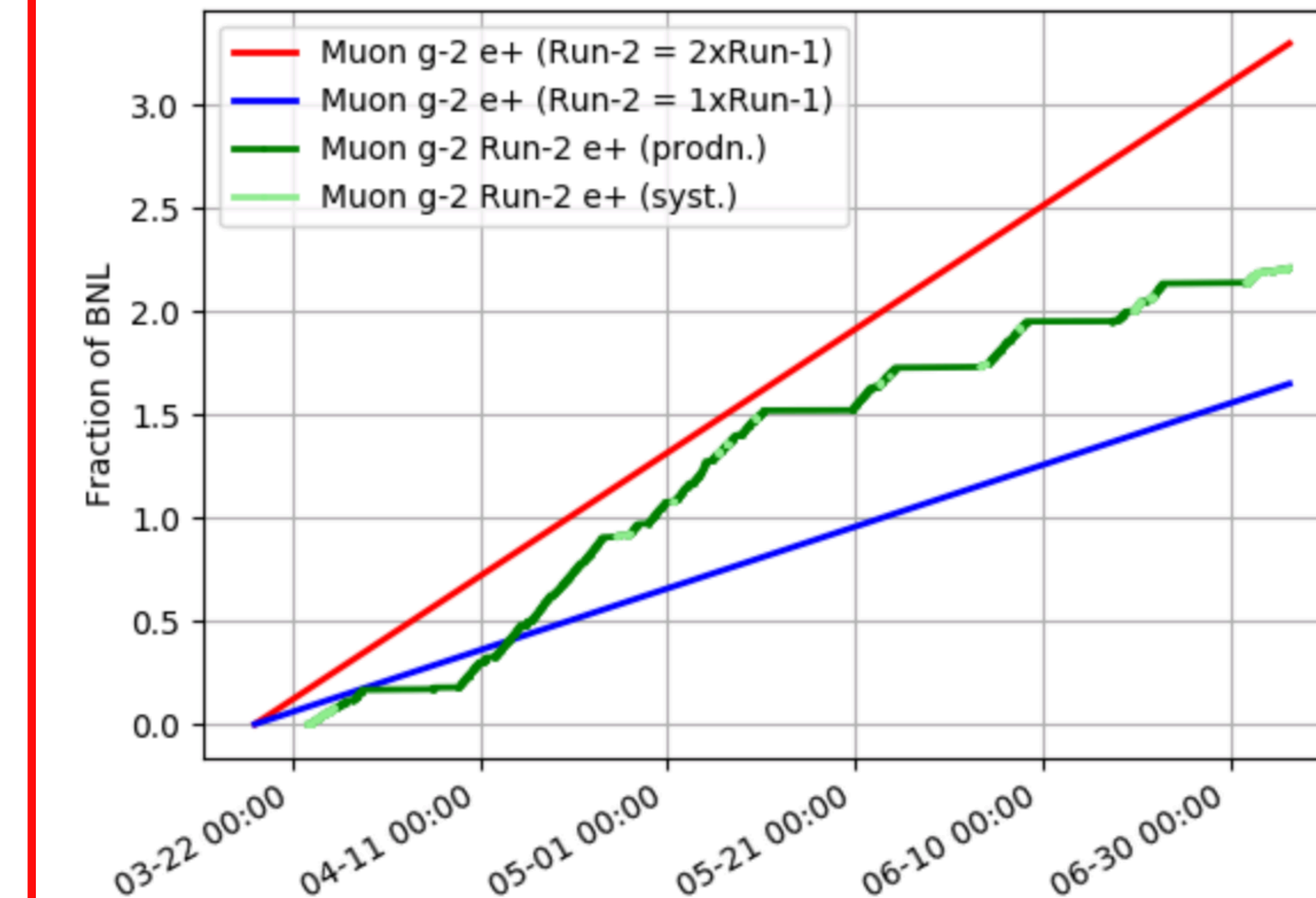


# Run 2 Overview

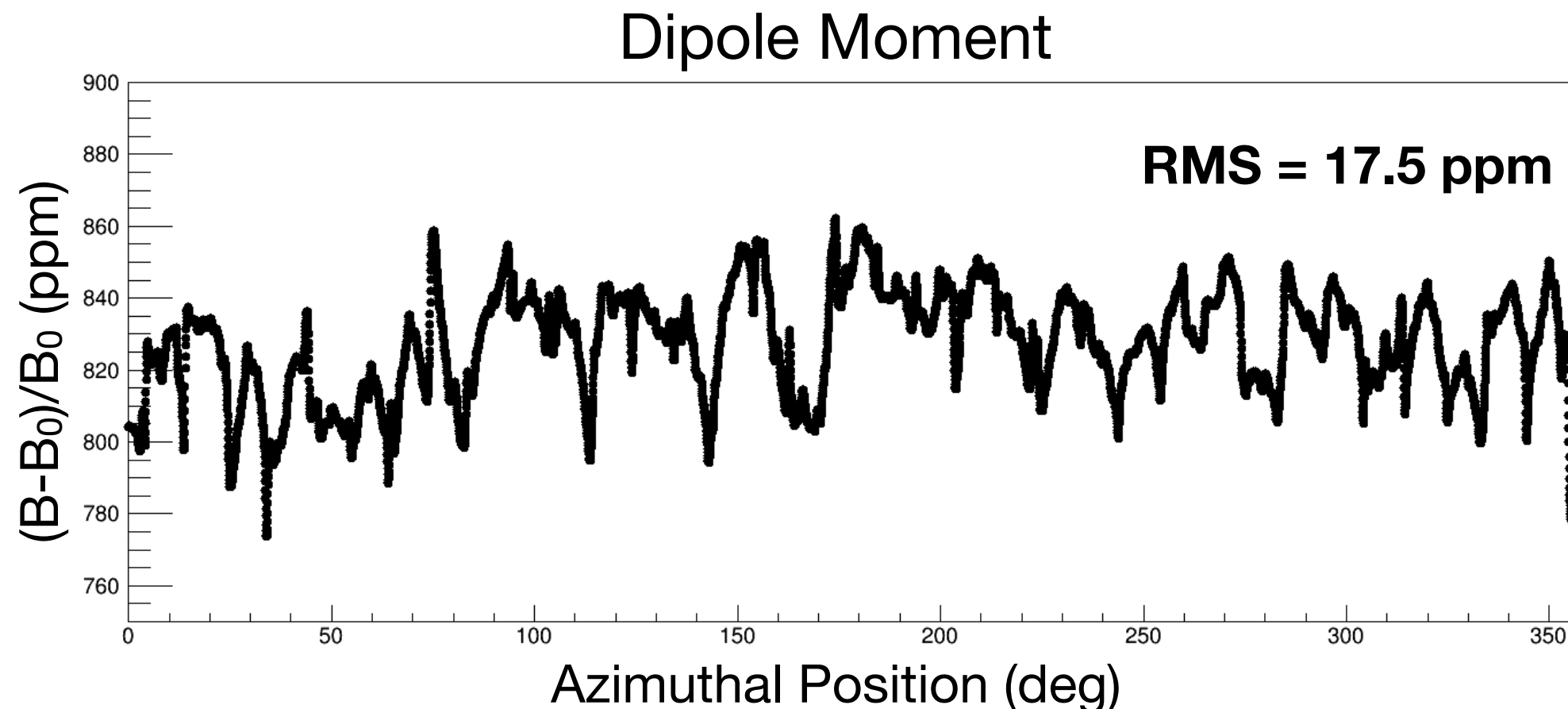
- Data taking period: March—July 2019
- Contiguous data set
- Accumulated  $\sim 1.9 \times$  BNL statistics  
(before data quality cuts)
- Field uniformity in very good condition



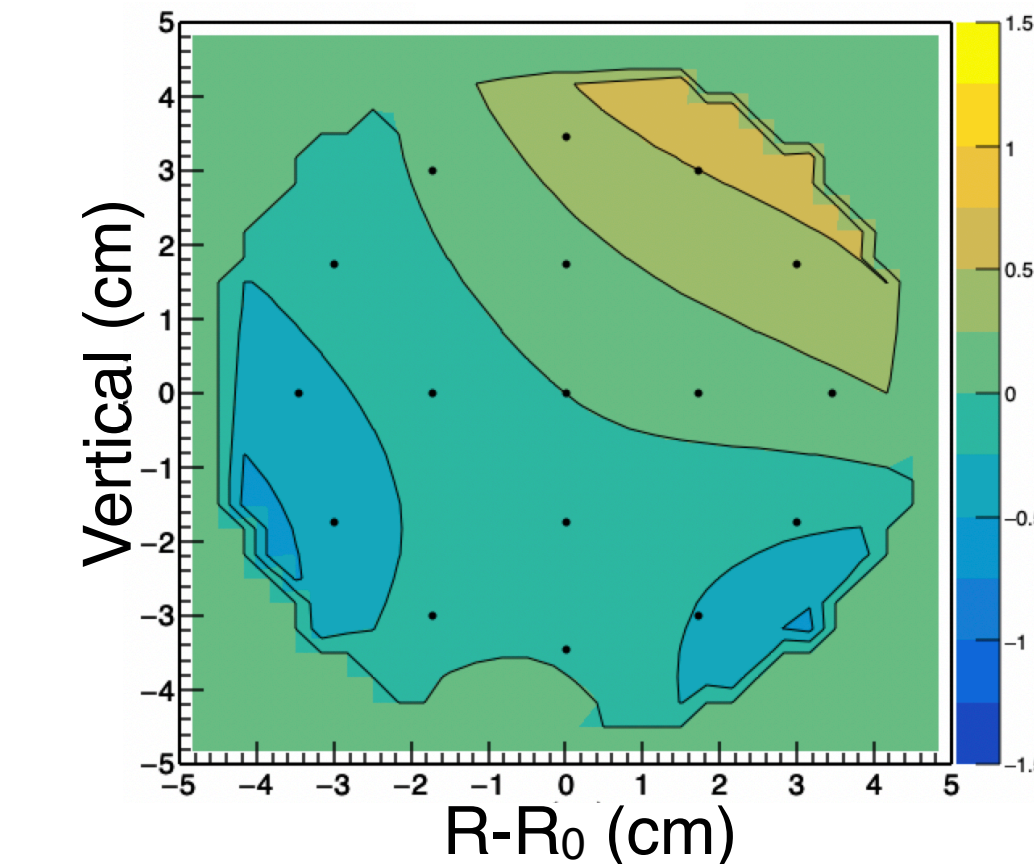
## Accumulated statistics



## Typical Field Map



Azimuthal average  
250-ppb contours



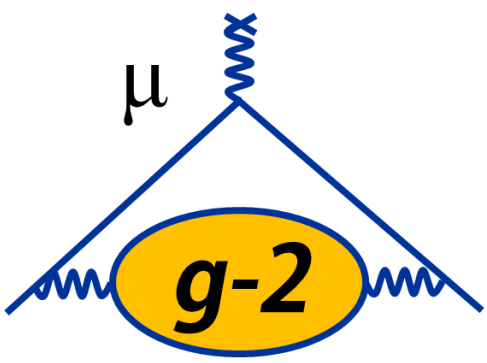
## Run 3

- To start in mid-November
- Aim to **triple** statistics accumulated to date
- Direct continuation of Run 2

# Run 1 Analysis Status — $\omega_a$

$$a_\mu = \frac{\omega_a}{\tilde{\omega}_p} \frac{\mu_p}{\mu_e} \frac{m_\mu}{m_e} \frac{g_e}{2}$$

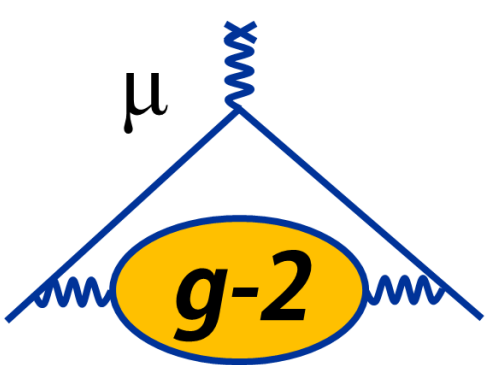
UMassAmherst



# Run 1 Analysis Status: $\omega_a$

- Account for a number of effects that can affect the extraction of  $\omega_a$

$$N(t) = N_0 e^{-t/\tau} [1 - A \cos(\omega_a t + \phi)]$$

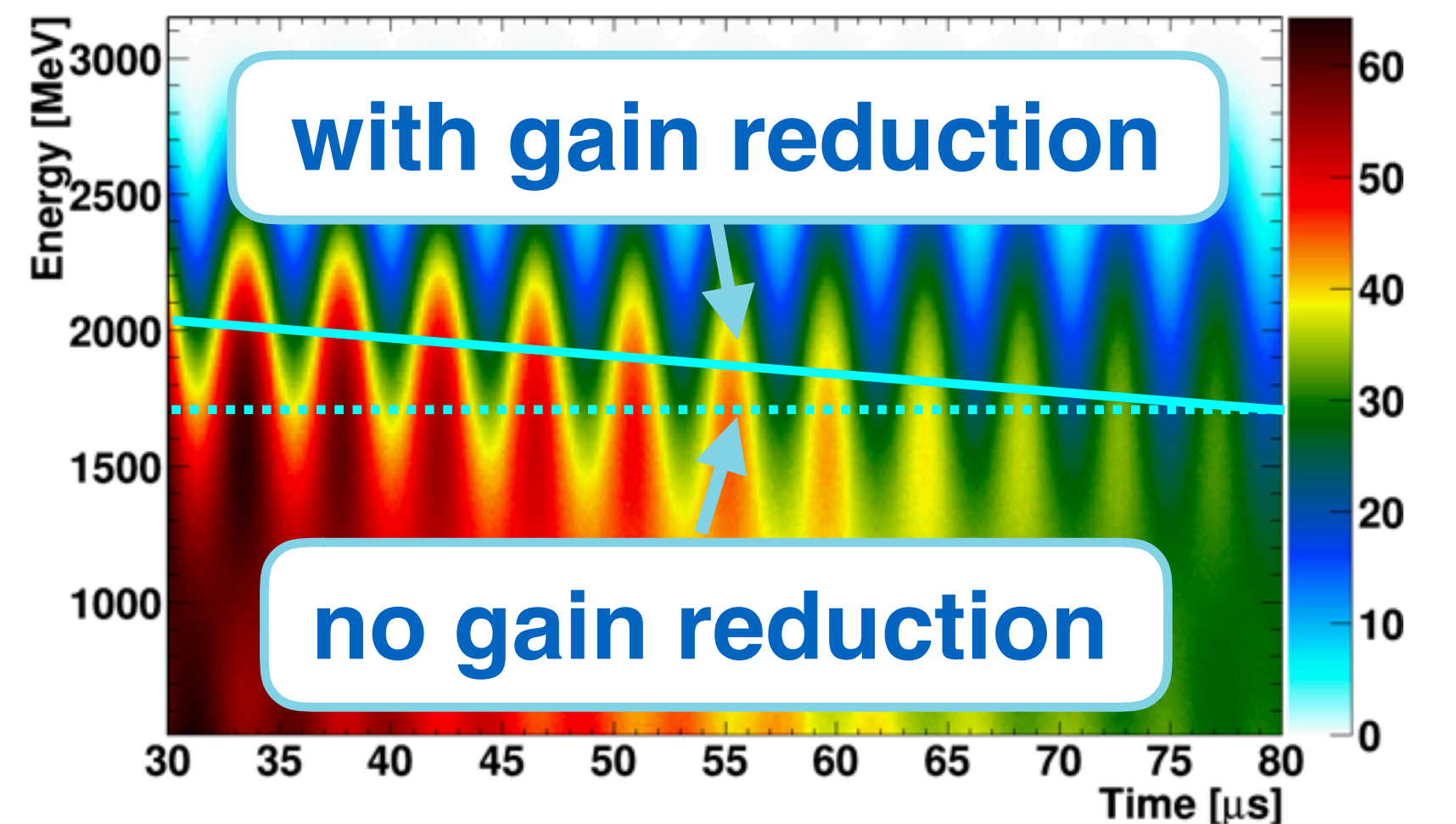


# Run 1 Analysis Status: $\omega_a$

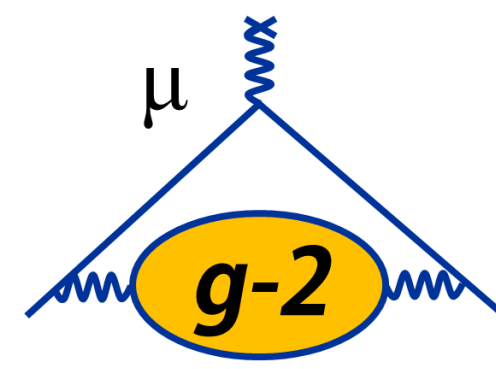
- Account for a number of effects that can affect the extraction of  $\omega_a$

$$N(t) = N_0 e^{-t/\tau} [1 - A \cos(\omega_a t + \phi)]$$

## Detector effects



- Gain changes over time in calorimeters affects phase of signal:  $N \rightarrow N(t)$ ,  $A \rightarrow A(t)$ ,  $\phi \rightarrow \phi(t)$
- Laser system provides corrections

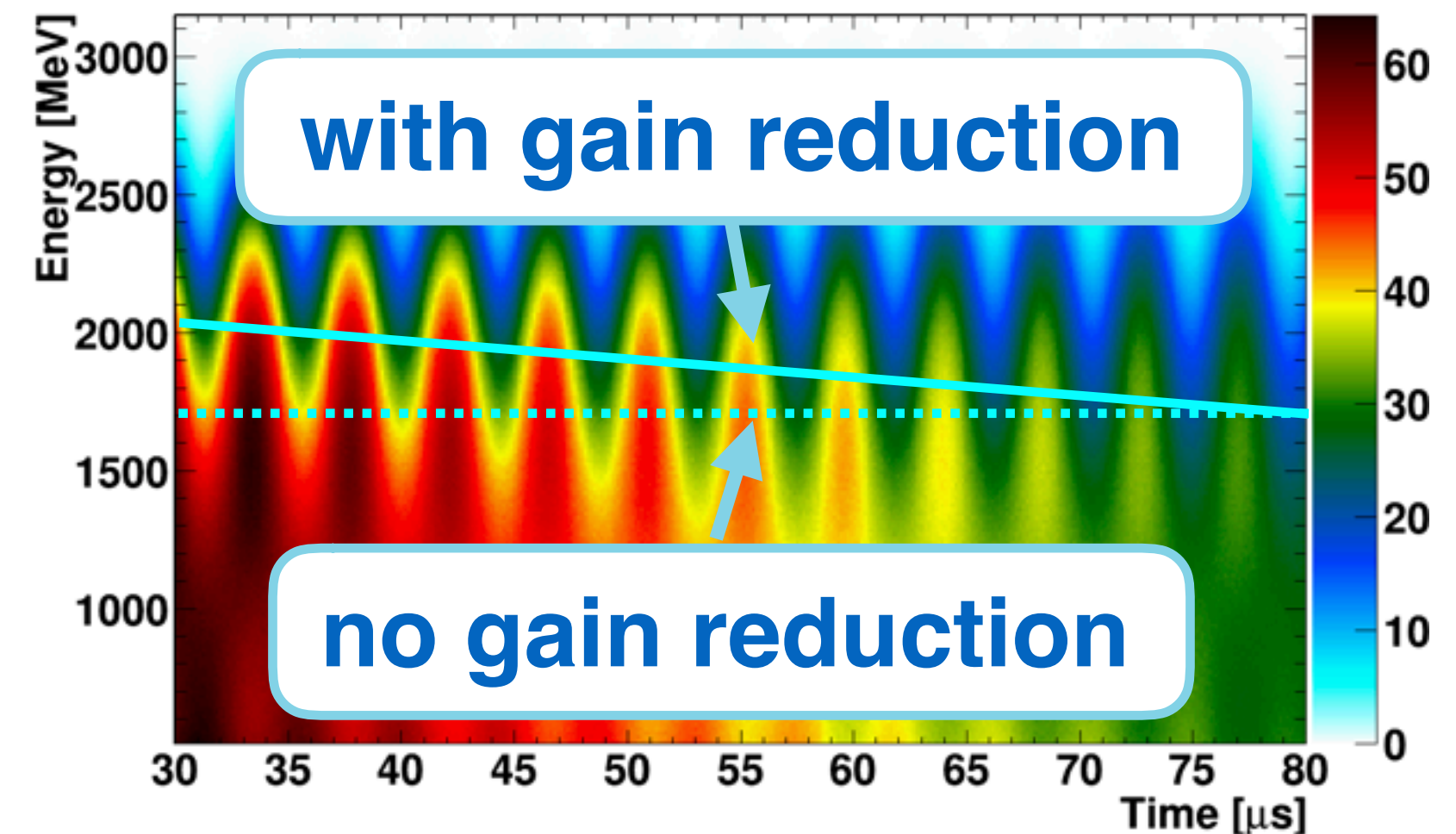


# Run 1 Analysis Status: $\omega_a$

- Account for a number of effects that can affect the extraction of  $\omega_a$

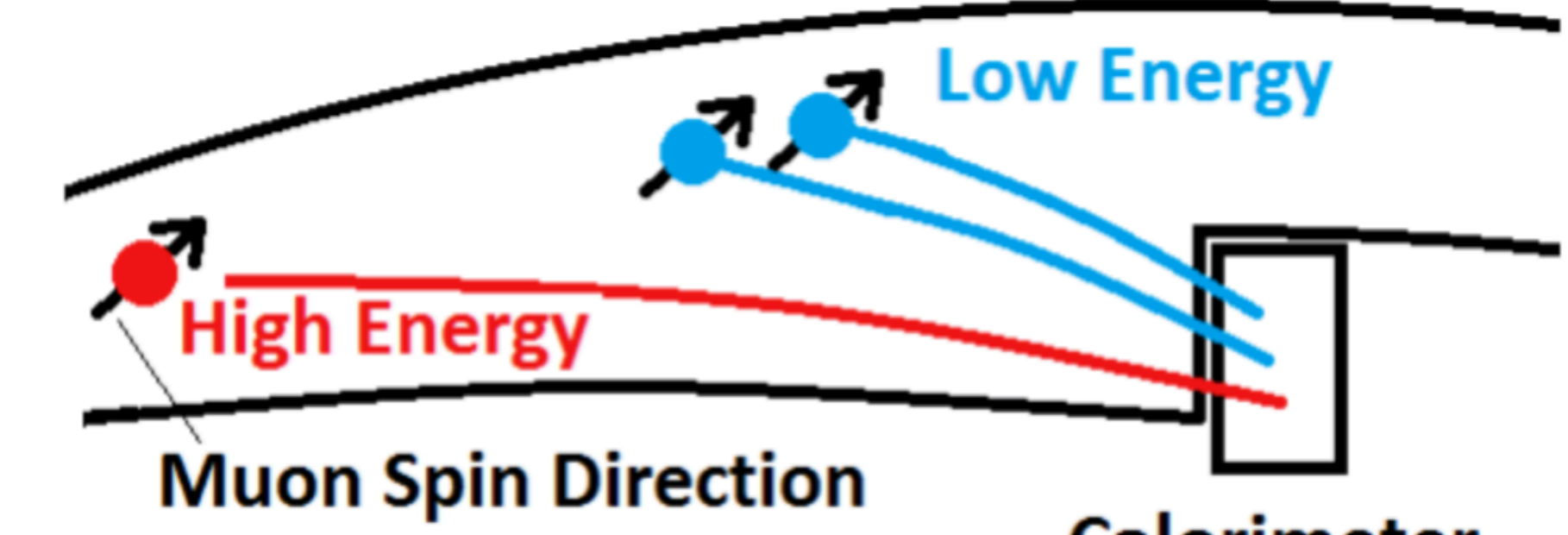
$$N(t) = N_0 e^{-t/\tau} [1 - A \cos(\omega_a t + \phi)]$$

## Detector effects

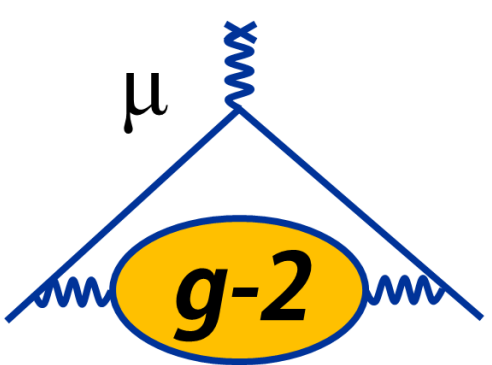


- Gain changes over time in calorimeters affects phase of signal:  $N \rightarrow N(t)$ ,  $A \rightarrow A(t)$ ,  $\phi \rightarrow \phi(t)$
- Laser system provides corrections

## Event pileup



- Low-energy events can mimic high-energy events in calorimeter
- Spin precession phase varies with energy — apparent high-energy decay carries phase of low-energy decays



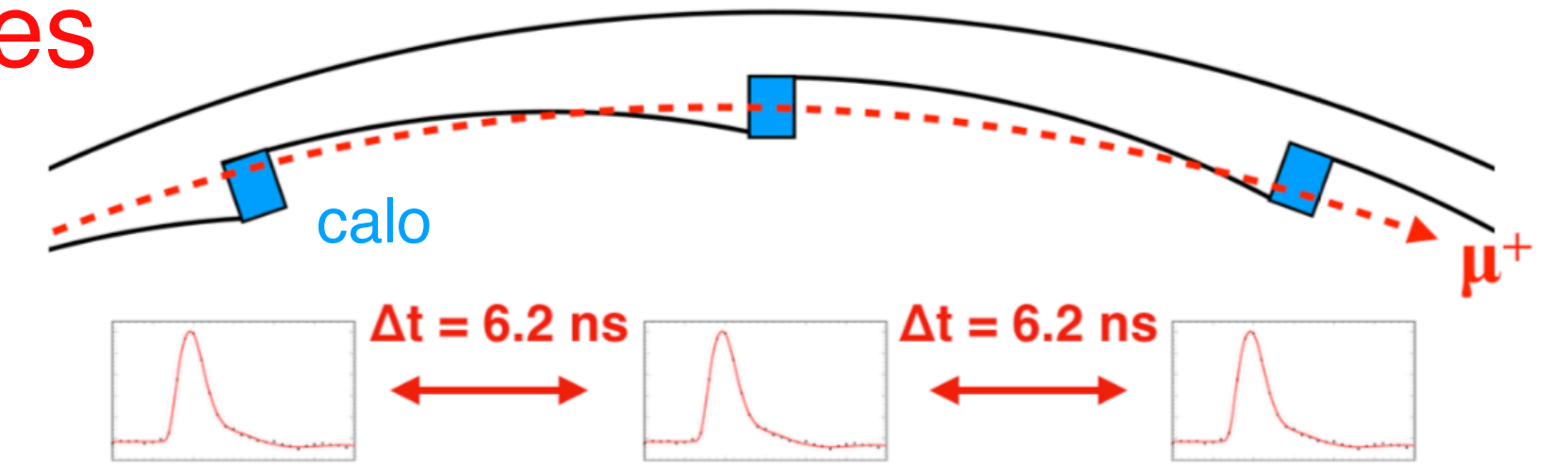
# Run 1 Analysis Status: $\omega_a$

- Account for a number of effects that can affect the extraction of  $\omega_a$

$$N(t) = N_0 e^{-t/\tau} [1 - A \cos(\omega_a t + \phi)]$$

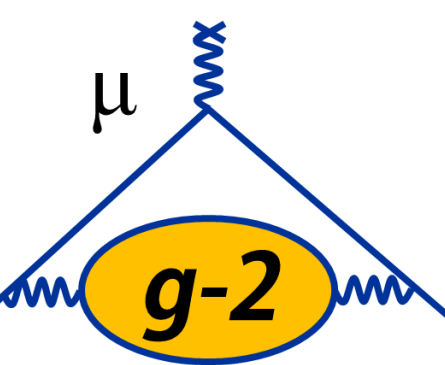
## Beam dynamics

### Muon losses



- Muons can leave storage ring by decaying or escaping
- Exhibit specific signature in multiple calorimeters
- Amplitude  $N_0$  scaled by:

$$\Lambda(t) = 1 - K_{\text{loss}} \int_0^t e^{t'/\tau} L(t') dt'$$



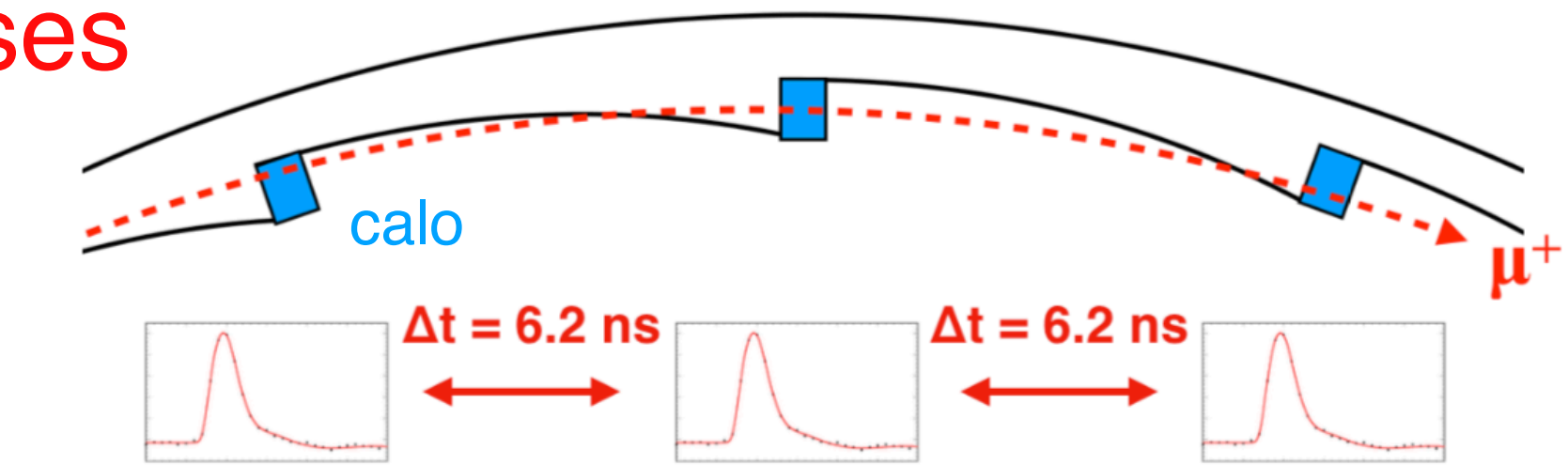
# Run 1 Analysis Status: $\omega_a$

- Account for a number of effects that can affect the extraction of  $\omega_a$

$$N(t) = N_0 e^{-t/\tau} [1 - A \cos(\omega_a t + \phi)]$$

## Beam dynamics

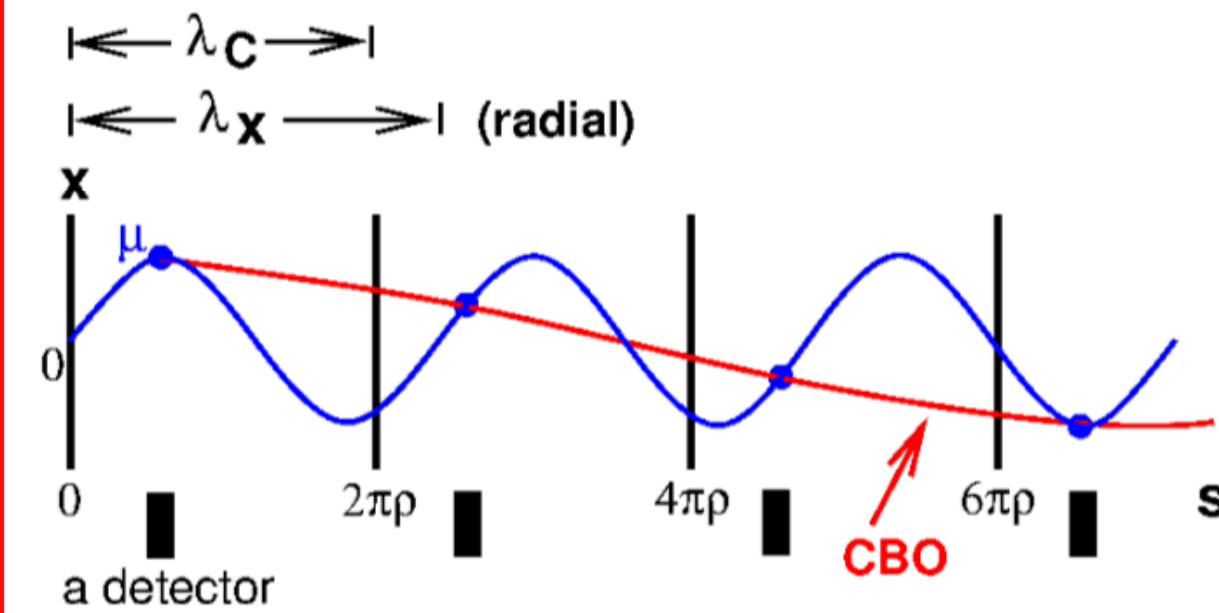
### Muon losses



- Muons can leave storage ring by decaying or escaping
- Exhibit specific signature in multiple calorimeters
- Amplitude  $N_0$  scaled by:

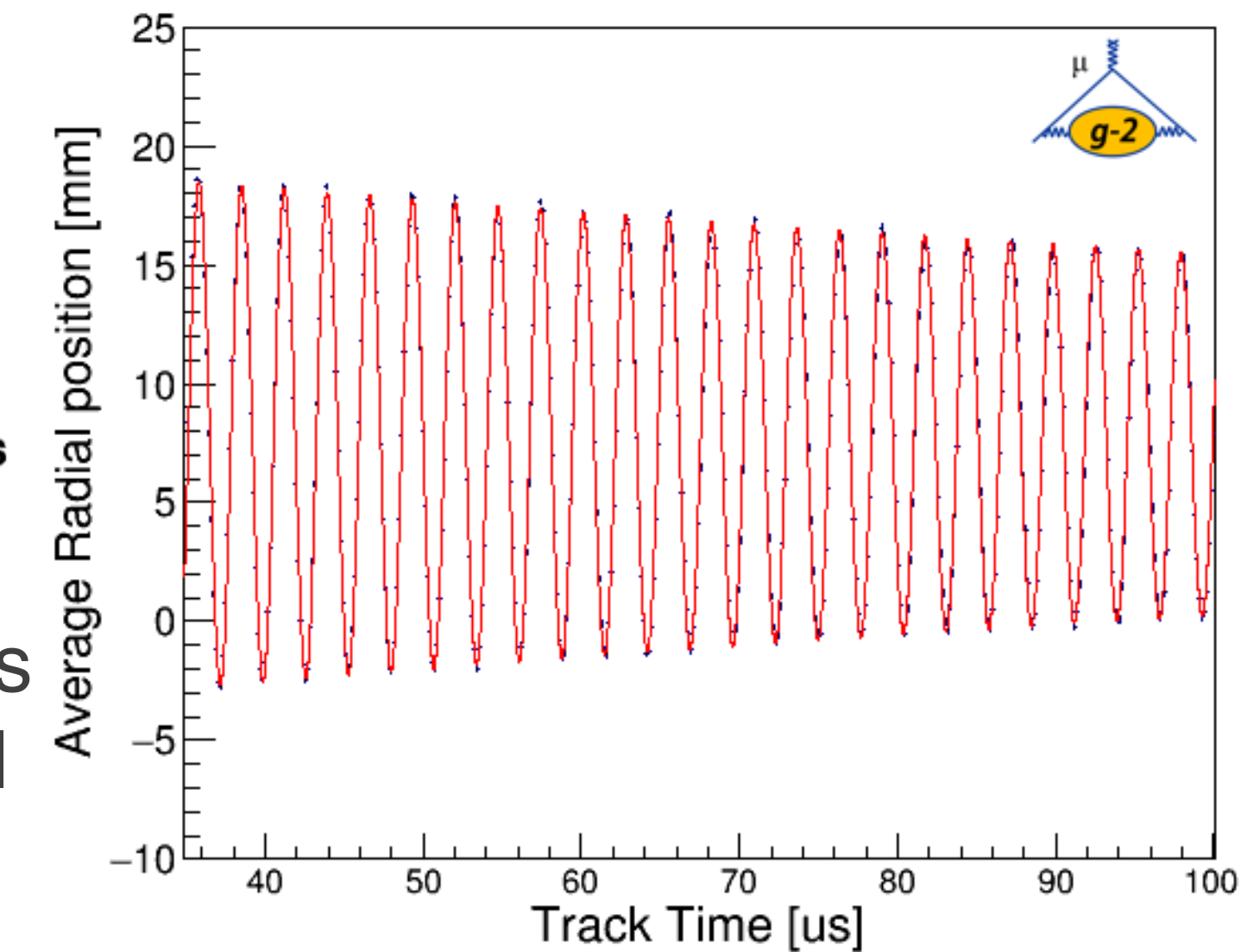
$$\Lambda(t) = 1 - K_{\text{loss}} \int_0^t e^{t'/\tau} L(t') dt'$$

### Coherent betatron oscillations (CBO)

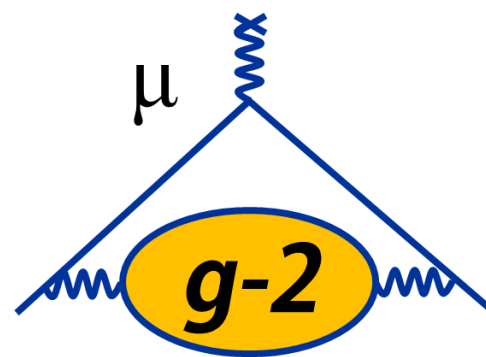


- Acceptance of calorimeters affected by coherent radial beam motion
- Amplitude  $N_0$  scaled by:

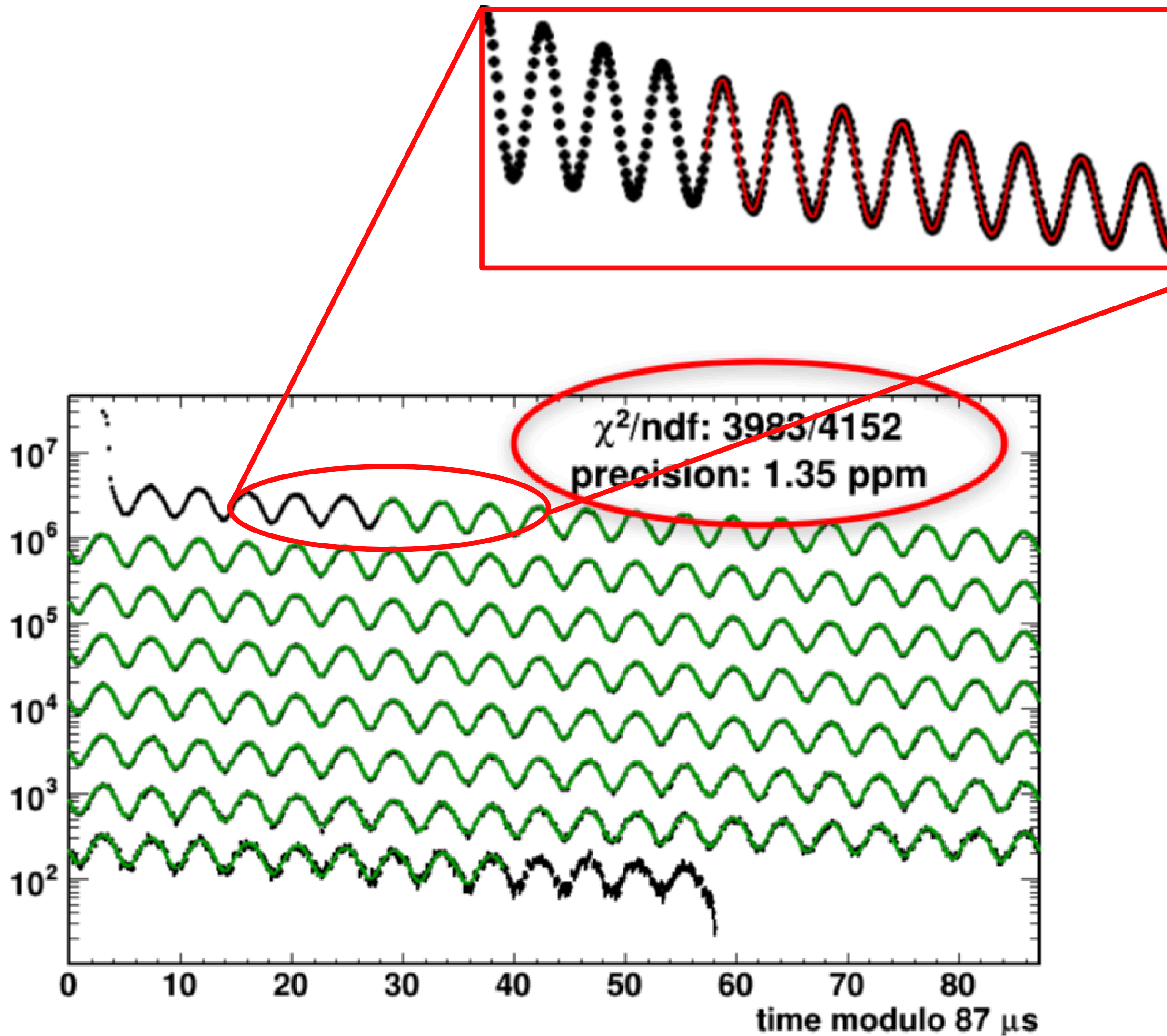
$$C(t) = 1 - e^{-t/\tau_{\text{CBO}}} A_1 \cos(\omega_{\text{CBO}} t + \phi_1)$$



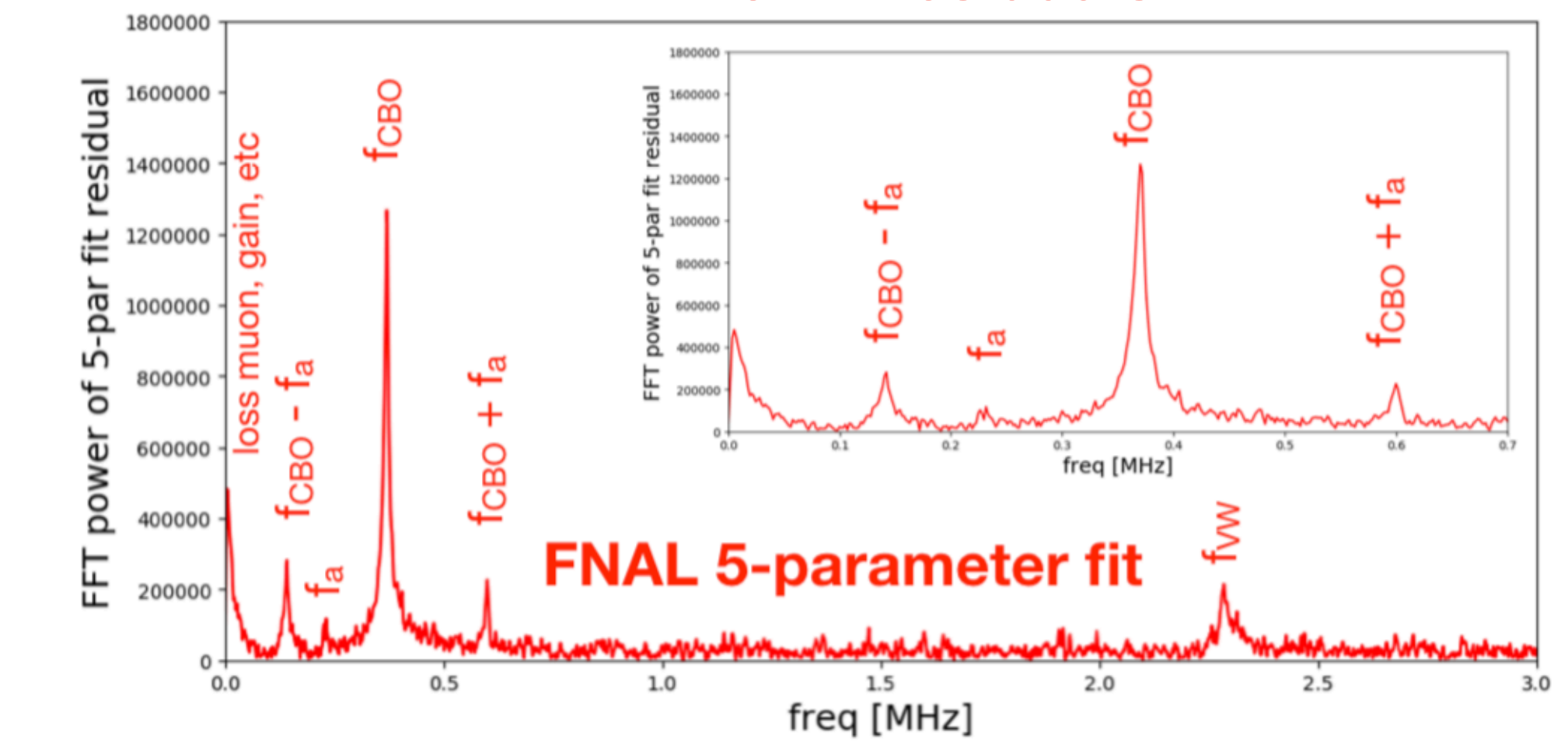
# Run 1 Analysis Status: $\omega_a$



Simple five-parameter fit

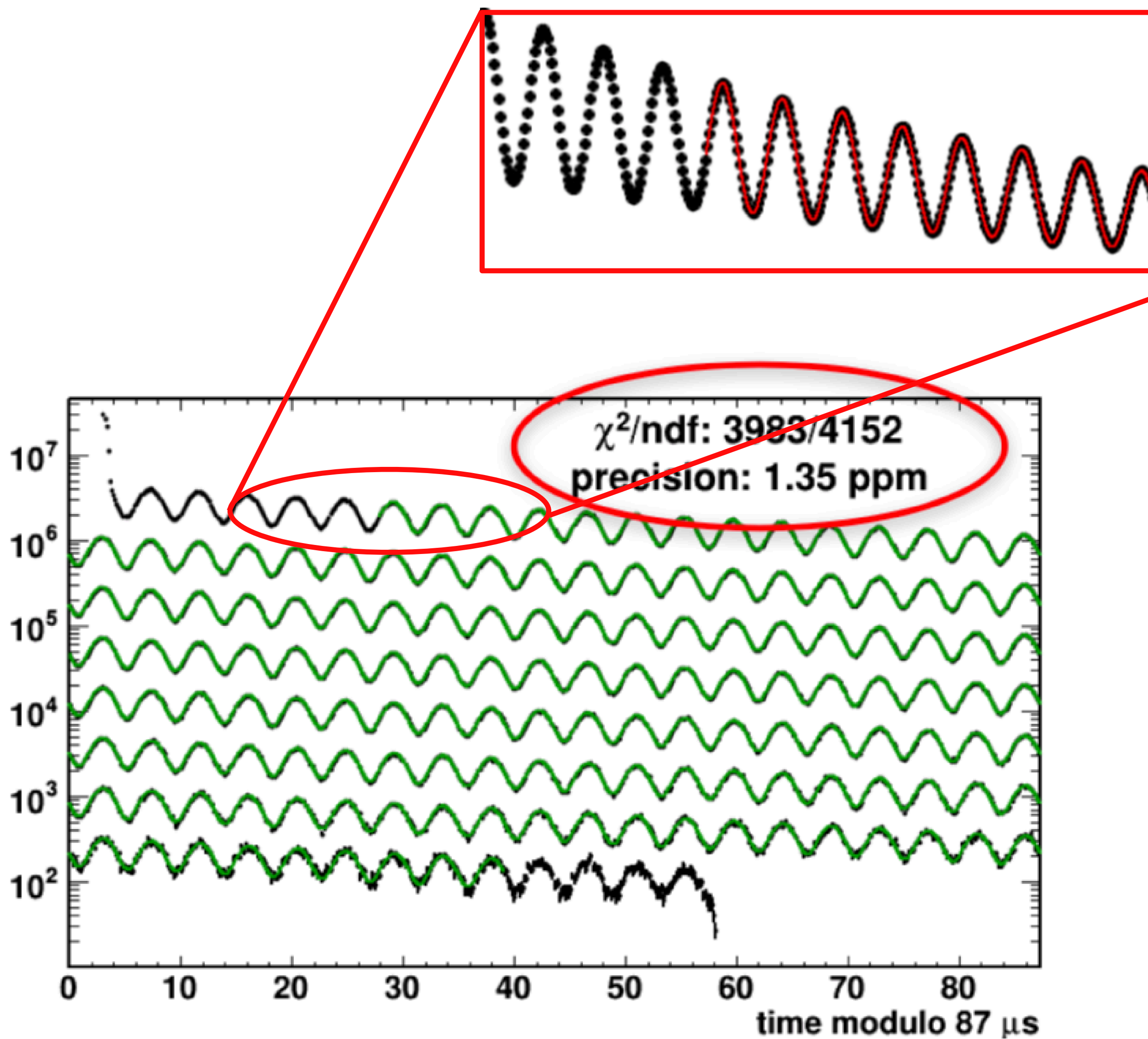
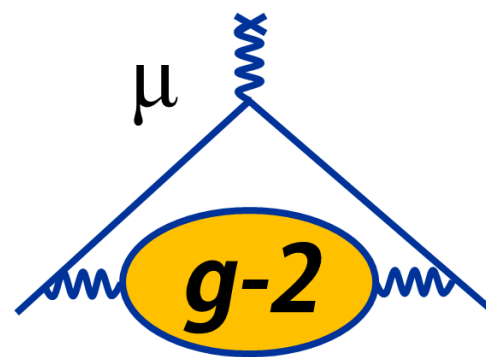


FFT of fit residuals



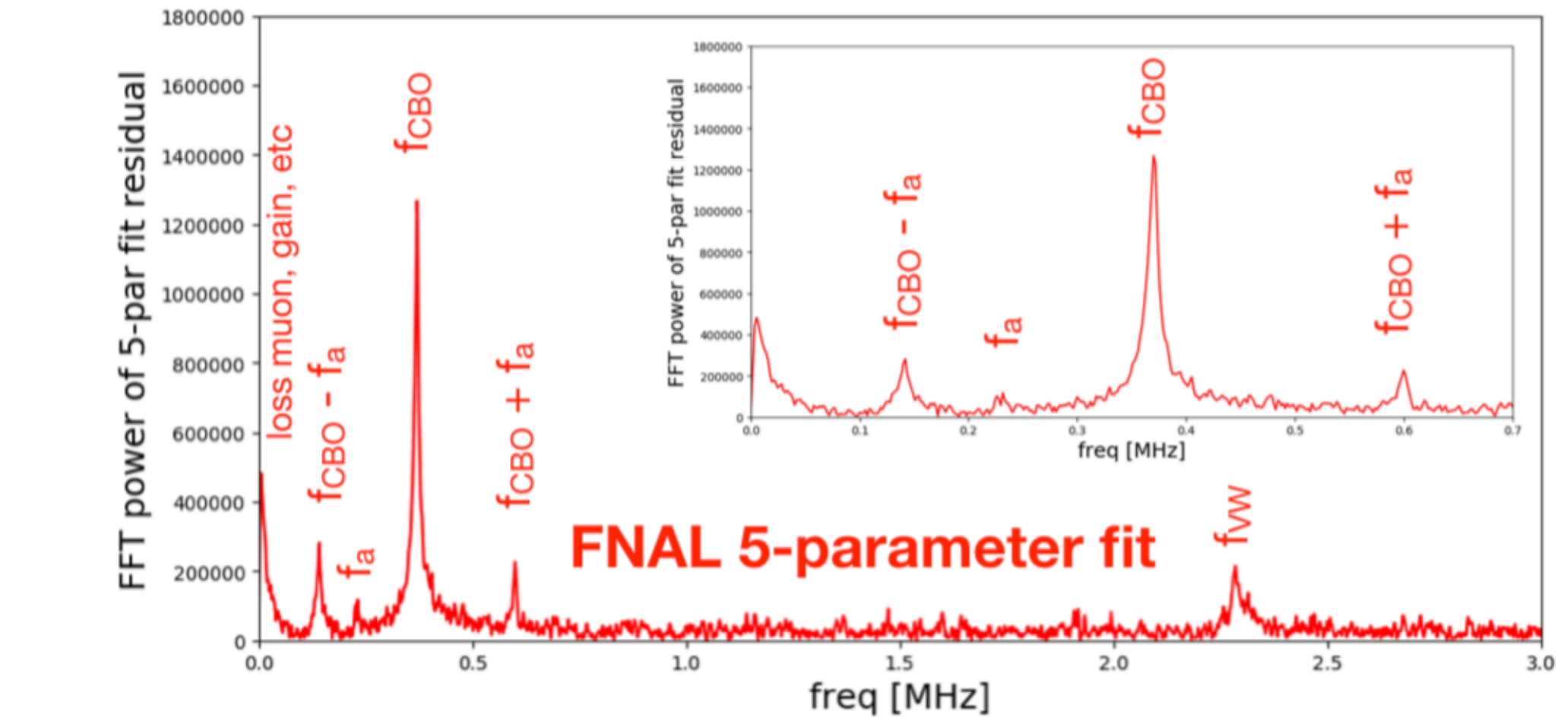
FNAL 5-parameter fit

# Run 1 Analysis Status: $\omega_a$

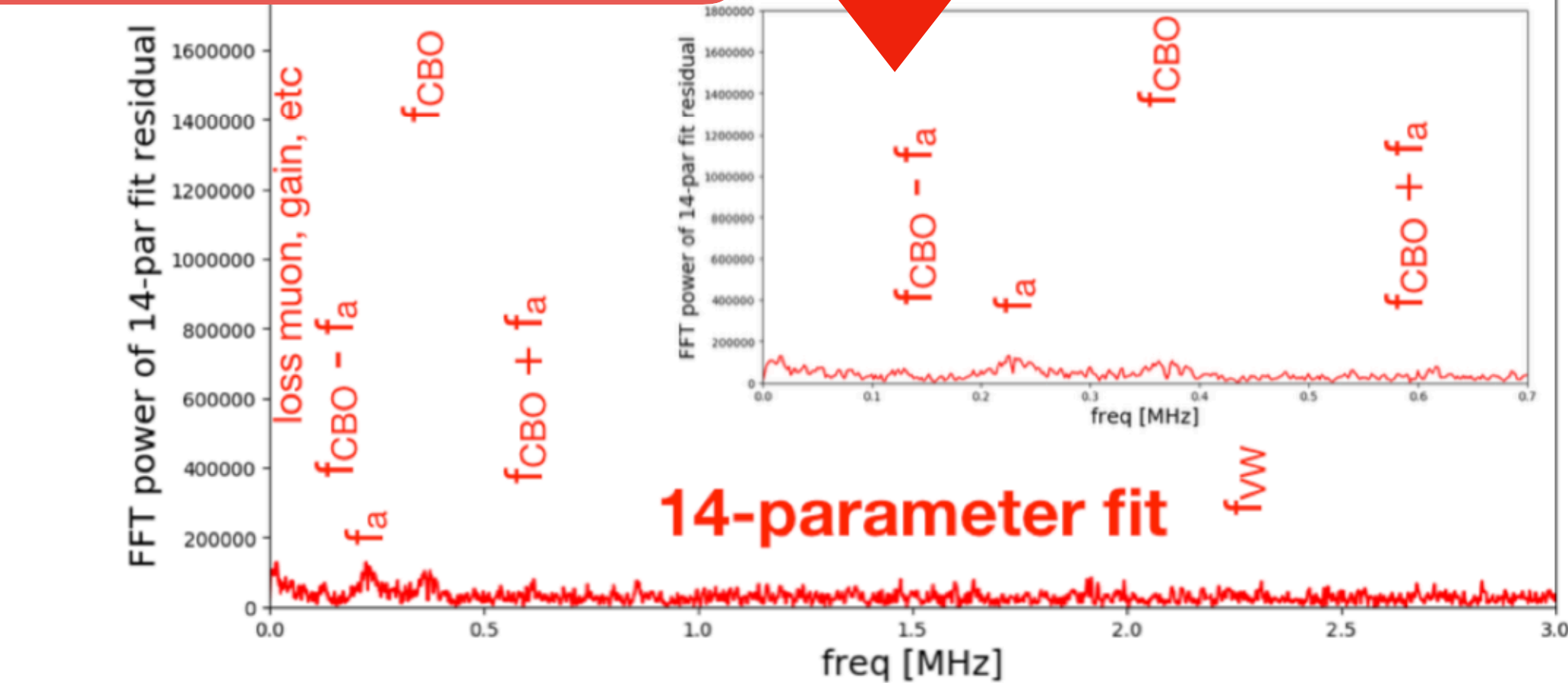


Simple five-parameter fit

FFT of fit residuals

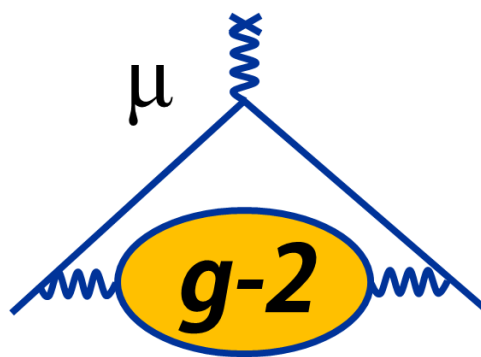


Big improvements when accounting  
for CBO, lost muons,...

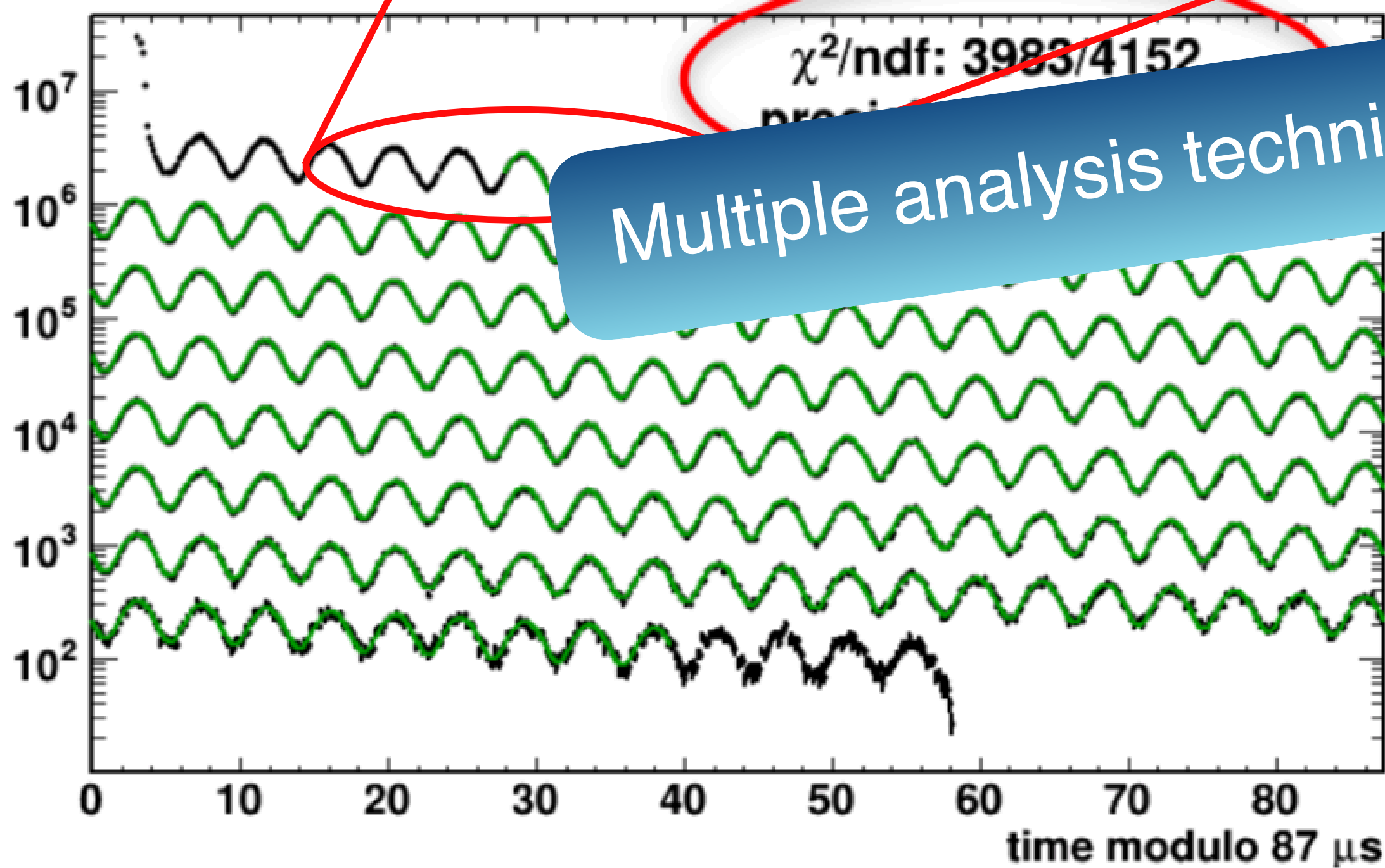


UMassAmherst

# Run 1 Analysis Status: $\omega_a$

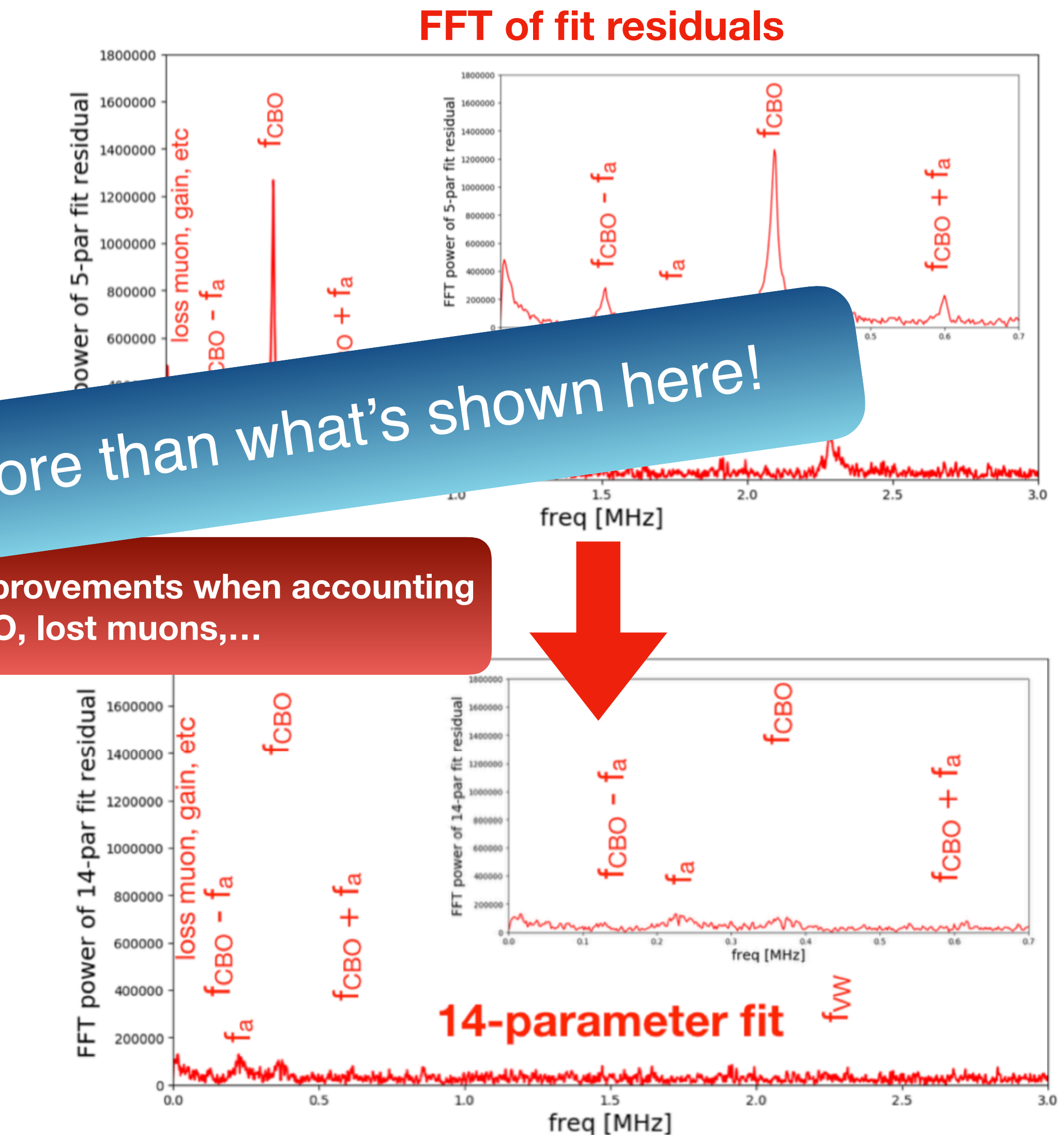


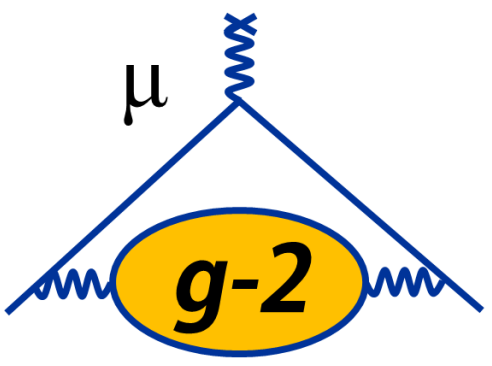
Simple five-parameter fit



Multiple analysis techniques – more than what's shown here!

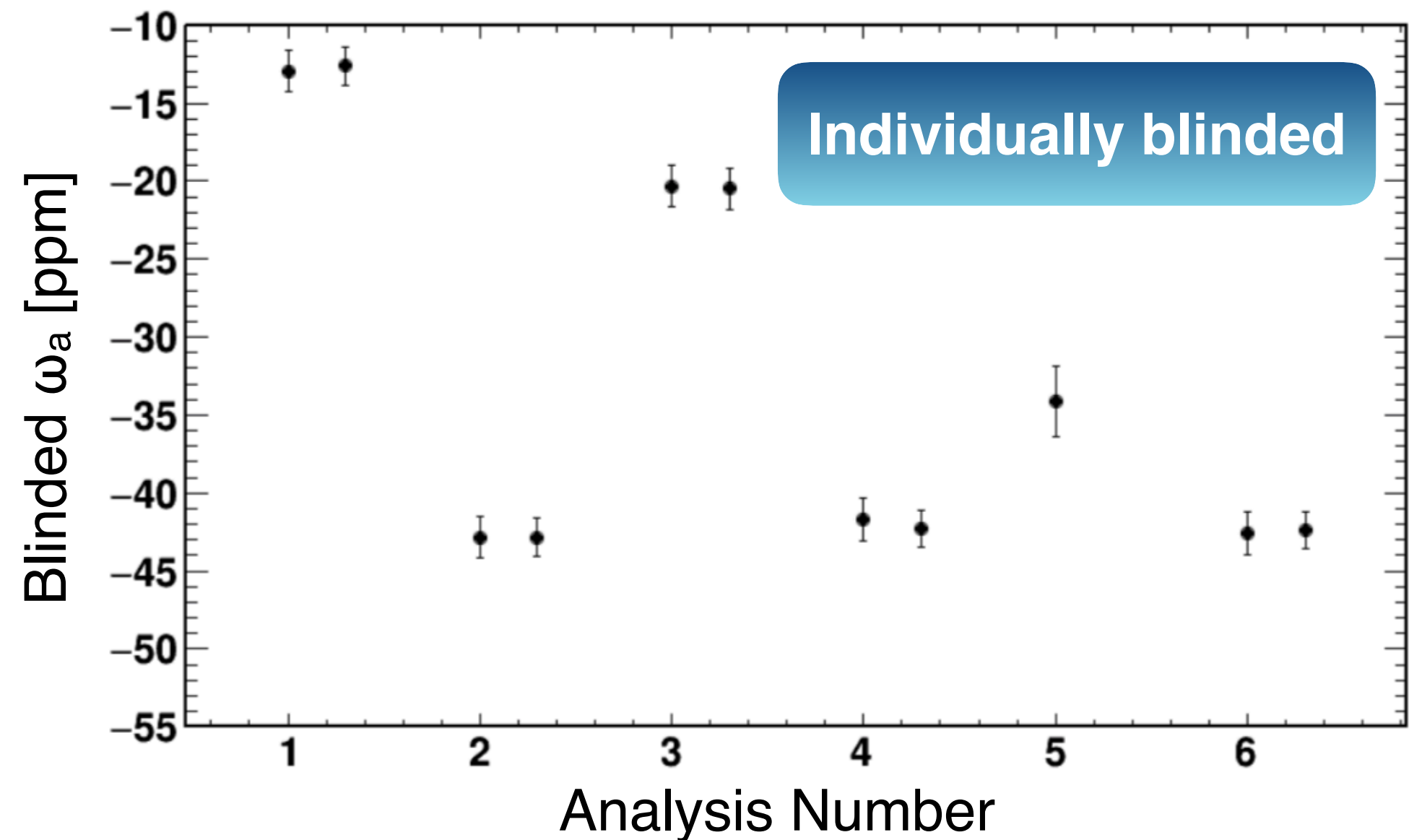
Big improvements when accounting  
for CBO, lost muons,...

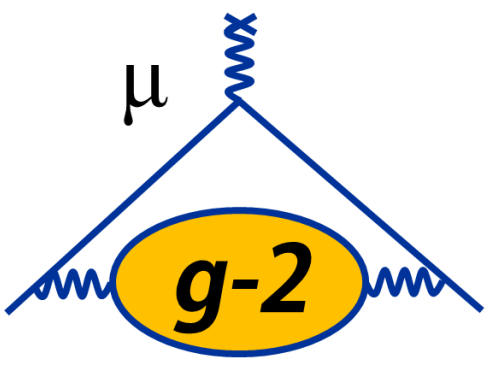




# Run 1 Analysis Status: Relative Unblinding for $\omega_a$

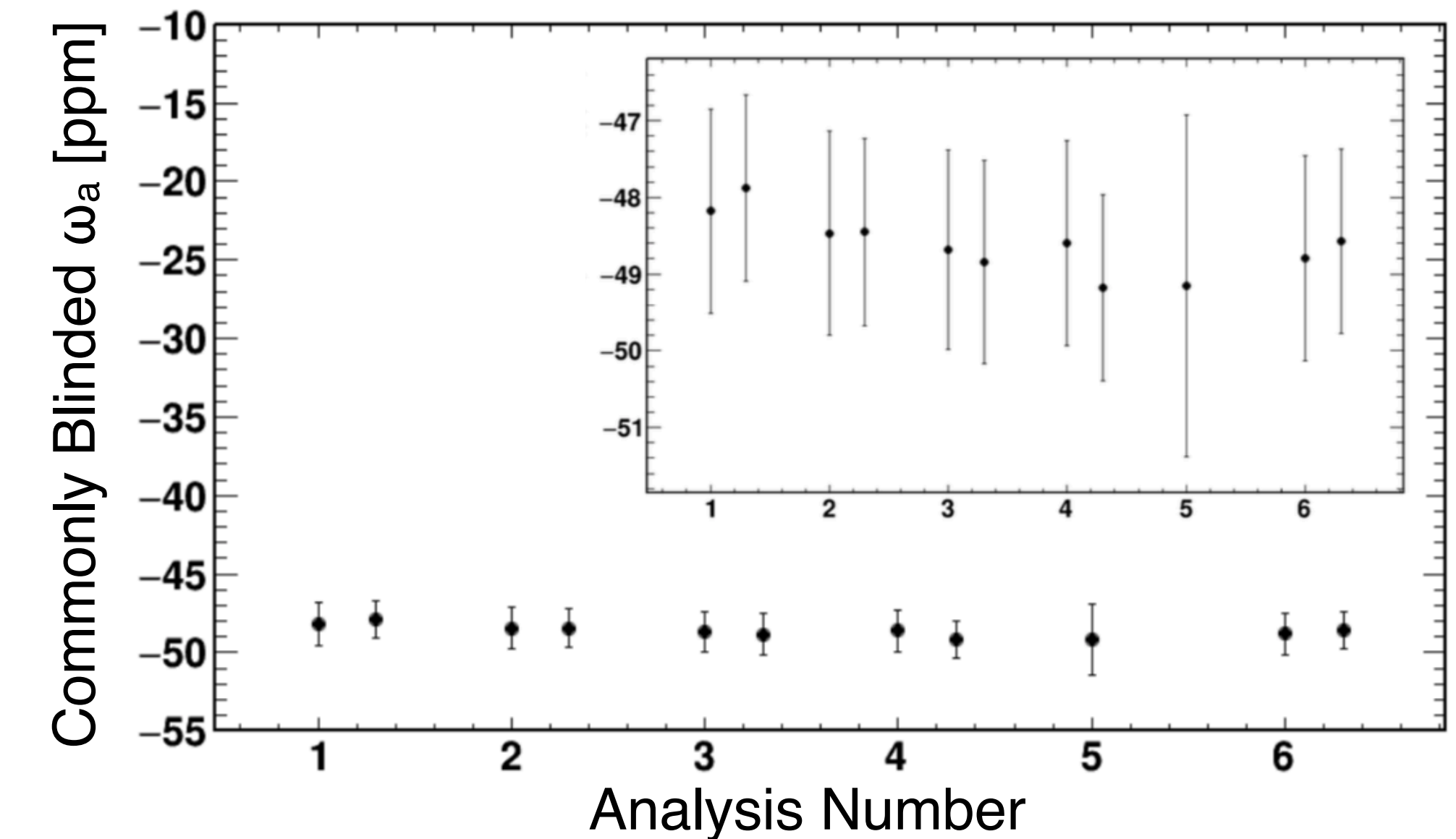
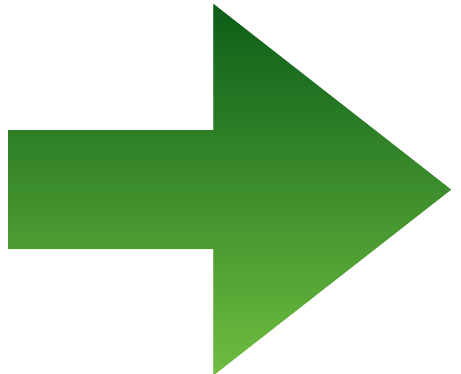
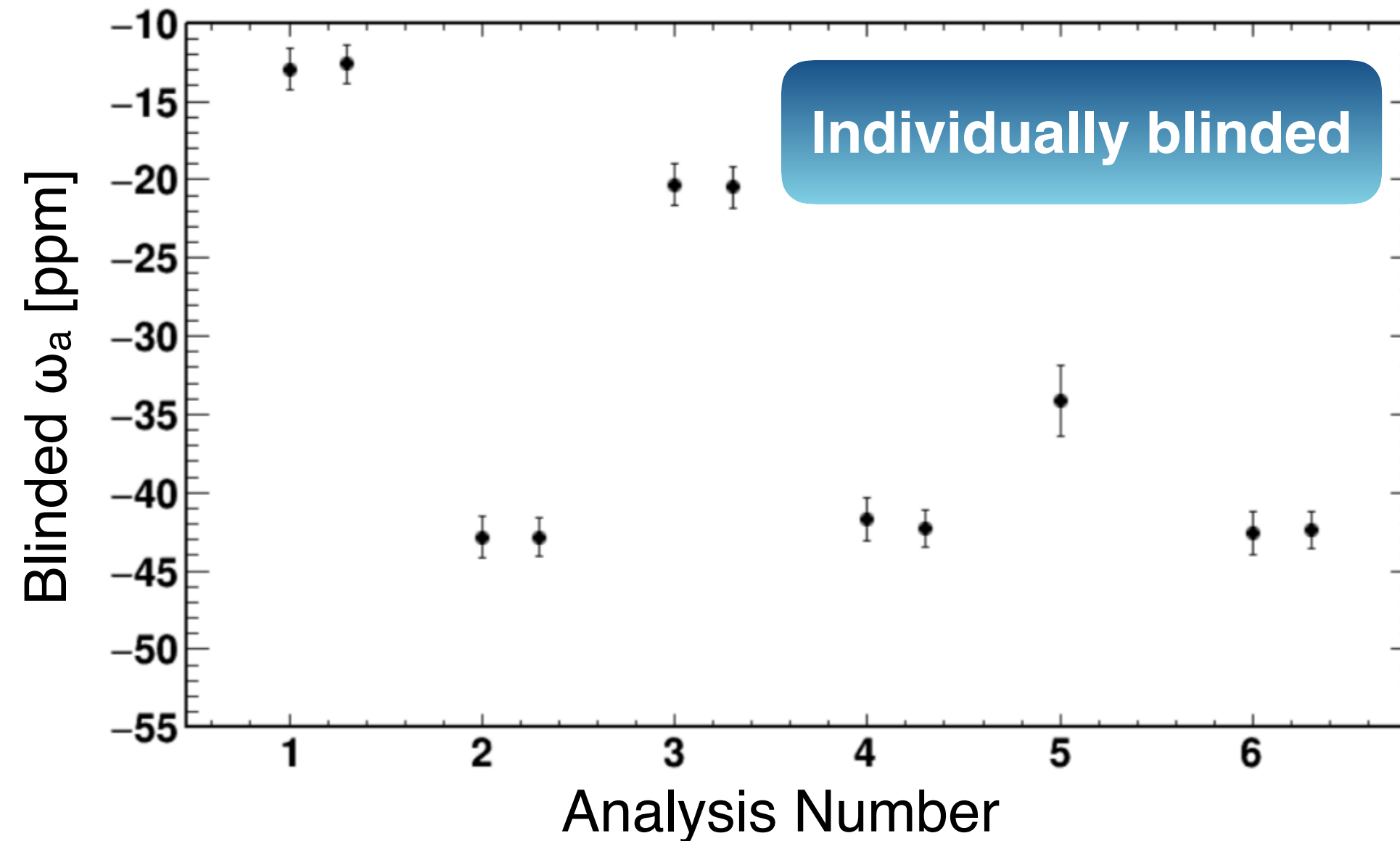
- Doubly-blinded in  $\omega_a$  measurement: Clock tuned to  $40 \text{ MHz} \pm 25 \text{ ppm}$
- Analyzers' results come with random frequency offset  $\omega_a \rightarrow \omega_a \pm 25 \text{ ppm}$
- Recently compared results on **subset of data** at a **common blinded value**





# Run 1 Analysis Status: Relative Unblinding for $\omega_a$

- Doubly-blinded in  $\omega_a$  measurement: Clock tuned to  $40 \text{ MHz} \pm 25 \text{ ppm}$
- Analyzers' results come with random frequency offset  $\omega_a \rightarrow \omega_a \pm 25 \text{ ppm}$
- Recently compared results on **subset of data** at a **common blinded value**



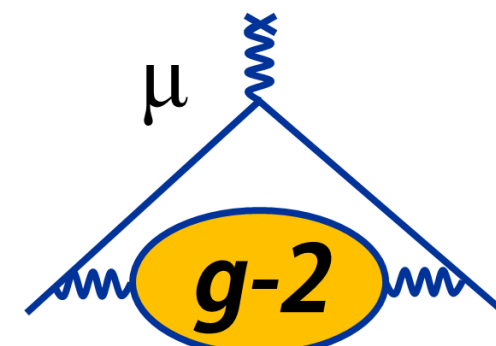
- Consistent results at **common blinded value** builds confidence in our analyses

Paramagnetism

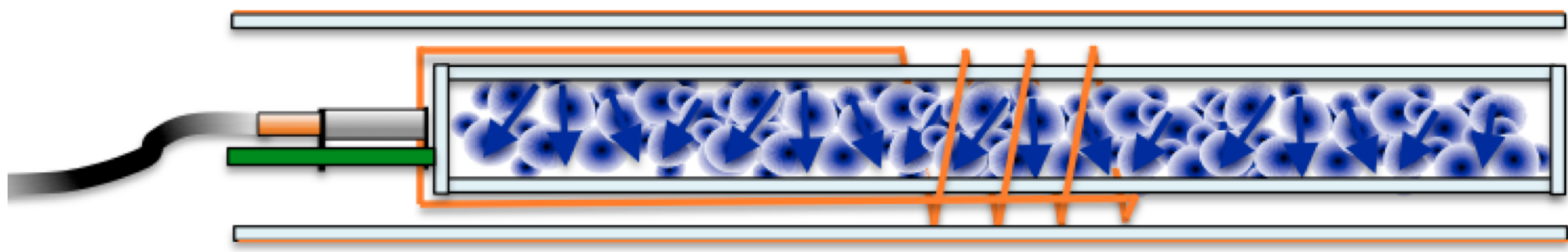
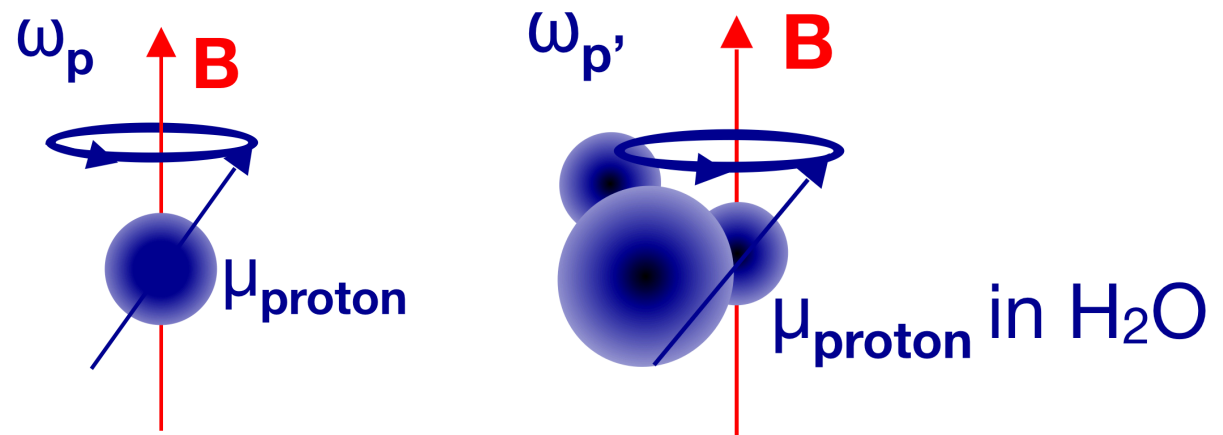
# Run 1 Analysis Status — $\omega_p$

$$a_\mu = \frac{\omega_a}{\tilde{\omega}_p} \frac{\mu_p m_\mu g_e}{\mu_e m_e 2}$$

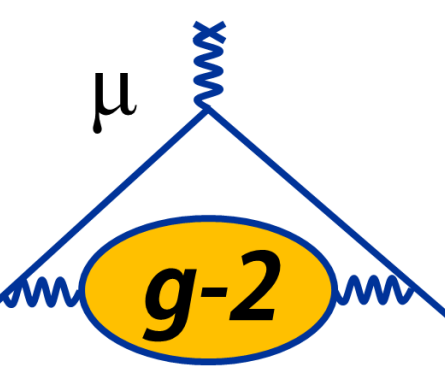
# Run 1 Analysis Status: $\omega_p$ – Field Calibration



- In the experiment, need to extract  $\omega_p$ ; however, don't have free protons
  - Need a calibration
- Field at the proton differs from the applied field

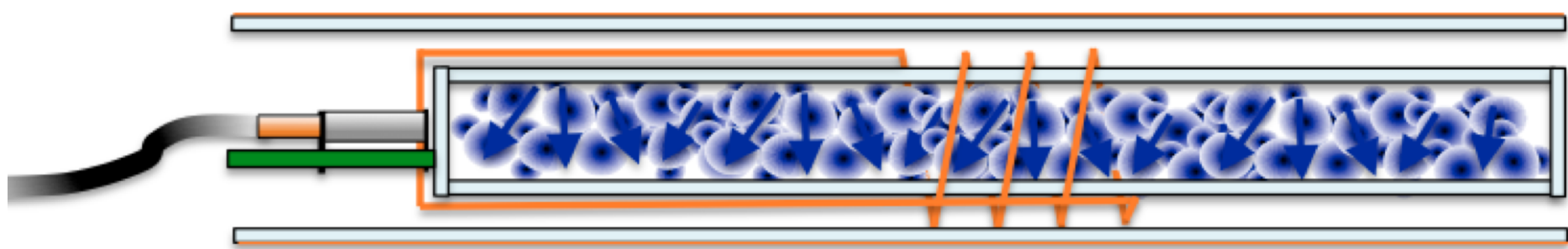
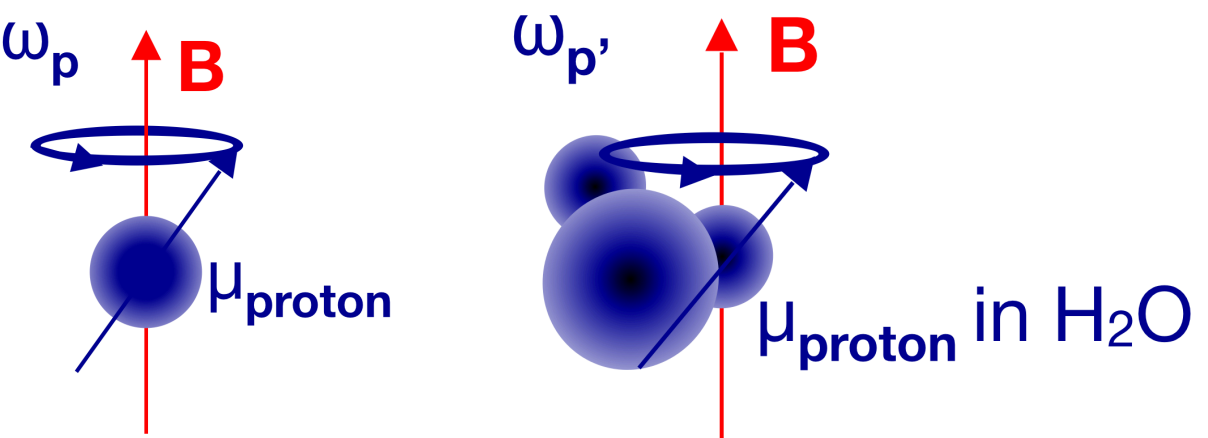


$$\omega_p^{\text{meas}} \approx \omega_p^{\text{free}}$$



# Run 1 Analysis Status: $\omega_p$ – Field Calibration

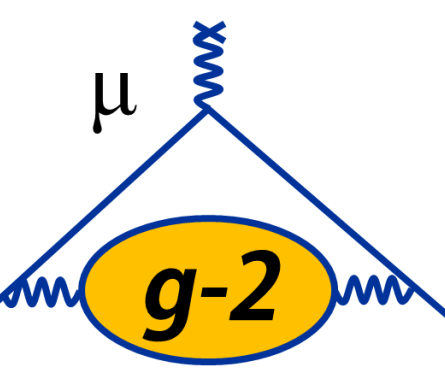
- In the experiment, need to extract  $\omega_p$ ; however, don't have free protons
  - Need a calibration
- Field at the proton differs from the applied field



$$\omega_p^{\text{meas}} = \omega_p^{\text{free}} \left[ 1 - \sigma(H_2O, T) \right]$$

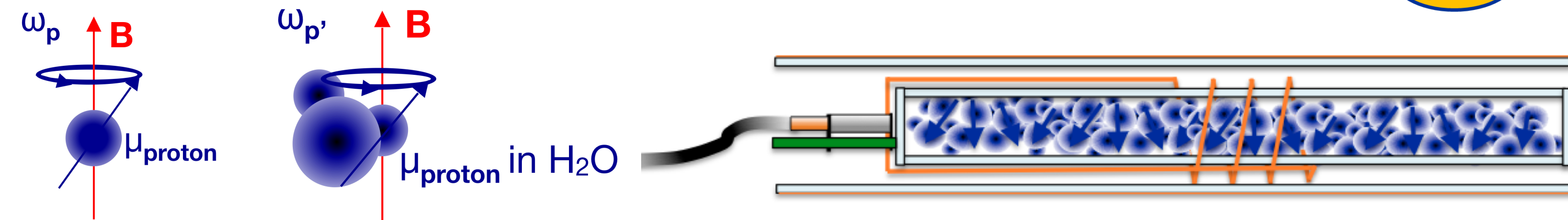
Protons in  $H_2O$  molecules, diamagnetism of electrons screens protons => local B changes

- $\sigma = 25\ 691(11) \times 10^{-9}$  at 25 deg C [P.J. Mohr et al, Rev. Mod. Phys. **84**, 1527 (2012)]



# Run 1 Analysis Status: $\omega_p$ – Field Calibration

- In the experiment, need to extract  $\omega_p$ ; however, don't have free protons
  - Need a calibration
- Field at the proton differs from the applied field



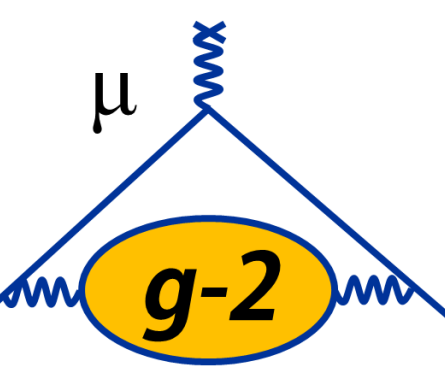
$$\omega_p^{\text{meas}} = \omega_p^{\text{free}} \left[ 1 - \sigma(\text{H}_2\text{O}, T) - \left( \frac{\varepsilon}{4\pi} - \frac{1}{3} \right) \chi(\text{H}_2\text{O}, T) \right]$$

Protons in  $\text{H}_2\text{O}$  molecules, diamagnetism of electrons screens protons => local B changes

- $\sigma = 25\ 691(11) \times 10^{-9}$  at 25 deg C [P.J. Mohr et al, Rev. Mod. Phys. **84**, 1527 (2012)]

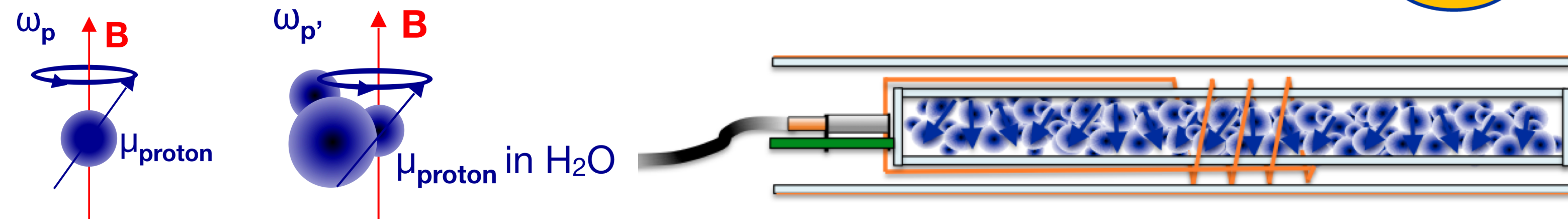
Magnetic susceptibility of water gives shape-dependent perturbation

- $\varepsilon = 4\pi/3$  (perfect sphere)
- $\varepsilon = 2\pi$  (infinite cylinder) when probe is perpendicular to B
- $\chi_{\text{H}_2\text{O}}(T = 20^\circ\text{C}) = -9049(9) \times 10^{-9}$  [world average]



# Run 1 Analysis Status: $\omega_p$ – Field Calibration

- In the experiment, need to extract  $\omega_p$ ; however, don't have free protons
  - Need a calibration
- Field at the proton differs from the applied field



$$\omega_p^{\text{meas}} = \omega_p^{\text{free}} \left[ 1 - \sigma(\text{H}_2\text{O}, T) - \left( \frac{\varepsilon}{4\pi} - \frac{1}{3} \right) \chi(\text{H}_2\text{O}, T) - \delta_s \right]$$

Protons in  $\text{H}_2\text{O}$  molecules, diamagnetism of electrons screens protons => local B changes

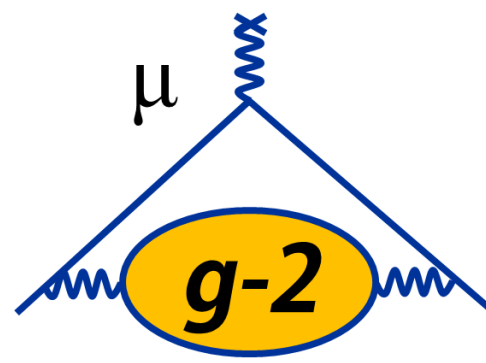
- $\sigma = 25\ 691(11) \times 10^{-9}$  at 25 deg C [P.J. Mohr et al, Rev. Mod. Phys. **84**, 1527 (2012)]

Magnetic susceptibility of water gives shape-dependent perturbation

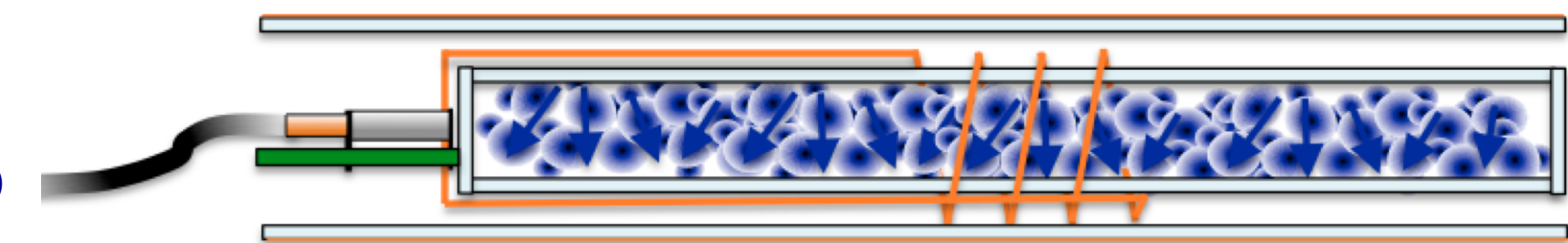
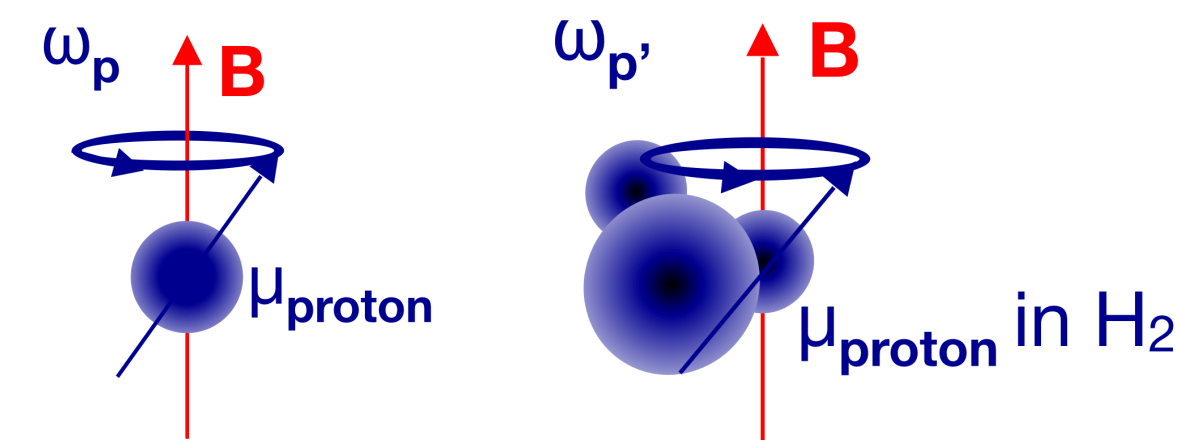
- $\varepsilon = 4\pi/3$  (perfect sphere)
- $\varepsilon = 2\pi$  (infinite cylinder) when probe is perpendicular to B
- $\chi_{\text{H}_2\text{O}}(T = 20^\circ\text{C}) = -9049(9) \times 10^{-9}$  [world average]

Magnetization of probe materials, geometry perturbs field experienced by protons

# Run 1 Analysis Status: $\omega_p$ – Field Calibration



- In the experiment, need to extract  $\omega_p$ ; however, don't have free protons
  - Need a calibration
- Field at the proton differs from the applied field



paramagnetic impurities in water sample

$$\omega_p^{\text{meas}} = \omega_p^{\text{free}} \left[ 1 - \sigma(\text{H}_2\text{O}, T) - \left( \frac{\varepsilon}{4\pi} - \frac{1}{3} \right) \chi(\text{H}_2\text{O}, T) - \delta_s - \delta_p \right]$$

Protons in  $\text{H}_2\text{O}$  molecules, diamagnetism of electrons screens protons => local B changes

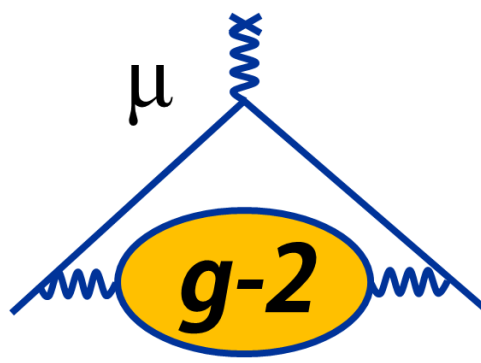
- $\sigma = 25\ 691(11) \times 10^{-9}$  at 25 deg C [P.J. Mohr et al, Rev. Mod. Phys. **84**, 1527 (2012)]

Magnetic susceptibility of water gives shape-dependent perturbation

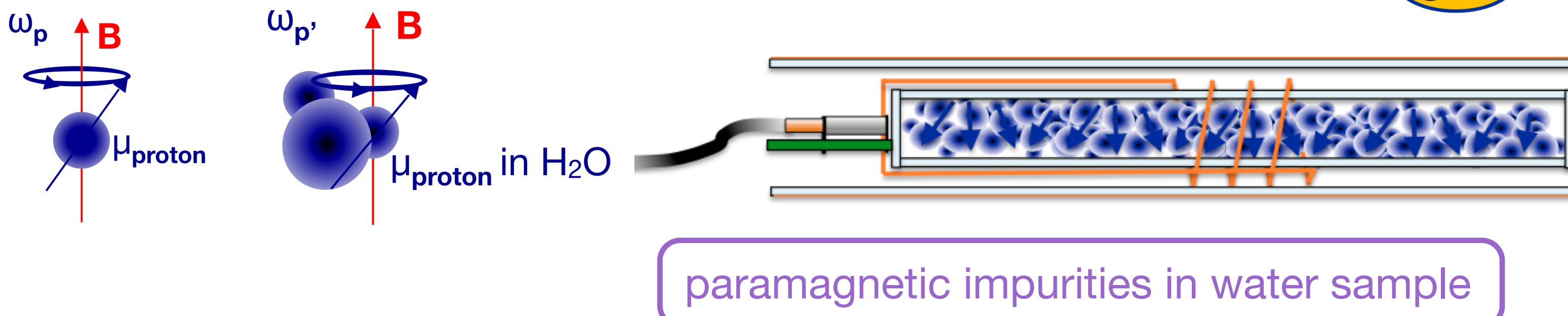
- $\varepsilon = 4\pi/3$  (perfect sphere)
- $\varepsilon = 2\pi$  (infinite cylinder) when probe is perpendicular to B
- $\chi_{\text{H}_2\text{O}}(T = 20^\circ\text{C}) = -9049(9) \times 10^{-9}$  [world average]

Magnetization of probe materials, geometry perturbs field experienced by protons

# Run 1 Analysis Status: $\omega_p$ – Field Calibration



- In the experiment, need to extract  $\omega_p$ ; however, don't have free protons
  - Need a calibration
- Field at the proton differs from the applied field



$$\omega_p^{\text{meas}} = \omega_p^{\text{free}} \left[ 1 - \sigma(\text{H}_2\text{O}, T) - \left( \frac{\varepsilon}{4\pi} - \frac{1}{3} \right) \chi(\text{H}_2\text{O}, T) - \delta_s - \delta_p - \delta_{\text{RD}} - \delta_d \right]$$

Protons in  $\text{H}_2\text{O}$  molecules, diamagnetism of electrons screens protons => local B changes

- $\sigma = 25\ 691(11) \times 10^{-9}$  at 25 deg C [P.J. Mohr et al, Rev. Mod. Phys. **84**, 1527 (2012)]

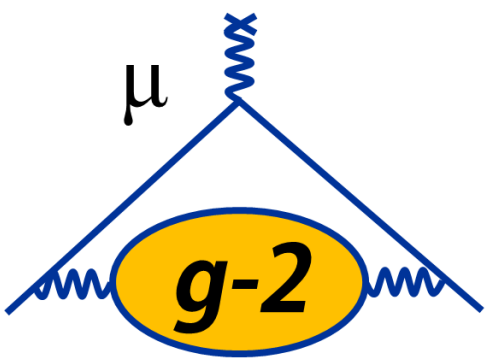
Magnetic susceptibility of water gives shape-dependent perturbation

- $\varepsilon = 4\pi/3$  (perfect sphere)
- $\varepsilon = 2\pi$  (infinite cylinder) when probe is perpendicular to B
- $\chi_{\text{H}_2\text{O}}(T = 20^\circ\text{C}) = -9049(9) \times 10^{-9}$  [world average]

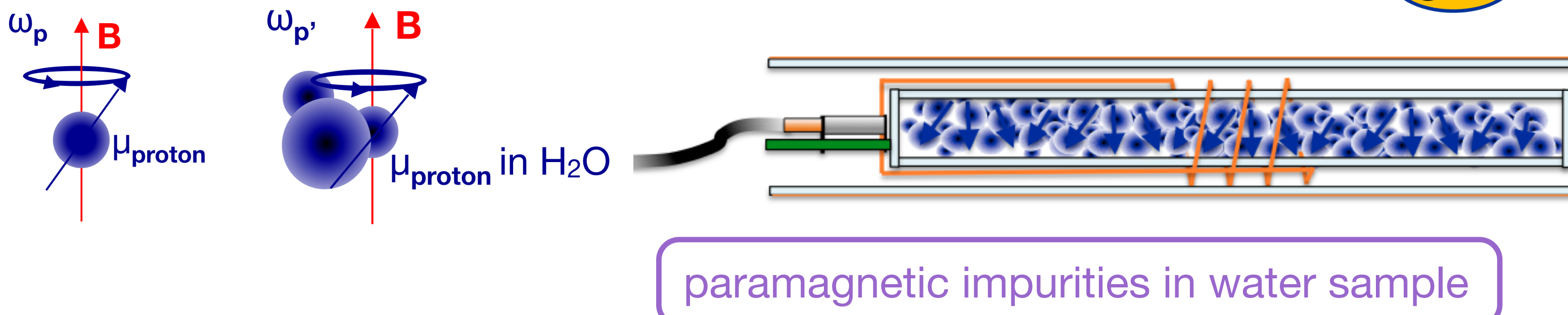
Magnetization of probe materials, geometry perturbs field experienced by protons

Dynamic effects: radiation damping, dipolar field from protons

# Run 1 Analysis Status: $\omega_p$ – Field Calibration



- In the experiment, need to extract  $\omega_p$ ; however, don't have free protons
  - Need a calibration
- Field at the proton differs from the applied field



$$\omega_p^{\text{meas}} = \omega_p^{\text{free}} \left[ 1 - \sigma(\text{H}_2\text{O}, T) - \left( \frac{\varepsilon}{4\pi} - \frac{1}{3} \right) \chi(\text{H}_2\text{O}, T) - \delta_s - \delta_p - \delta_{\text{RD}} - \delta_d \right]$$

Protons in  $\text{H}_2\text{O}$  molecules, diamagnetism of electrons screens protons => local B changes

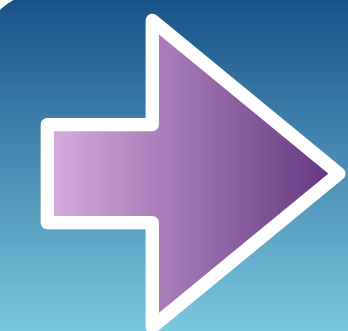
- $\sigma = 25\ 691(11) \times 10^{-9}$  at 25 deg C [P.J. Mohr et al, Rev. Mod. Phys. **84**, 1527 (2012)]

Magnetic susceptibility of water gives shape-dependent perturbation

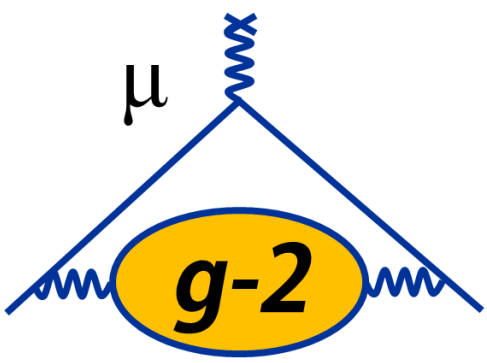
- $\varepsilon = 4\pi/3$  (perfect sphere)
- $\varepsilon = 2\pi$  (infinite cylinder) when probe is perpendicular to B
- $\chi_{\text{H}_2\text{O}}(T = 20^\circ\text{C}) = -9049(9) \times 10^{-9}$  [world average]

Magnetization of probe materials, geometry perturbs field experienced by protons

Dynamic effects: radiation damping, dipolar field from protons



Goal: Determine total correction to  $\leq 35$  ppb accuracy



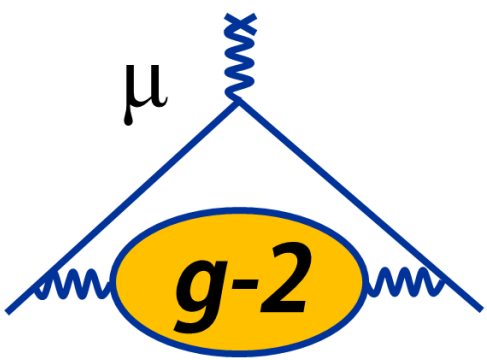
# Run 1 Analysis Status: $\omega_p$ – Field Calibration

## Plunging Probe

- Achieved **small perturbation of plunging probe ( $\delta_s + \delta_p + \delta_{RD} + \delta_d$ ): (-0.2 ± 11.4) ppb**
- Quantified uncertainties on plunging probe material, dynamic effects – **under budget of 35 ppb by a factor of > 2**

| Plunging Probe Perturbations |               |                   |
|------------------------------|---------------|-------------------|
| Quantity                     | Symbol        | Uncertainty (ppb) |
| Material Perturbation        | $\delta_s$    | 10.9              |
| Paramagnetic Impurities      | $\delta_p$    | 1.1               |
| Radiation Damping            | $\delta_{RD}$ | 2                 |
| Proton Dipolar Fields        | $\delta_d$    | 2.3               |
| Bulk Magnetic Susceptibility | $\delta_b$    | 2                 |
| Water Diamagnetic Shielding  | $\sigma$      | 11                |
| <b>TOTAL</b>                 |               | <b>15.9</b>       |

# Run 1 Analysis Status: $\omega_p$ – Field Calibration



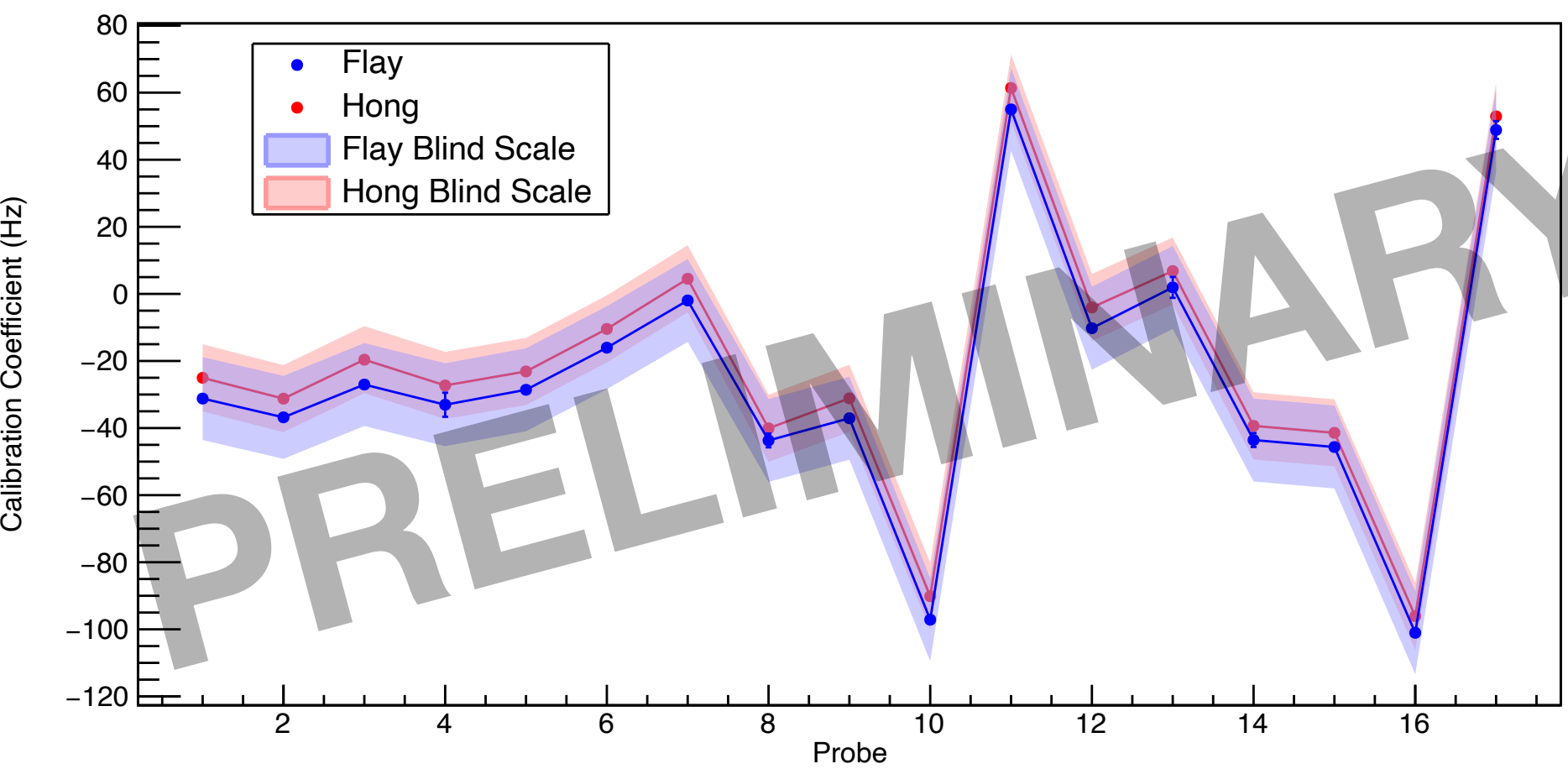
## Plunging Probe

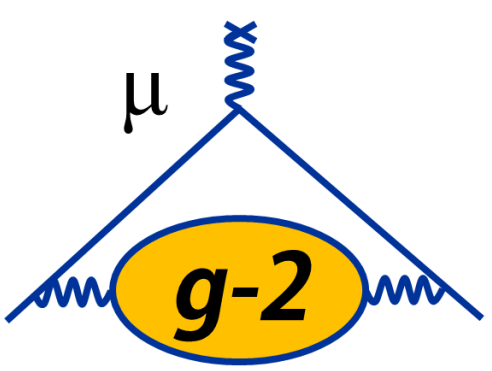
- Achieved **small perturbation of plunging probe ( $\delta_s + \delta_p + \delta_{RD} + \delta_d$ ): (-0.2 ± 11.4) ppb**
- Quantified uncertainties on plunging probe material, dynamic effects – **under budget of 35 ppb by a factor of > 2**

| Plunging Probe Perturbations |               |                   |
|------------------------------|---------------|-------------------|
| Quantity                     | Symbol        | Uncertainty (ppb) |
| Material Perturbation        | $\delta_s$    | 10.9              |
| Paramagnetic Impurities      | $\delta_p$    | 1.1               |
| Radiation Damping            | $\delta_{RD}$ | 2                 |
| Proton Dipolar Fields        | $\delta_d$    | 2.3               |
| Bulk Magnetic Susceptibility | $\delta_b$    | 2                 |
| Water Diamagnetic Shielding  | $\sigma$      | 11                |
| TOTAL                        |               | 15.9              |

## Trolley Calibration

- Calibration of trolley probes under control**
- Factor of  $\geq 2$  improvement on uncertainties for nearly all probes compared to E821
- Uncertainty is  $< \sim 40$  ppb on average per probe – **on budget**

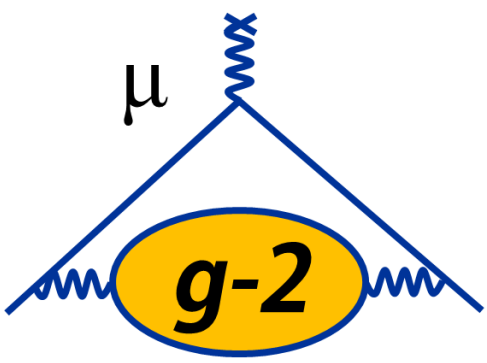




# Run 1 Analysis Status: $\omega_p$ – Field Interpolation

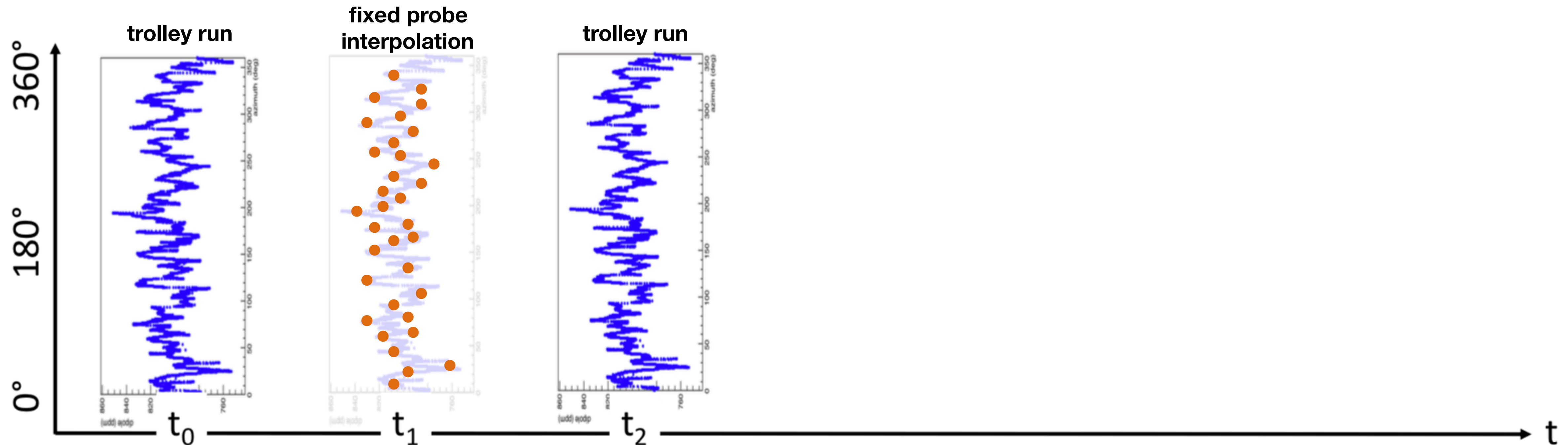
- Need to determine  $\omega_p$  at all times while storing muons => interpolate between trolley maps using fixed probe data



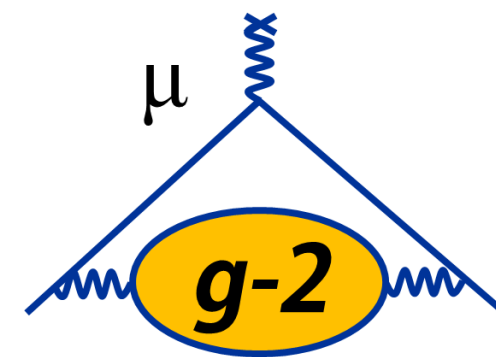


# Run 1 Analysis Status: $\omega_p$ – Field Interpolation

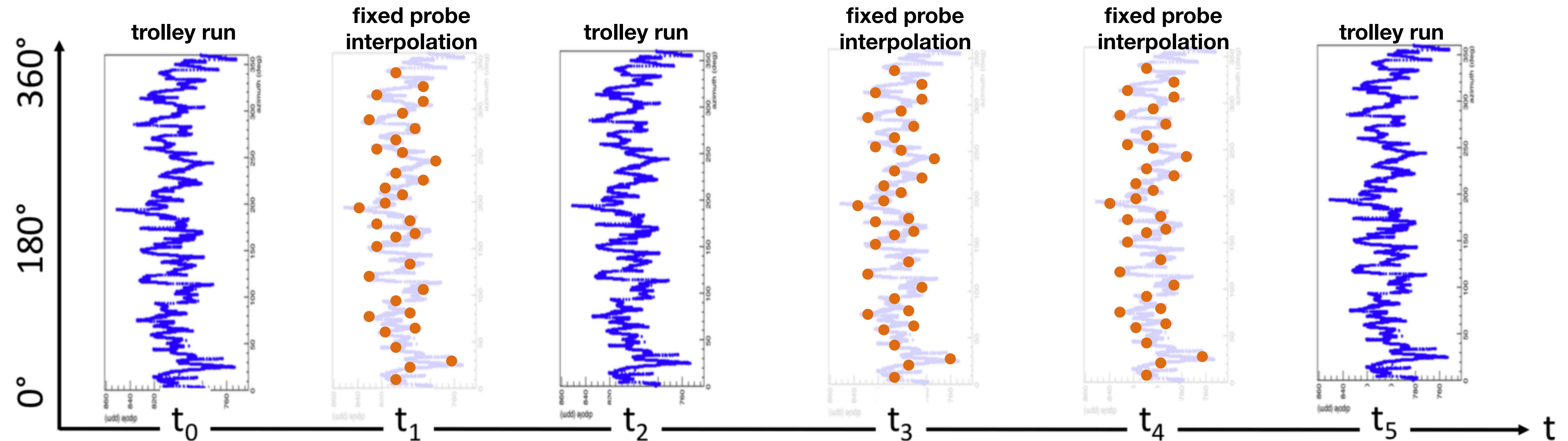
- Need to determine  $\omega_p$  at all times while storing muons => interpolate between trolley maps using fixed probe data



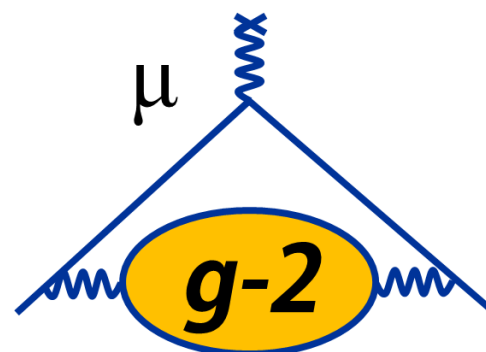
# Run 1 Analysis Status: $\omega_p$ – Field Interpolation



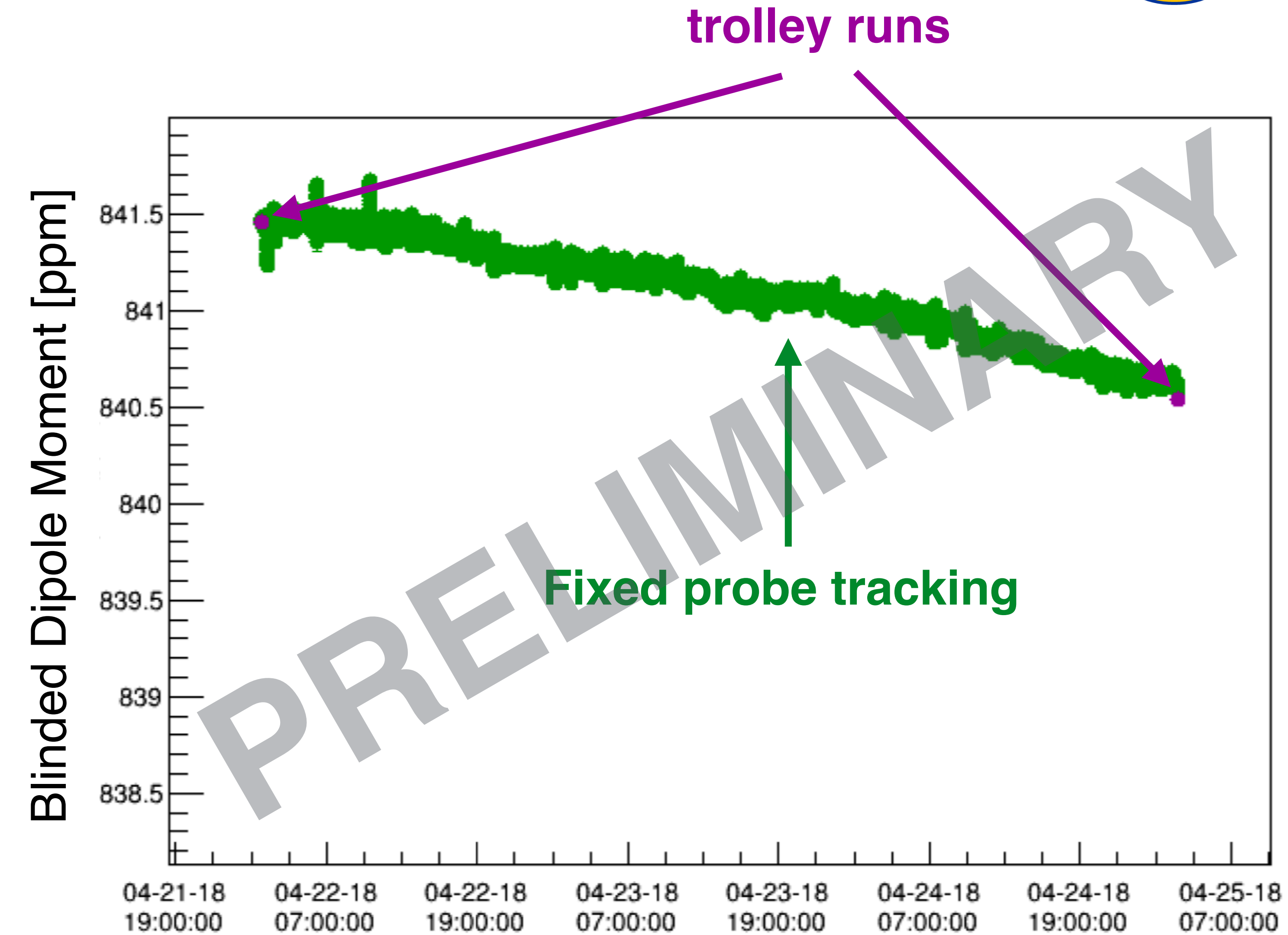
- Need to determine  $\omega_p$  at all times while storing muons => interpolate between trolley maps using fixed probe data

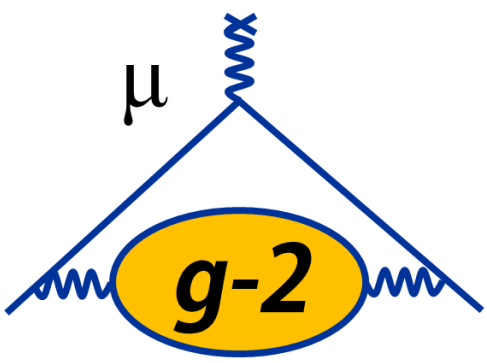


# Run 1 Analysis Status: $\omega_p$ – Field Interpolation



- Example from subset of data
- Tracking algorithms showing good agreement with trolley runs
- Also tracking higher-order multipole moments – important for extracting muon-weighted field  $\tilde{\omega}_p$





# Summary

- The Muon g-2 Experiment is a highly sensitive test of the SM
    - Discrepancy between theory and experiment for  $a_\mu > \sim 3\sigma$
- ✓ Completed Run 1 in July 2018 (1.1x BNL statistics)
- Analyses are mature and progressing towards a result in **early 2020**
- ✓ Completed Run 2 in July 2019 (1.9x BNL statistics)
  - Starting to organize analysis efforts
  - Run 3 starting this November: aiming to **triple** statistics to date

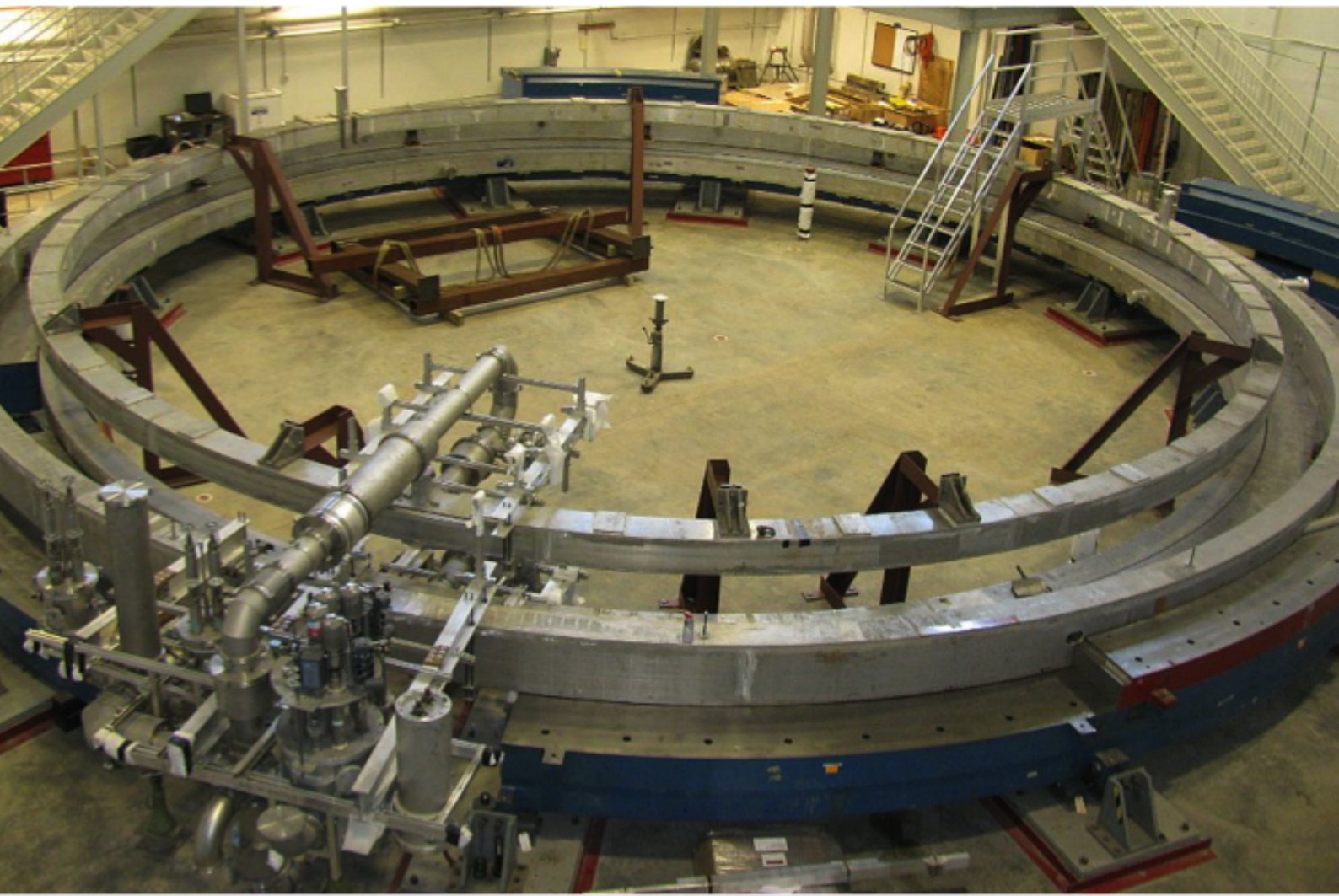
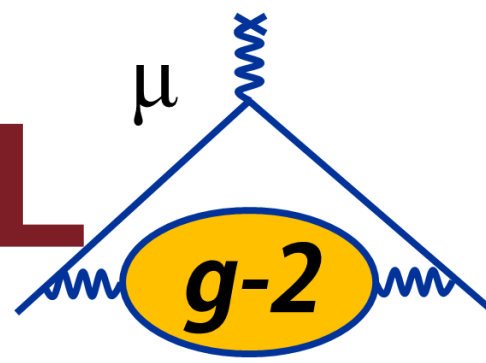
# Thank You!



A wide-angle photograph of a coastal scene. In the foreground, there's a rocky shoreline with various sizes of dark rocks and some low-lying vegetation. To the left, a rocky pier or breakwater extends into the ocean. The ocean itself is a deep blue, with sunlight reflecting off the surface, creating bright highlights. The sky is clear and light blue. Overlaid on the center of the image is the word "Backup" in a large, white, sans-serif font.

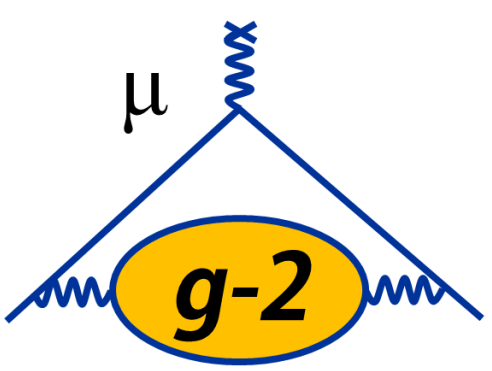
Backup

# The Big Move: Transporting the Ring from BNL to FNAL



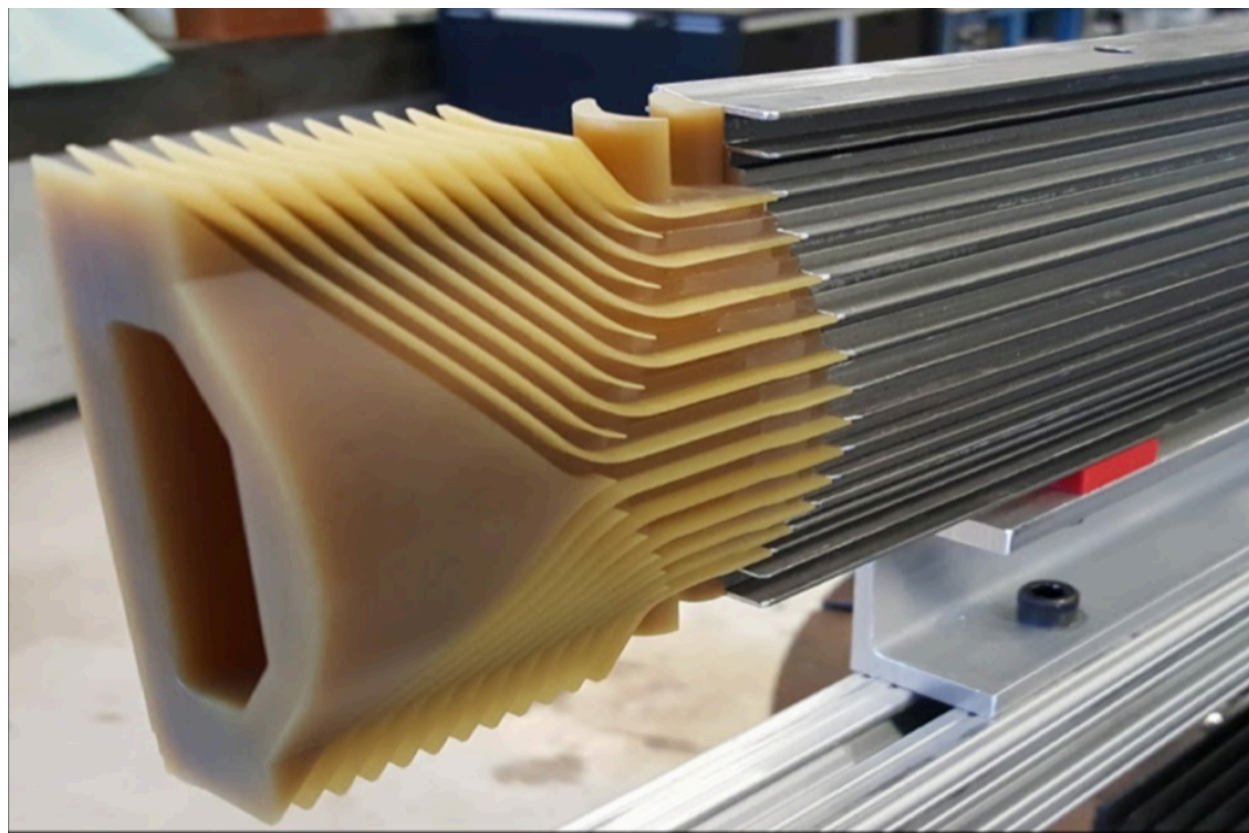
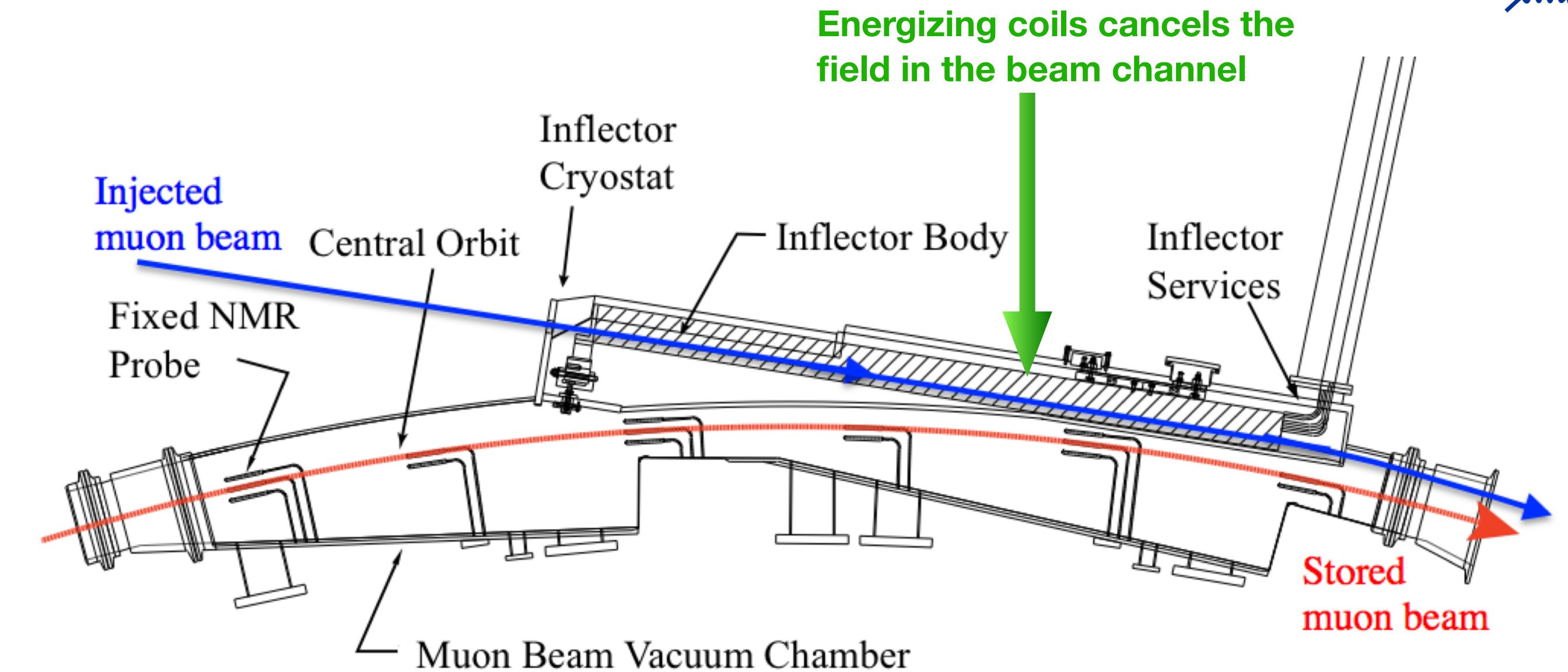
- June 2013—June 2015
- Ring deconstructed at BNL, transported by barge/flatbed trailer
- Reassembled at FNAL
- Ring successfully cooled and powered to 1.45 T in September 2015 — remarkable achievement!

UMassAmherst

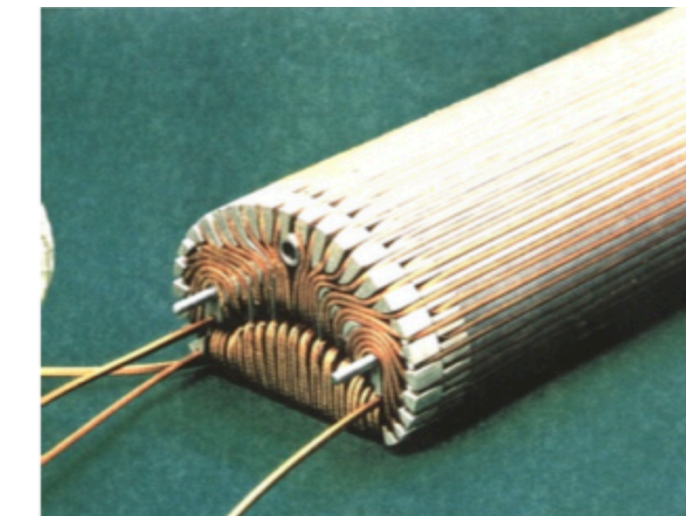


# Getting Muons Into the Ring: Inflector Magnet

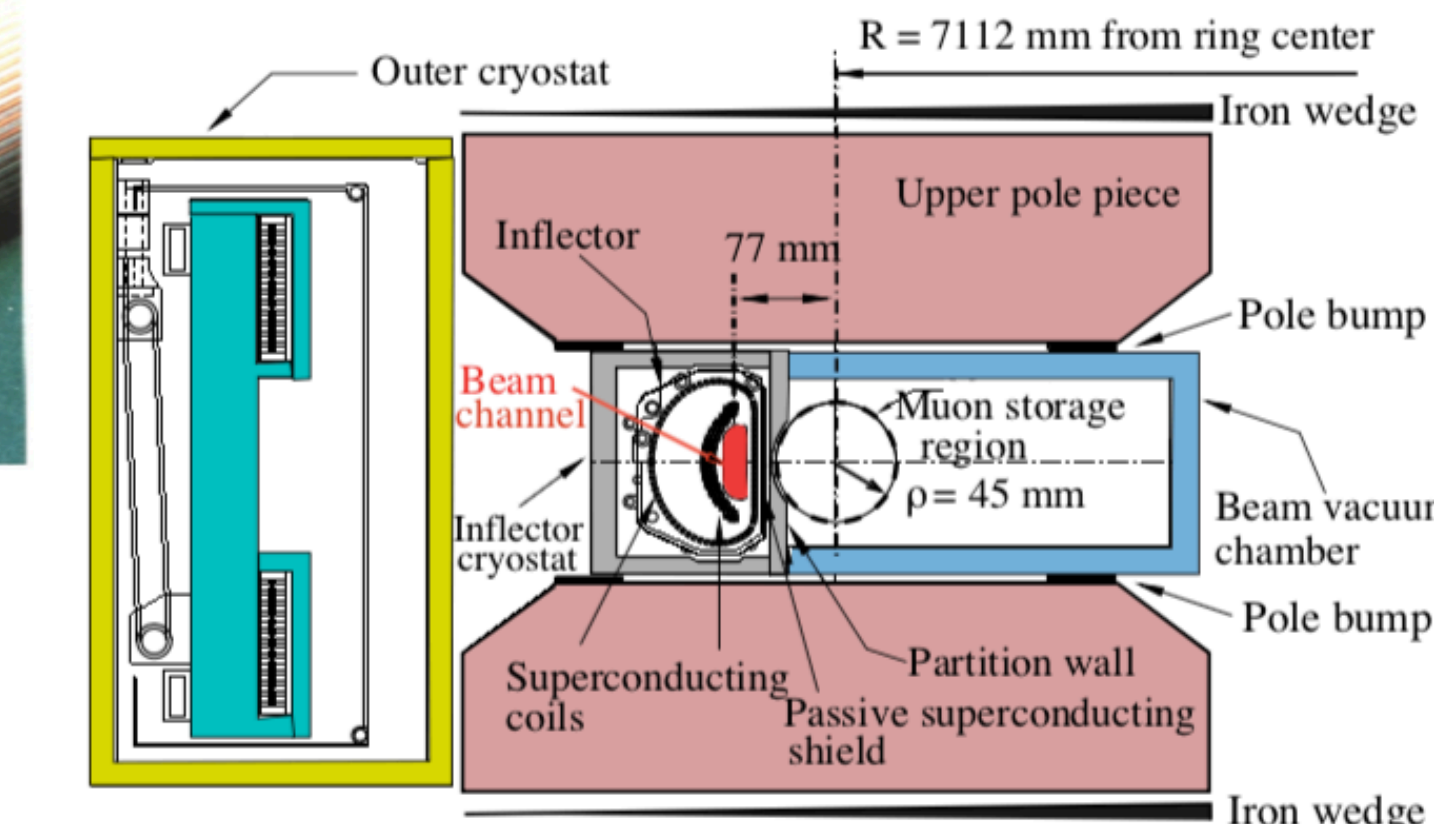
- Outside ring:  $B = 0 \text{ T}$ , inside:  $B = 1.45 \text{ T}$
- Need to cancel field in order to get muons in (strong deflection otherwise)
- No perturbation to field outside shield
- New inflector design with higher transmission under development
- **Improve injection by 40%**



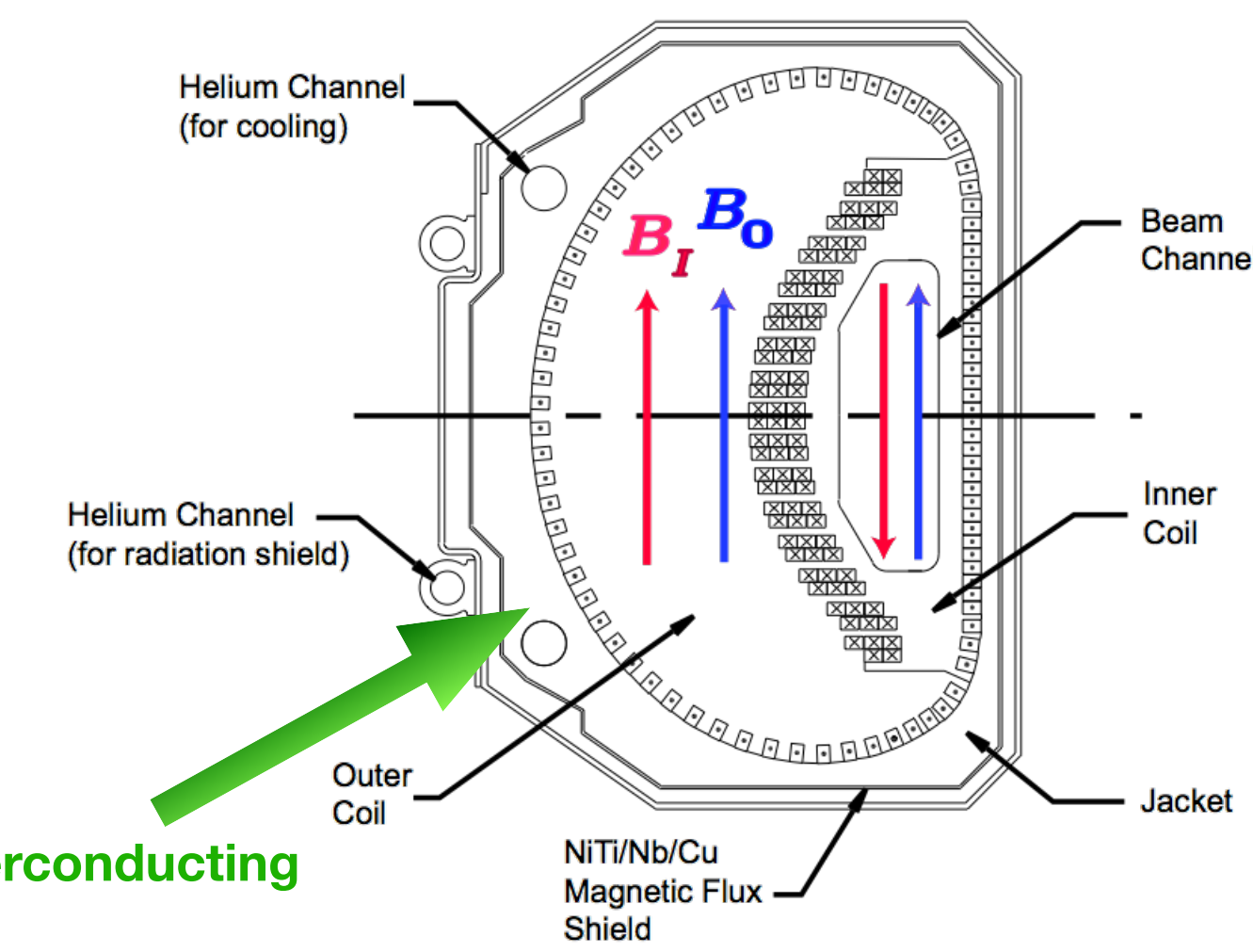
New inflector coil winding mount



Present inflector

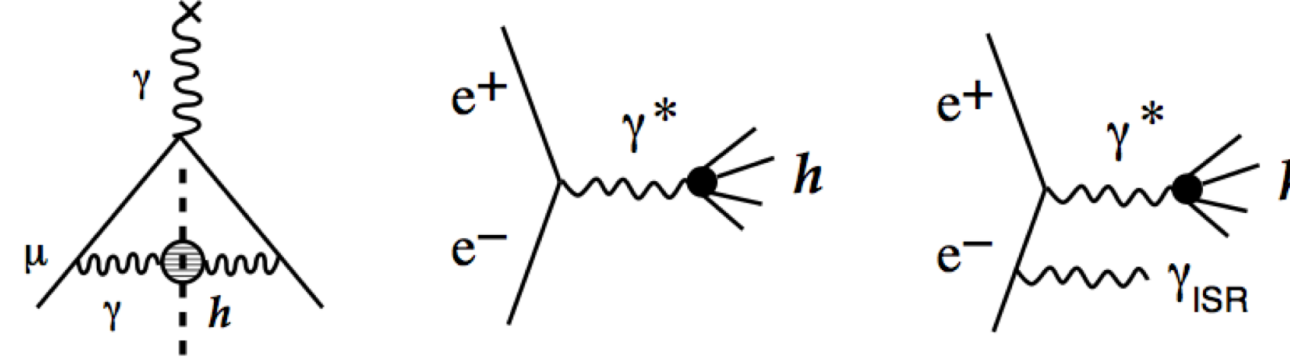
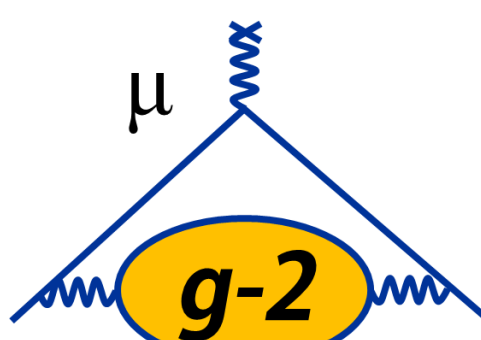


Super currents in passive superconducting shield prevents flux leakage



UMassAmherst

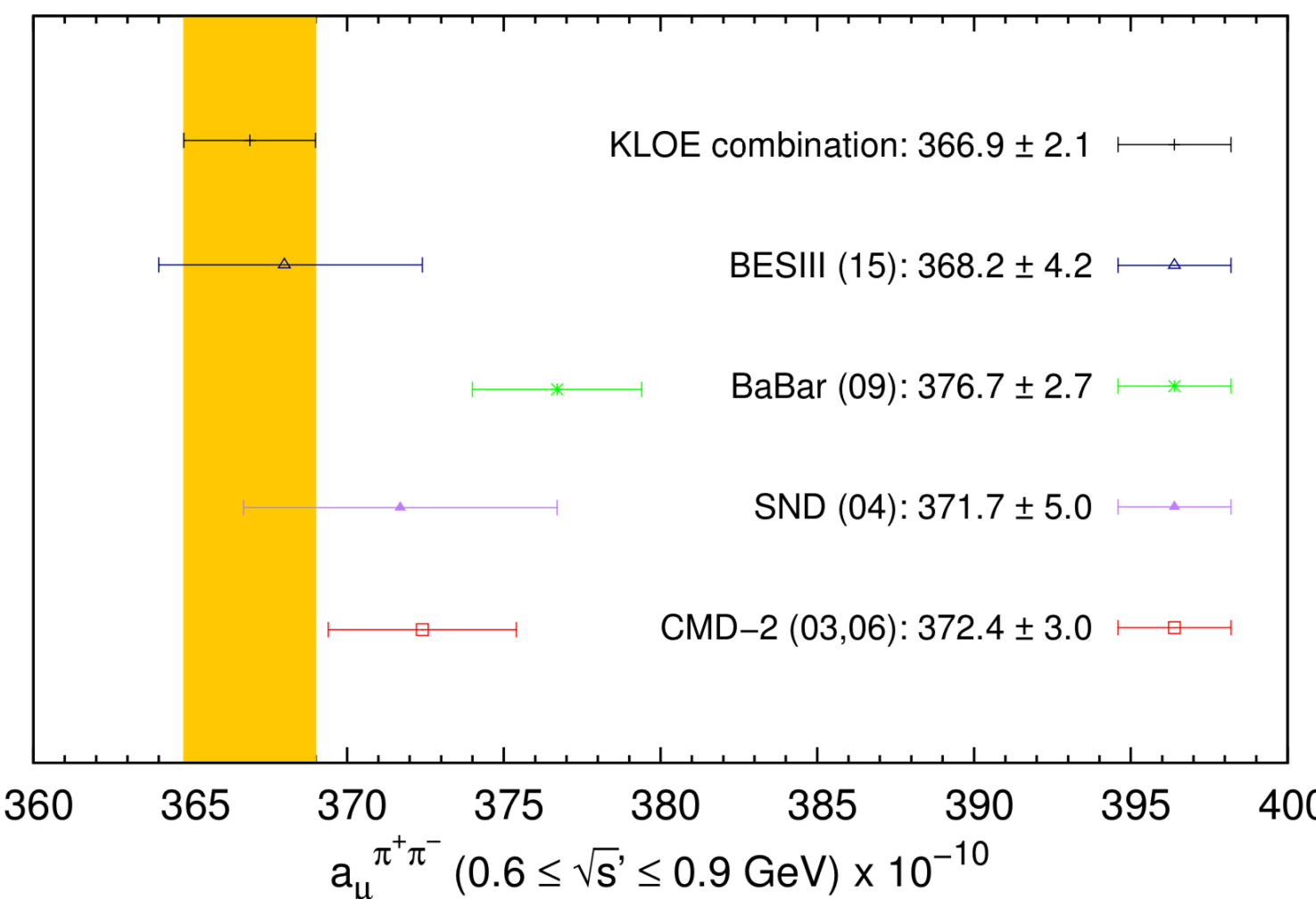
# Theory Status of Hadronic Contribution to $a_\mu$



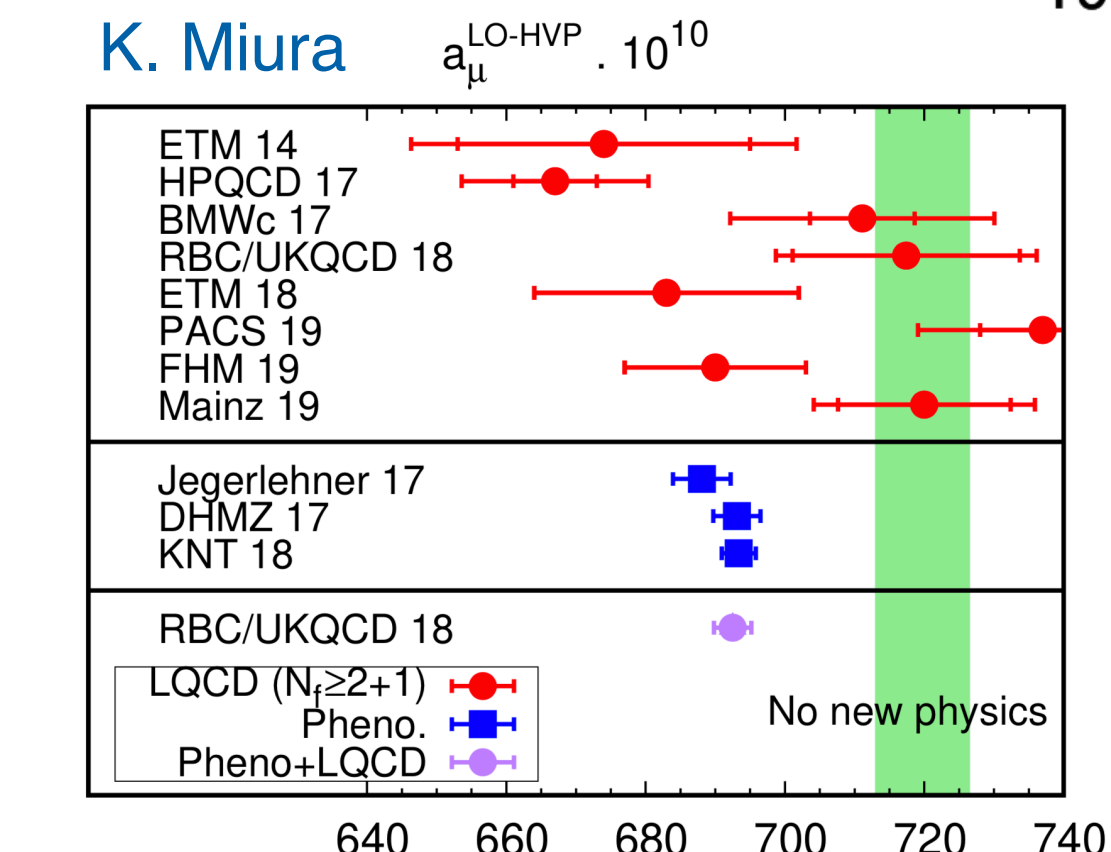
$$a_\mu^{\text{had;LO}} = \left( \frac{\alpha m_\mu}{3\pi} \right)^2 \int_{m_\pi^2}^{\infty} \frac{ds}{s^2} K(s) R(s)$$

$$R \equiv \frac{\sigma_{\text{tot}}(e^+e^- \rightarrow \text{hadrons})}{\sigma(e^+e^- \rightarrow \mu^+\mu^-)}$$

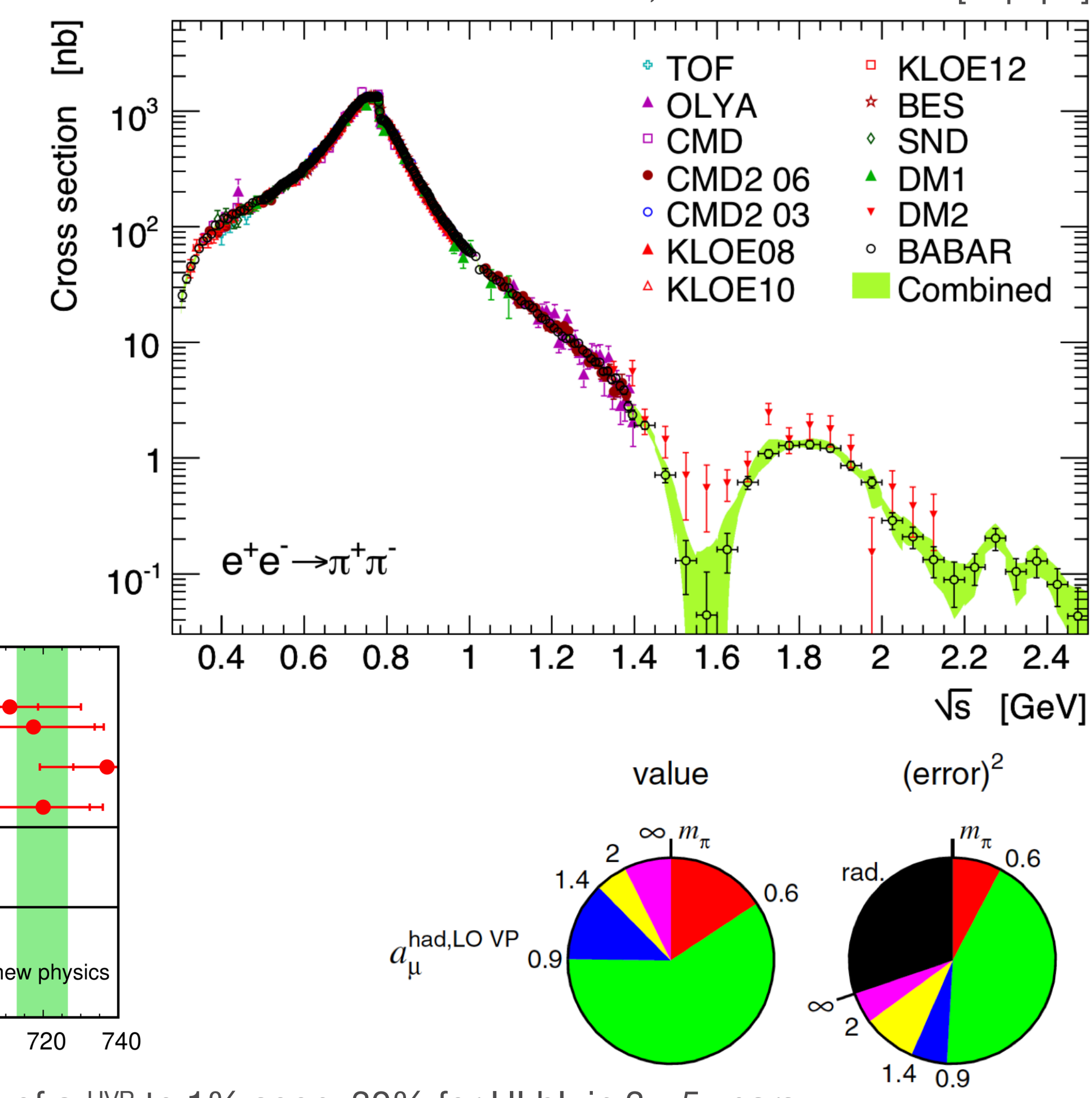
- **Critical input to HVP** from  $e^+e^-$  colliders (SND, CMD3, BaBar, KLOE, Belle, BESIII)
- **BESIII:** 3x more data available, luminosity measurement improvements
- **VEPP-2000:** Aiming for 0.3% (fractional) uncertainty; radiative return + energy scan
- **CMD3:** Will measure up to 2 GeV (energy scan, ISR – good cross check)



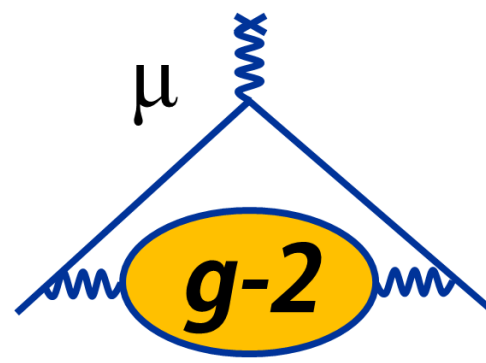
A. Anastasi et al., arXiv:1711.03085 [hep-ex]



- **Lattice calculations** of  $a_\mu^{\text{HVP}}$  to 1% soon, 30% for HLbL in 3–5 years



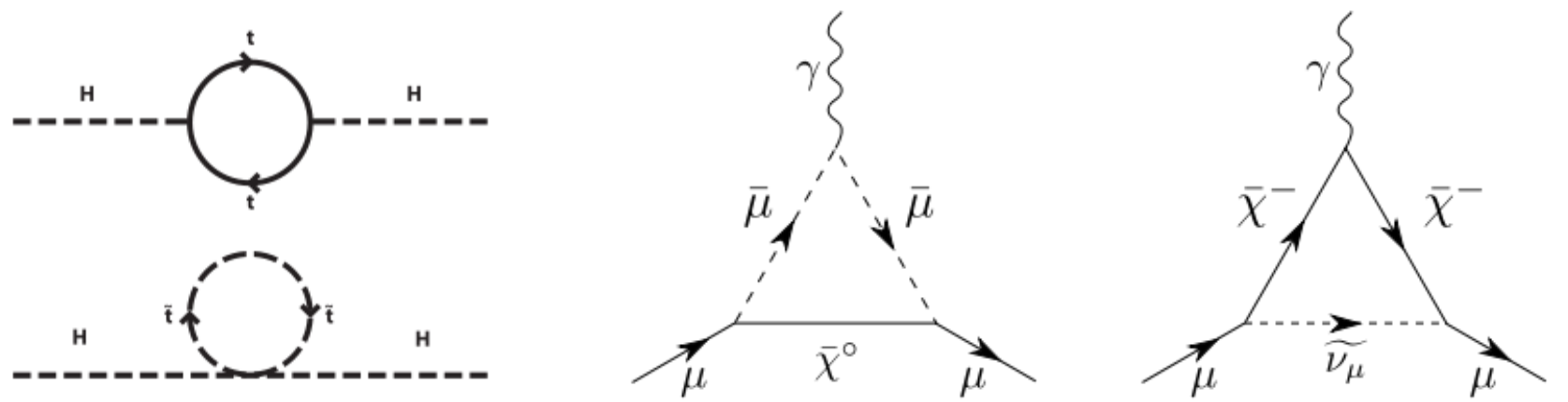
# Physics Beyond the Standard Model?



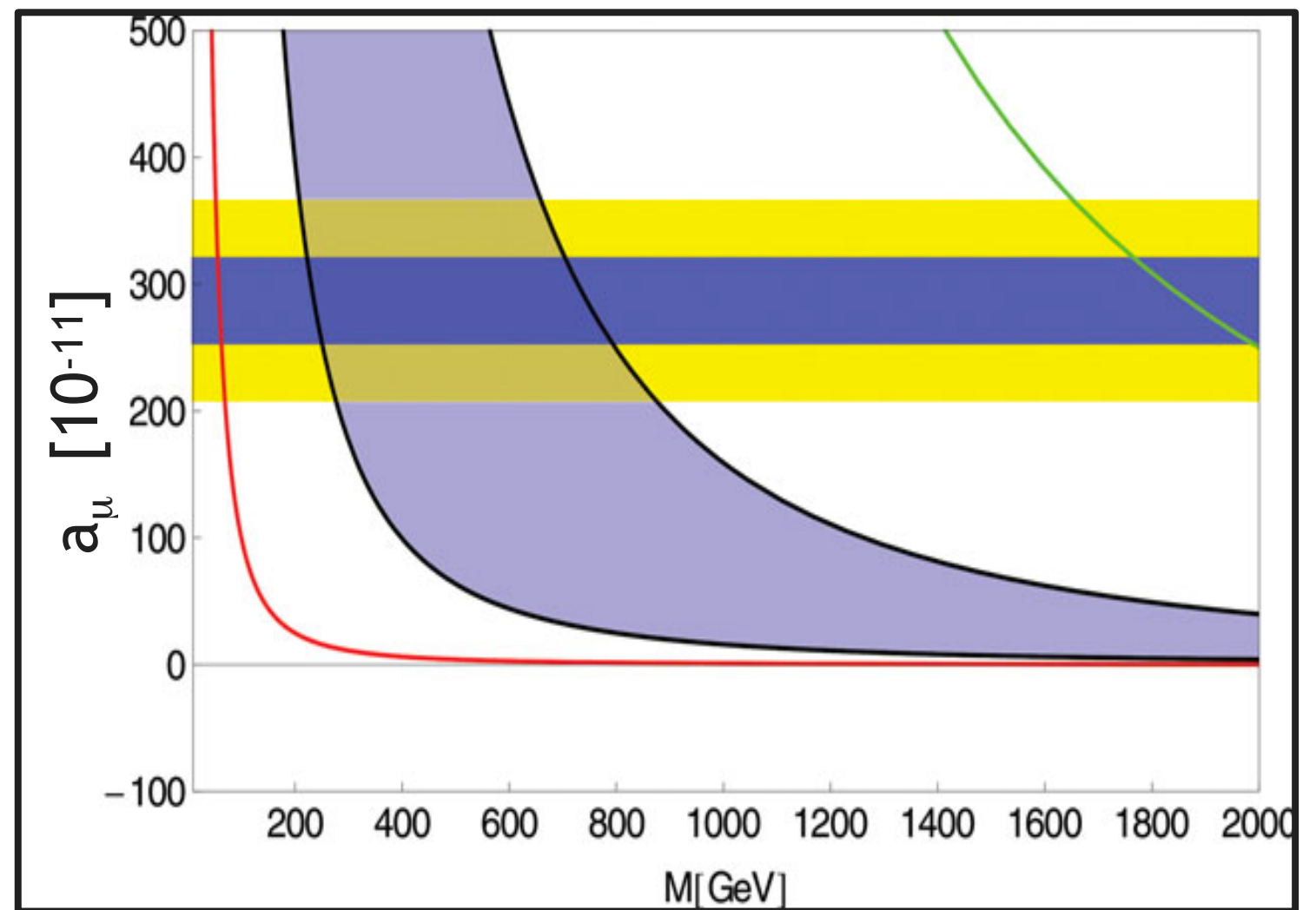
## SUSY, TeV-Scale Models

- Higgs measured at the LHC to be 125 GeV
- Theory: Higgs should acquire much heavier mass from loops with heavy SM particles (e.g., top quark)

- Supersymmetry: new class of particles** that enters such loops and **cancels this contribution**



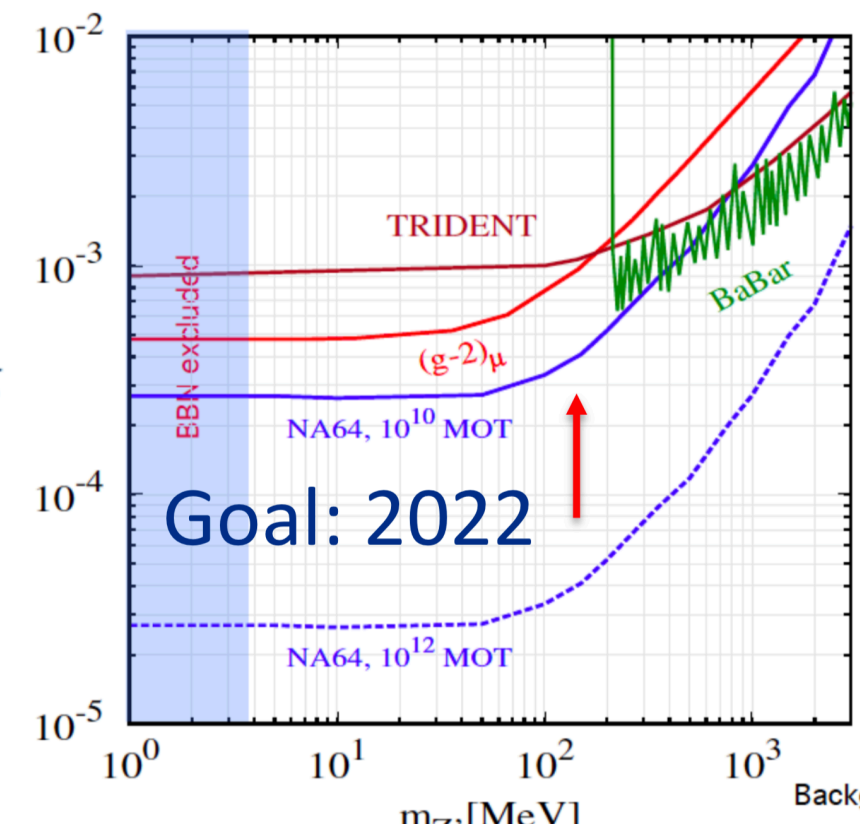
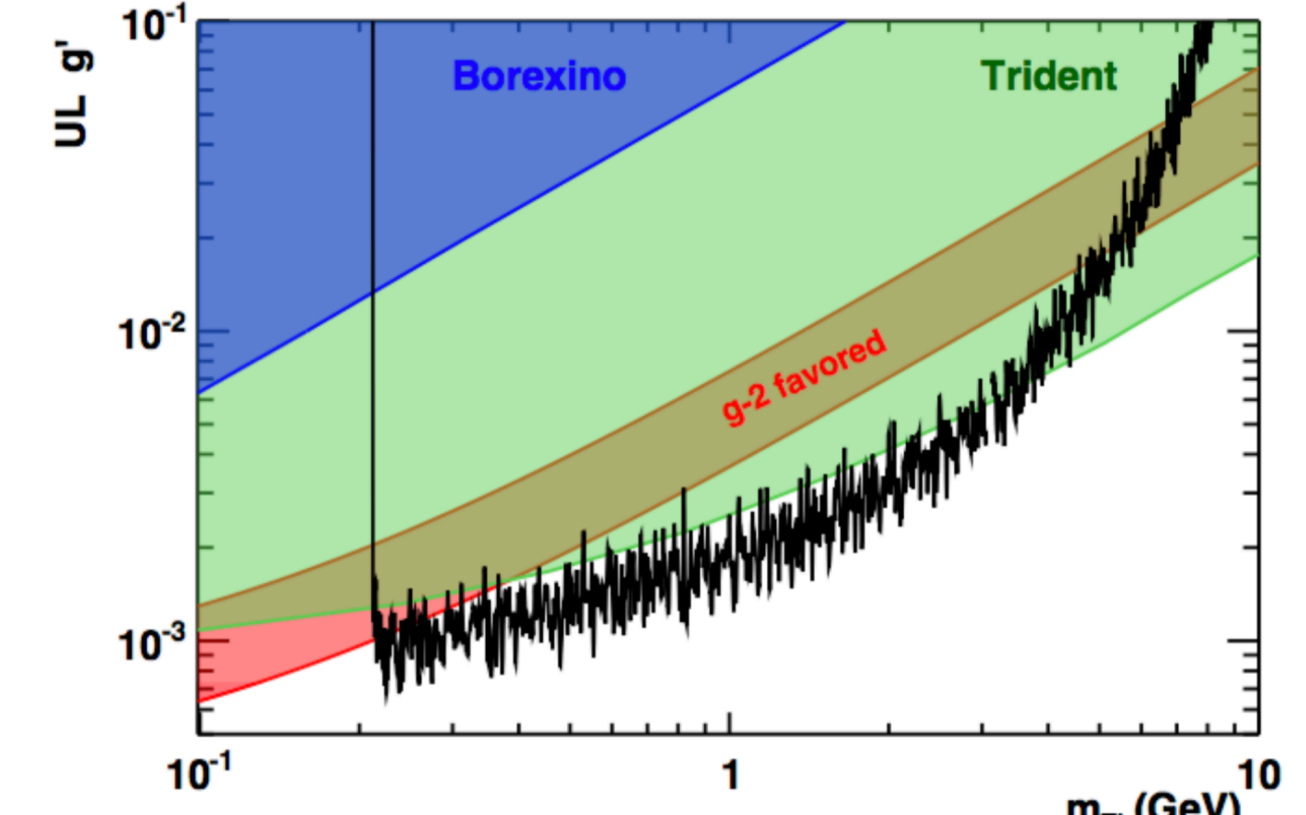
- Complementary to direct searches at the LHC**
  - Sensitivity to  $\text{sgn}(\mu)$ ,  $\tan(\beta)$
  - Contributions to  $a_\mu$  arise from charginos, sleptons
  - LHC searches sensitive to squarks, gluinos



D. Hertzog, Ann. Phys. (Berlin), 2015, courtesy D. Stockinger

- Z', W', UED, Littlest Higgs**
  - Assumes typical weak coupling
- Radiative muon mass generation
- Unparticles, Extra Dimension Models, SUSY ( $\tan \beta = 5$  to 50)

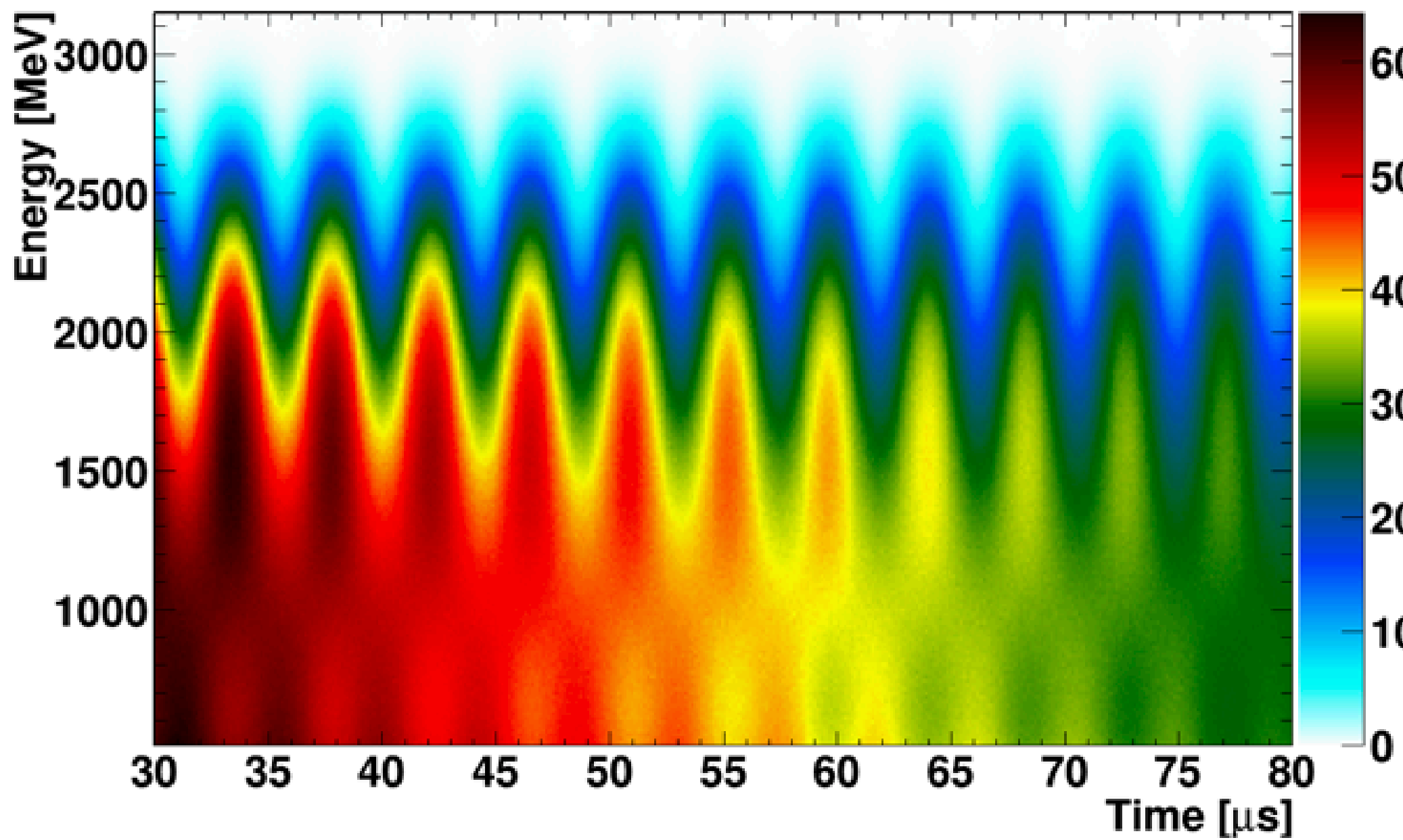
## Z' Possibilities



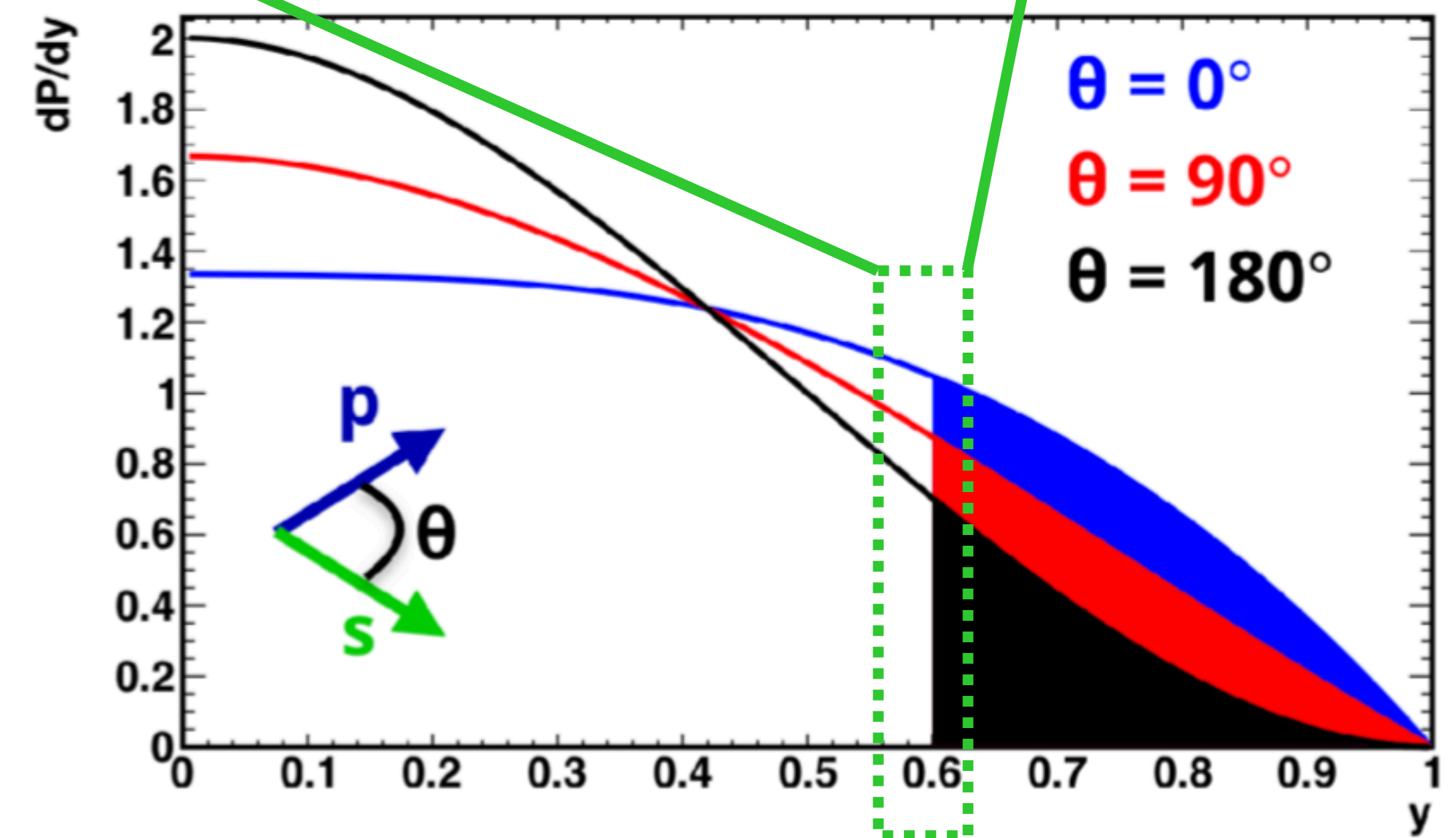
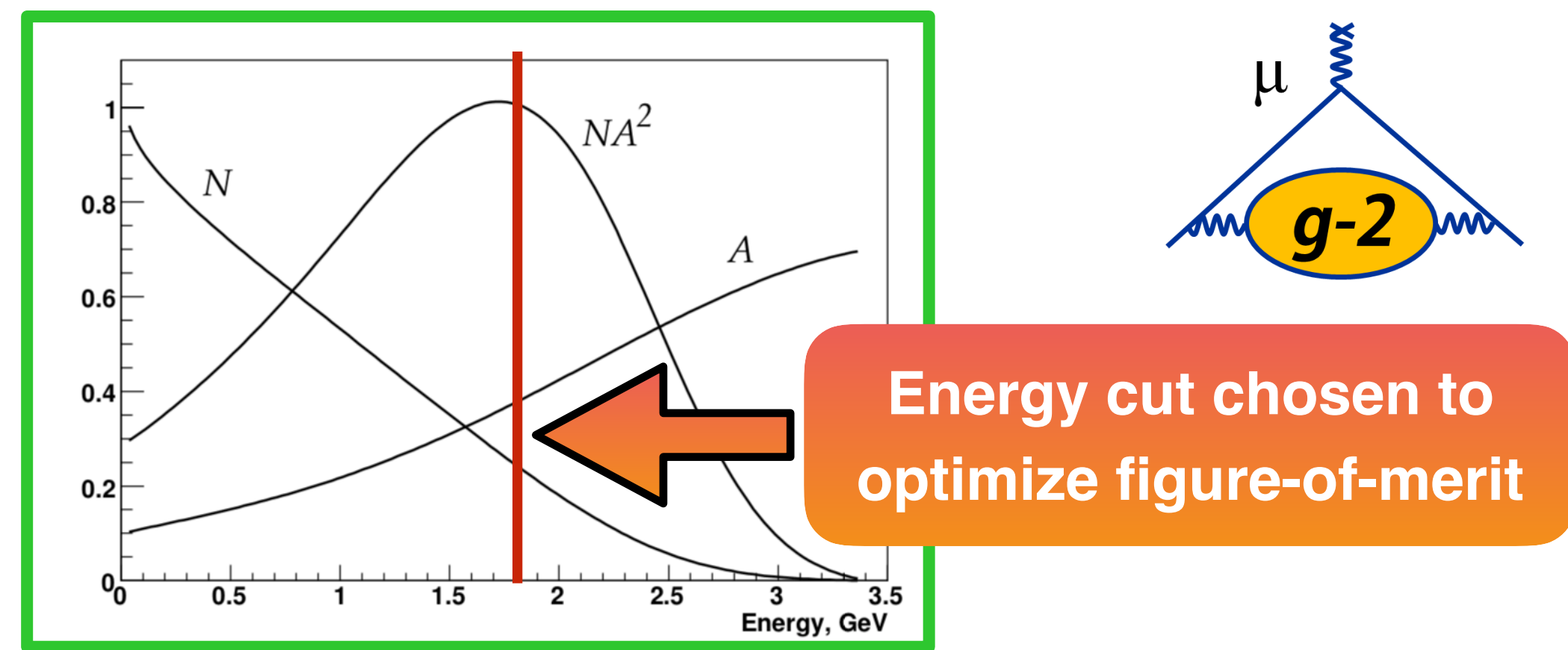
## Others...

- Axion-like particles
- Dark photons (invisible)
- Extended Higgs/leptoquarks

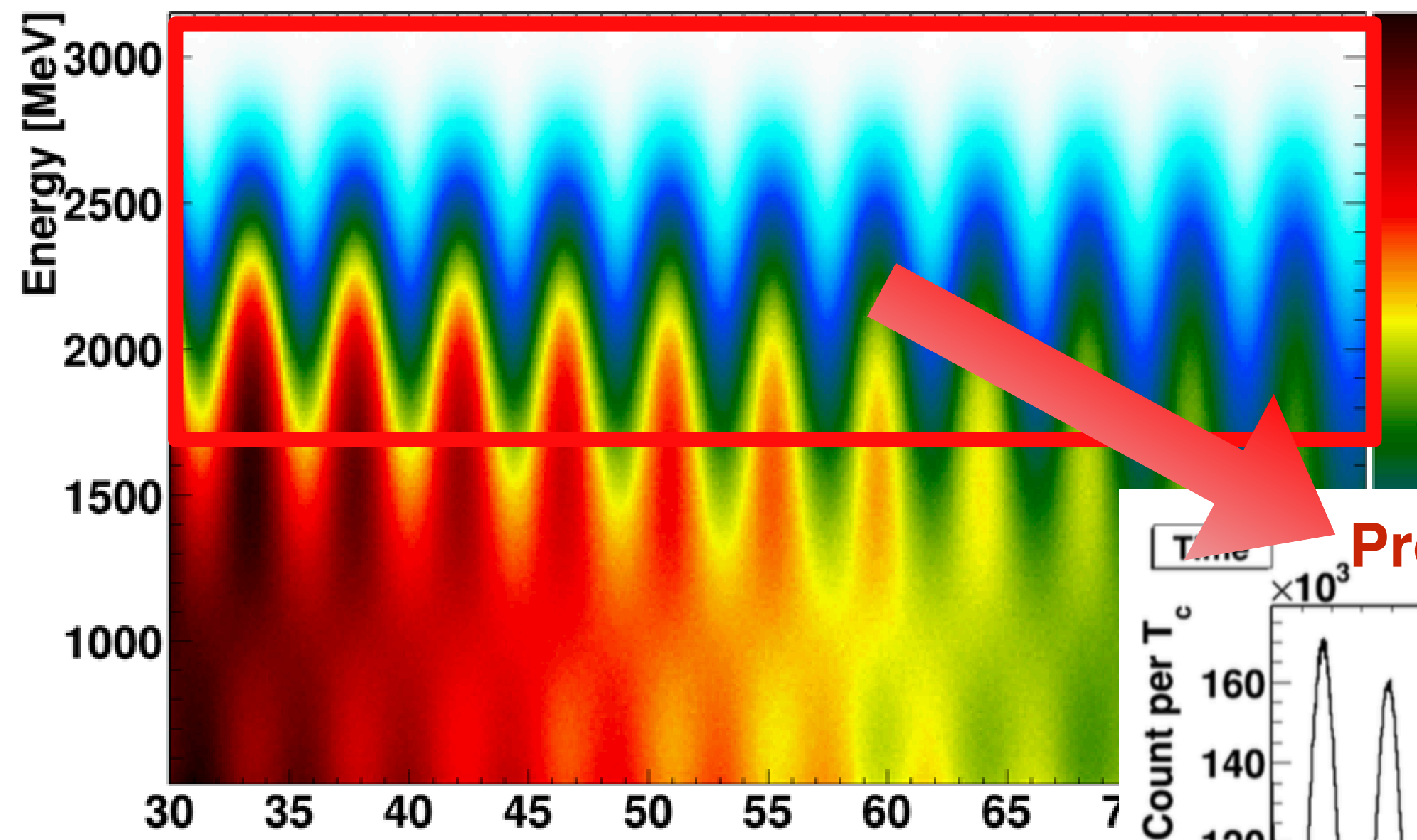
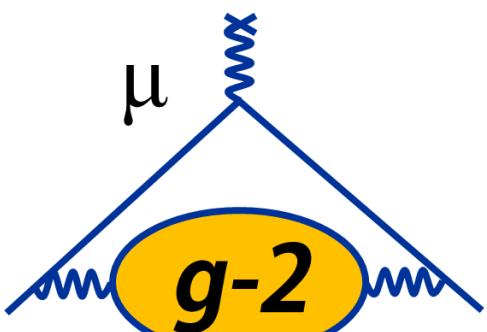
# Analysis Details: $\omega_a$



$$\frac{\delta\omega_a}{\omega_a} = \frac{\sqrt{2}}{2\pi f_a \tau_\mu N^{\frac{1}{2}} A}$$

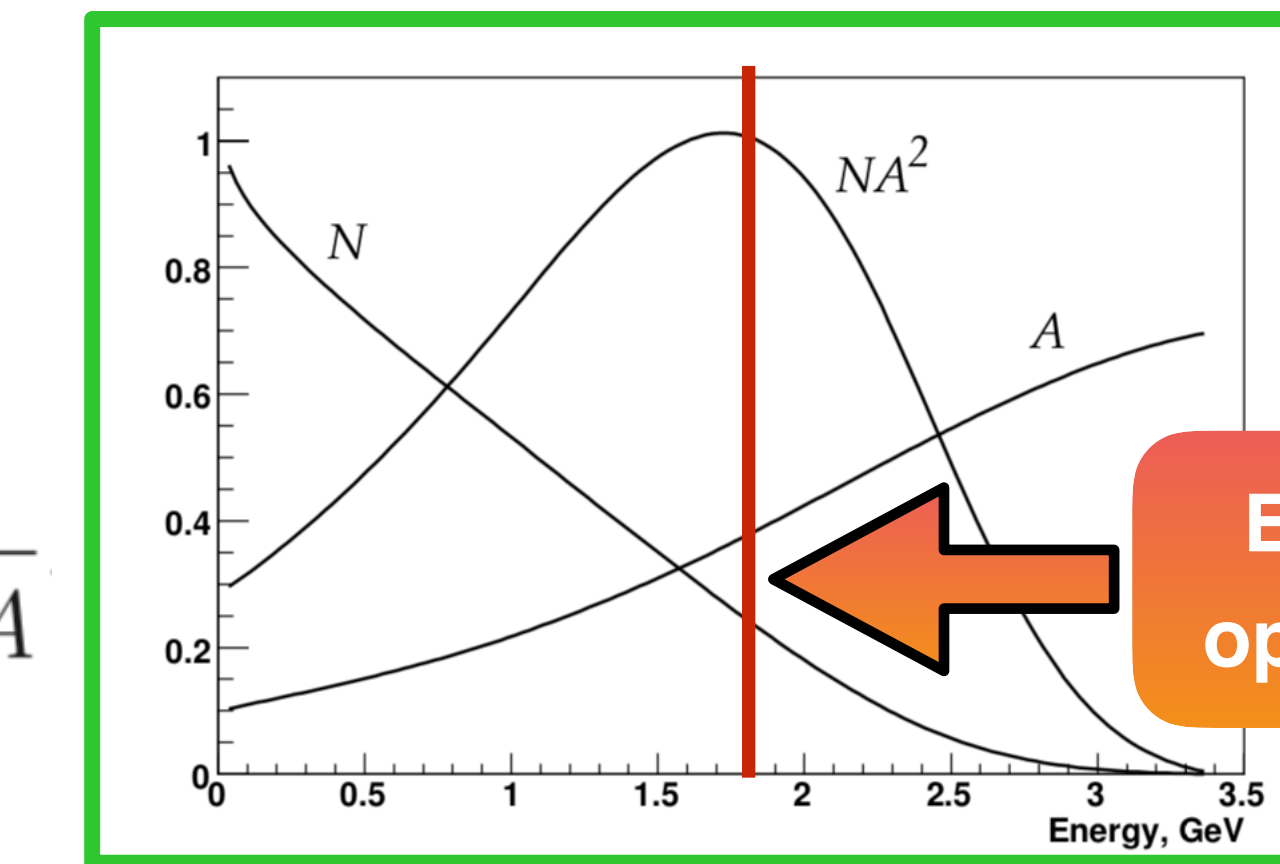
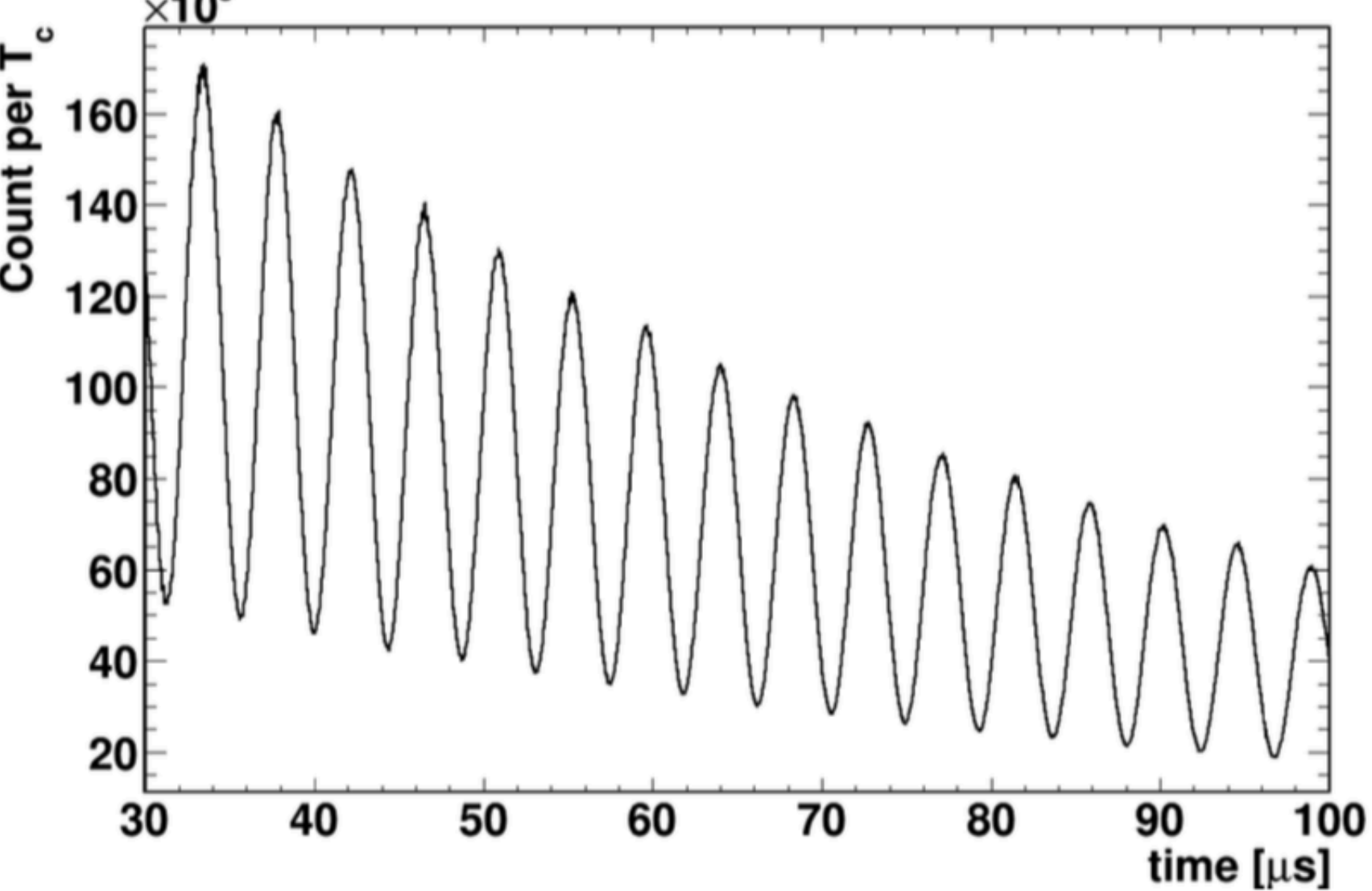


# Analysis Details: $\omega_a$

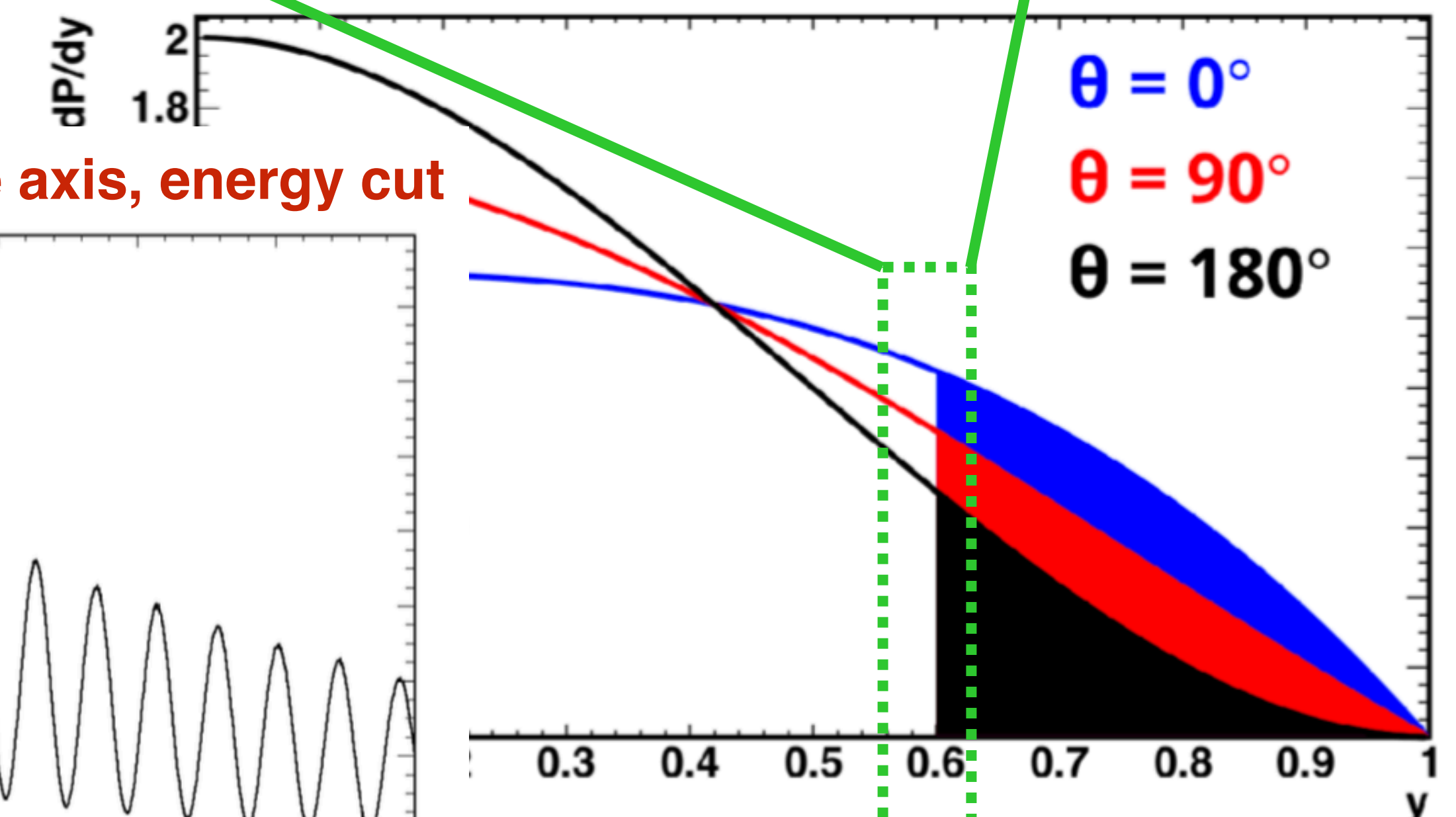


$$\frac{\delta\omega_a}{\omega_a} = \frac{\sqrt{2}}{2\pi f_a \tau_\mu N^{\frac{1}{2}} A}$$

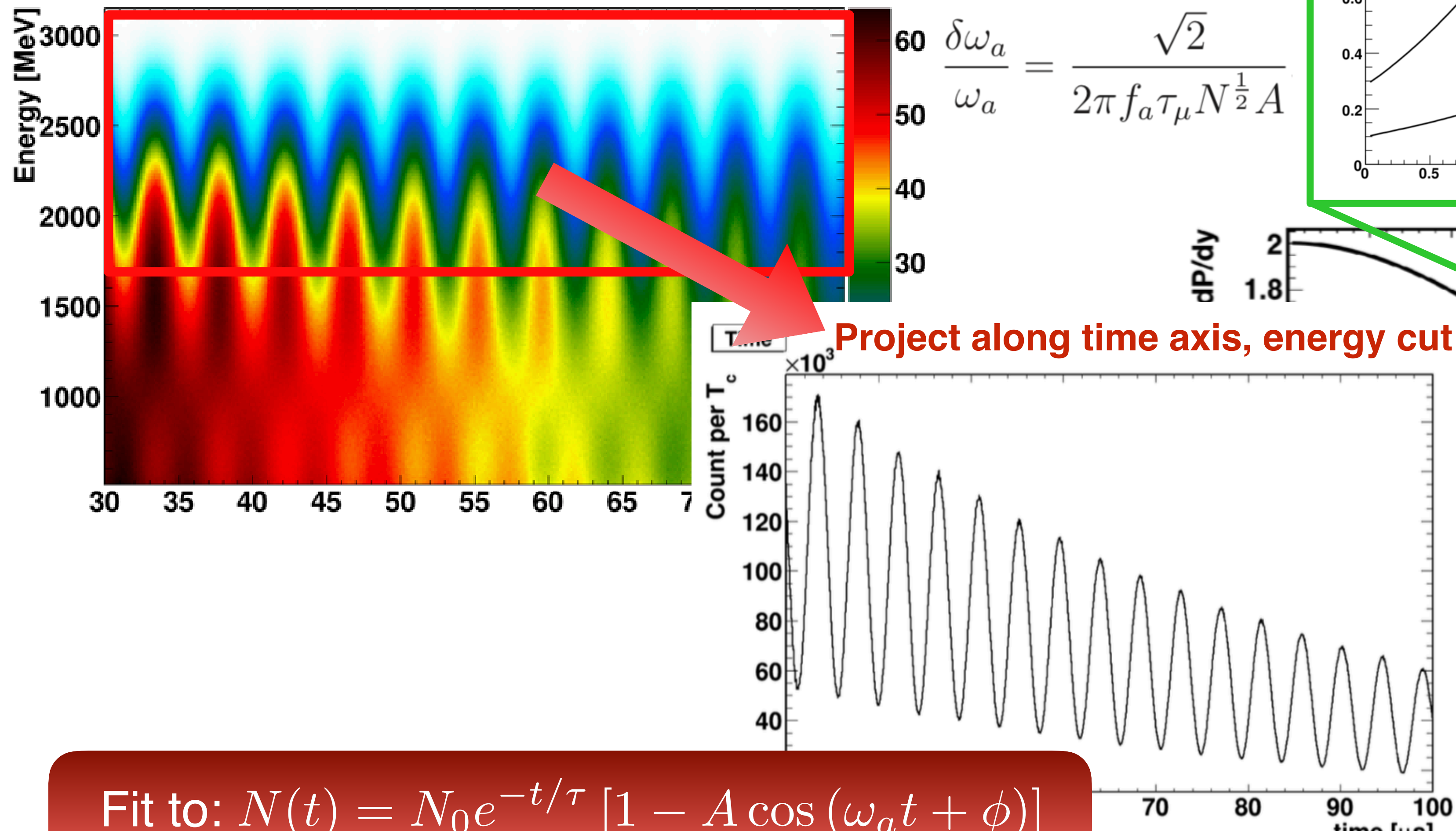
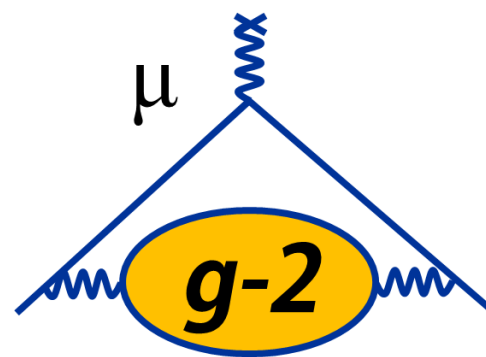
Project along time axis, energy cut



Energy cut chosen to optimize figure-of-merit

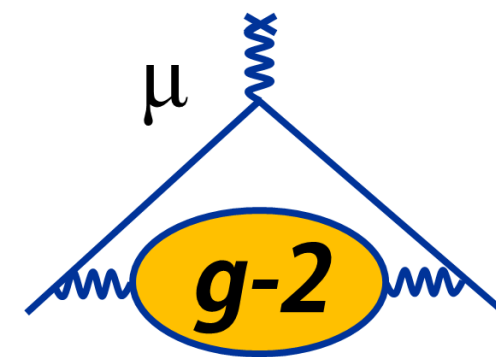


# Analysis Details: $\omega_a$



Fit to:  $N(t) = N_0 e^{-t/\tau} [1 - A \cos(\omega_a t + \phi)]$

# Beam Dynamics Corrections



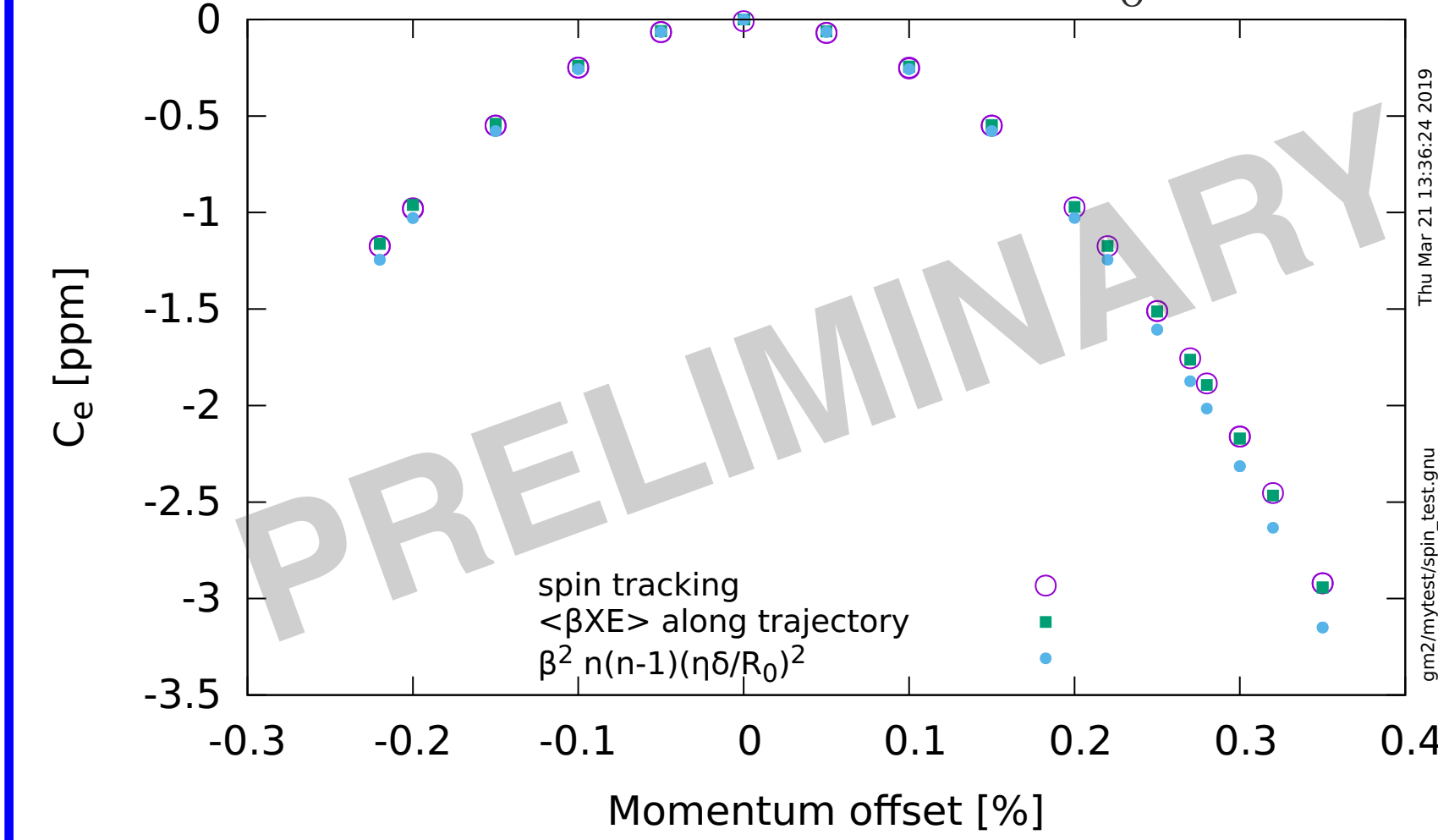
- Full expression for  $\omega_a$ :

$$\vec{\omega}_a = \vec{\omega}_S - \vec{\omega}_C = -\frac{e}{mc} \left[ a_\mu \vec{B} - \left( a_\mu - \frac{1}{\gamma^2 - 1} \right) \vec{\beta} \times \vec{E} \right] - a_\mu \left( \frac{\gamma}{\gamma + 1} \right) (\vec{\beta} \cdot \vec{B}) \vec{\beta}$$

- Choose  $\gamma = 29.3$  ( $p_\mu = 3.094$  GeV/c)

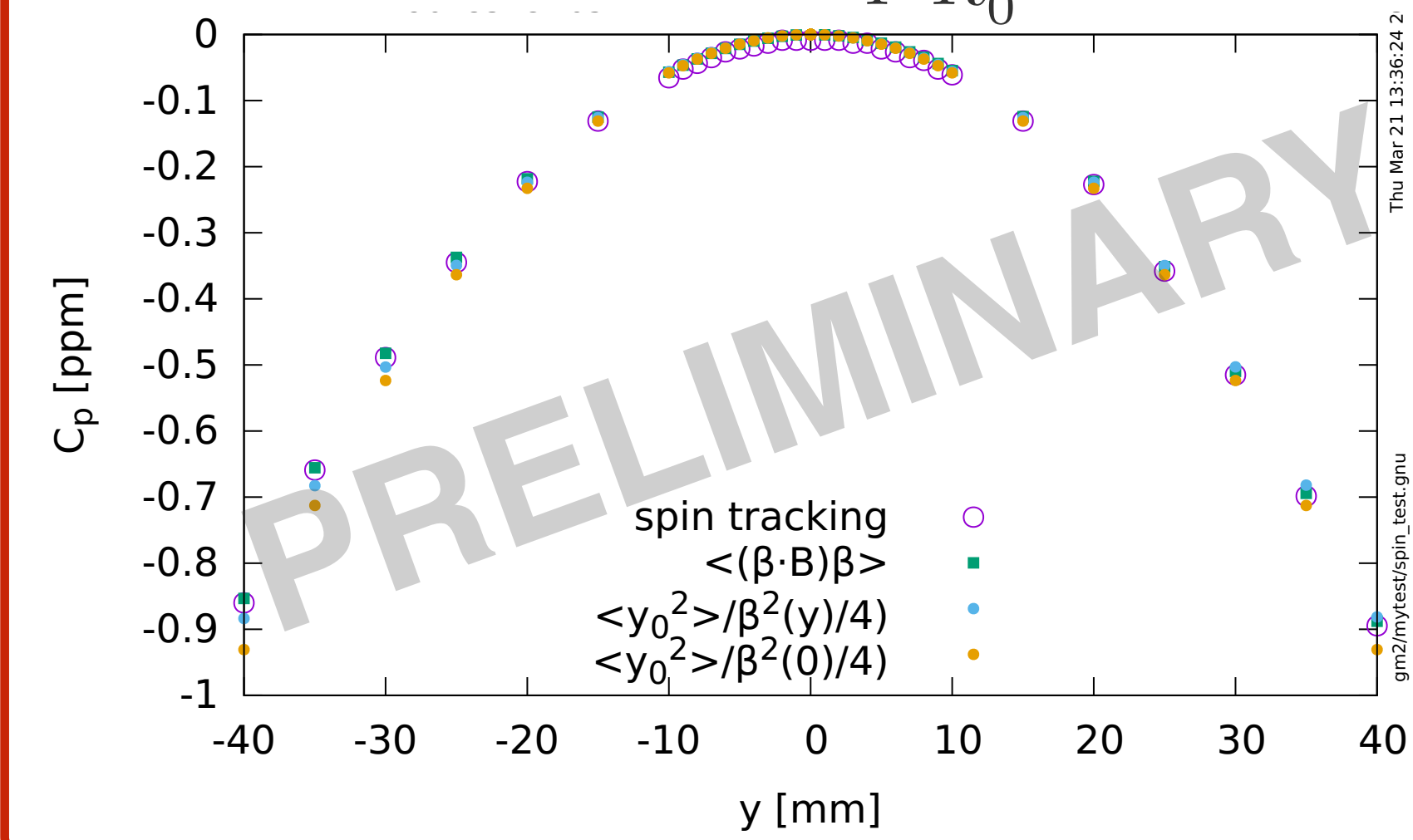
Not all  $\mu^+$  at this  $\gamma \rightarrow$  **E-field correction**

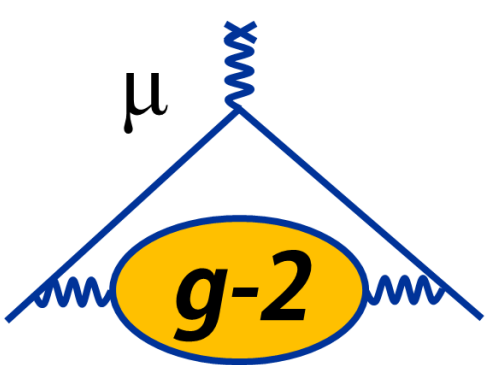
$$C_E = -2n(1-n)\beta^2 \frac{\langle x_e^2 \rangle}{R_0^2}$$



Vertical beam oscillations  $\rightarrow$  **pitch correction**

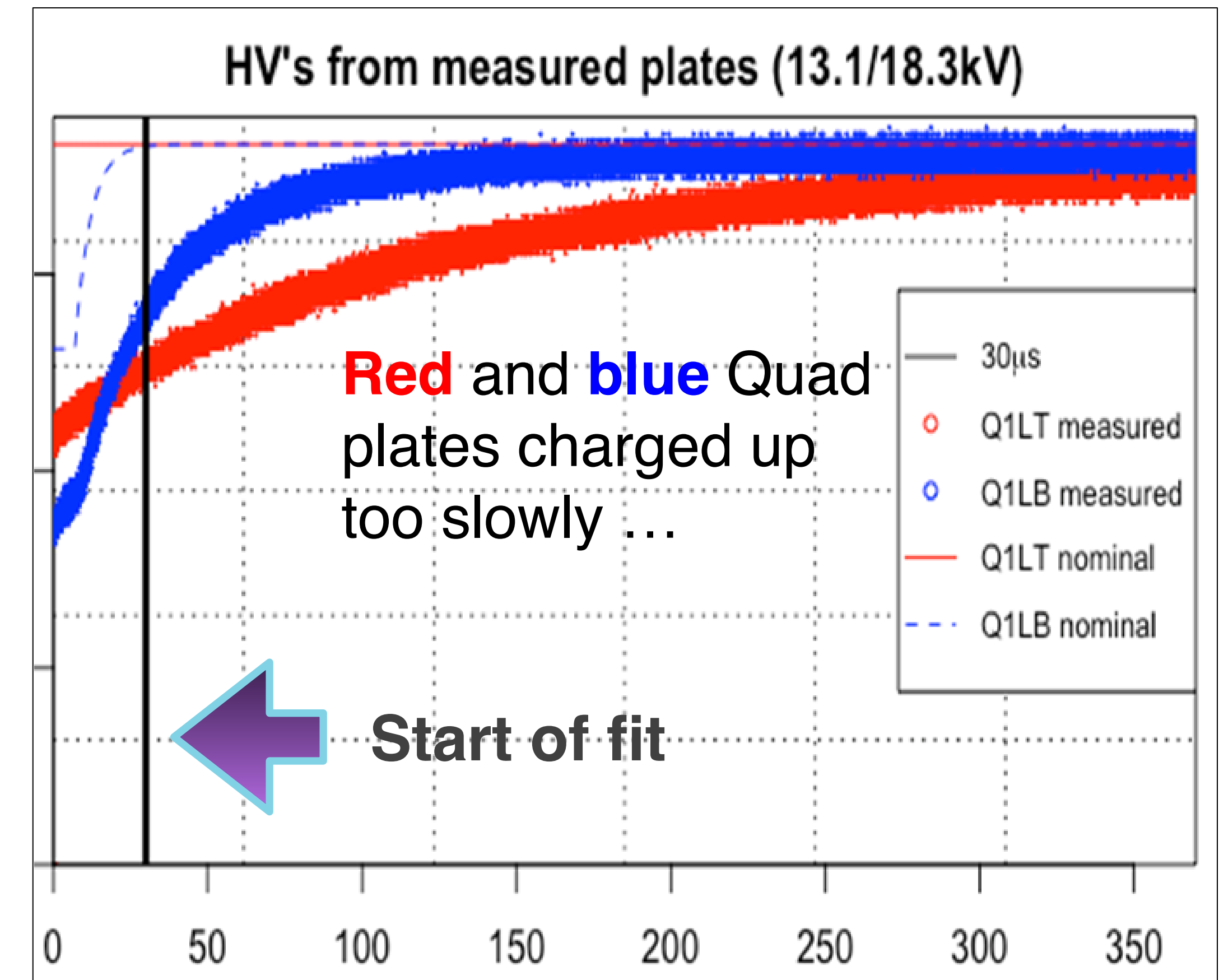
$$C_p = -\frac{n}{4} \frac{\langle y^2 \rangle}{R_0^2}$$





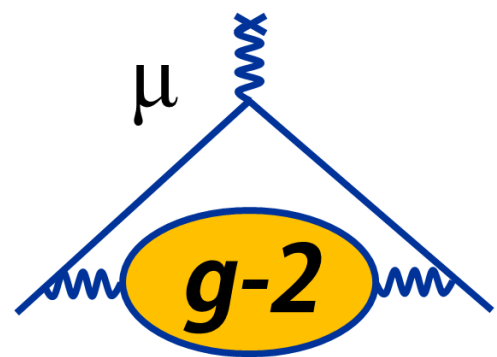
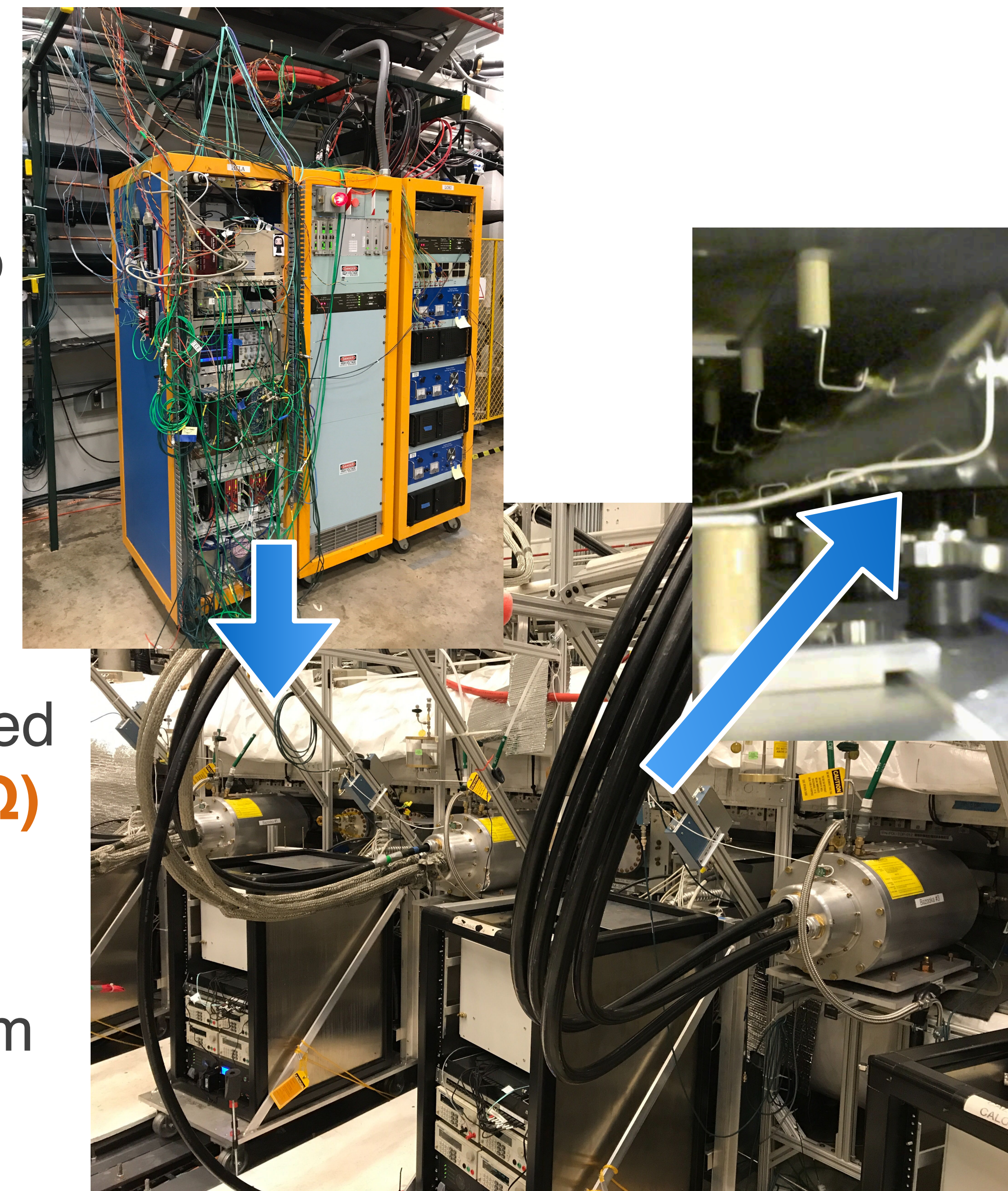
# Quad Challenges (Run 1)

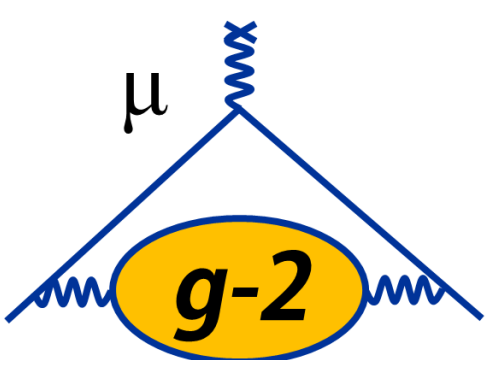
- 2 of 32 HV resistors on quad plates were flawed => did not stabilize in time for “fit start time”
- Mean of vertical muon distribution moves down by 0.6 mm
  - Investigating impact on  $\omega_a$  (calculations, systematic measurements)
- Problem was fixed for Run 2



# How is a Kick Made?

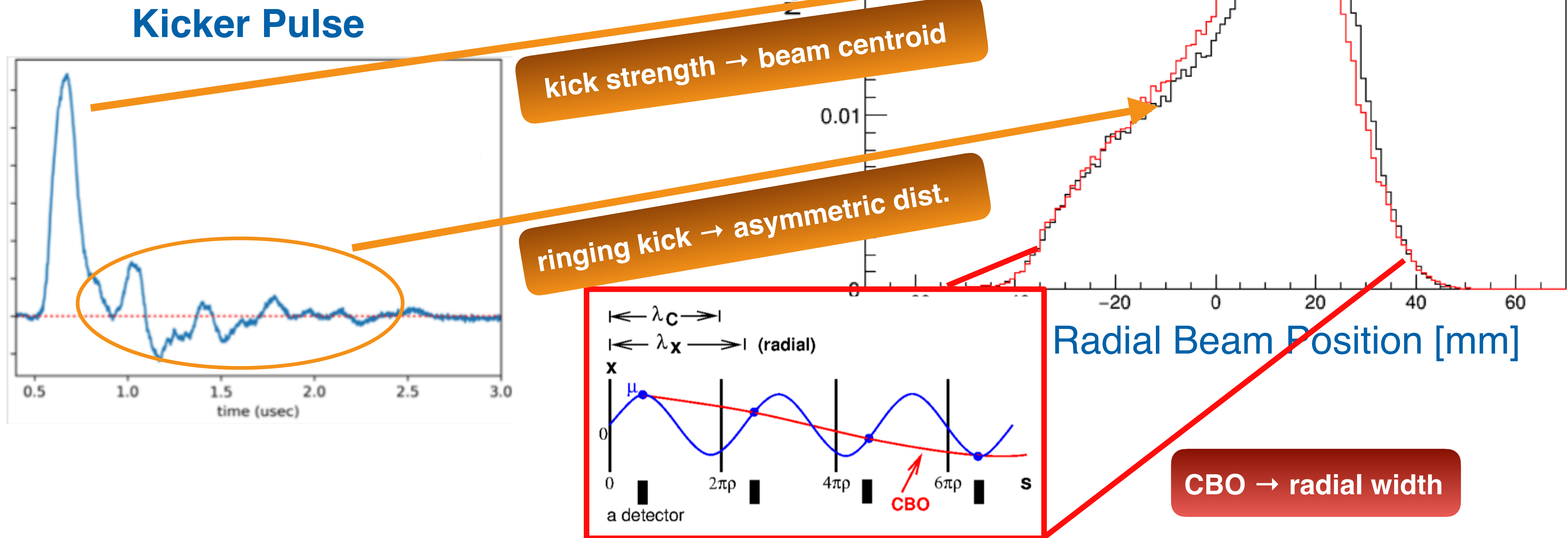
- A **charging power supply** charges up a **capacitor bank** to 700 V
- Capacitors are **discharged** through a transformer into a **Blumlein** (a HV capacitor up to 55 kV)
- Current in **Blumlein** is discharged into a **resistive load ( $Z = 12.5 \Omega$ )**
- Current delivered to plates, producing a **~200 G magnetic field**, rotating muon's momentum vector

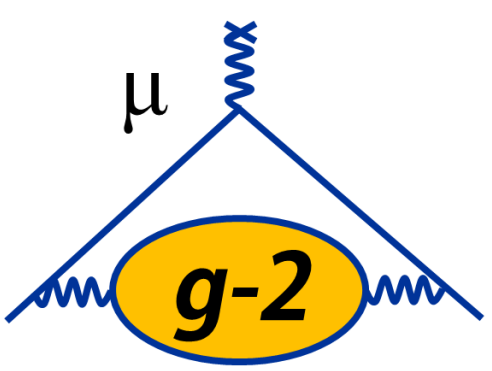




# What Affects the Beam Shape?

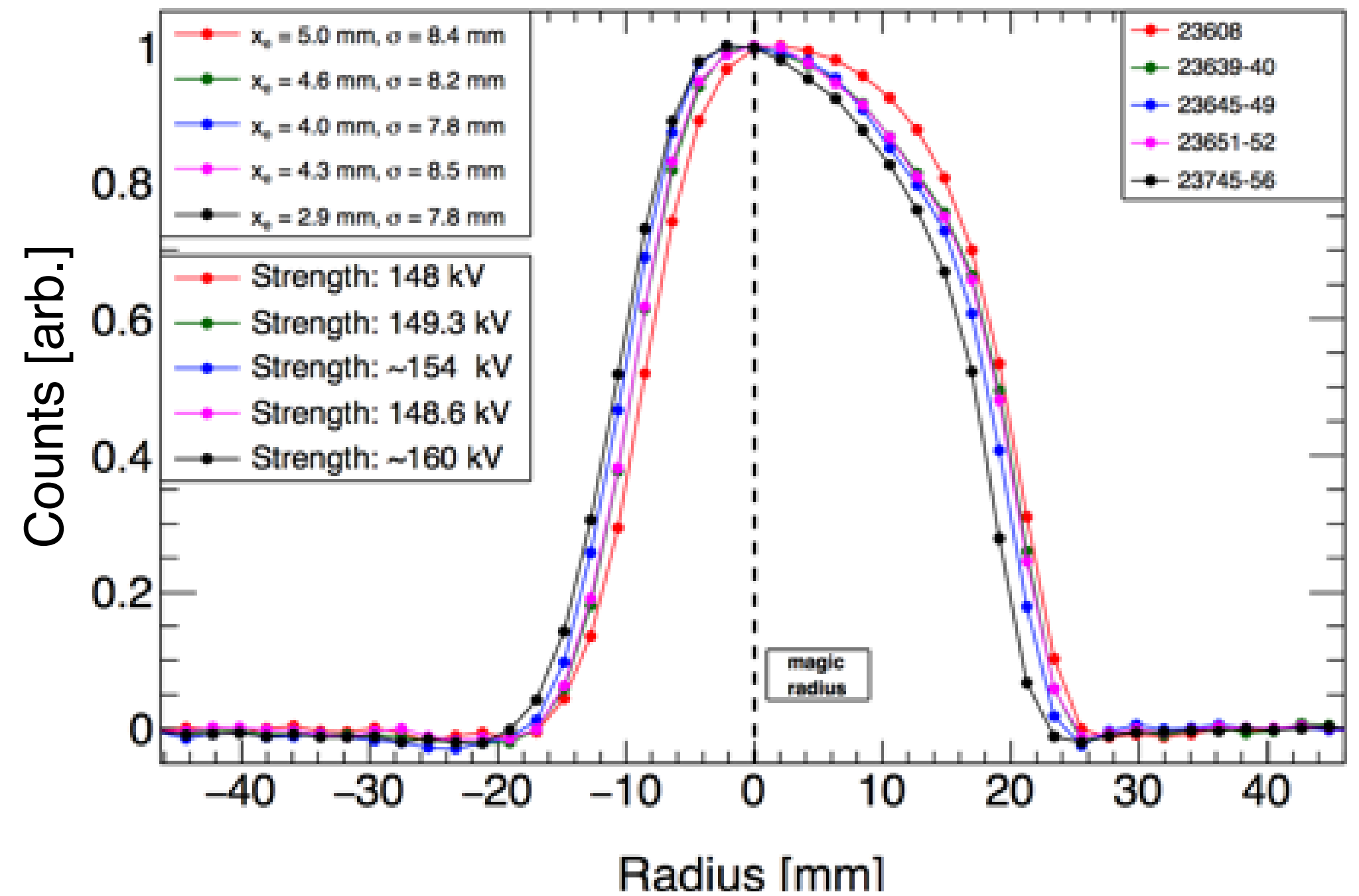
- **Kicker pulse** strength, shape affects structure of beam
- **Beam width** affected by dynamics





# Kicker Challenges

- Need to deflect beam by ~11 mrad on the first turn, then turn off (< 149 ns)
- Engineering challenge never fully realized at BNL — and not yet for us

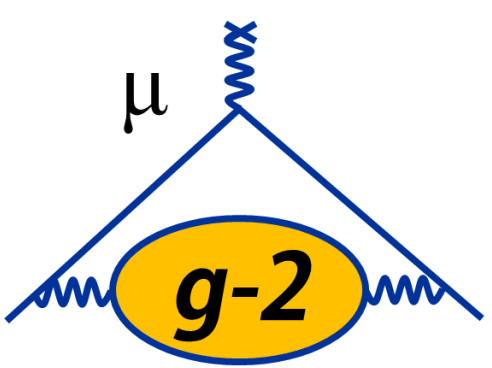


Radial beam distribution at various kick strengths; well contained, but not centered

**Take away: we can live with this — we just don't like it**



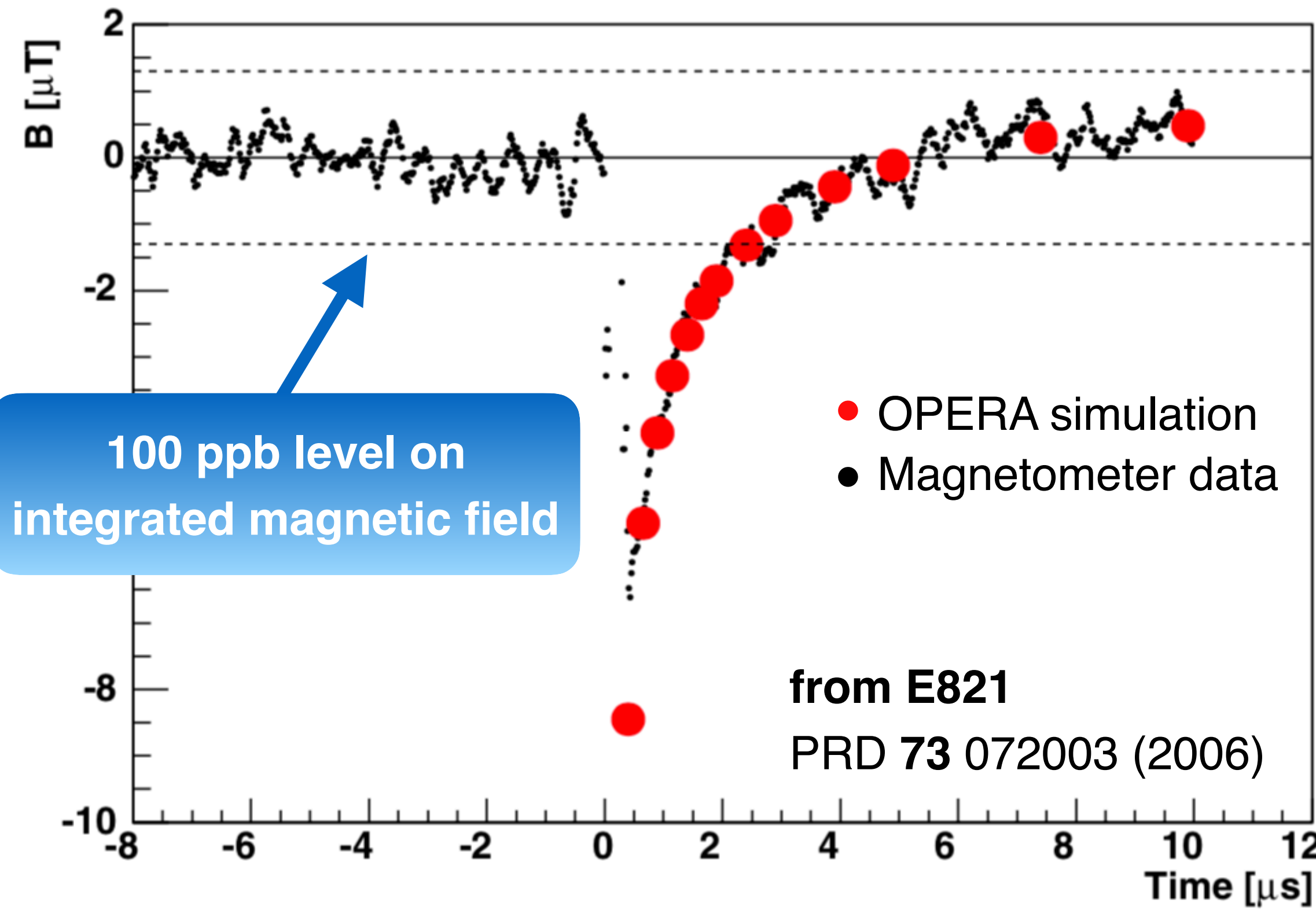
Running at high voltages (~ 50 kV) burns out cables — had to back off



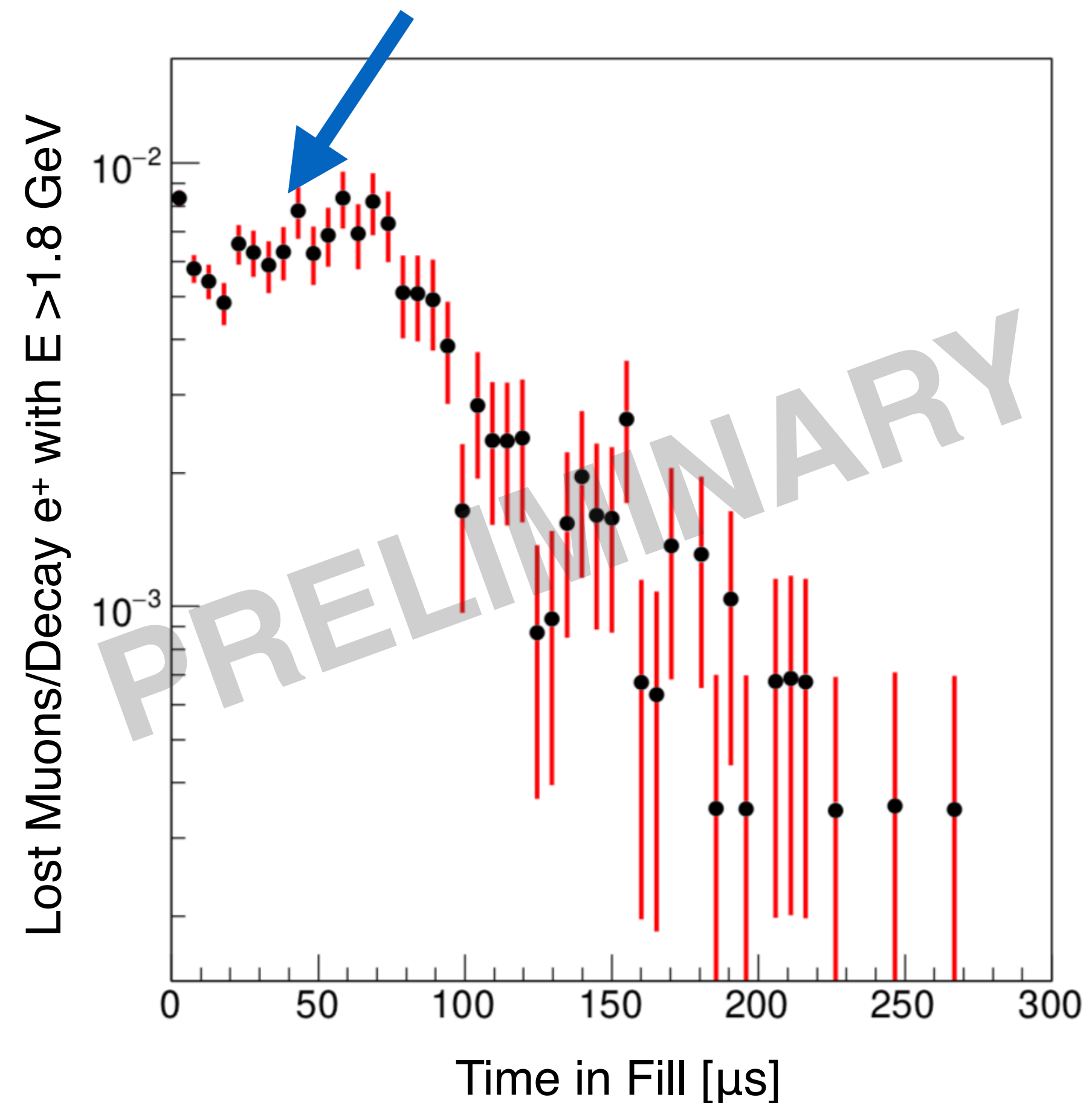
# What Drives the $\omega_a$ Fit Start Time?

- Start fit window to extract  $\omega_a$  at  $\sim 30 \mu\text{s}$  to avoid:

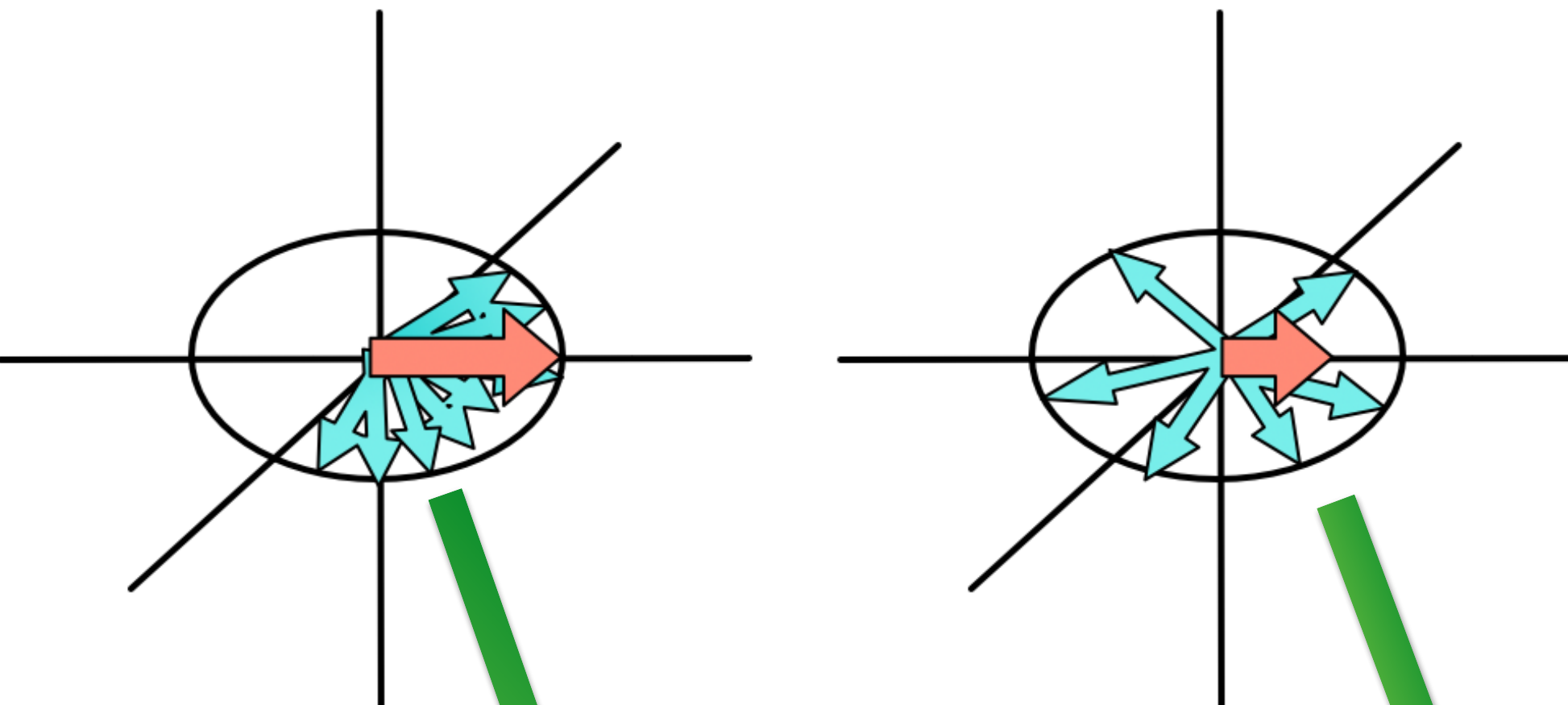
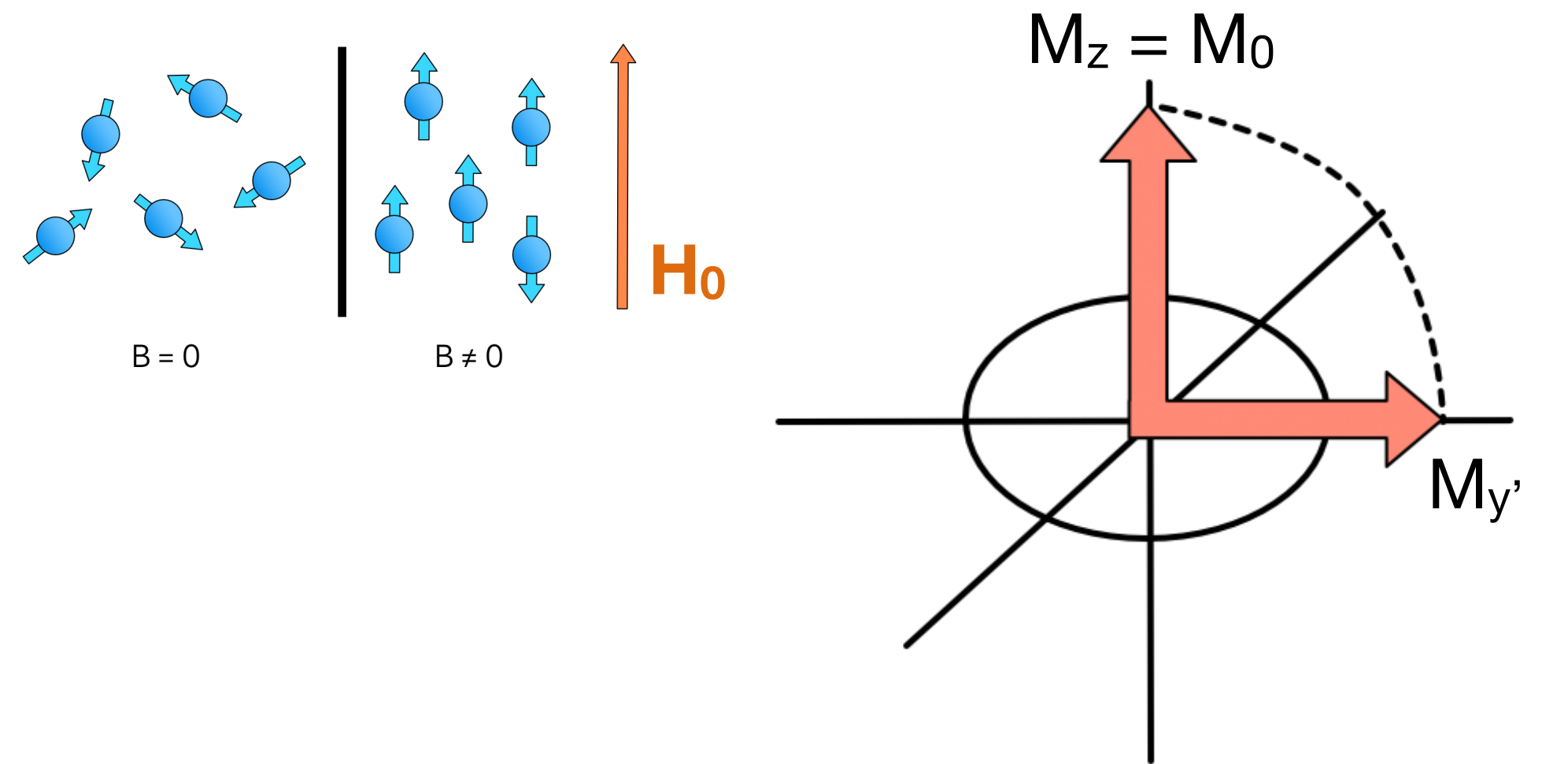
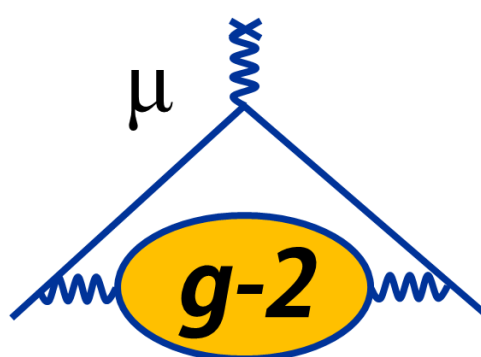
Kicker eddy currents affect the magnetic field



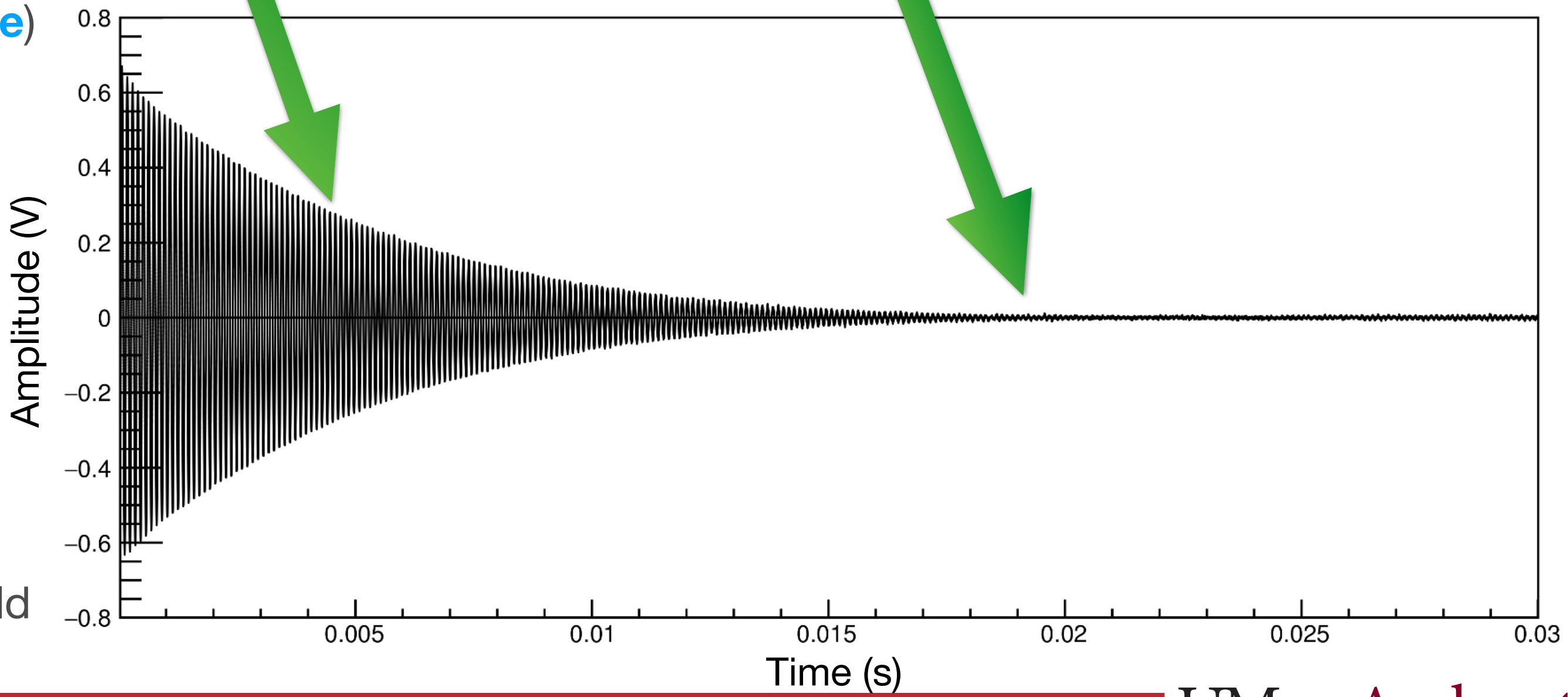
Quad scraping at early times to reduce losses



# Pulsed Nuclear Magnetic Resonance



- Apply an RF pulse for a short time to the sample at Larmor frequency — tips spins perpendicular to external B field ( **$\pi/2$  pulse**)
- Spin precession induces an EMF in the pickup coil
  - So-called **Free-Induction Decay (FID)**
- Decay of signal driven by:
  - Spin-spin interactions (dephasing) (pure  $T_2$ )
  - Field inhomogeneities ( $T_2^*$ )
  - Simultaneously, spins relax back to alignment with holding field (spin-lattice relaxation,  $T_1$ )



# Magnetic Circuits

$$\mathcal{E} = \oint \vec{f}_s \cdot d\vec{\ell} = V = IR$$

Can write a similar equation for magnets

$$\mathcal{F} = \oint \vec{H} \cdot d\vec{\ell} = NI$$

**Magnetomotive Force (mmf)**

$$\vec{B} = \mu_0 (1 + \chi_m) \vec{H} = \mu \vec{H}$$

**Rewrite H in terms of B**

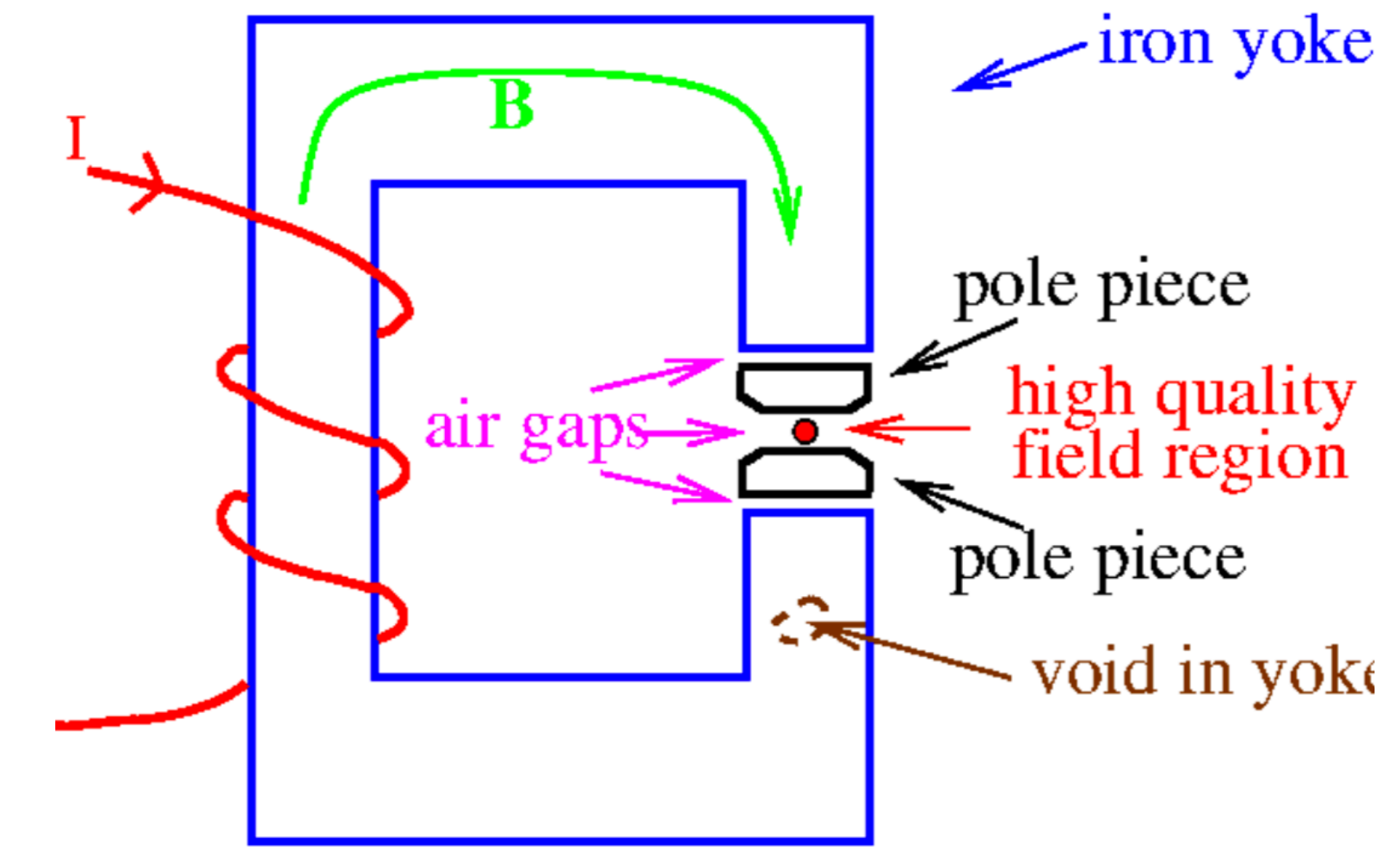
$$\Phi = \vec{B} \cdot \vec{A} = \mu \vec{H} \cdot \vec{A}$$

**Consider magnetic flux**

$$\Phi \oint \frac{d\ell}{\mu A} = \mathcal{F} \Rightarrow \boxed{\mathcal{R} = \oint \frac{d\ell}{\mu A} = \frac{\mathcal{F}}{\Phi}}$$

## Magnetic Reluctance

- Analogous to resistance in an electrical circuit
- Current flows along a path of least resistance while field lines will take a path of least reluctance
- While the emf drives electric charges (Ohm's Law), the mmf "drives" magnetic field lines (Hopkinson's Law)



# Magnet Anatomy

- For E821, Gordon Danby had a brilliant magnet design

$$\mathbf{B} = 1.45 \text{ T } (\sim 5200 \text{ A})$$

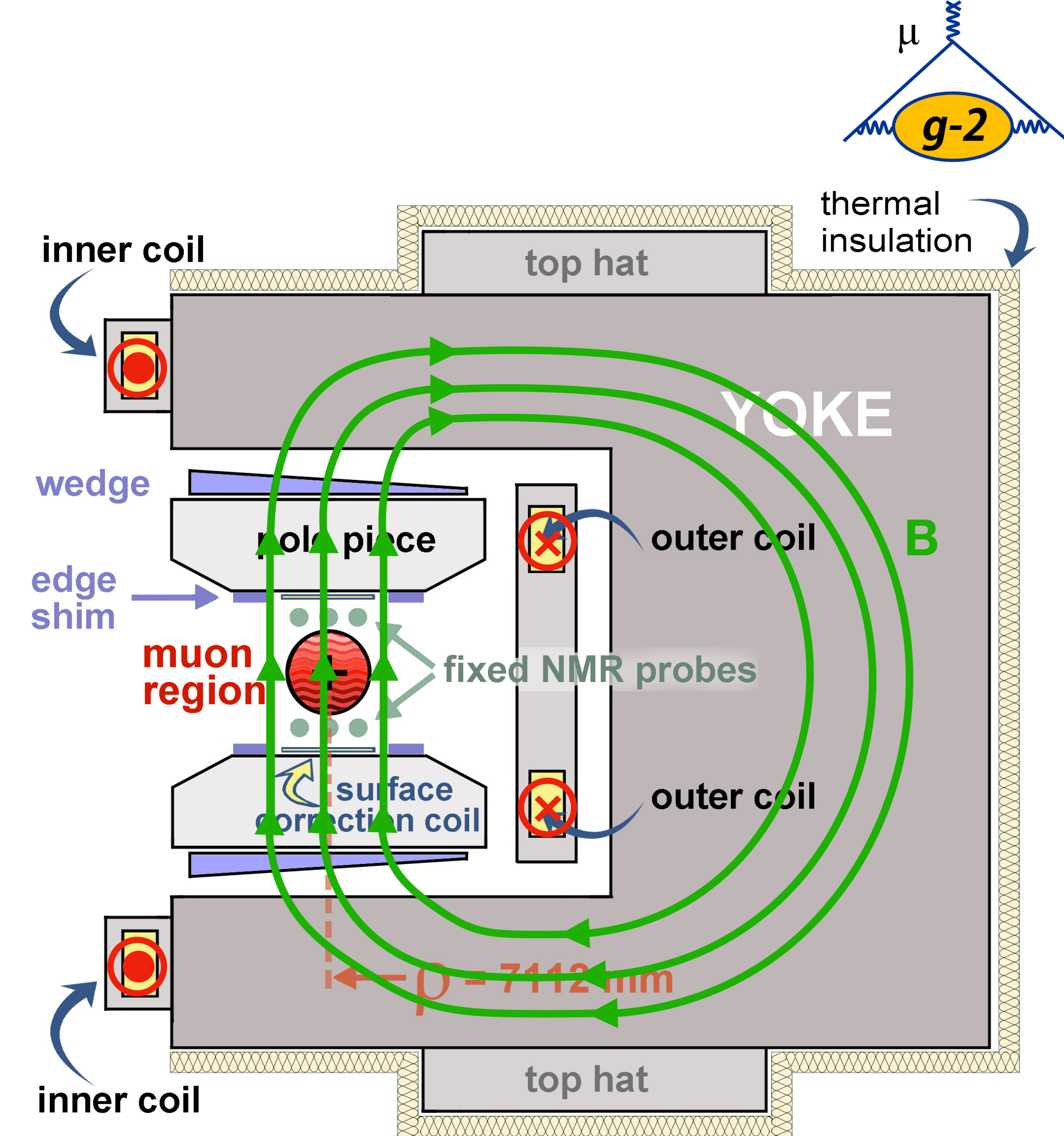
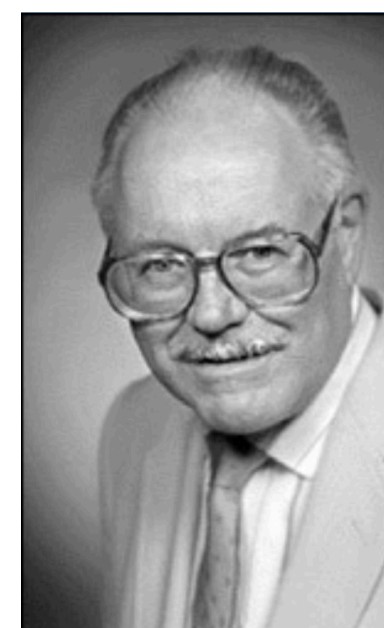
- Non-persistent current: fine-tuning of field in real time

## 12 C-shaped yokes

- 3 upper and 3 lower poles per yoke
- 72 total poles

## Shimming knobs

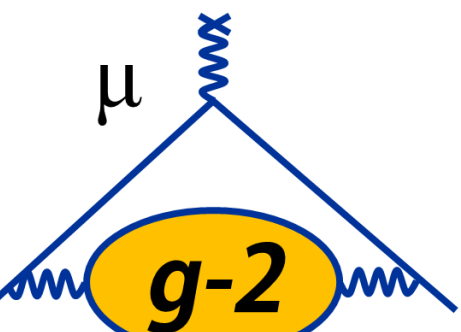
- Pole separation determines field: pole tilts, non-flatness affect uniformity
- Top hats (30 deg effect, dipole)
- Wedges (10 deg effect, dipole, quadrupole)
- Edge shims (10 deg effect, dipole, quadrupole, sextupole)
- Laminations (1 deg effect, dipole, quadrupole, sextupole)
- Surface coils (360 deg effect, quadrupole, sextupole,...)



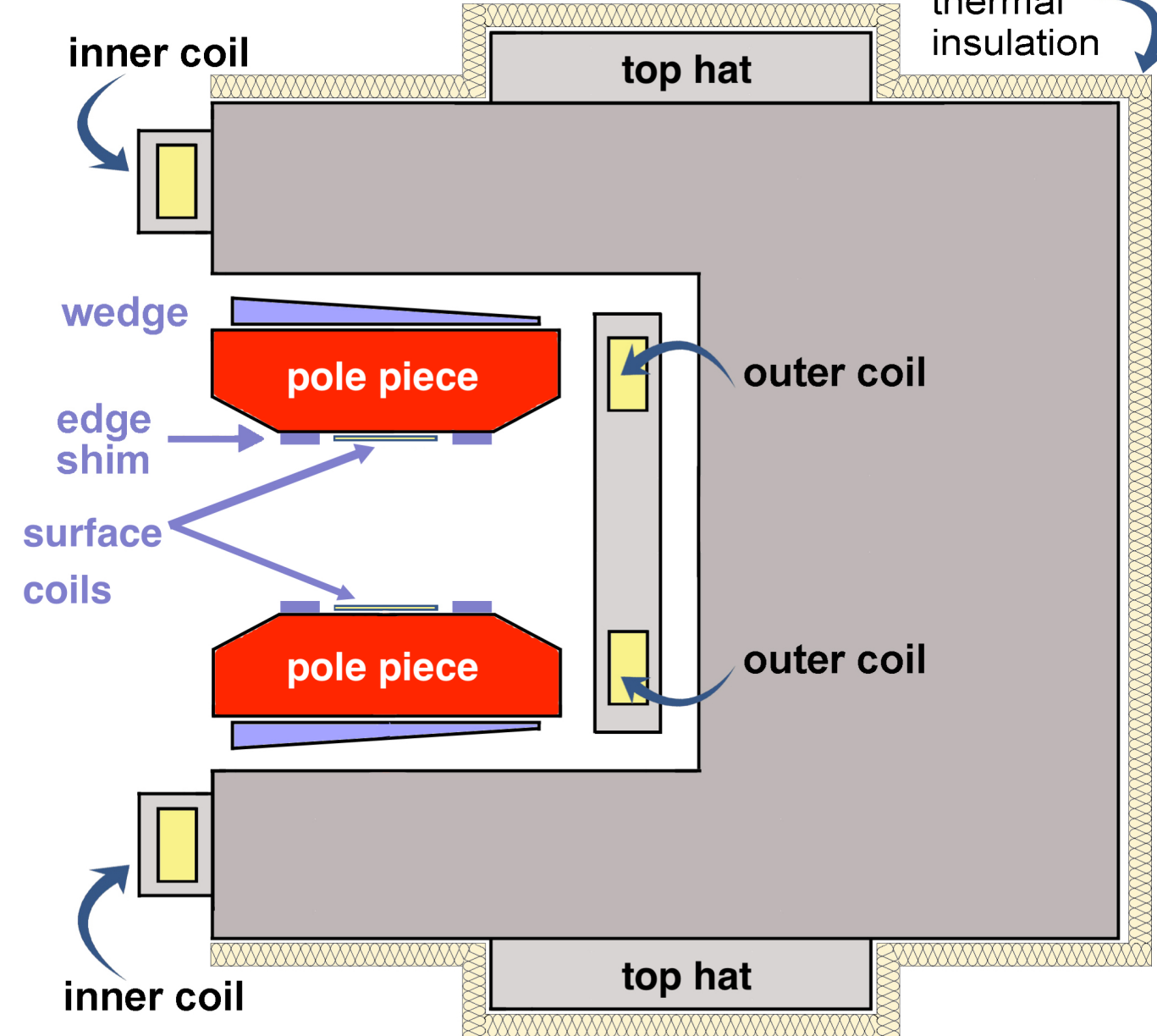
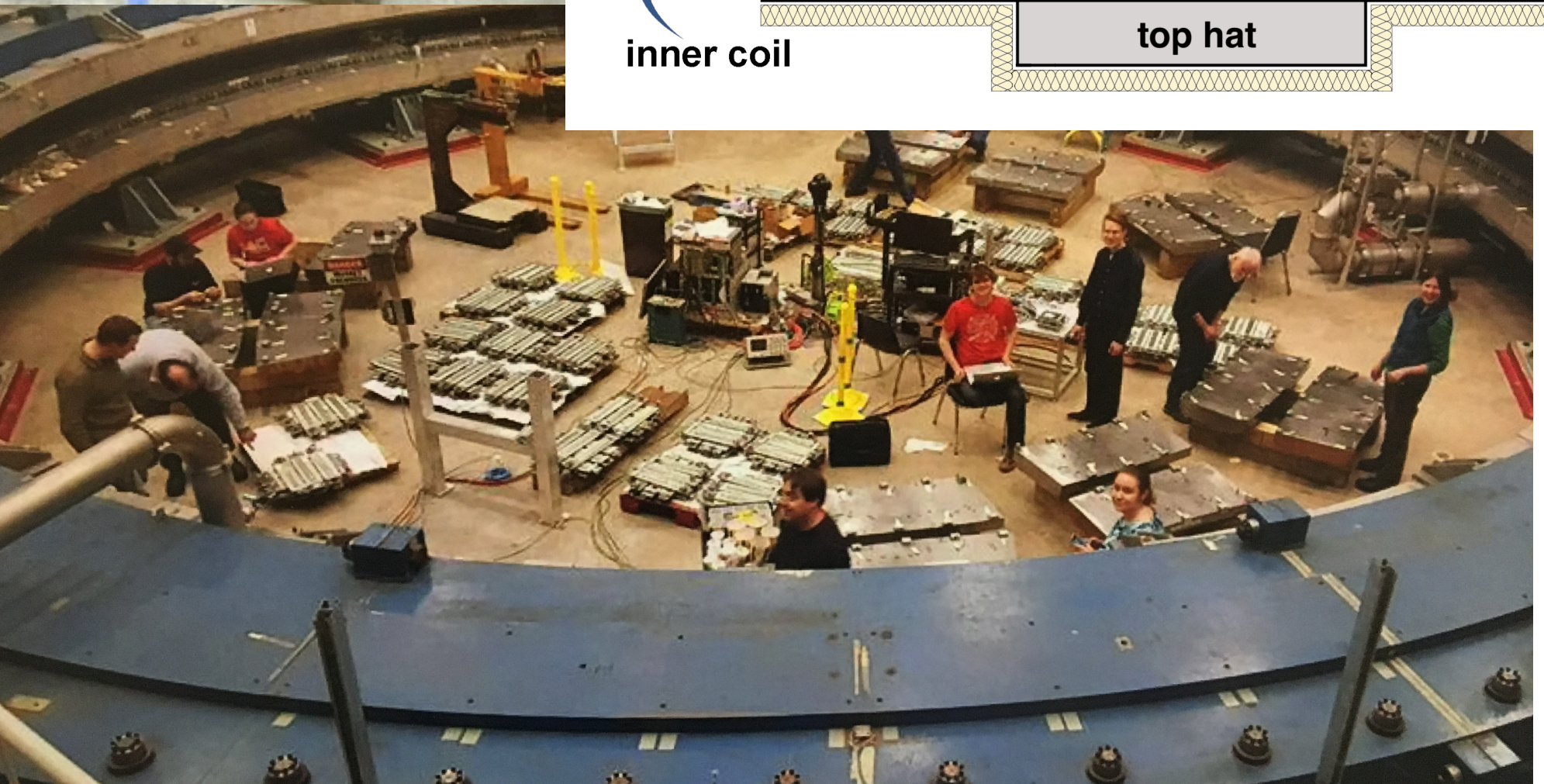
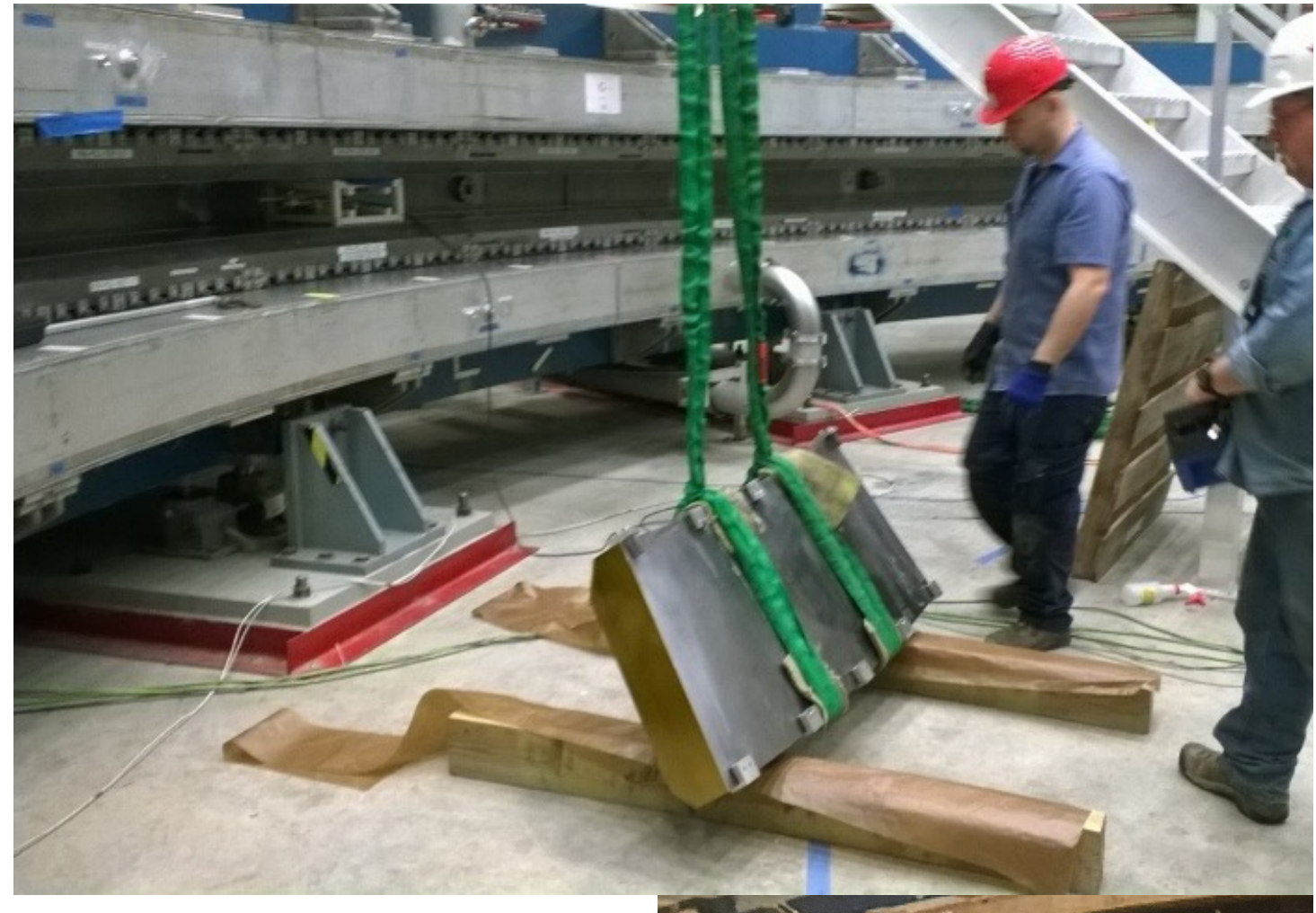
Current direction indicated by red markers

UMassAmherst

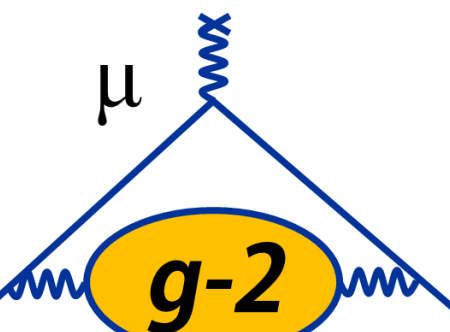
# Optimizing the Dipole Moment



- Want to optimize the vertical component of the field
- Step and tilt discontinuities in pole surfaces yield large variations in the field
- To reduce/remove such effects, make adjustments to pole feet, which changes the magnet gaps and tilts
  - Use 0.001–0.010" thick shims
  - Requires removal of poles from the ring
- Informed by a computer model that optimizes the pole configurations
  - Requires global continuity between pole surfaces
  - Allows only three adjacent poles to be moved at a time (preserves alignment)



# Minimizing the Quad, Sext, Octu Moments



## Calibrated shimming knobs

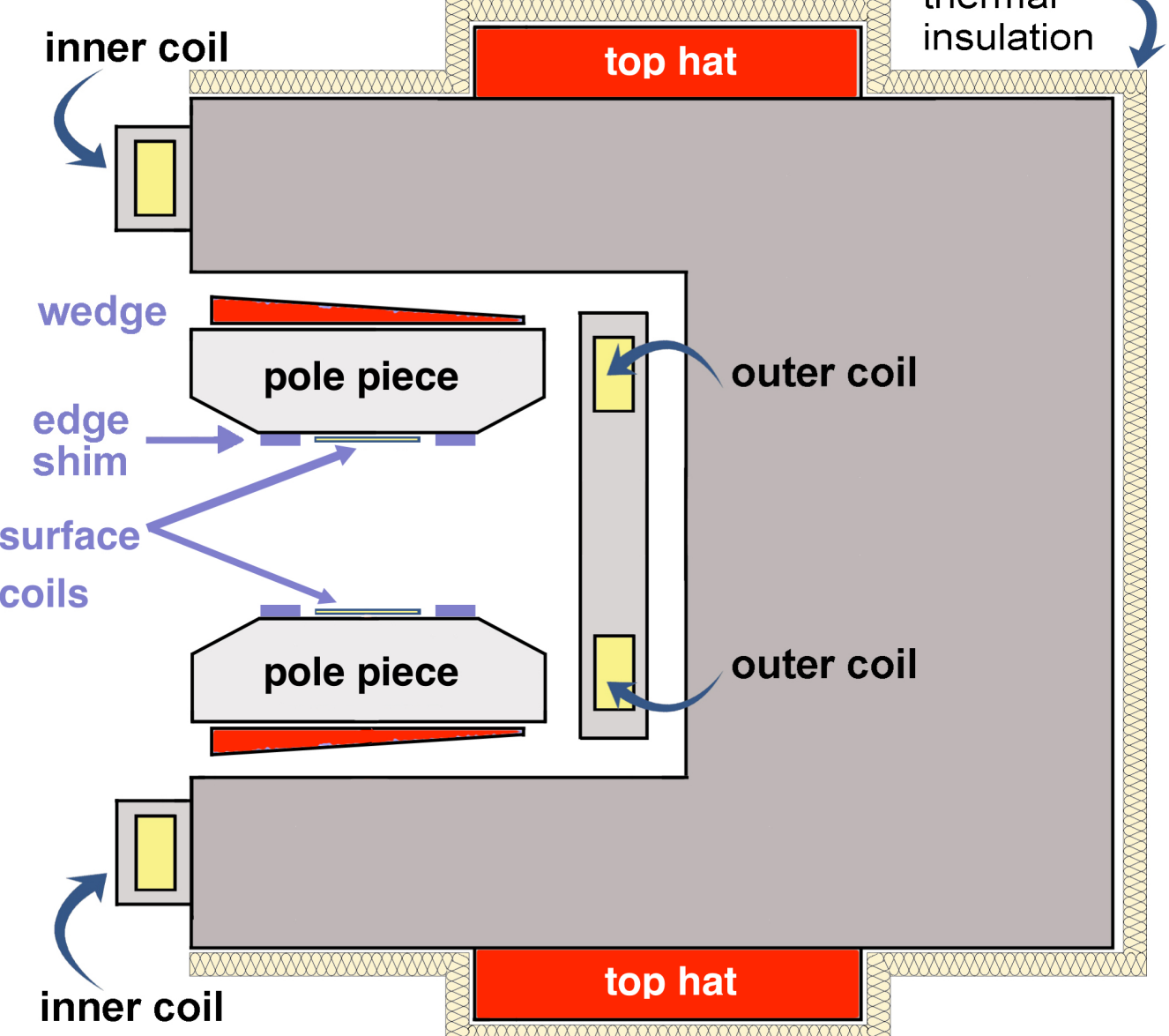
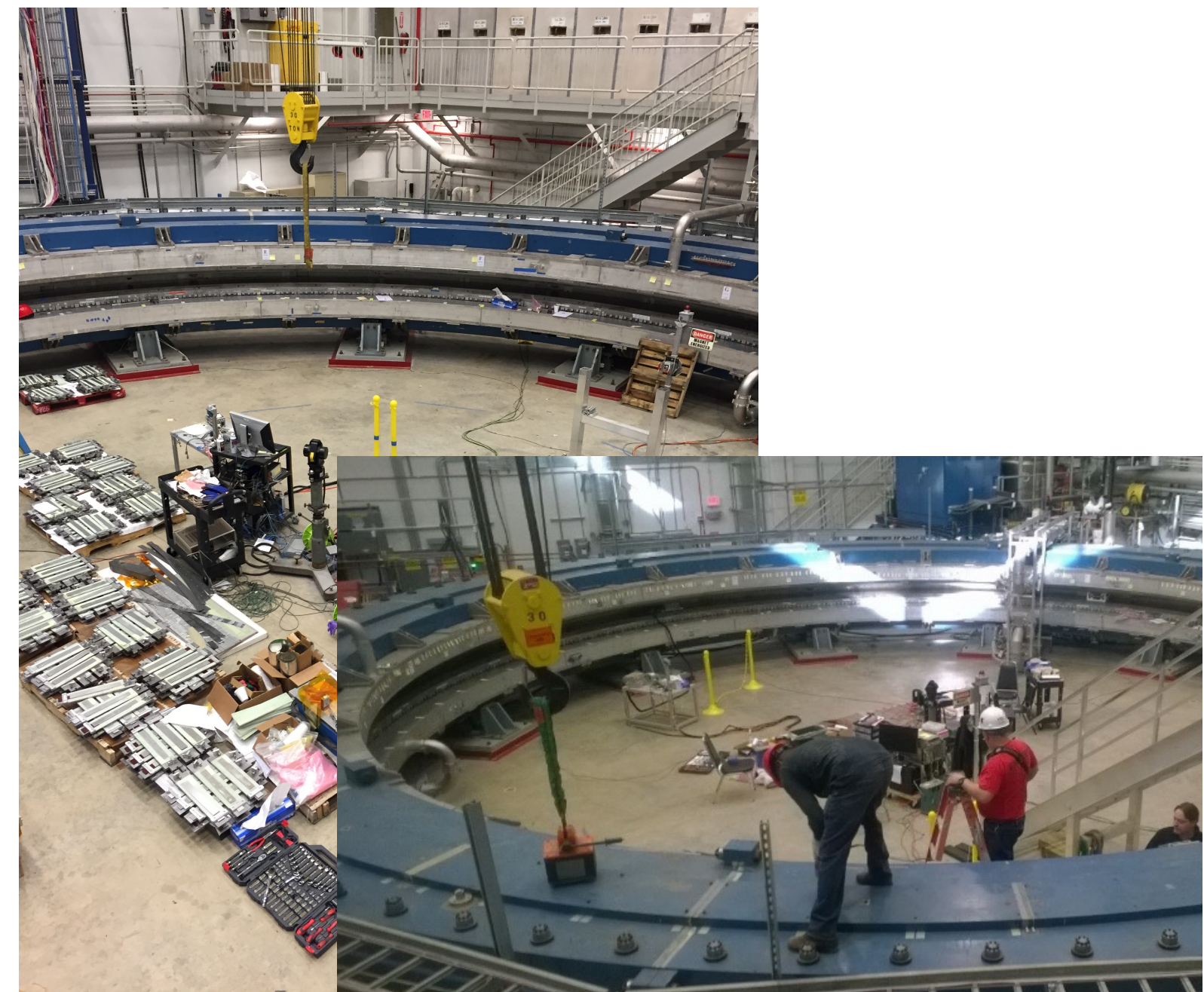
- 48 top hats
- 864 wedges
- ~8400 iron foils (on pole surfaces)

**Coarse tuning:** top hat & wedge adjustments (**dipole, quadrupole**)

- Least-squares fit to field maps predicts top hat and wedge positions

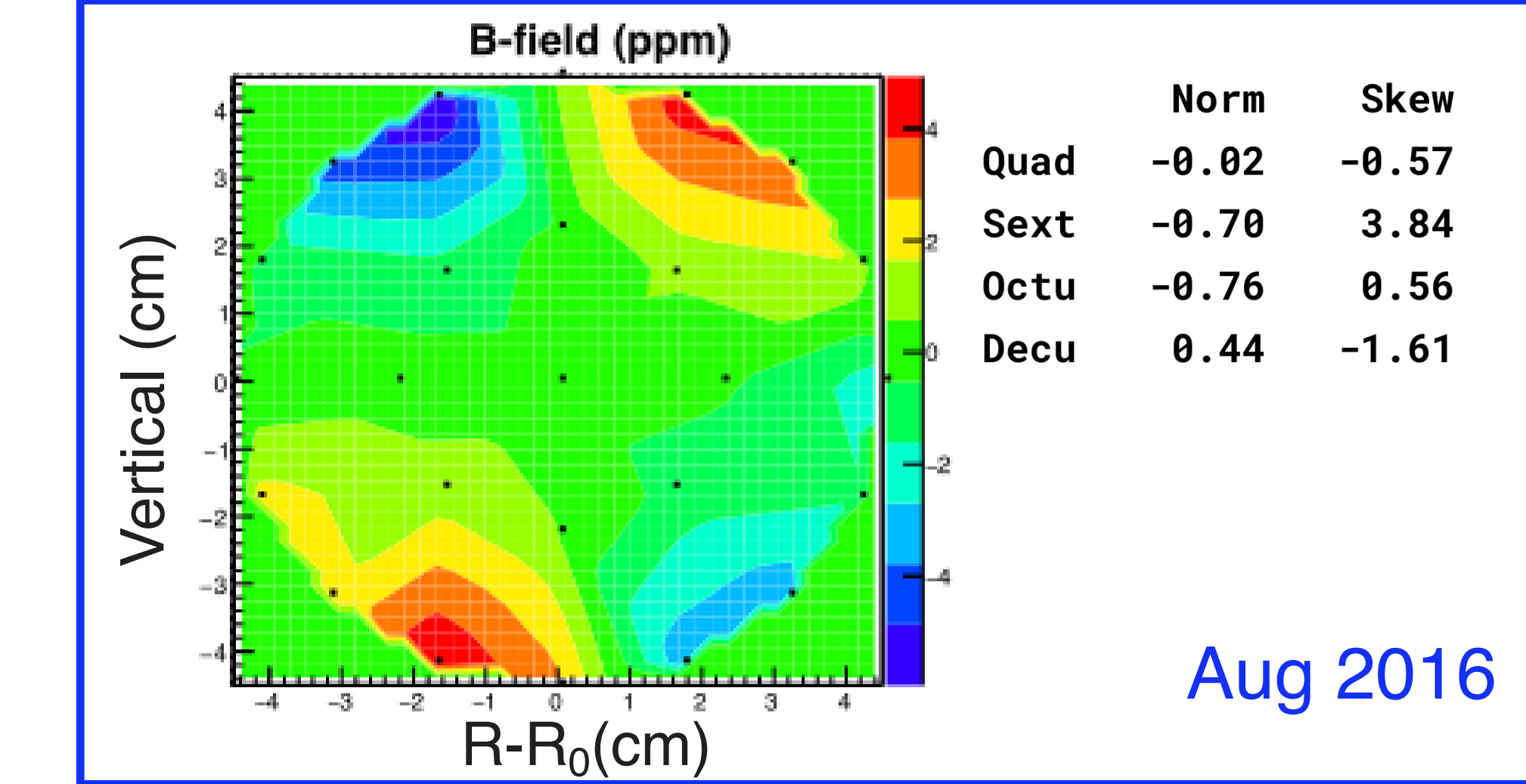
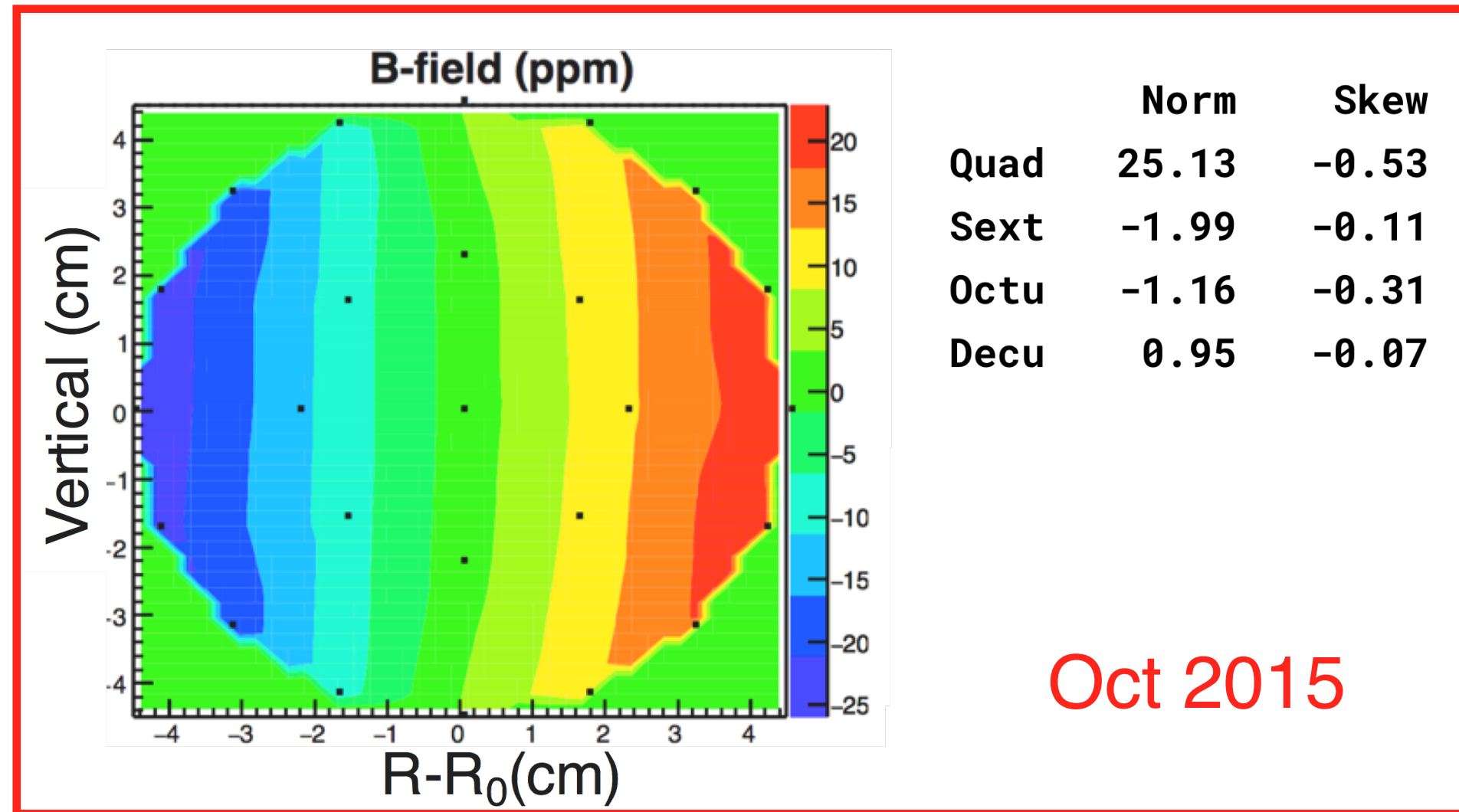
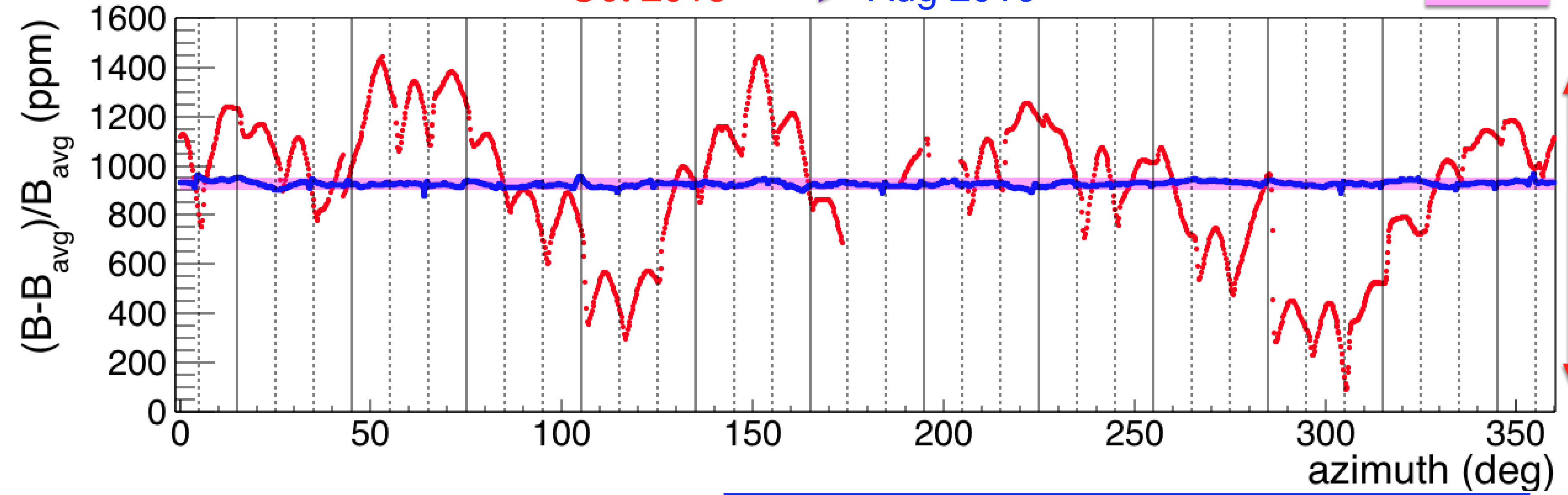
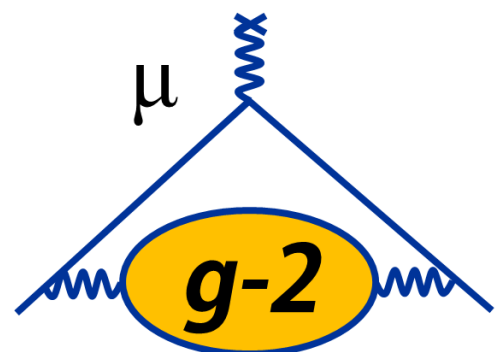
**Fine tuning:** iron foils (**quadrupole, sextupole,...**)

- Modeled as saturated dipoles in 1.45 T field
- Computer code predicts foil width (mass) distribution to fill in the valleys of the field map

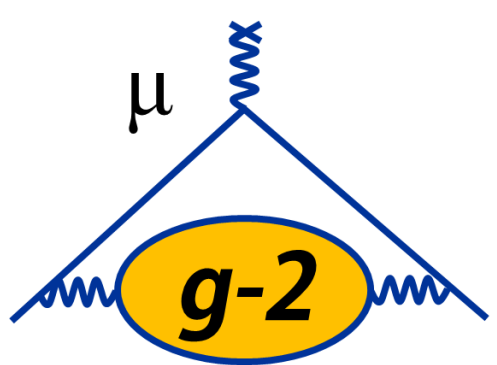


# Rough Shimming Results

Oct 2015 → Aug 2016

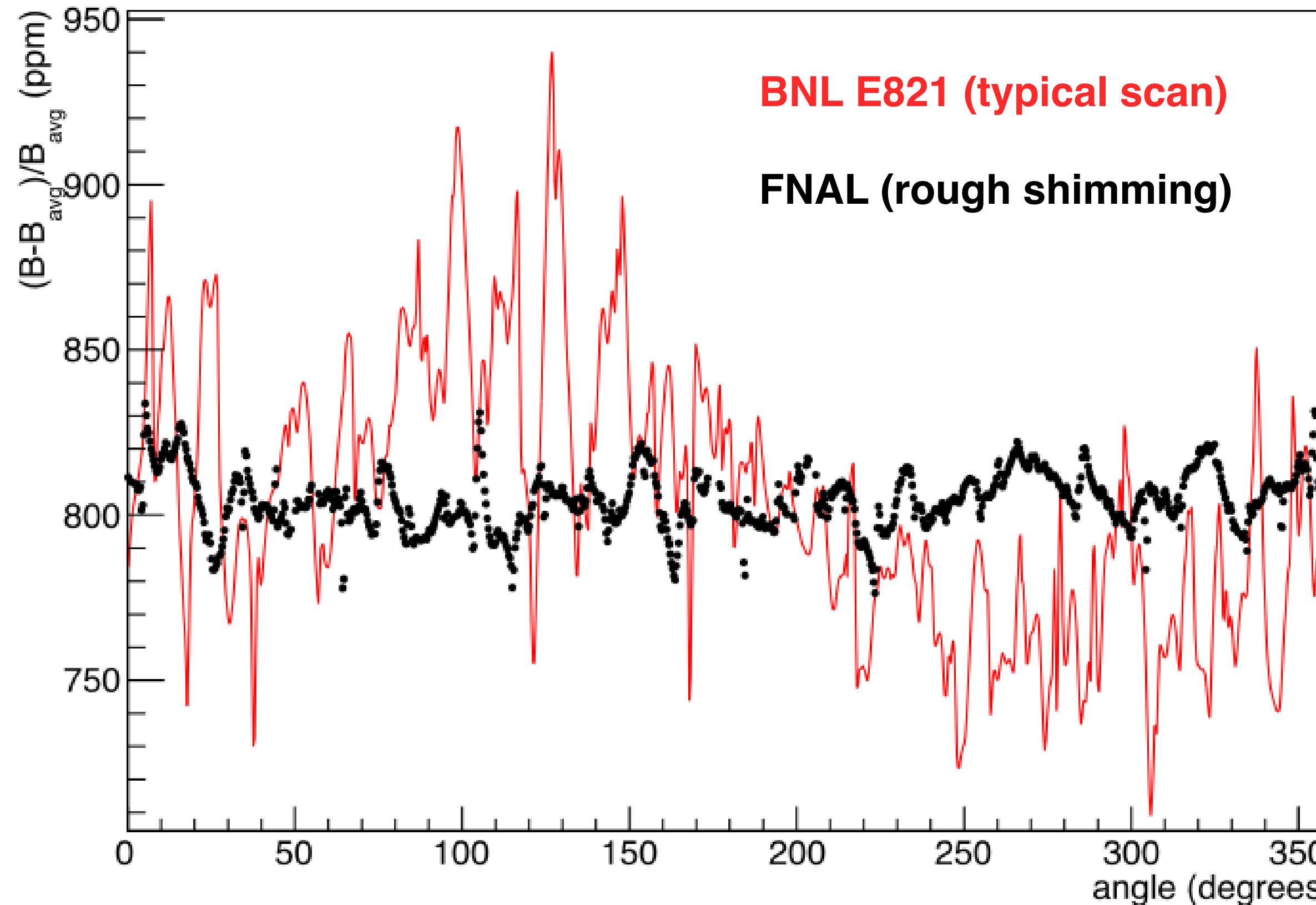


UMassAmherst



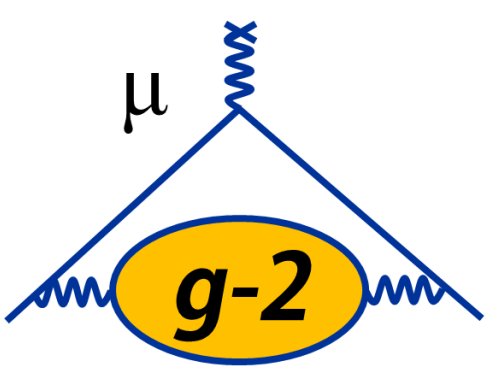
# Magnetic Field Comparison: BNL 821 and FNAL E989

Dipole Vs Azimuth



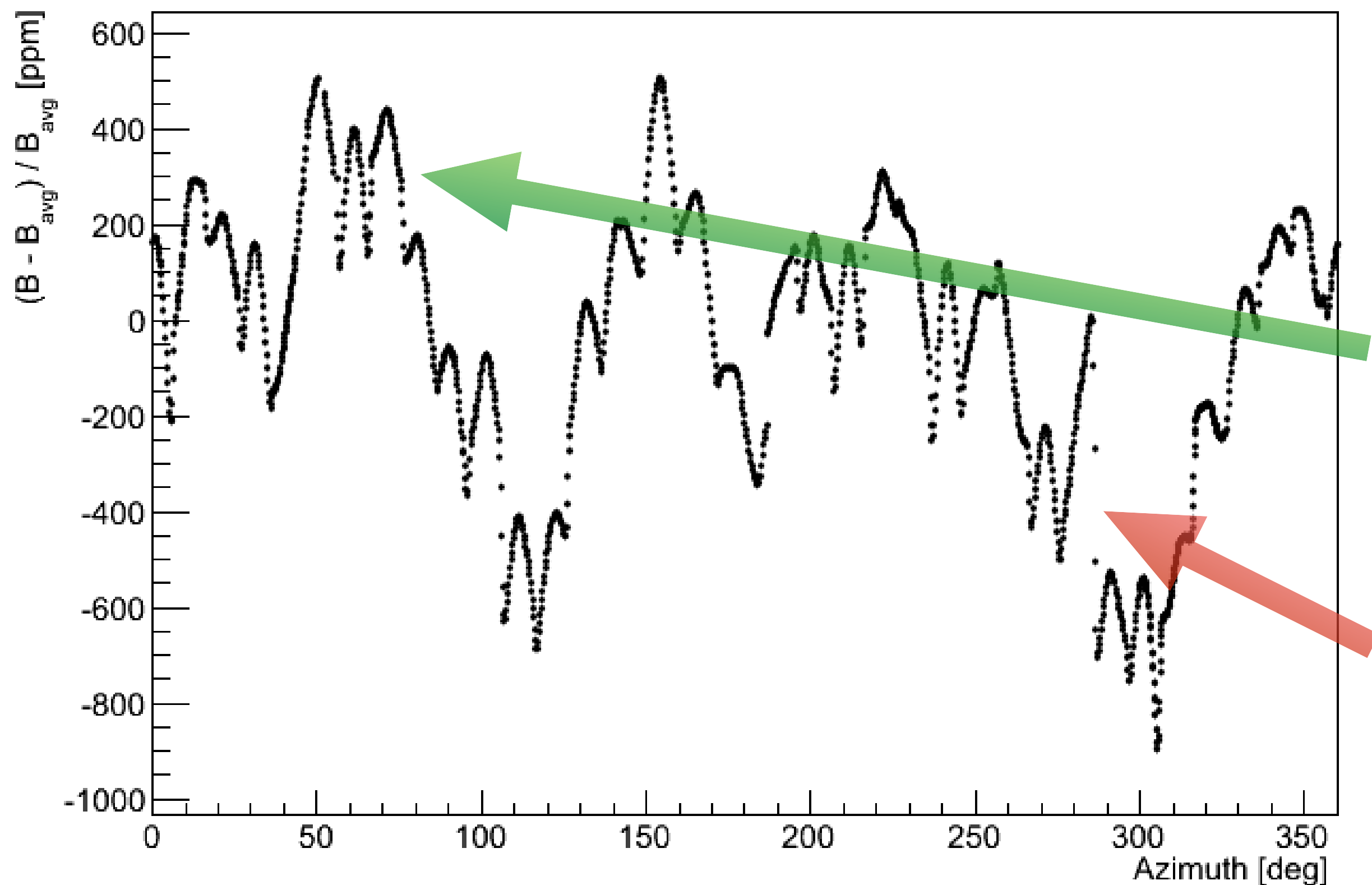
- Laminations very successful in reducing field variations

- BNL E821: 39 ppm RMS (dipole), 230 ppm peak-to-peak
- FNAL rough shimming: 10 ppm RMS (dipole), 75 ppm peak-to-peak

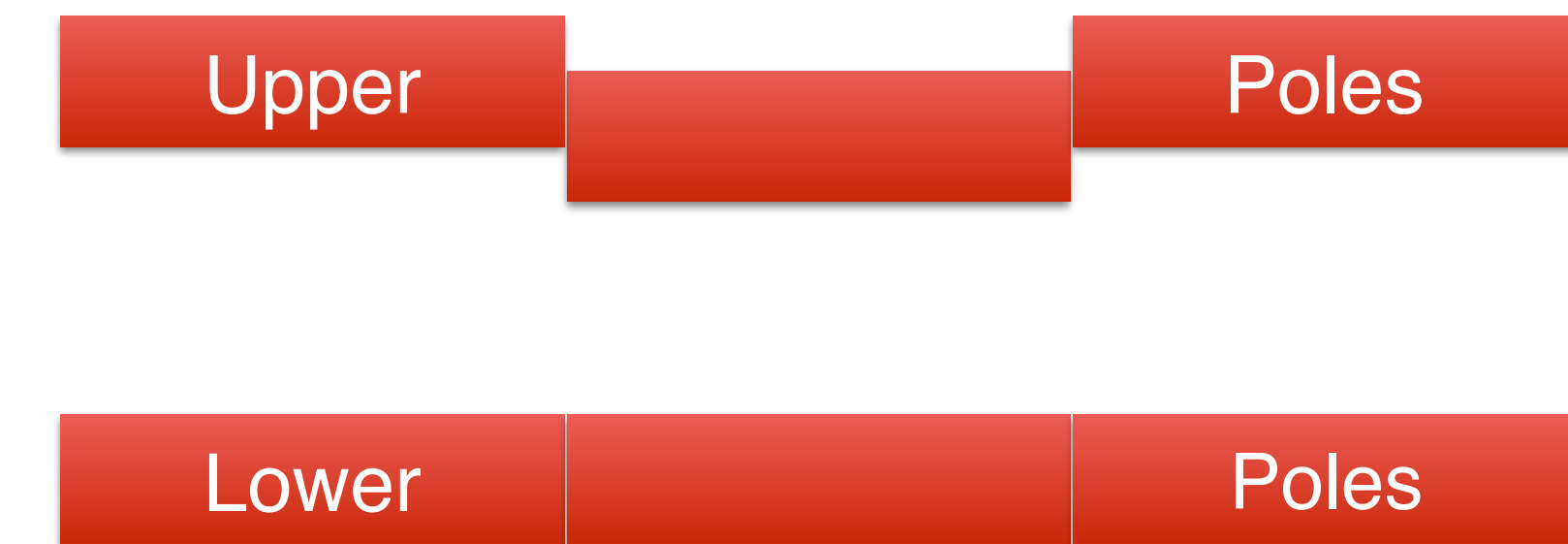


# Magnetic Field Variations

First Magnetic Field Map, Oct 14 2015

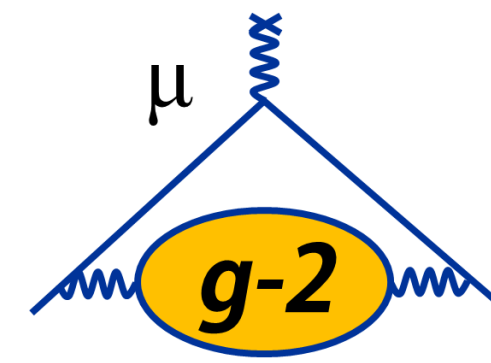


- Gradual drift from materials, pole gap changes
- 36 pairs of poles  $\rightarrow$  10-degree structure
- Pole shape:
- Pole-to-pole discontinuities



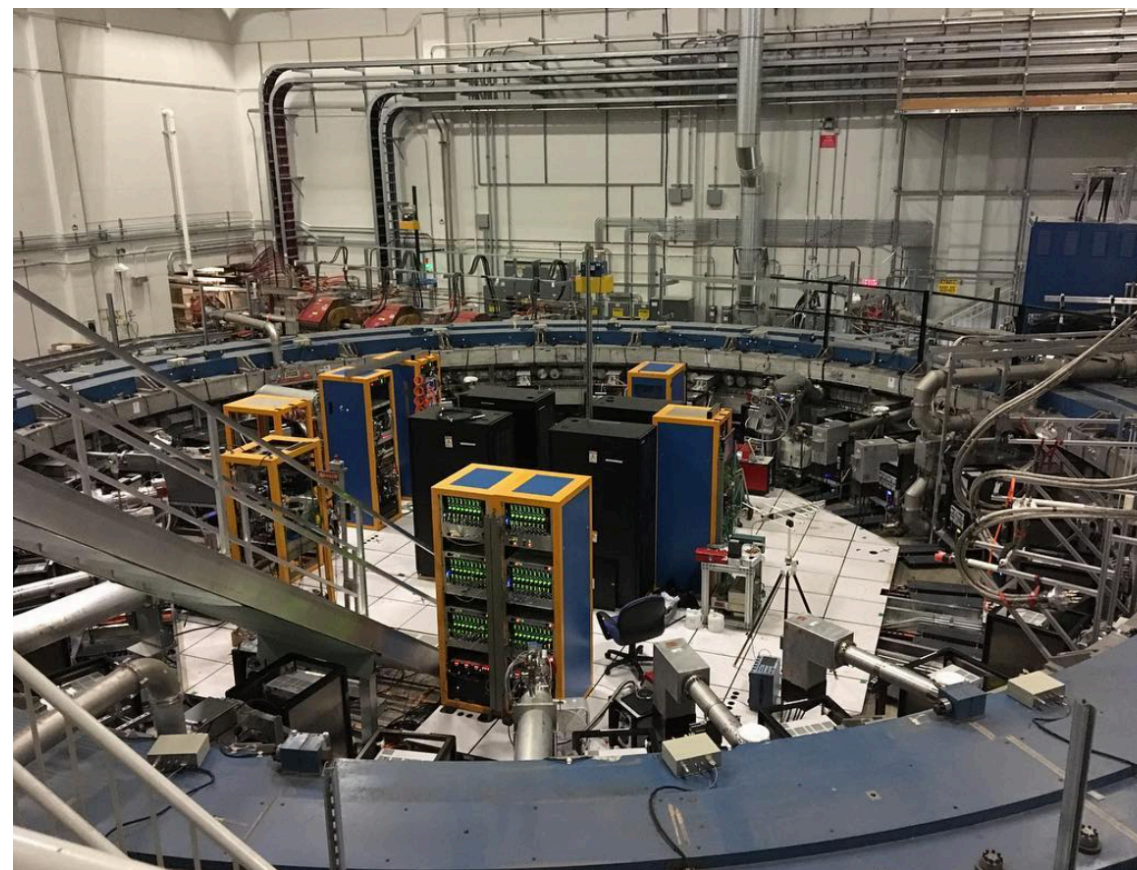
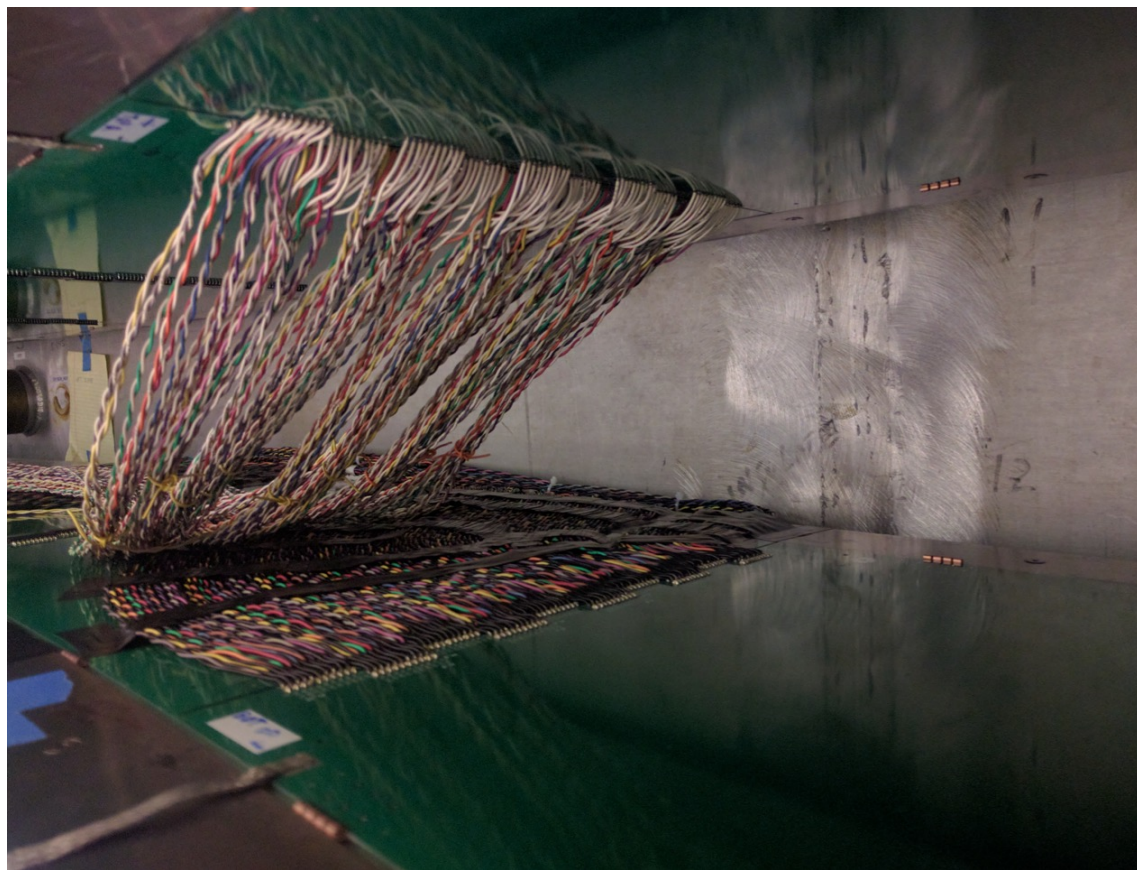
UMassAmherst

# Auxiliary Field Systems



## Surface Correction Coils

- Continuous PCB traces going around the ring on pole surfaces
- 100 concentric traces on upper poles, 100 on lower poles
- Programmable range:  $\pm 20$  ppm on the field
- Used to cancel higher-order multipole moments in the magnetic field (on average)



## Power Supply Feedback

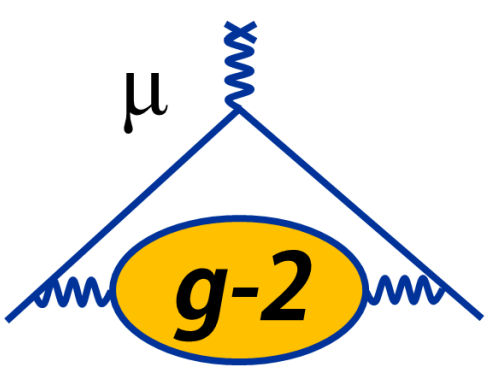
- Programmable current source with a range of  $\pm 5$  ppm on the field
- Uses data from **fixed probe** system to stabilize the field at a specified set point



## Fluxgates

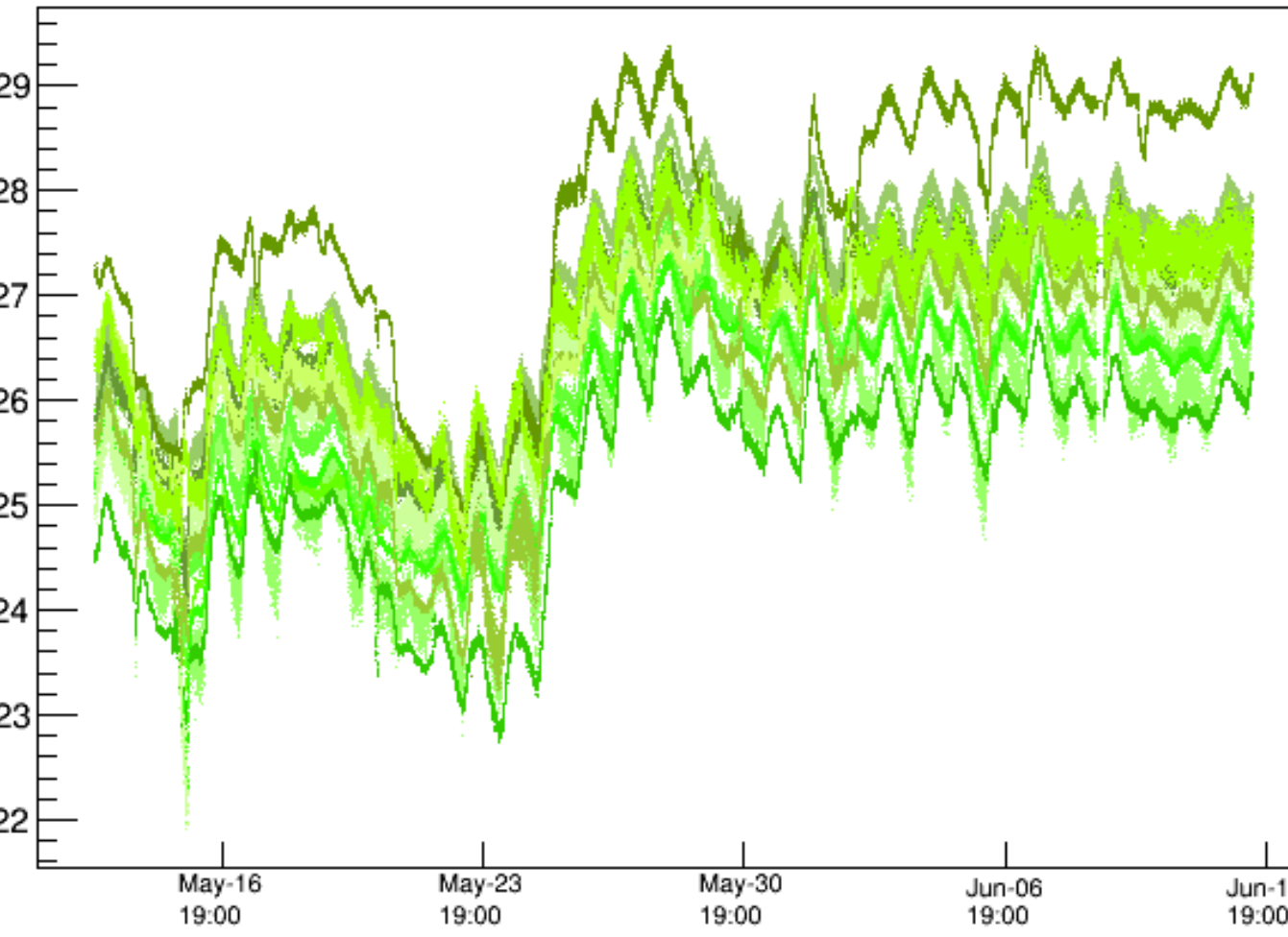
- Measure (x,y,z) components of transient fields in the hall
- Sensitive down to  $10^{-9}$  T (DC or AC) fields
- Bandwidth up to 1 kHz



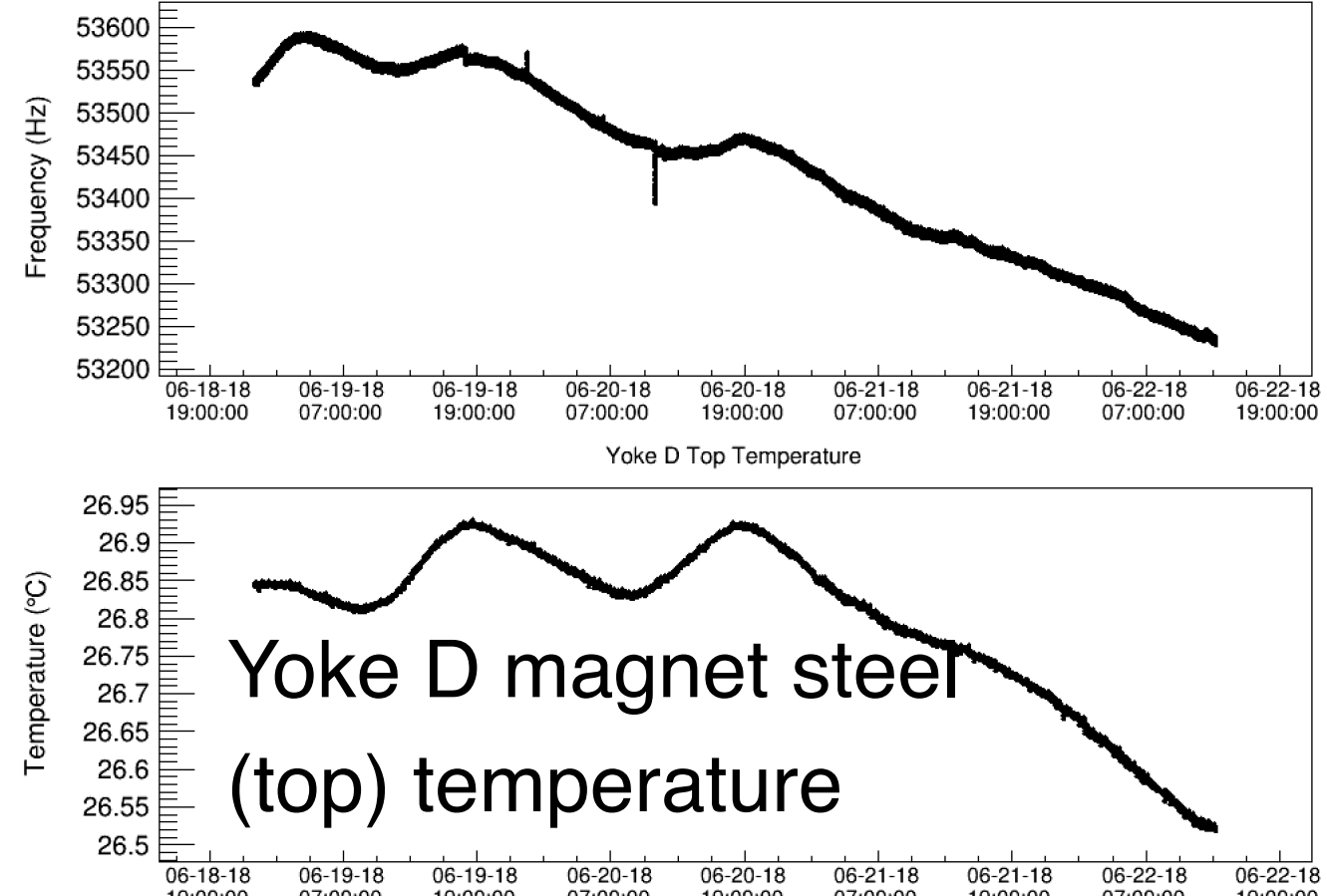


# Magnet Insulation

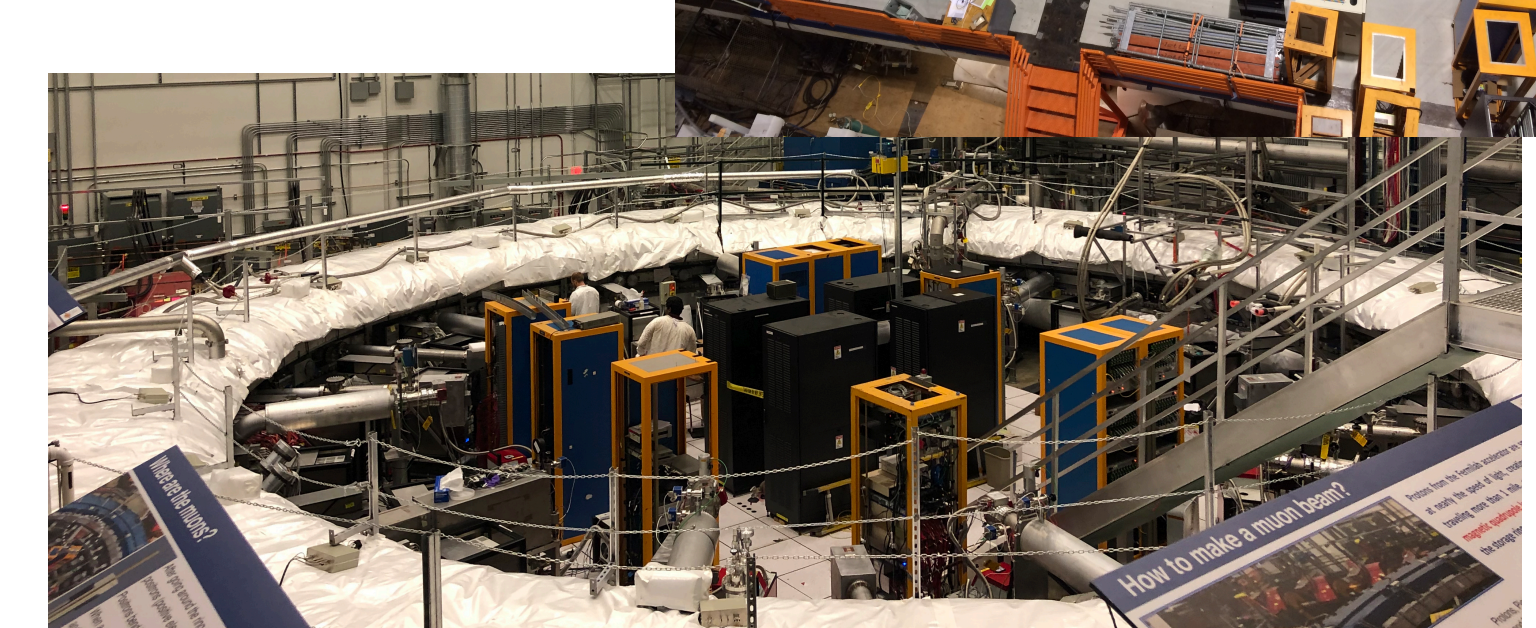
- Temperature variations in the hall affect the quality of the magnetic field
  - Observed  $\sim 20$  ppm/deg C effects on the dipole moment during the run
  - Also affects ability to track higher-order multipoles
- Two main issues
  - Large changes in average temperature over time ( $2\text{--}3^\circ\text{C}$ )
  - Differential changes across the magnet ( $\sim 3^\circ\text{C}$ )
- Two-pronged solution:
  - Improved cooling system in the hall
  - Install fiberglass insulation blanket on magnet steel

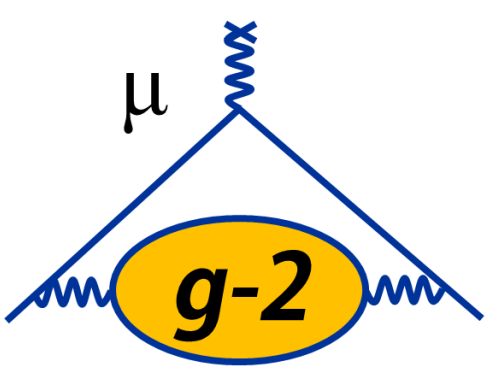


Fixed probe on yoke D vacuum chamber (top)



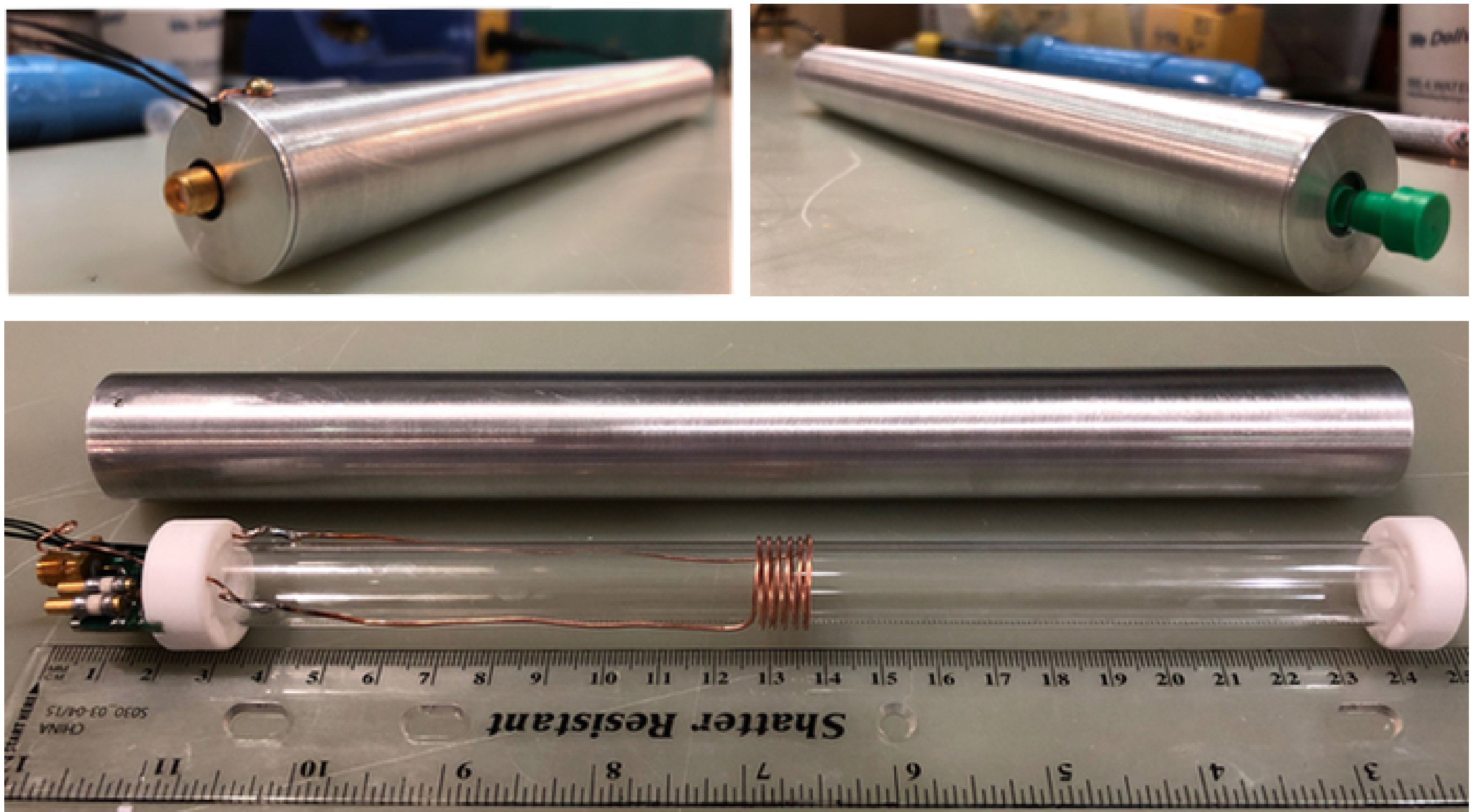
Installed blankets  
summer 2018



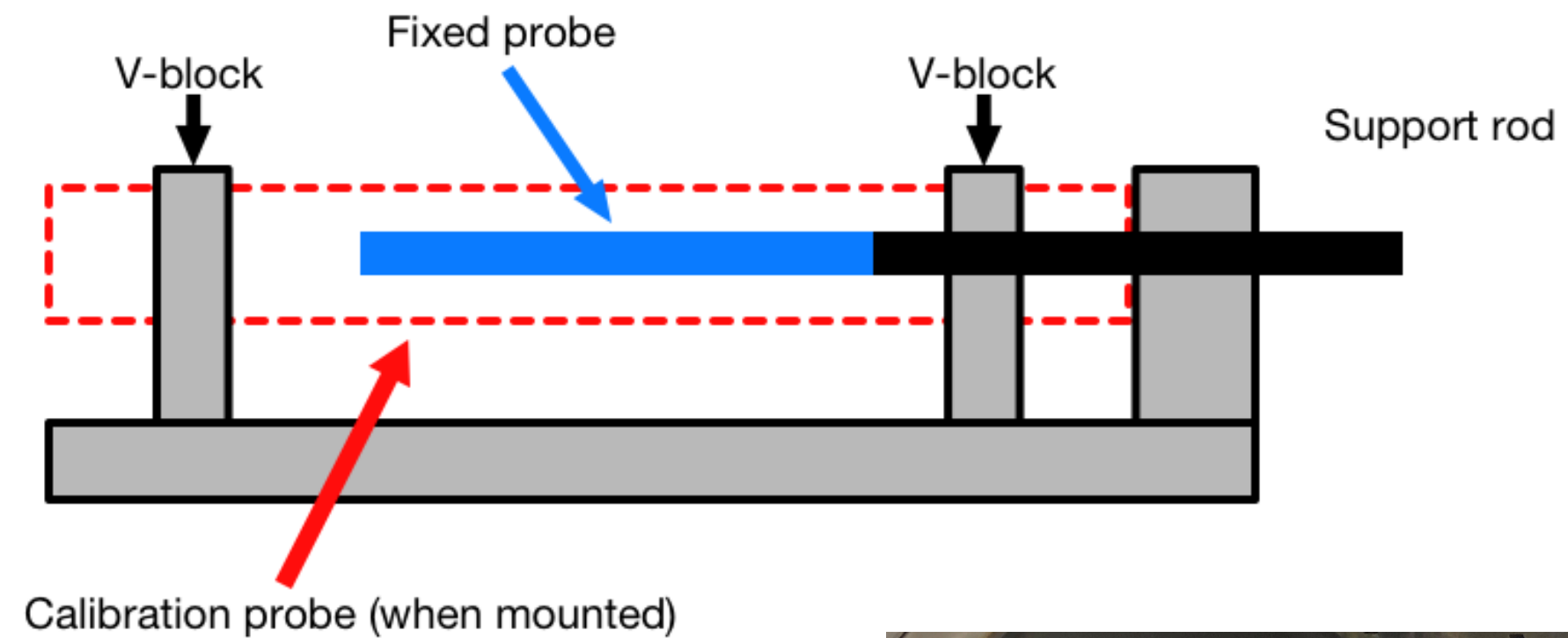
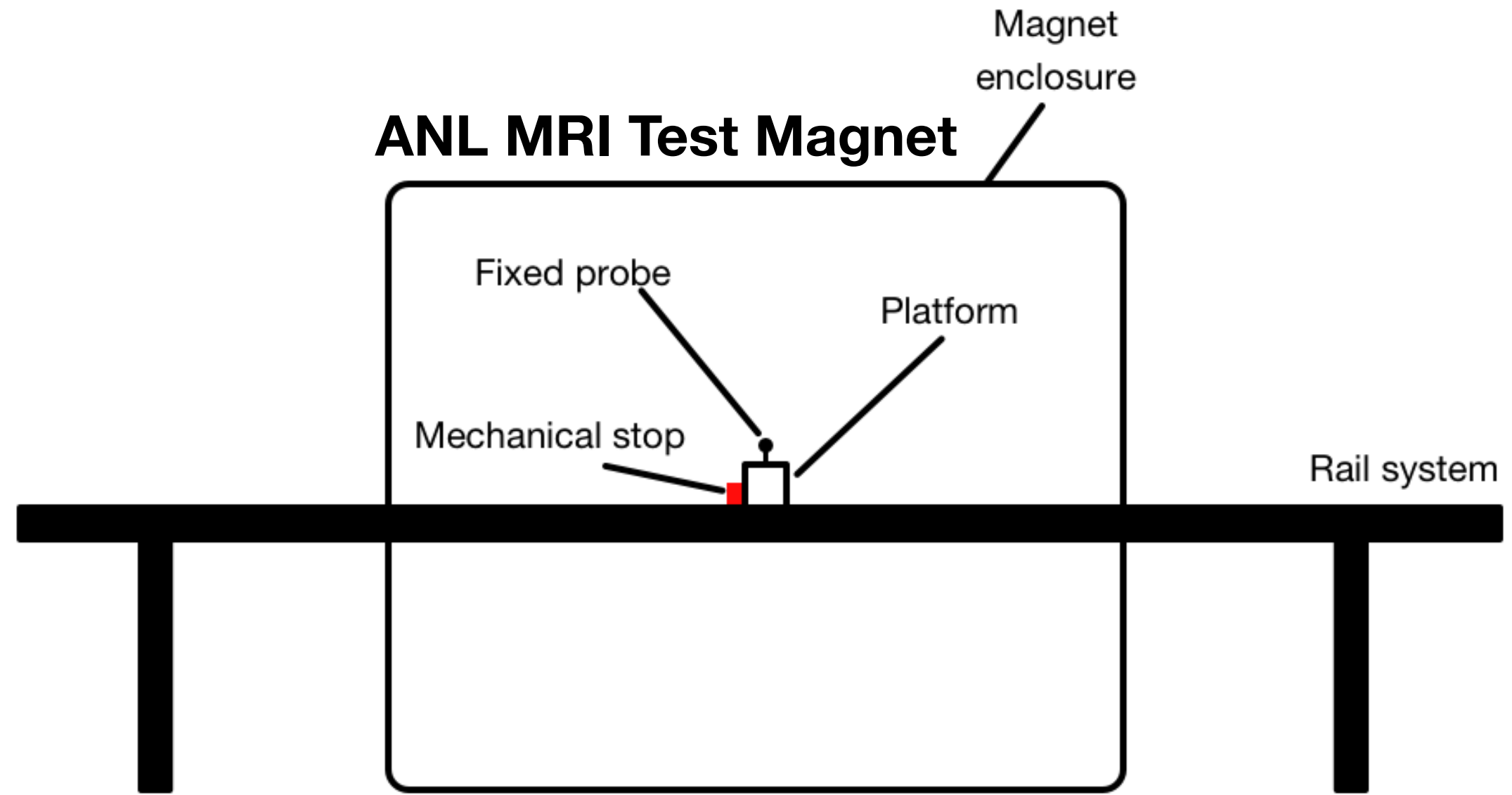
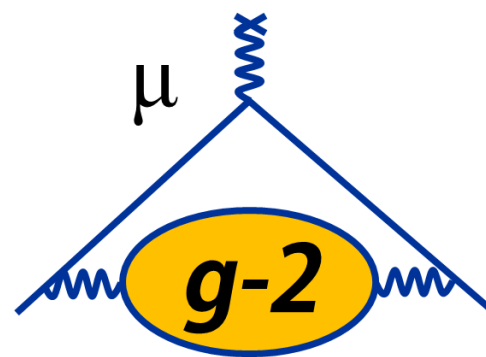


# Plunging Probe Design

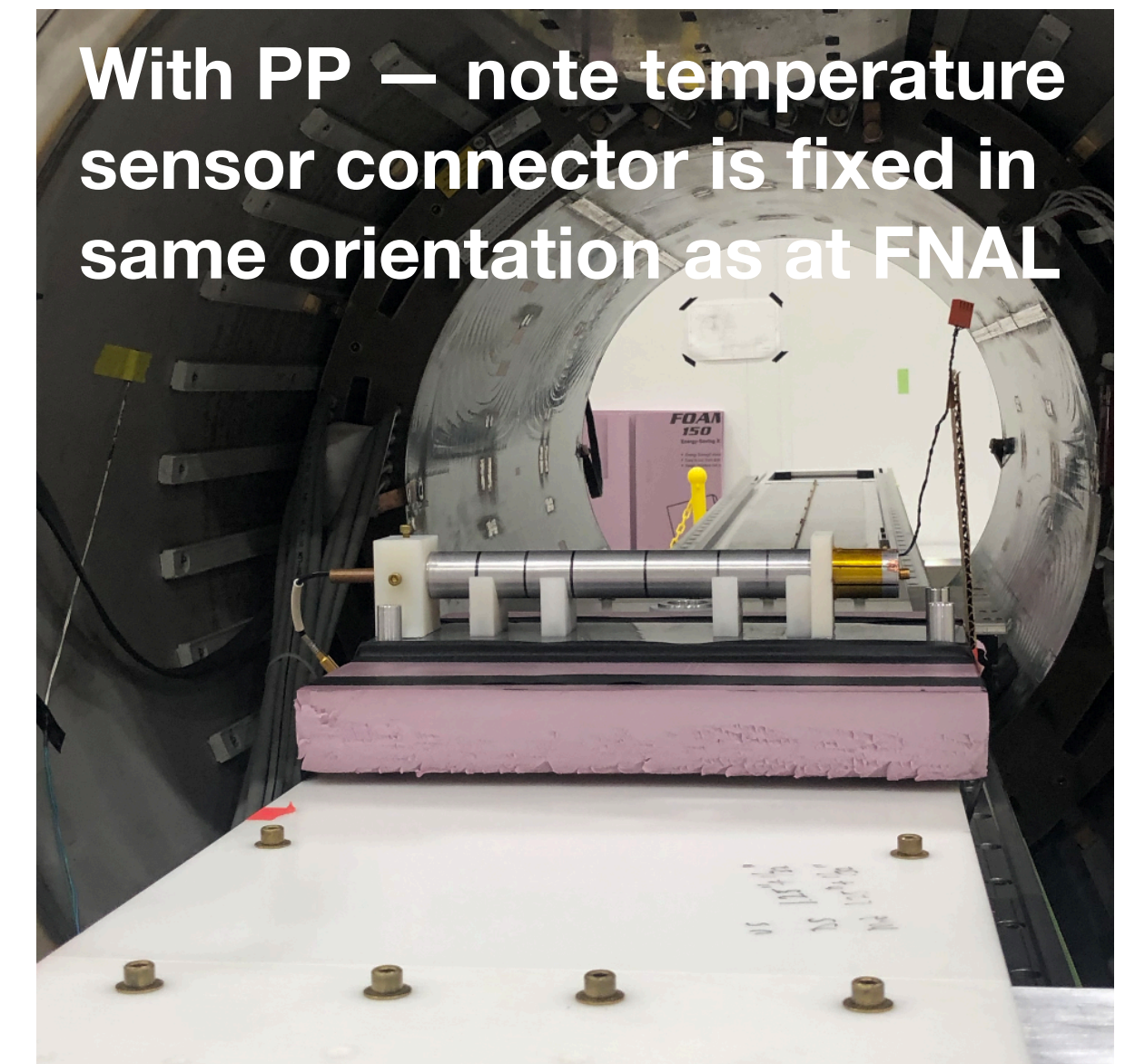
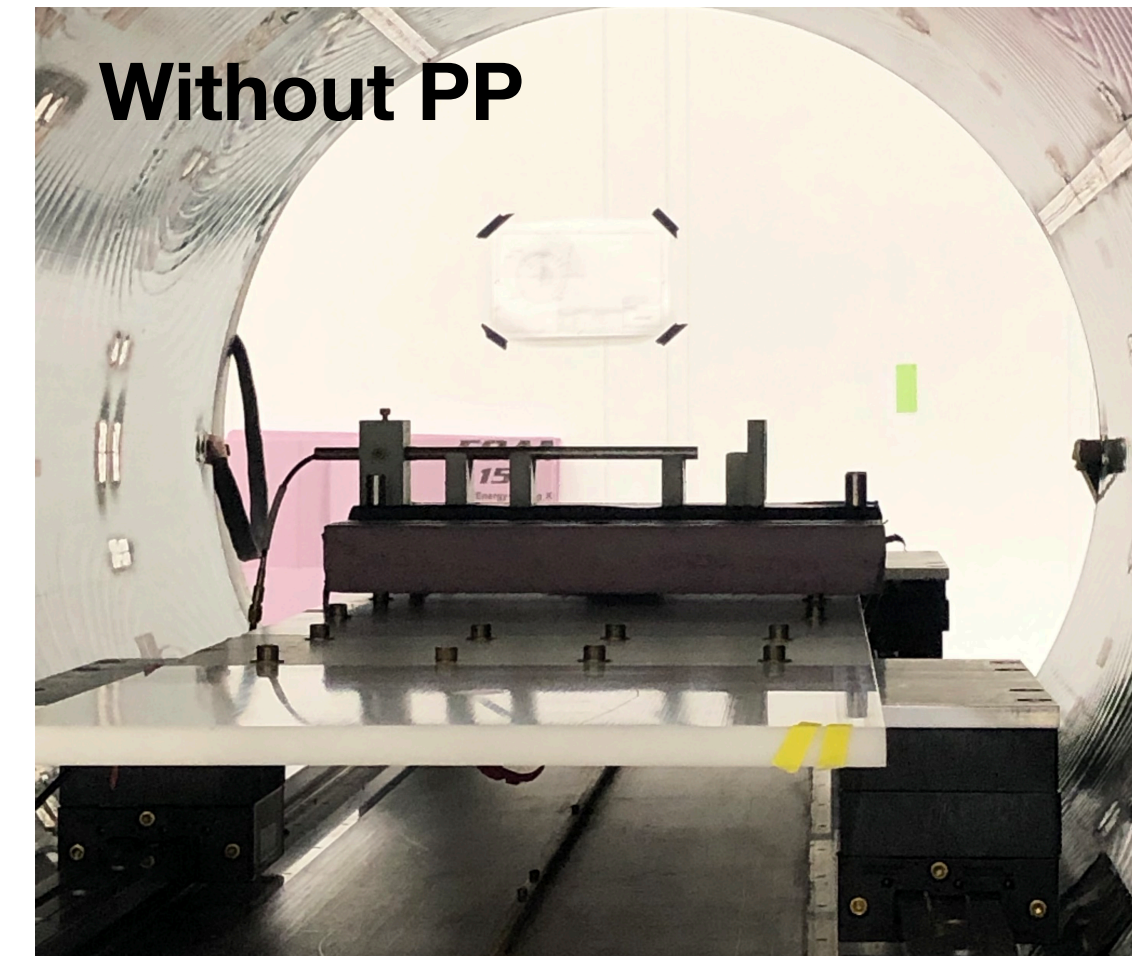
- Used to calibrate the **trolley** NMR probes
- **Symmetry** is very important => minimizes field perturbations => reduced systematic uncertainties
- **RF coil support**: 15-mm OD high-precision glass cylinder
  - Macor supports ensure alignment of **RF coil** (zero- $\chi$  0.97-mm OD wire)
- **Ground shield**: 1" OD, 1-mm wall 2024-T3 Al
  - Stabilizes probe tune, reduces noise pickup
- **Vacuum compatible**



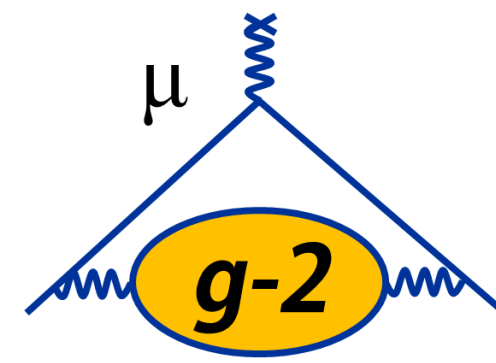
# Plunging Probe: Measuring Perturbations



- Take measurements of the field using the **fixed probe**
- **Compare** measurements without and with the PP mounted on stand
- **Difference** with and without gives the effect



# Plunging Probe: Material Perturbations ( $\delta_s$ )

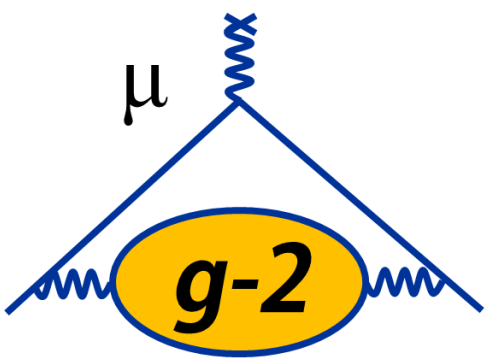


How much the field changes due to probe presence

Dependence on orientation about its **own** axis

Dependence on orientation relative to **field** axis

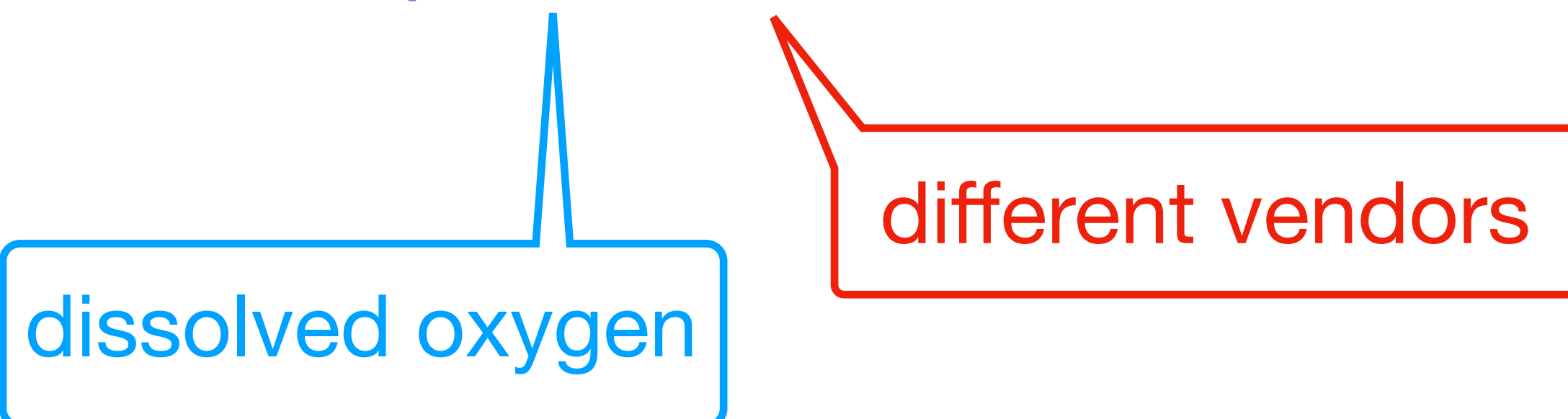
| Quantity                      | Symbol                                      | Value (ppb)                       |
|-------------------------------|---|-----------------------------------|
| General Material Perturbation | $\delta_{\text{mat}} + \delta_{\text{mag}}$ | $4.2 \pm 8.0$                     |
| SMA Cable Perturbation        | $\delta_{\text{cable}}$                     | $-1.4 + 3.0$                      |
| Probe Temperature             | $\delta_T$                                  | $0 \pm 5$                         |
| Roll Effect                   | $\delta_{\text{roll}}$                      | $0 \pm 1$                         |
| Pitch Effect                  | $\delta_{\text{pitch}}$                     | $-4.4 \pm 4.4$                    |
| Water Sample Camber           | $\delta_c$                                  | $0 \pm 1$                         |
| <b>TOTAL</b>                  | <b><math>\delta_s</math></b>                | <b><math>-1.6 \pm 10.9</math></b> |



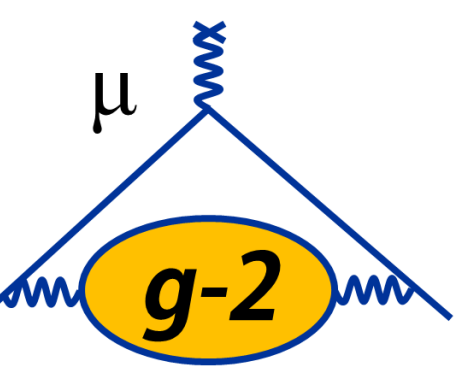
# Plunging Probe: Water Purity ( $\delta_p$ )

- Impurities in the water sample will perturb the field – paramagnetic contamination (e.g., dissolved oxygen) will increase the field
- Conduct two tests:
  1. Measure field when we **degas** the water – that is, heat up water just enough so that oxygen escapes. Compare to nominal water sample (at same T)
  2. Compare field measurements using water from two different vendors

- Define  $\delta_p = \delta_{O_2} + \delta_w$



| Quantity             | Symbol                       | Value (ppb)                     |
|----------------------|------------------------------|---------------------------------|
| Oxygen Contamination | $\delta_{O_2}$               | $1.4 \pm 0.5$                   |
| Different Vendors    | $\delta_w$                   | $0 \pm 1$                       |
| <b>TOTAL</b>         | <b><math>\delta_p</math></b> | <b><math>1.4 \pm 1.1</math></b> |

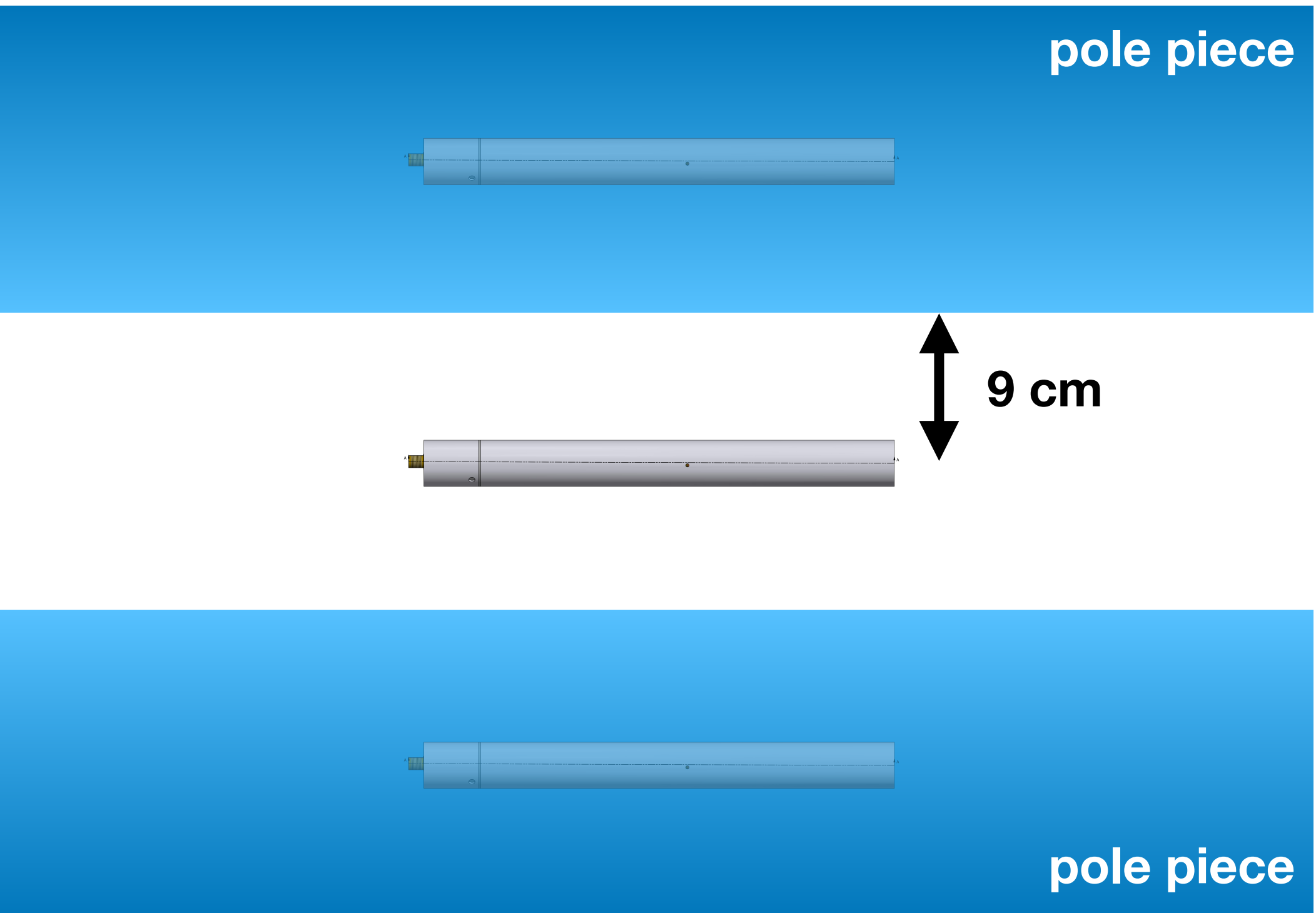


# Plunging Probe: Magnetic Images

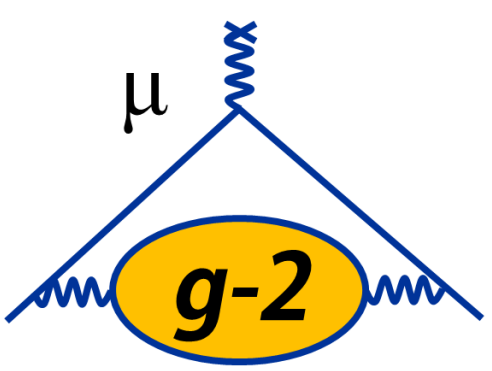
- Need to account for the effect due to magnetic images of the PP in the pole pieces
- For an infinite plane with magnetic permeability  $\mu_r$ , the field due to the image of a material with perturbation  $\Delta B$  is:

$$\Delta B' \approx \left( \frac{\mu_r - 1}{\mu_r + 1} \right) \Delta B(x, y, z') \approx \Delta B(x, y, z')$$

For  $\mu_r \gg 1$  ( $\sim 1450$  for the magnet\*). Evaluate the perturbation at image distance  $z'$  in the pole piece (upper **and** lower)



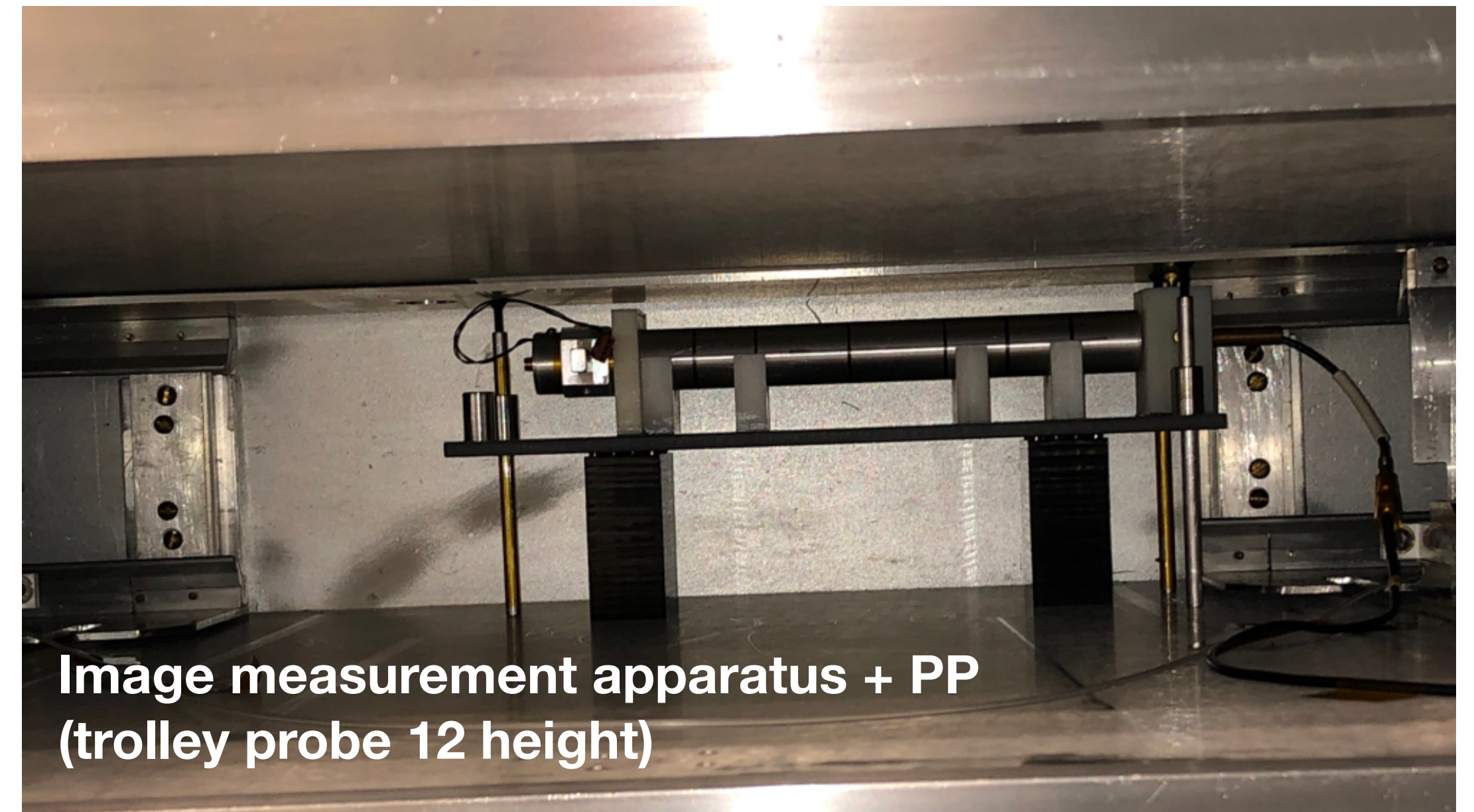
\* G. T. Danby *et al*, Nucl. Instrum. Meth. A **457**, 151 (2001)



# Plunging Probe: Measuring the Images at FNAL

- Use a stage to mount a fixed probe along the axis of the PP, which can slide over fixed probe
- Compare field measurements with and without PP installed on the stage
- Repeat measurements at height of center trolley probe, and highest trolley probe location
- Also conduct measurements with PP mounting rod attached/detached

Rod composition may not be pure aluminum (typically up to ~20% variation in  $\chi \Rightarrow$  imperfect predictions)



| Type         | Height Above Midplane (mm) | Image + Perturbation (ppb)      | Calculated Prediction (ppb) |
|--------------|----------------------------|---------------------------------|-----------------------------|
| PP + Holder  | 35.5                       | $6.1 \pm 4.4$                   | 11.5                        |
| PP + Holder  | -0.2                       | $7.3 \pm 5.4$                   | 4.3                         |
| Rod          | -0.2                       | $-3.1 \pm 5.6$                  | -12.9                       |
| <b>TOTAL</b> | <b>-0.2</b>                | <b><math>4.2 \pm 8.0</math></b> | <b>-8.6</b>                 |

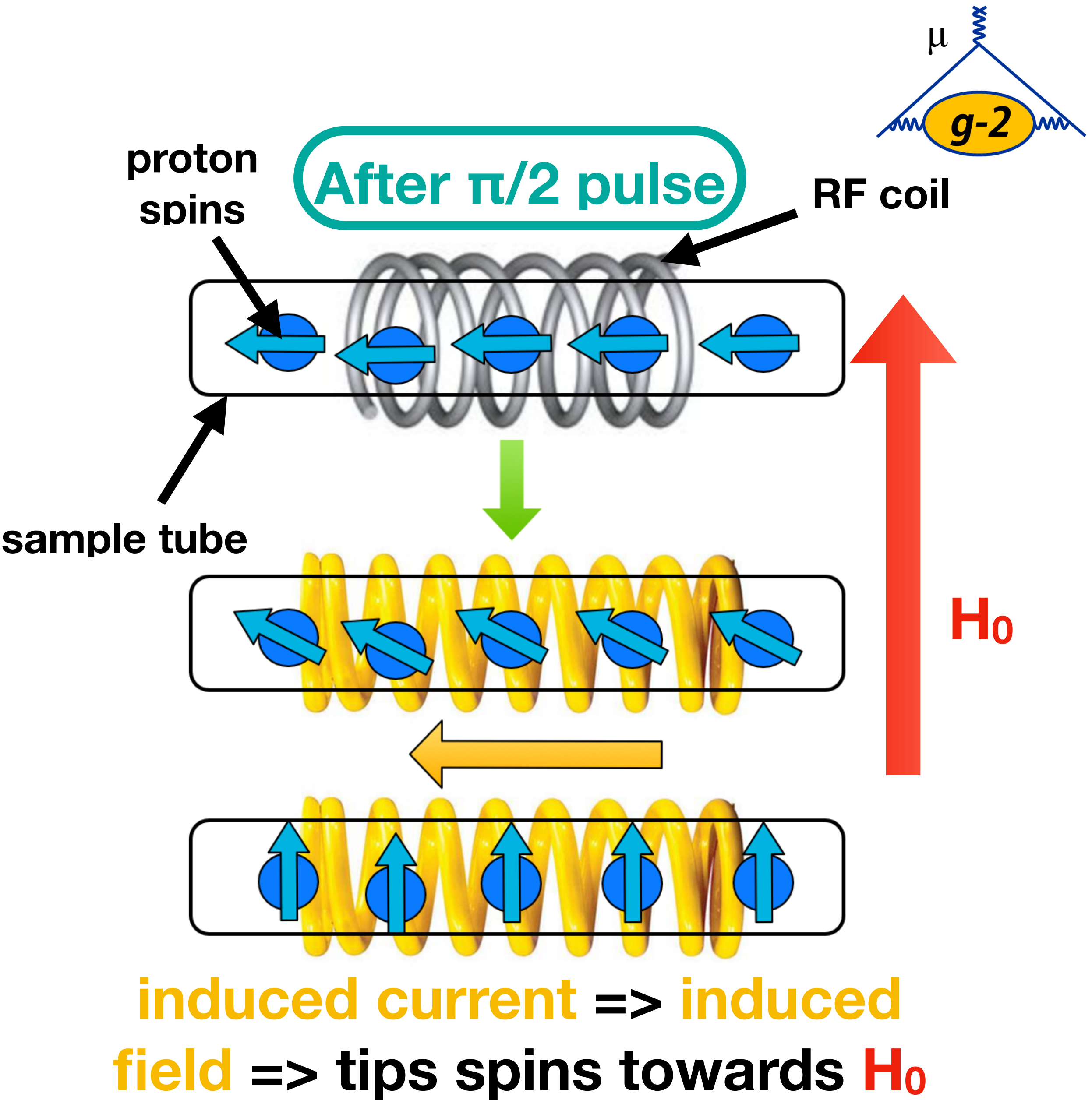
# Radiation Damping

## What is it?

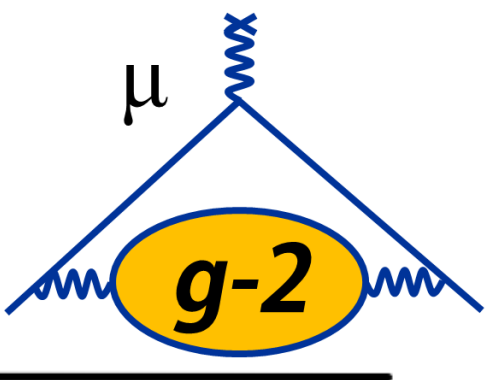
- Precessing spins induce emf in pickup coil; this in turn generates an alternating magnetic field that **acts to rotate spins back towards the main field**
- **Size of effect:**  $\delta_{RD} \sim [(f_0 - f_L)/f_0]\eta Q M_z(t)/\tau_{RD}$ 
  - $f_0$  = resonant frequency of circuit;  $f_L$  = Larmor frequency
  - $\eta$  = filling factor;  $Q$  = quality factor of circuit
  - $M_z(t)$  = magnetization of sample,  $\tau_{RD}$  = time scale of effect

## How to quantify?

- Use coils to produce a longitudinal field
  - Precise control over main field to mimic damping effect
- Vary  $\pi/2$  pulse  $\Rightarrow$  vary  $M_z(t) \Rightarrow$  changes  $\delta_{RD}$

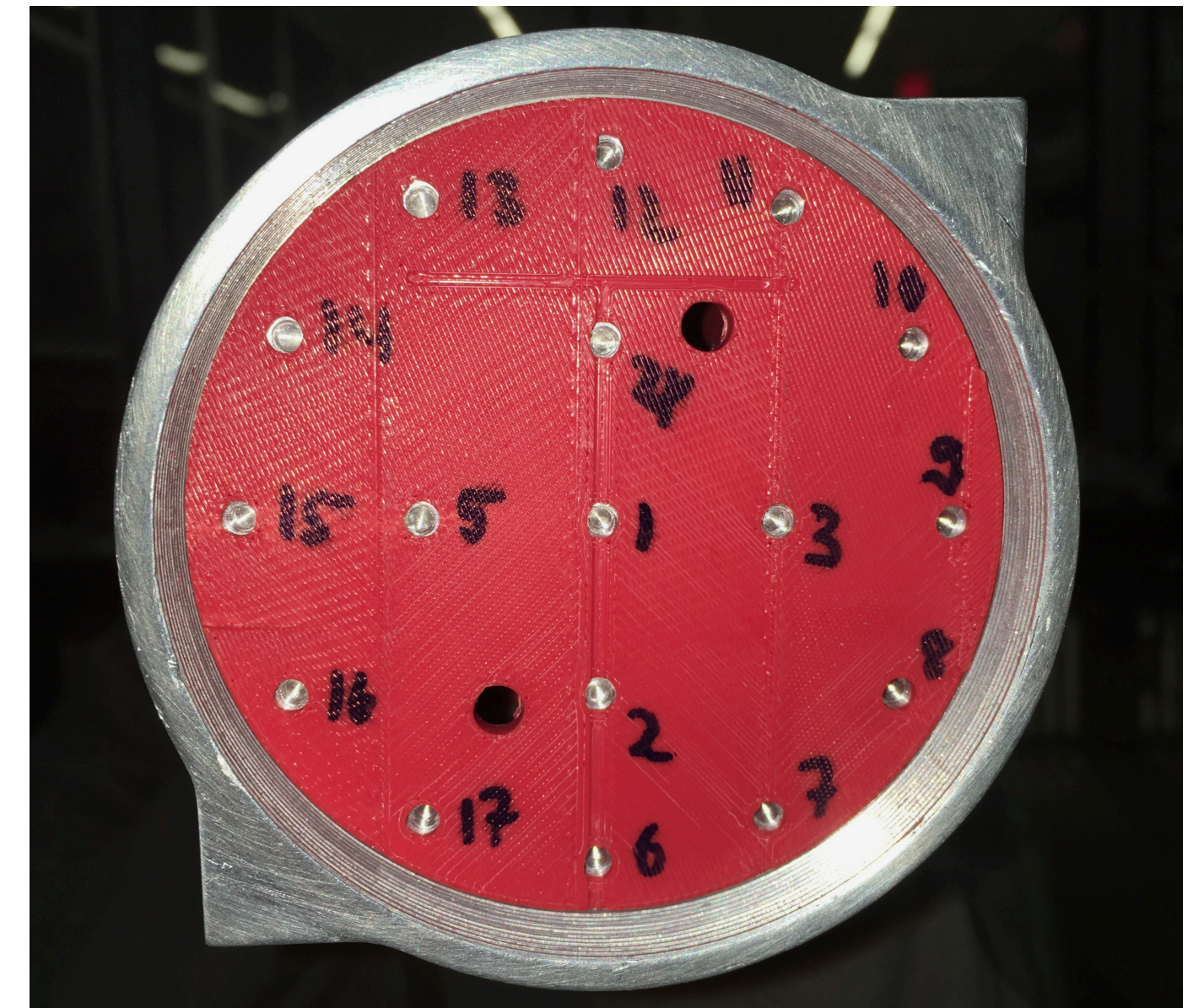
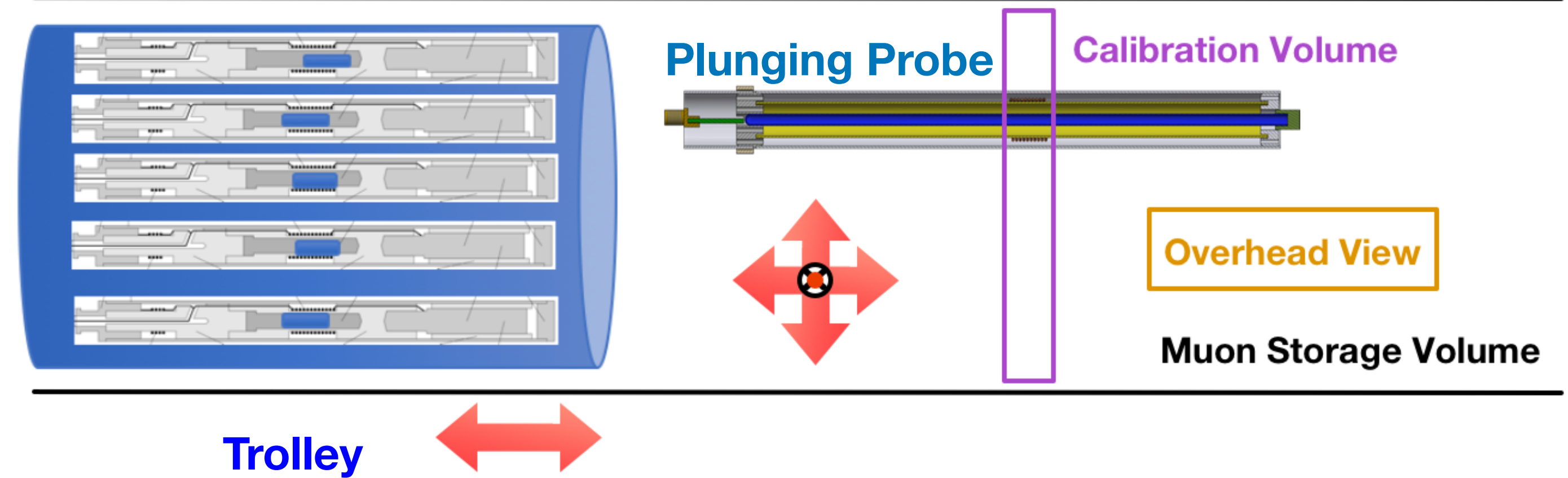


# Calibrating the Trolley



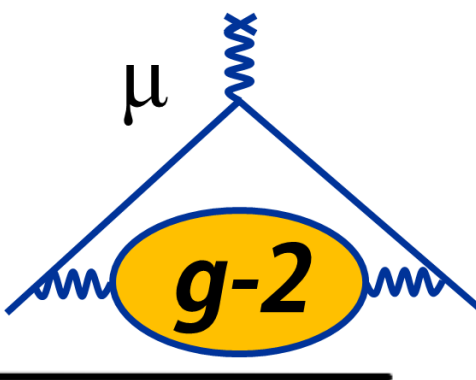
## Procedure

- Select **trolley** probe to calibrate



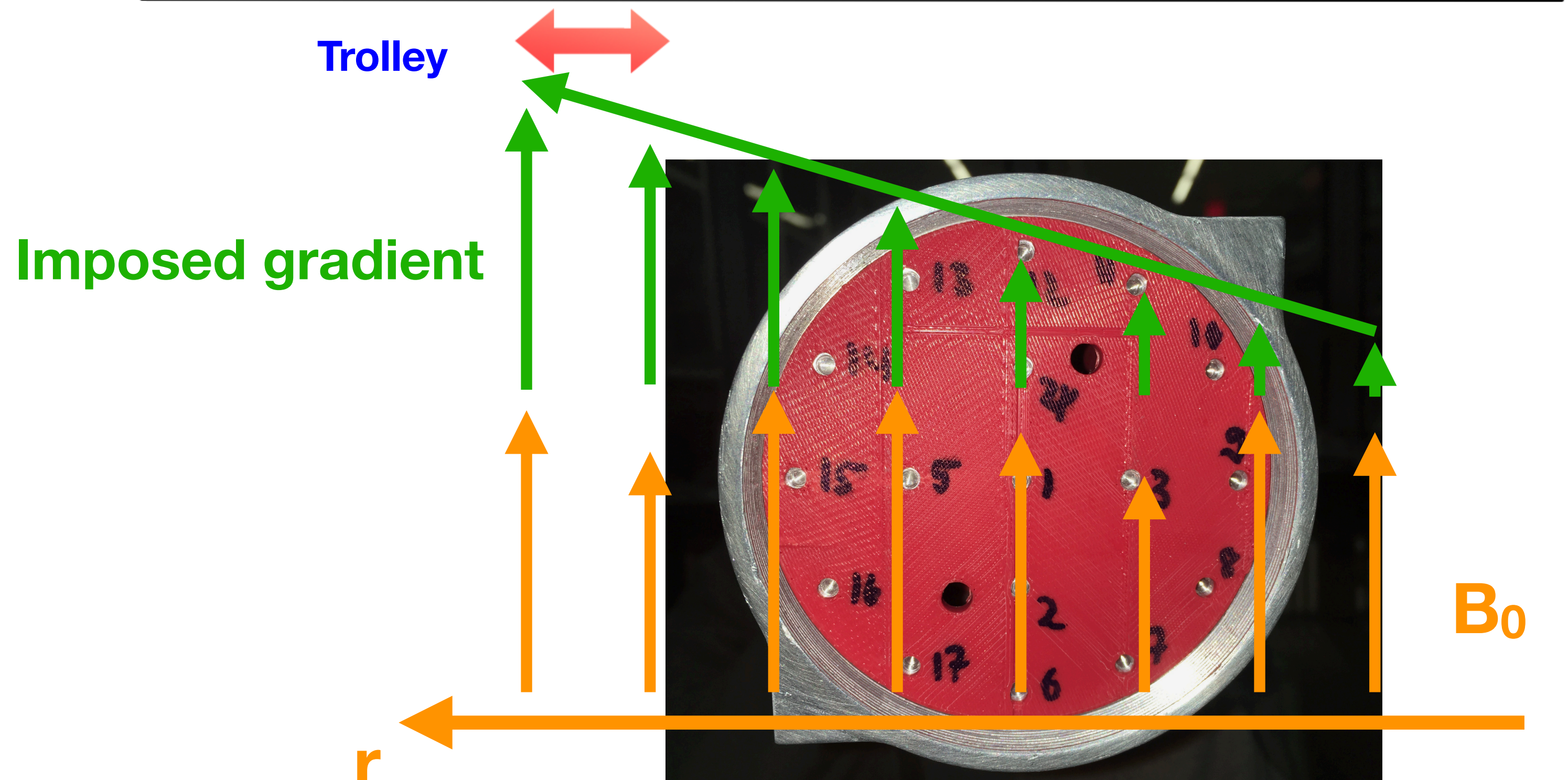
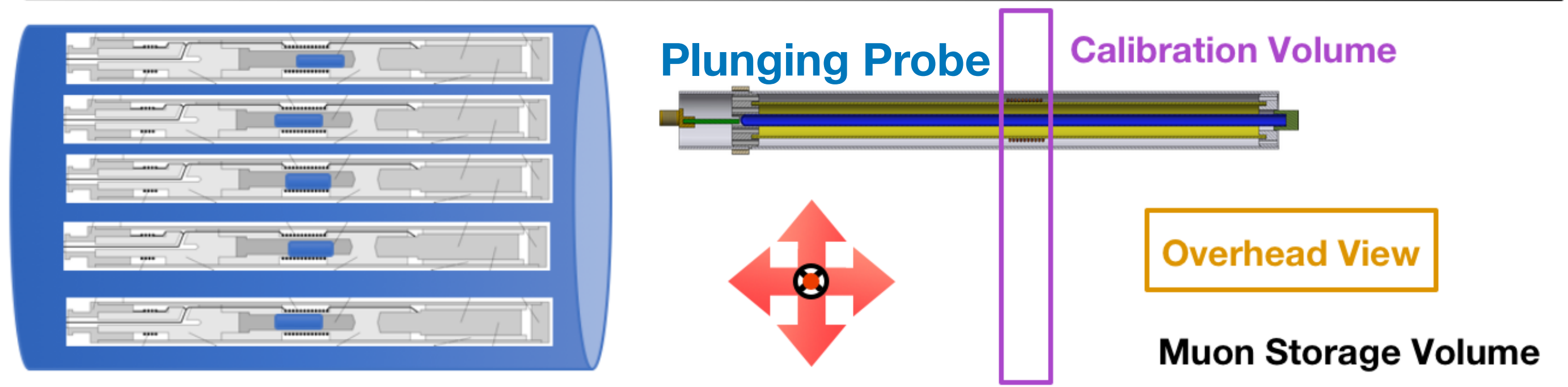
UMassAmherst

# Calibrating the Trolley



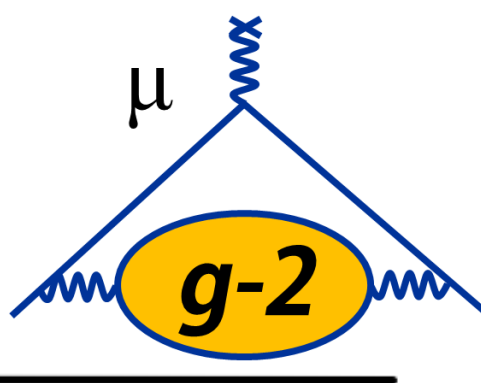
## Procedure

- Select **trolley** probe to calibrate
- Impose a **known gradient** across the trolley; compare to **bare field  $B_0$** . Define  $\Delta B = B(I \neq 0) - B(I=0)$
- Unique  $\Delta B$  for each **trolley** probe gives position



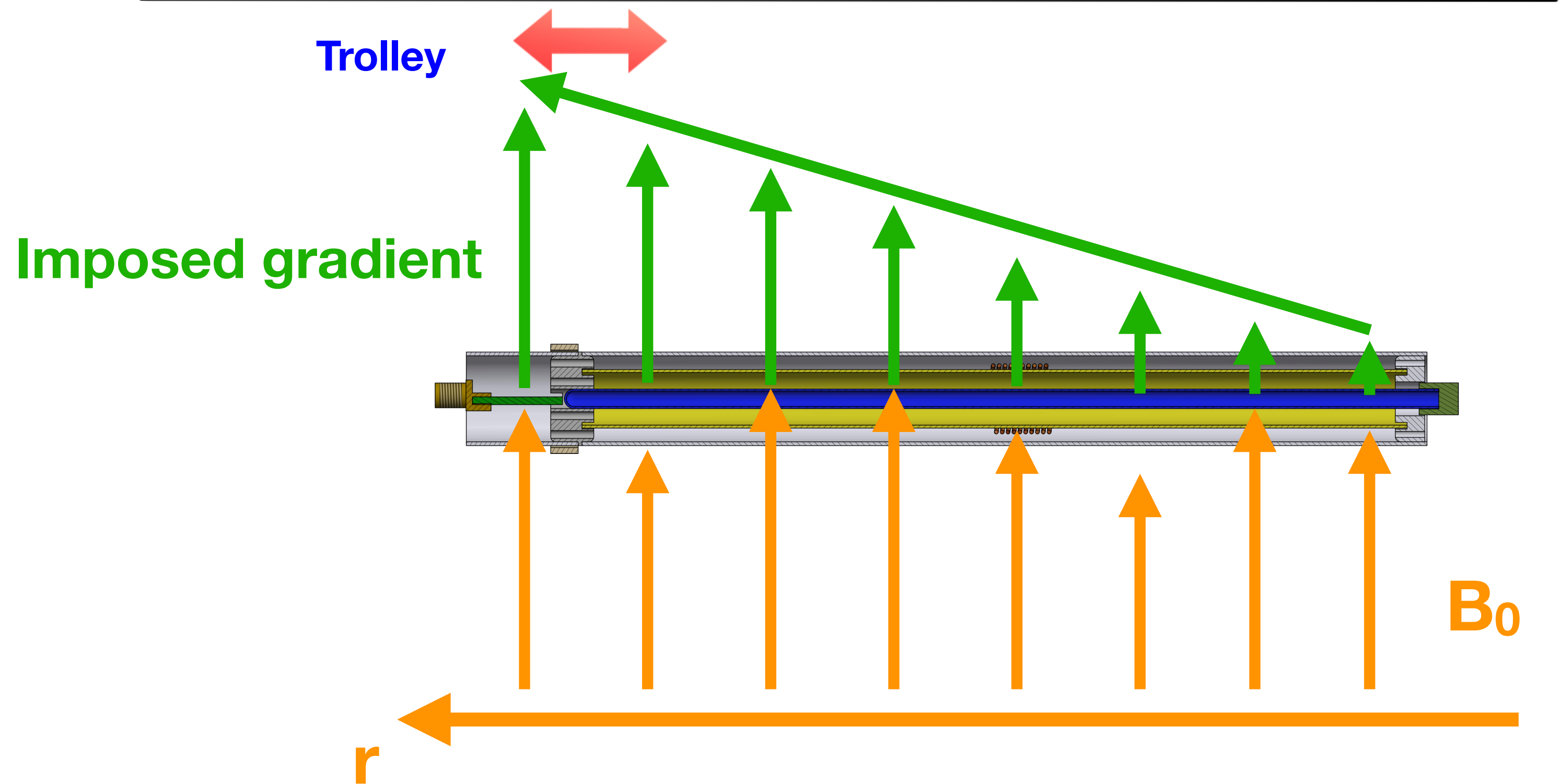
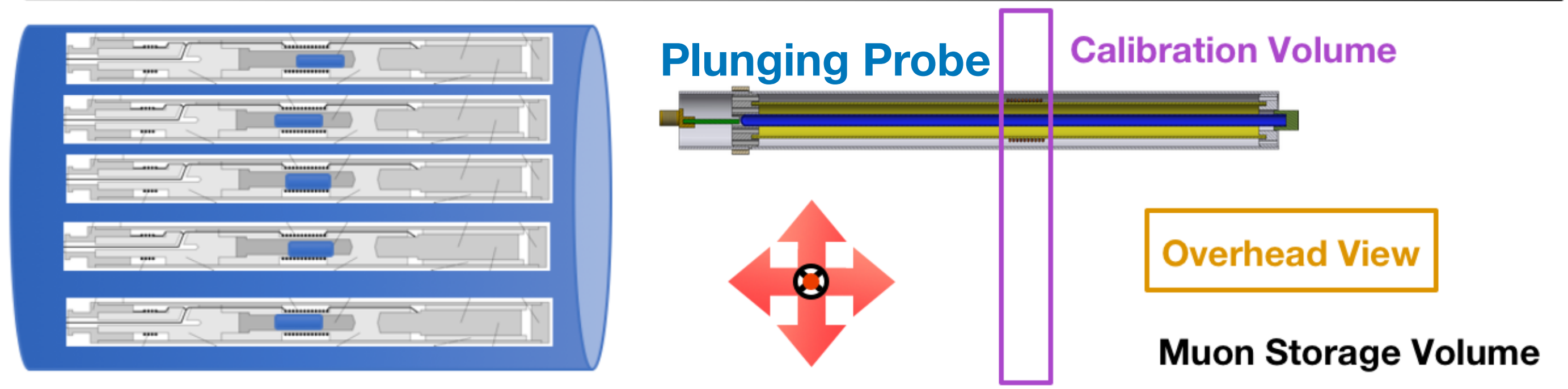
UMassAmherst

# Calibrating the Trolley



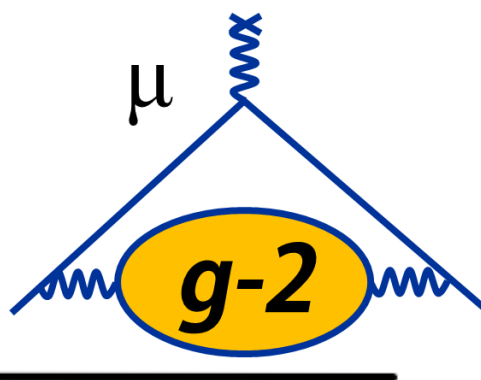
## Procedure

- Select **trolley** probe to calibrate
- Impose a **known gradient** across the trolley; compare to **bare field  $B_0$** . Define  $\Delta B = B(l \neq 0)$ 
  - $B(l=0)$
- Unique  $\Delta B$  for each **trolley** probe gives position
- Move **plunging probe** into volume; measure  $\Delta B$  and determine distance to move **plunging probe**
- Iterate until **plunging probe**  $\Delta B$  matches **trolley** probe  $\Delta B$
- Perform for radial, vertical, azimuthal coordinates



UMassAmherst

# Calibrating the Trolley



## Procedure

- Select **trolley** probe to calibrate
- Impose a **known gradient** across the trolley; compare to **bare field  $B_0$** . Define  $\Delta B = B(I \neq 0) - B(I=0)$
- Unique  $\Delta B$  for each **trolley** probe gives position
- Move **plunging probe** into volume; measure  $\Delta B$  and determine distance to move **plunging probe**
- Iterate until **plunging probe**  $\Delta B$  matches **trolley** probe  $\Delta B$
- Perform for radial, vertical, azimuthal coordinates
- Shim the field to be highly uniform, and measure using the **PP** and the **trolley** (rapid swapping)

